

Quantum Transport in Electron Devices and Novel Materials

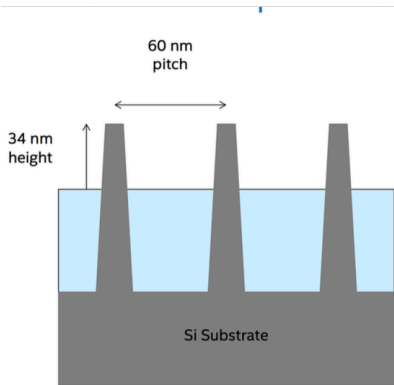
ECE 5390/MSE 5472

Fall, 2017

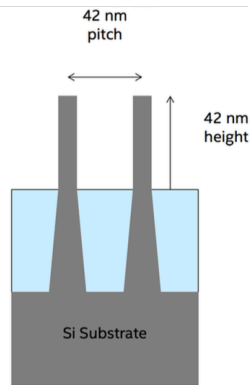
Debdeep Jena (djena@cornell.edu)

ECE & MSE, Cornell University

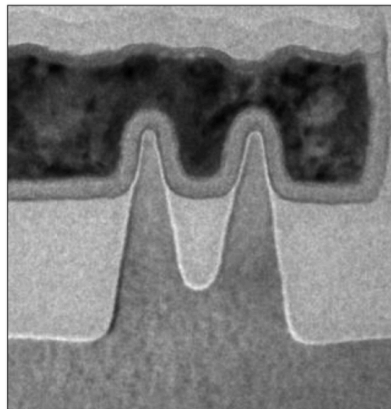
About the class



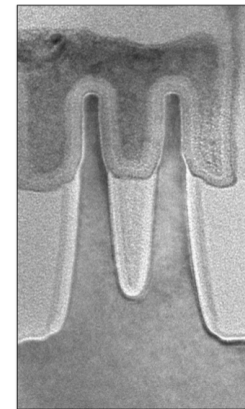
22 nm Process



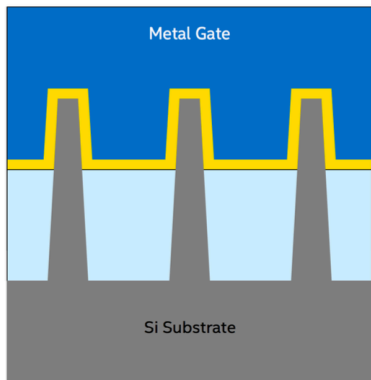
14 nm Process



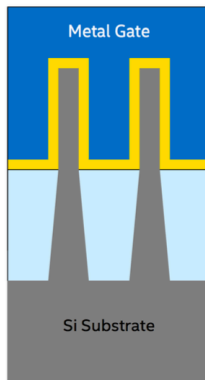
22 nm 1st Generation Tri-gate Transistor



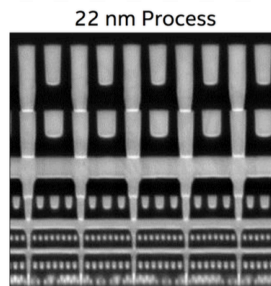
14 nm 2nd Generation Tri-gate Transistor



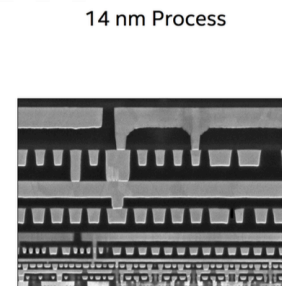
22 nm 1st Generation Tri-gate Transistor



14 nm 2nd Generation Tri-gate Transistor



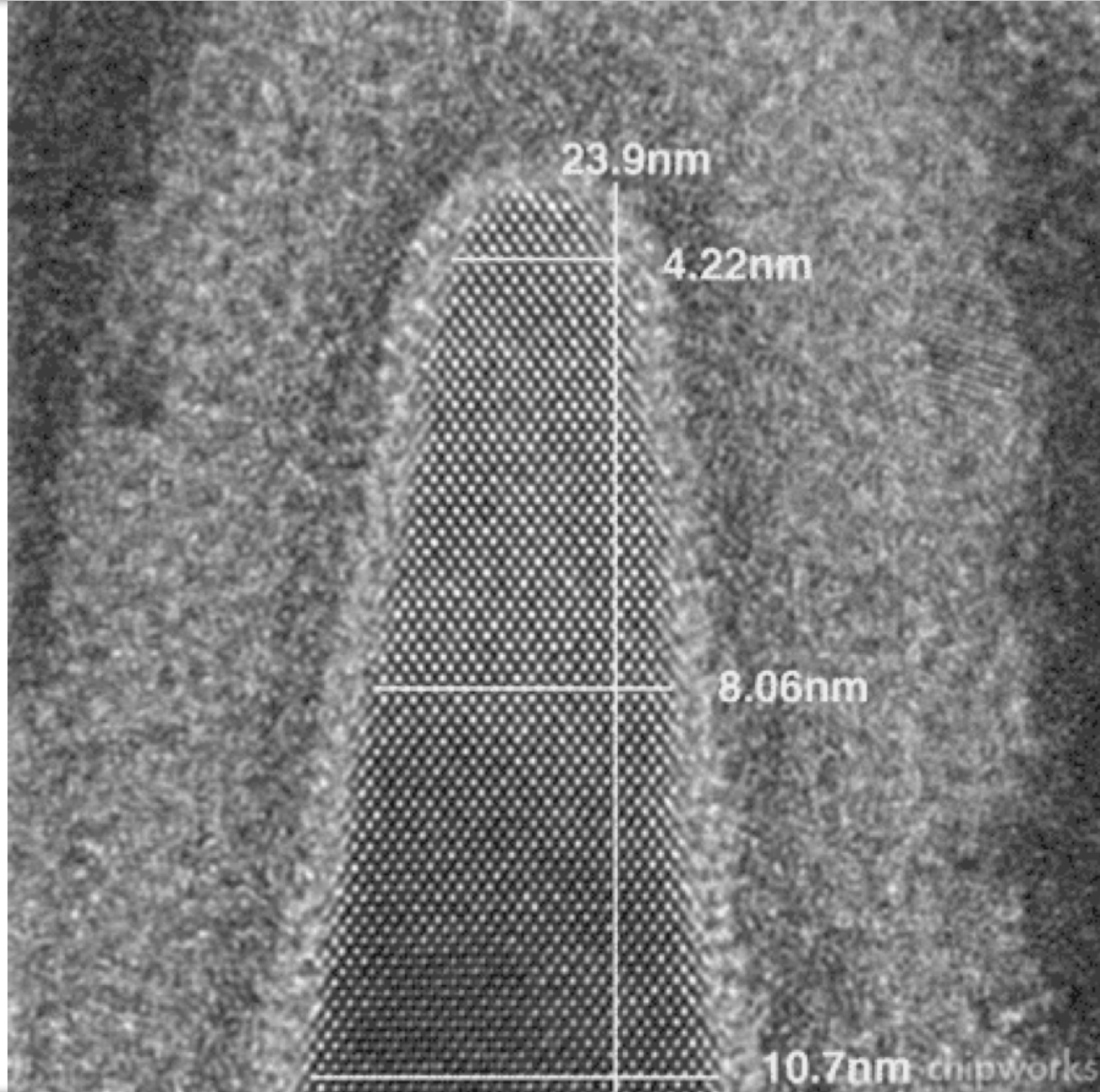
80 nm minimum pitch



52 nm (0.65x) minimum pitch

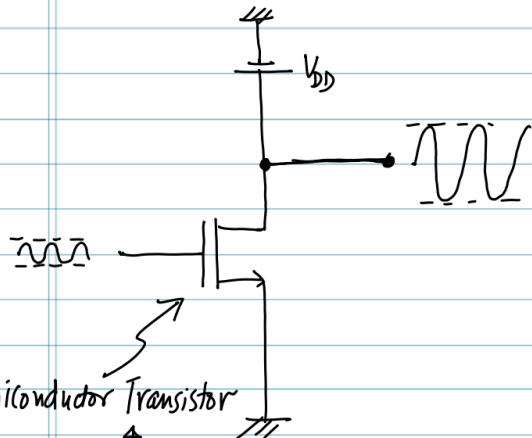


About the class

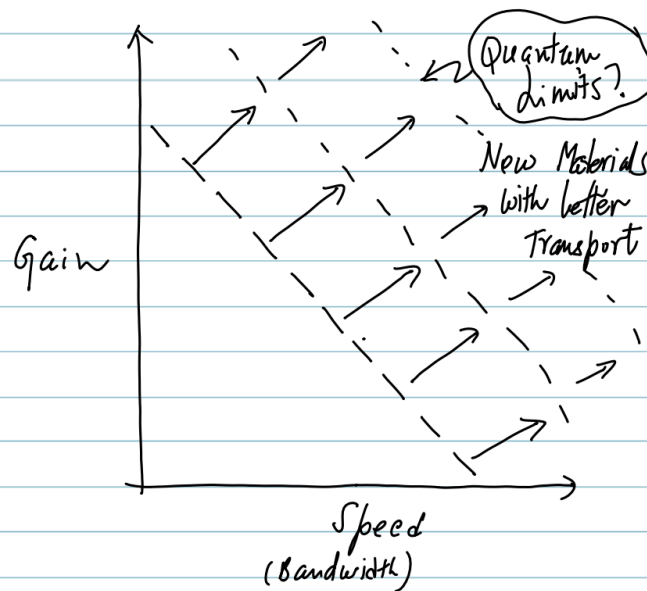


Our goals in this course

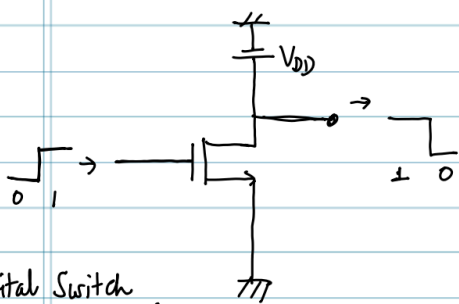
Communication Devices



- Semiconductor Transistor
- Vacuum tube

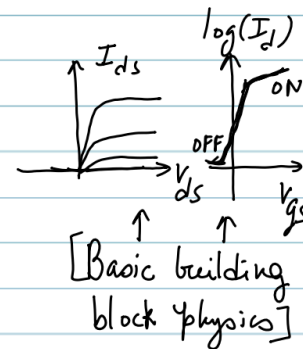
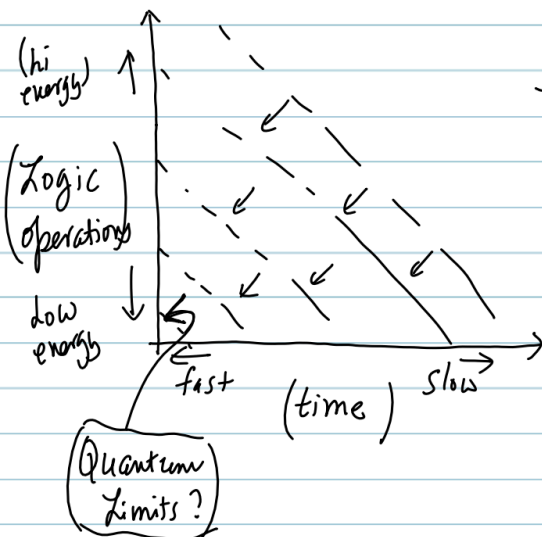


Logic Devices



- Digital Switch
- Mechanical relay

- Charge-based
- Spin-based
- Correlated/Phase transitions.



Our goals in this course



As engineers, cards we are dealt with:

Si N
All elements in the periodic table

Our tasks:

- ① Improve (Gain) * (Bandwidth) ← better Communications
- ② Lower energy cost of computation ← better 'logic'.

How do we coax electrons and the elements to do these things for us?

- Learn the physics of transport in materials (semiconductors, metals, etc.).
- Learn how to control the electron's population, spins, etc. . . .
- Learn the 'traditional' or semi-classical transport properties such as drift, diffusion, scattering, etc. Examine limitations on devices.
- Learn "emergent" phenomena in transport: e.g. Gunn Oscillations, Superconductivity, Quantum Hall effects, and Metal-Insulator transitions, etc. . . .
- Learn the most modern tools for coherent/quantum transport such as the NEGF approach. Expose its limitations.
- Learn how historically new transport phenomena have led to new device applications.

Periodic Table of Elements

1	2	3	4	5	6	7	8	9	10	11	12	13	14	15	16	17	18
1 H Hydrogen 1.00794	2 He Helium 4.002602																
3 Li Lithium 6.941	4 Be Beryllium 9.012182																
5 B Boron 10.811	6 C Carbon 12.0107	7 N Nitrogen 14.00644	8 O Oxygen 15.999	9 F Fluorine 18.9984032	10 Ne Neon 20.1797												
11 Na Sodium 22.98976928	12 Mg Magnesium 24.304																
13 Al Aluminum 26.9815386	14 Si Silicon 28.0855	15 P Phosphorus 30.973762	16 S Sulfur 32.06	17 Cl Chlorine 35.45	18 Ar Argon 39.948												
19 K Potassium 39.0983	20 Ca Calcium 40.078	21 Sc Scandium 44.955912	22 Ti Titanium 47.88	23 V Vanadium 50.9415	24 Cr Chromium 51.9961	25 Mn Manganese 54.938045	26 Fe Iron 55.845	27 Co Cobalt 58.933195	28 Ni Nickel 58.6934	29 Cu Copper 63.546	30 Zn Zinc 65.38	31 Ga Gallium 69.723	32 Ge Germanium 72.64	33 As Arsenic 74.9216	34 Se Selenium 78.96	35 Br Bromine 79.904	36 Kr Krypton 83.796
37 Rb Rubidium 85.4678	38 Sr Strontium 87.62	39 Y Yttrium 88.90584	40 Zr Zirconium 91.224	41 Nb Niobium 92.90638	42 Mo Molybdenum 95.94	43 Tc Technetium 98.90625	44 Ru Ruthenium 101.07	45 Rh Rhodium 102.9055	46 Pd Palladium 106.42	47 Ag Silver 107.8682	48 Cd Cadmium 112.411	49 In Indium 114.818	50 Sn Tin 118.710	51 Sb Antimony 121.757	52 Te Tellurium 127.603	53 I Iodine 126.905	54 Xe Xenon 131.29
55 Cs Cesium 132.90545196	56 Ba Barium 137.327	57-71 Lanthanides	72 Hf Hafnium 178.49	73 Ta Tantalum 180.94788	74 W Tungsten 183.84	75 Re Rhenium 186.207	76 Os Osmium 190.23	77 Ir Iridium 192.222	78 Pt Platinum 195.084	79 Au Gold 196.966569	80 Hg Mercury 200.59	81 Tl Thallium 204.3833	82 Pb Lead 207.2	83 Bi Bismuth 208.9804	84 Po Polonium (209)	85 At Astatine (210)	86 Rn Radon 222
87 Fr Francium (223)	88 Ra Radium (226)	89-103 Actinides	104 Rf Rutherfordium (261)	105 Db Dubnium (262)	106 Sg Seaborgium (263)	107 Bh Bohrium (264)	108 Hs Hassium (265)	109 Mt Meitnerium (266)	110 Ds Darmstadtium (271)	111 Rg Roentgenium (272)	112 Uub Ununbium (285)	113 Uut Ununtrium (284)	114 Uuq Ununquadium (289)	115 Uup Ununpentium (288)	116 Uuq Ununhexium (289)	117 Uus Ununseptium (289)	118 Uuo Ununoctium (294)

For elements with no stable isotopes, the mass number of the isotope with the longest half-life is in parentheses.

Design and Interface Copyright © 1997 Michael Dayah (michael@dayah.com). <http://www.ptable.com>

About the class

Course Title: ECE 5390/MSE 5472: Quantum Transport in Electron Devices and Novel Materials

Author: Prof. Debdeep Jena, ECE and MSE

Authorship or Revision Date: 8/10/2017

Credit Hours: 4 hours

Catalog Description:

Charge, heat, and spin transport in semiconductors, 2D crystals, and correlated oxides. Electronic gain and speed and its link to transport. Rigorous quantum transport in semiconductors, ballistic transport, quantized conductance, non-equilibrium Green's functions. Boltzmann transport equation, scattering, Fermi's golden rule, and electron-phonon interactions. Transport coefficients, thermoelectric properties. Mobility, high-field saturation and impact ionization. Gunn and IMPATT devices. ultrafast (THz) semiconductor electronics. Tunneling transport, backward diodes, negative differential resistance. Magnetotransport/Quantum Hall effect, Berry phase, Chern numbers. Edge-state/surface transport phenomena in emerging chiral semiconductors such as TMDs, topological insulators, and correlated transport in BCS superconductivity in semiconductors such as diamond and 2D Crystals.

Course Frequency:

Offered every 2nd spring

Prerequisites:

ECE 4070/MSE 6050 or equivalent Solid-State Physics, ECE 4060/MSE 5715 or equivalent Quantum Mechanics, or permission of the instructor

Corequisites:

ECE 4570 strongly recommended

Student Preparation Summary:

Math: Students enrolling in this class must be comfortable with the basics of algebra, linear algebra and matrices, and differential equations.

Physics: Students should be familiar with the basics of classical electromagnetism and fields and waves, charge and current, resistance and capacitance, and Ohm's Law. Prior familiarity with quantum mechanical concepts such as the wave/particle duality and the Heisenberg uncertainty principle, the Schrodinger wave equation, and eigenvalues and eigenfunctions will help in the initial portions of the course. Basic notions of statistical mechanics such as Maxwell-Boltzmann, Fermi-Dirac, and Bose-Einstein distributions should be familiar to those who enroll in the class.

Programming: Students should be comfortable in using the computer to solve equations symbolically (e.g. using Mathematica) and numerically (e.g. using Mathematica, MATLAB or Python) and to produce graphical plots.

Textbook(s) and/or Other Required Materials:

- Course notes distributed via the class website
- Selected reading materials distributed via class website
- Etc

ECE Open CourseWare Link [if available]:

Class and Laboratory Schedule:

Lectures: Two 75 min lectures per week

Recitations: None required.

Labs: None

Assignments, Exams and Projects:

Homework: Biweekly assignments. Total of ~5 homework assignments per semester. Collaboration with students is encouraged.

Exams: One take-home written exam at the middle of the semester.

Design Projects: One research project through the last half of the semester for which there will be 2 in-class presentations, and 2 reports. The research project will integrate, refine, and advance the materials learnt in the class.

Course Grading Scheme: 70% Homeworks, 10% Prelim, 20% Research Project

Detailed List of Topics Covered:

Part I: Review of fundamentals

- 1.1: Review of classical and quantum mechanics
- 1.2: Current flow in quantum mechanics, classical and quantum continuity equations
- 1.3: Drift, diffusion, recombination, and space-charge currents
- 1.4: Quantum statistics and thermodynamics, quest for equilibrium as the driver for transport

Part II: Single-particle transport

- 2.1: Ballistic transport: Quantized conductance, Ballistic MOSFETs
- 2.2: Transmission and tunneling, Tunneling FETs and resonant tunneling diodes
- 2.3: Closed vs. open systems, the Non-Equilibrium Green's Function approach to transport
- 2.4: Diffusive transport, Boltzmann transport equation, scattering
- 2.5: Fermi's golden rule, Electron-phonon interactions, mobility and velocity saturation
- 2.6: High-field effects, Gunn diodes and oscillators for high-frequency power
- 2.7: Feynman path integrals, the Aharonov Bohm effect and Weak Localization

Part III: Geometrical and topological quantum mechanics, unification with relativity

- 3.1: Spin, transport in a magnetic field
- 3.2: Berry phase in quantum mechanics, Quantum Hall effect, Anomalous Hall Effect
- 3.3: Chern numbers, Edge/Topological states, Topological insulators and Majorana Fermions

Part IV: Many-particle correlated transport

- 4.1: Fock-space way of thinking transport, second quantization, conductance anomalies
- 4.2: BCS theory of superconductivity, Josephson junctions
- 4.3: Landau/Ginzburg superconductivity theories of phase transitions due to broken symmetry

Student Outcomes [ABET]:

1. Demonstrate fundamental in-depth quantum mechanical understanding of electron transport in electron devices such as diodes, transistors, and LEDs and Lasers.
2. Demonstrate understanding of single and multi-particle transport properties by showing ability to develop and explain experimental data using theoretical models, and make predictions.
3. Demonstrate an understanding of electronic transport phenomena across materials families of insulators, amorphous solids, 3D 2D 1D and 0D semiconductors, topological insulators, metals, and superconductors.
4. Demonstrate an ability to apply the knowledge to design electronic materials and device structures that perform specific actions such as high-speed switching, negative differential resistance, electronic gain, high magnetoresistance, control of spin currents, protected quantum states robust to scattering and decoherence.

Academic Integrity:

Students expected to abide by the Cornell University Code of Academic Integrity with work submitted for credit representing the student's own work. Discussion and collaboration on homework and laboratory assignments is permitted and encouraged, but final work should represent the student's own understanding. Specific examples of this policy implementation will be distributed in class. Course materials posted on Blackboard are intellectual property belonging to the author. Students are not permitted to buy or sell any course materials without the express permission of the instructor. Such unauthorized behavior will constitute academic misconduct.

Outline

Part I: Review of fundamentals

- 1.1: Review of classical and quantum mechanics
- 1.2: Current flow in quantum mechanics, classical and quantum continuity equations
- 1.3: Drift, diffusion, recombination, and space-charge currents
- 1.4: Quantum statistics and thermodynamics, quest for equilibrium as the driver for transport

Part II: Single-particle transport

- 2.1: Ballistic transport: Quantized conductance, Ballistic MOSFETs
- 2.2: Transmission and tunneling, Tunneling FETs and resonant tunneling diodes
- 2.3: Closed vs. open systems, the Non-Equilibrium Green's Function approach to transport
- 2.4: Diffusive transport, Boltzmann transport equation, scattering
- 2.5: Fermi's golden rule, Electron-phonon interactions, mobility and velocity saturation
- 2.6: High-field effects, Gunn diodes and oscillators for high-frequency power
- 2.7: Feynman path integrals, the Aharonov Bohm effect and Weak Localization

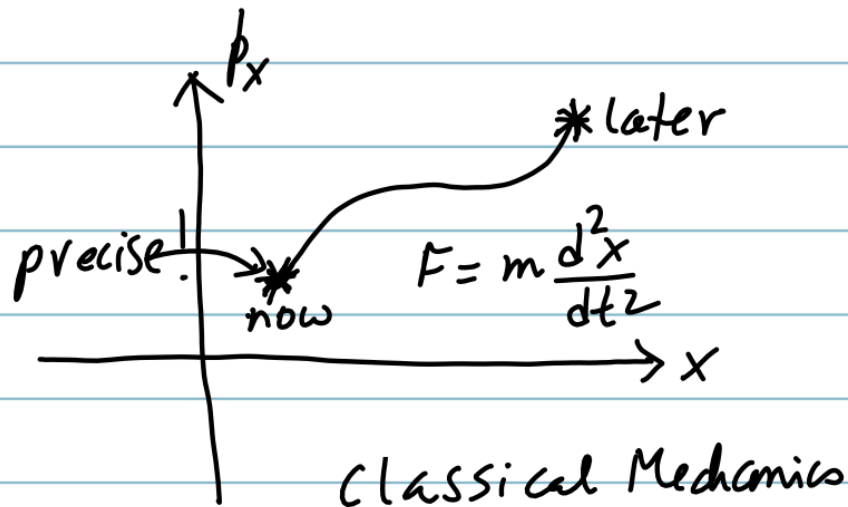
Part III: Geometrical and topological quantum mechanics, unification with relativity

- 3.1: Spin, transport in a magnetic field
- 3.2: Berry phase in quantum mechanics, Quantum Hall effect, Anomalous Hall Effect
- 3.3: Chern numbers, Edge/Topological states, Topological insulators and Majorana Fermions

Part IV: Many-particle correlated transport

- 4.1: Fock-space way of thinking transport, second quantization, conductance anomalies
- 4.2: BCS theory of superconductivity, Josephson junctions
- 4.3: Landau/Ginzburg superconductivity theories of phase transitions due to broken symmetry

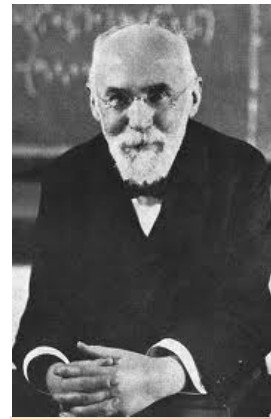
Time-evolution of a classical 'charged' object



Newton

$$\mathbf{F} = -\nabla V(r) = \frac{d\mathbf{p}}{dt}$$

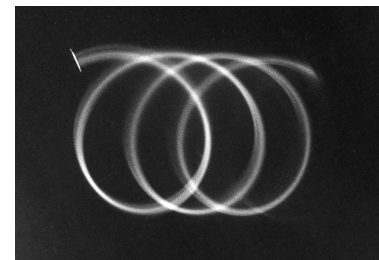
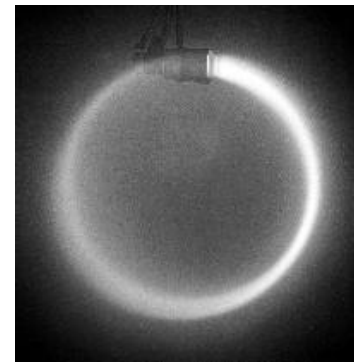
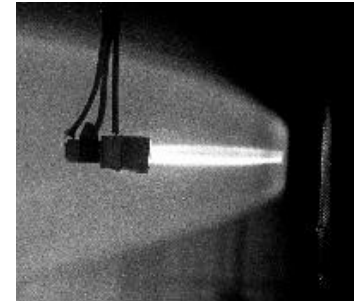
Path is deterministic



Lorentz

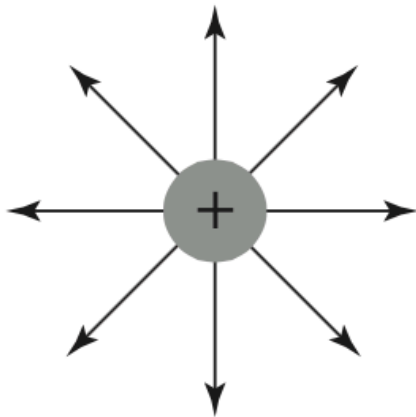
$$\mathbf{F} = q(\mathbf{E} + \mathbf{v} \times \mathbf{B})$$

Path is deterministic

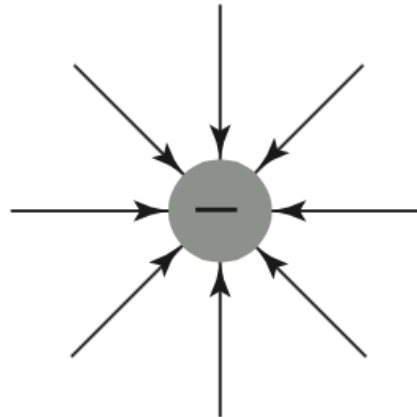


Maxwell's equations: Classical EMag

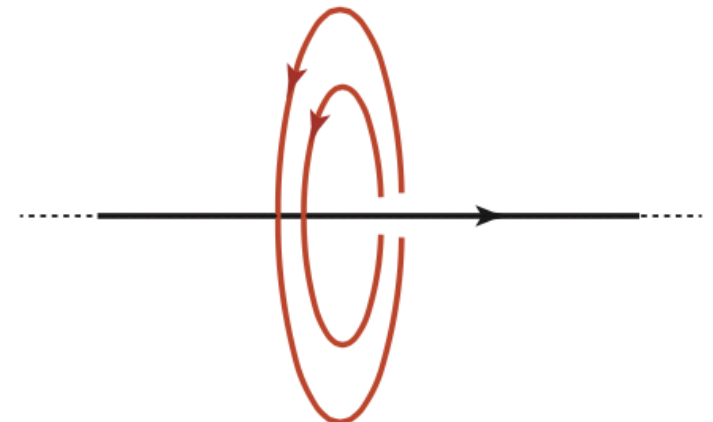
$\nabla \cdot \mathbf{D}$	$= \rho,$	Gauss's law
$\nabla \cdot \mathbf{B}$	$= 0,$	Gauss's law
$\nabla \times \mathbf{E}$	$= -\frac{\partial \mathbf{B}}{\partial t},$	Faraday's law
$\nabla \times \mathbf{H}$	$= \mathbf{J} + \frac{\partial \mathbf{D}}{\partial t},$	Ampere's law.



$$\nabla \cdot \mathbf{E} > 0$$



$$\nabla \cdot \mathbf{E} < 0$$



$$\nabla \times \mathbf{H} = \mathbf{J}$$

Maxwell's equations: Classical EMag

$$\begin{aligned}(\nabla^2 - \frac{1}{c^2} \frac{\partial^2}{\partial t^2}) \mathbf{E} &= 0, \quad \text{Wave Equations} \\(\nabla^2 - \frac{1}{c^2} \frac{\partial^2}{\partial t^2}) \mathbf{B} &= 0.\end{aligned}$$

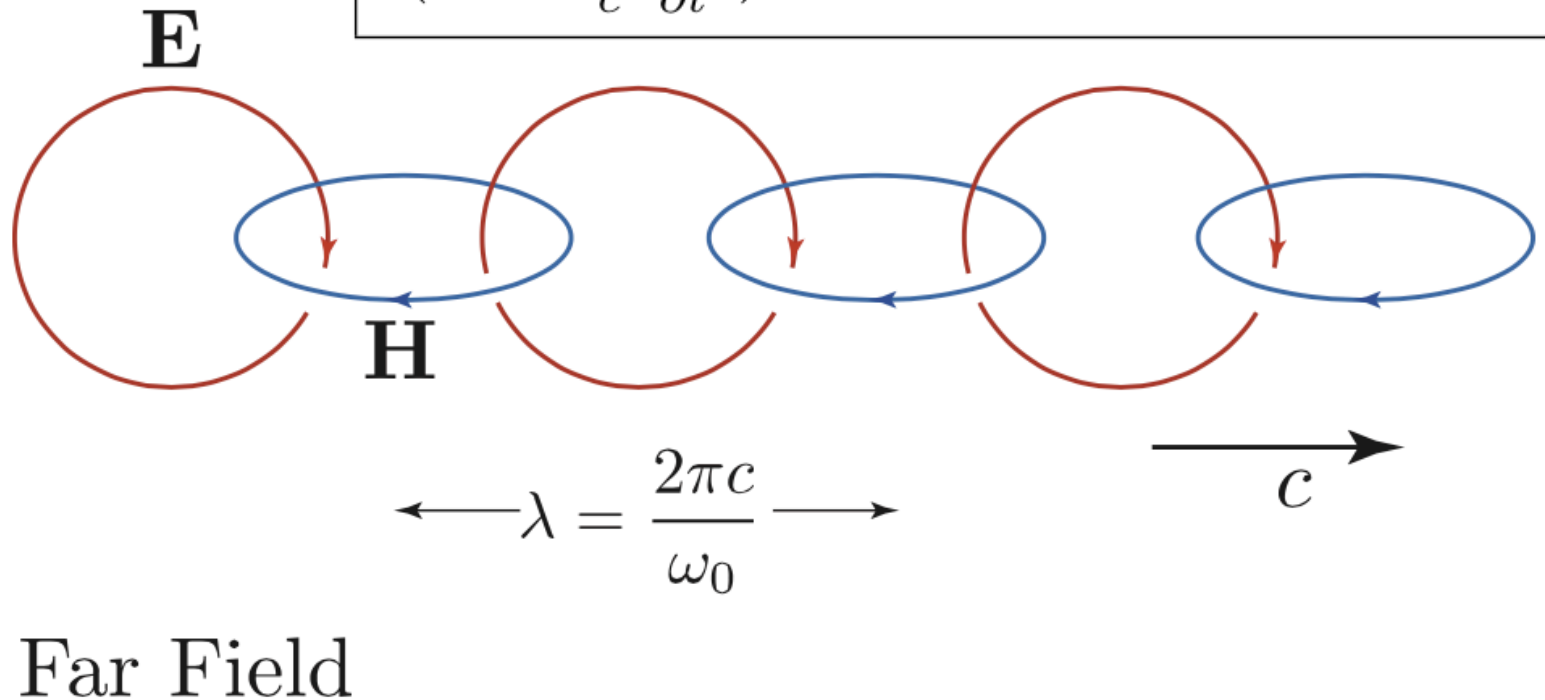
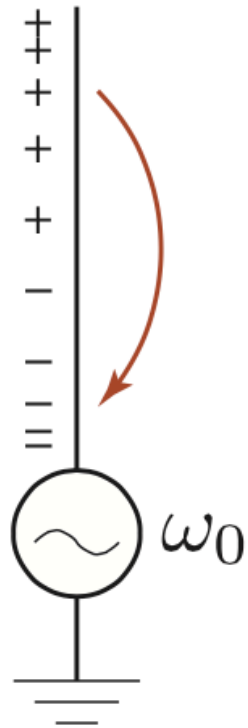


FIGURE 20.2: Antenna producing an electromagnetic wave.

Maxwell's equations: Birth of Light

$$\begin{aligned} (\nabla^2 - \frac{1}{c^2} \frac{\partial^2}{\partial t^2}) \mathbf{E} &= 0, & \text{Wave Equations} \\ (\nabla^2 - \frac{1}{c^2} \frac{\partial^2}{\partial t^2}) \mathbf{B} &= 0. \end{aligned}$$

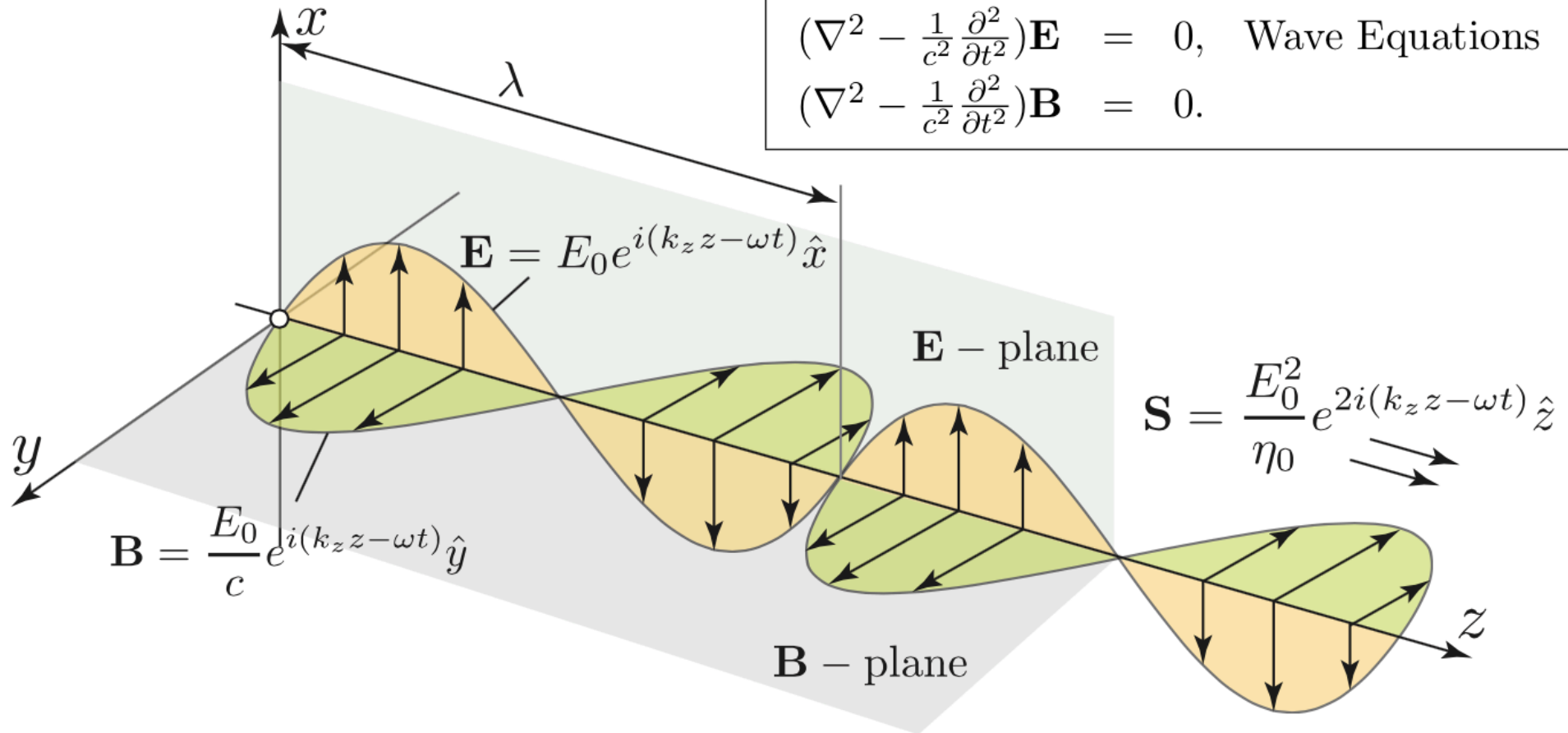


FIGURE 20.3: Electromagnetic wave.

Maxwell's equations: Response of solids

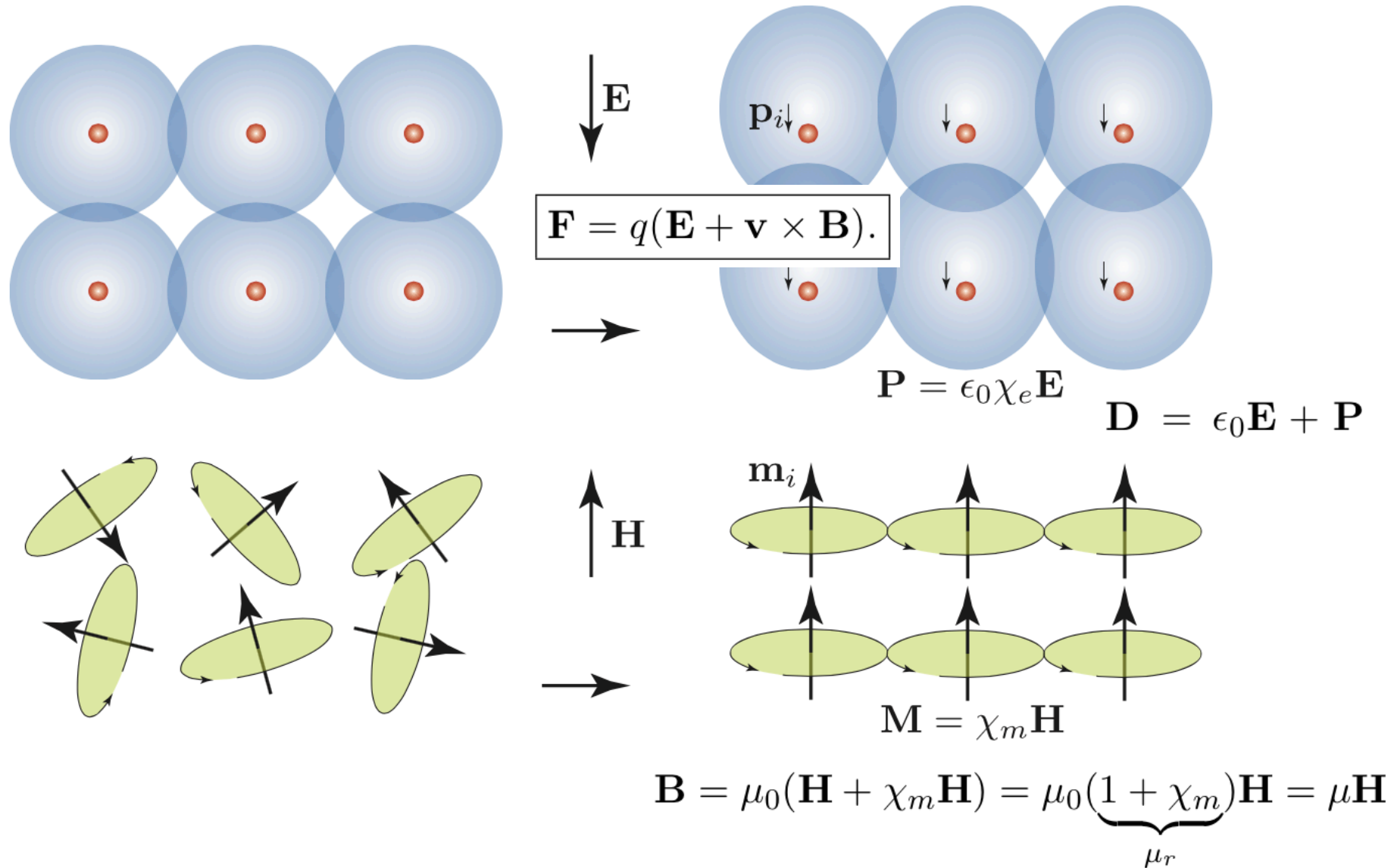
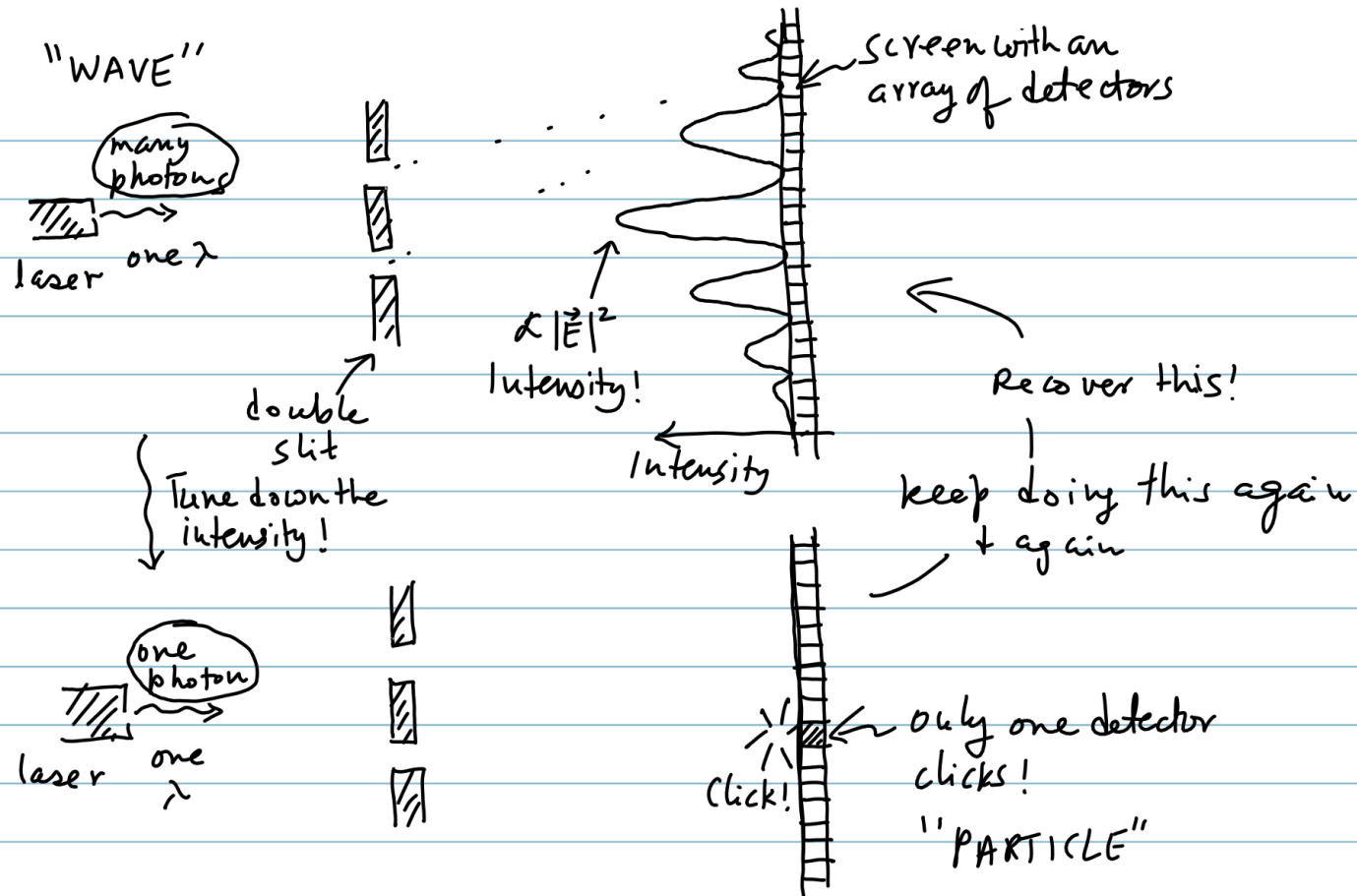
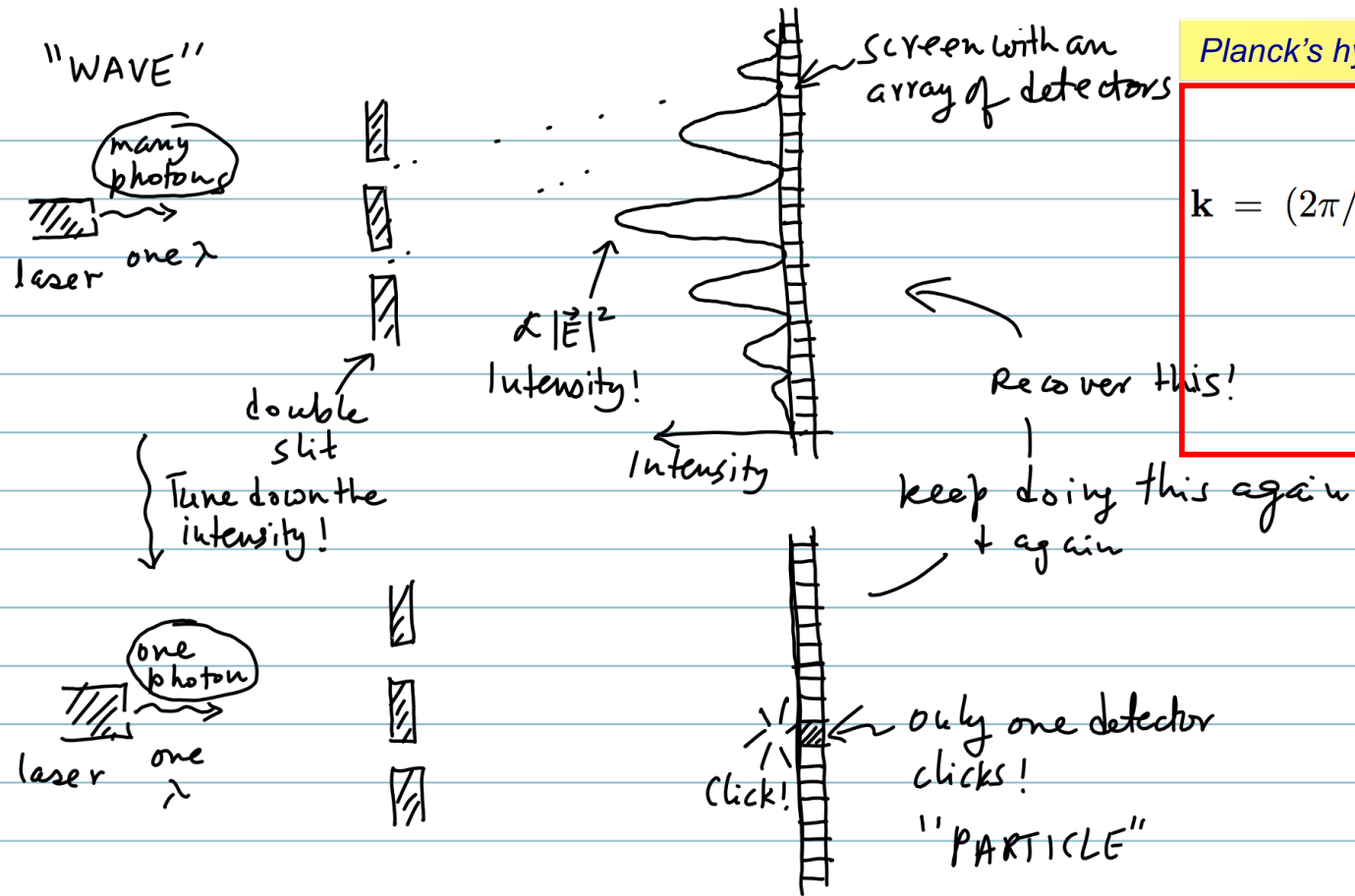


FIGURE 20.4: Dielectric and Magnetic materials. Orientation of electric and magnetic dipoles by external fields, leading to electric and magnetic susceptibilities.

Experiment: Light is a wave... or a particle?



Experiment: Light is a wave... or a particle?



Planck's hypothesis for photons to explain expts:

$$\mathbf{p} = \hbar \mathbf{k}$$

$$\mathbf{k} = (2\pi/\lambda)\hat{\mathbf{n}}, \hat{\mathbf{n}} \text{ the direction of propagation}$$

$$\omega = c|\mathbf{k}| \text{ with } c \text{ the speed of light}$$

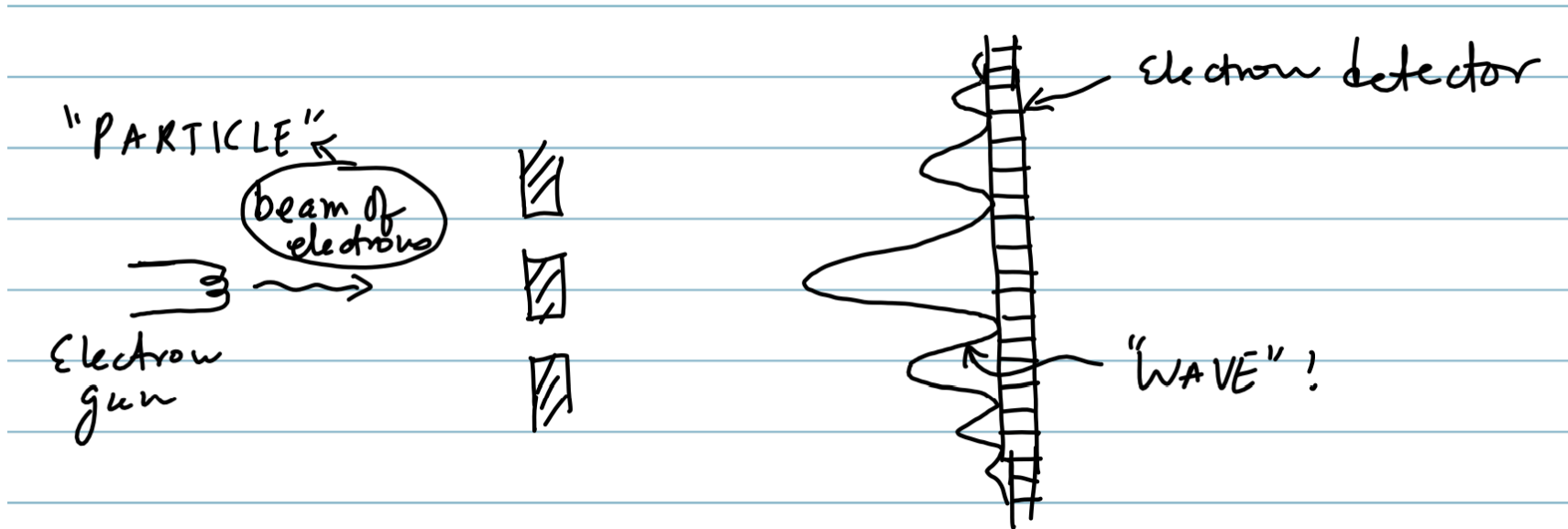
$$E = \hbar\omega$$

Einstein: look downstairs!

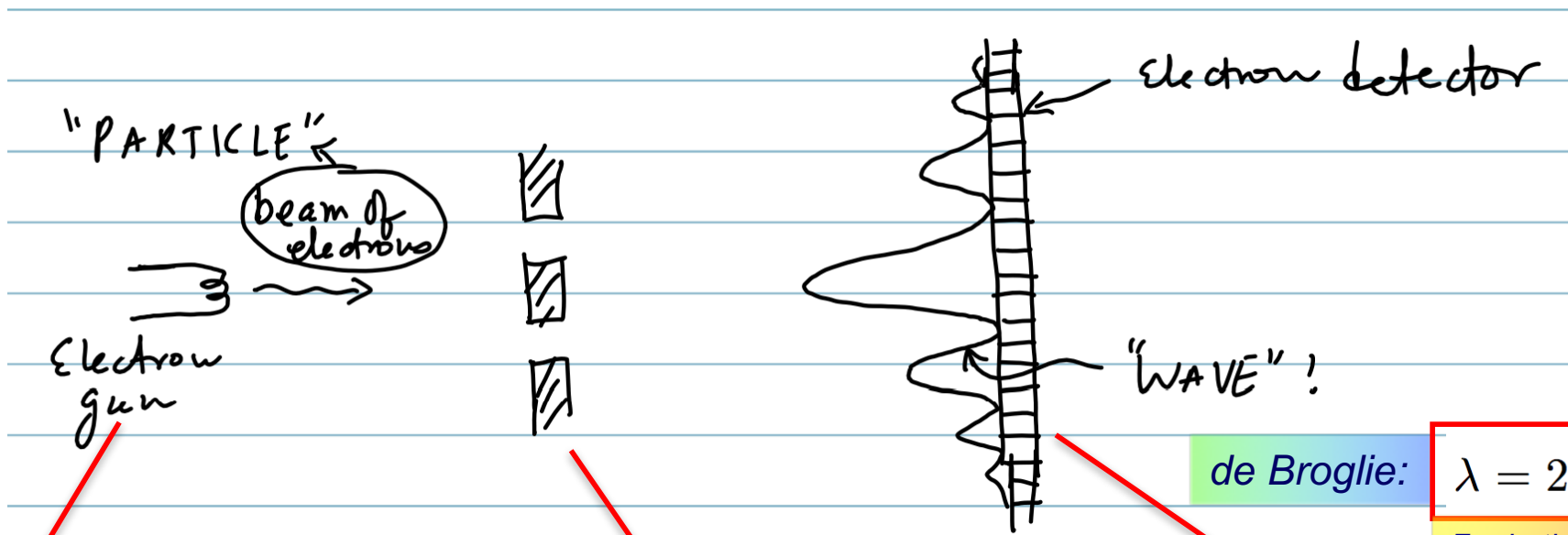
$$p = mv / \sqrt{1 - (v/c)^2}$$

- The only way an object of mass $m=0$ can have momentum is if its speed $v=c$, or the speed of light.
- A photon is exactly such an object. No mass, all energy, and a finite momentum!

An electron is a particle... or a wave?

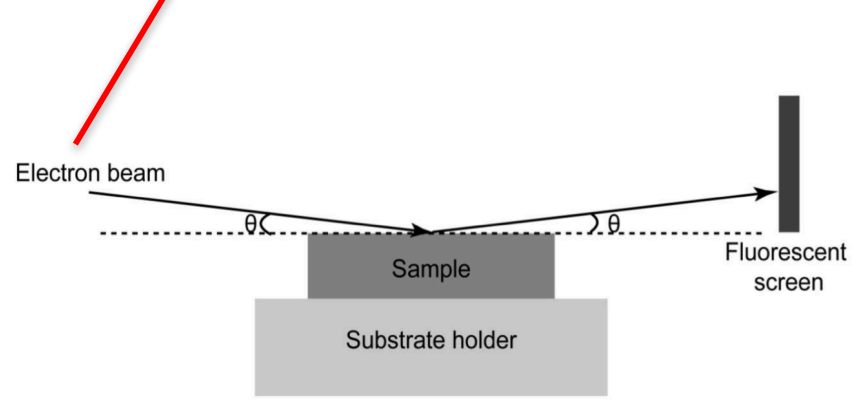


An electron is a particle... or a wave?

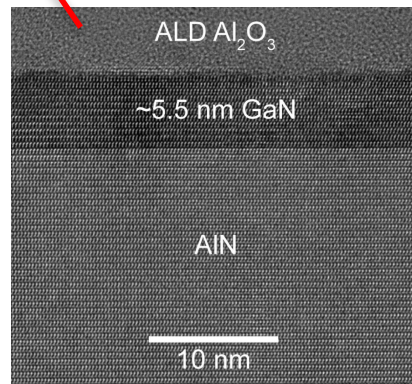


de Broglie: $\lambda = 2\pi\hbar/|p|$
 For both waves, and particles!

Guowang Li (Results from our lab!)



Electron beam incident on a crystal (RHEED)



Atomic structure of a crystal (grating!)

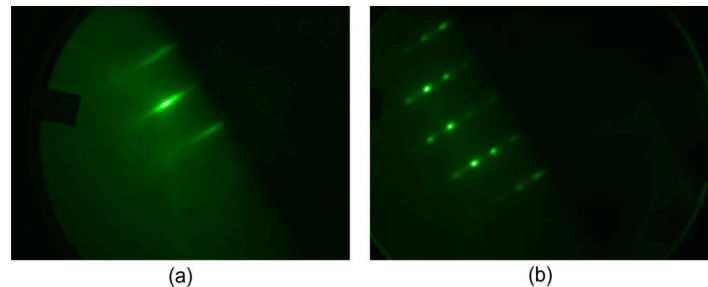
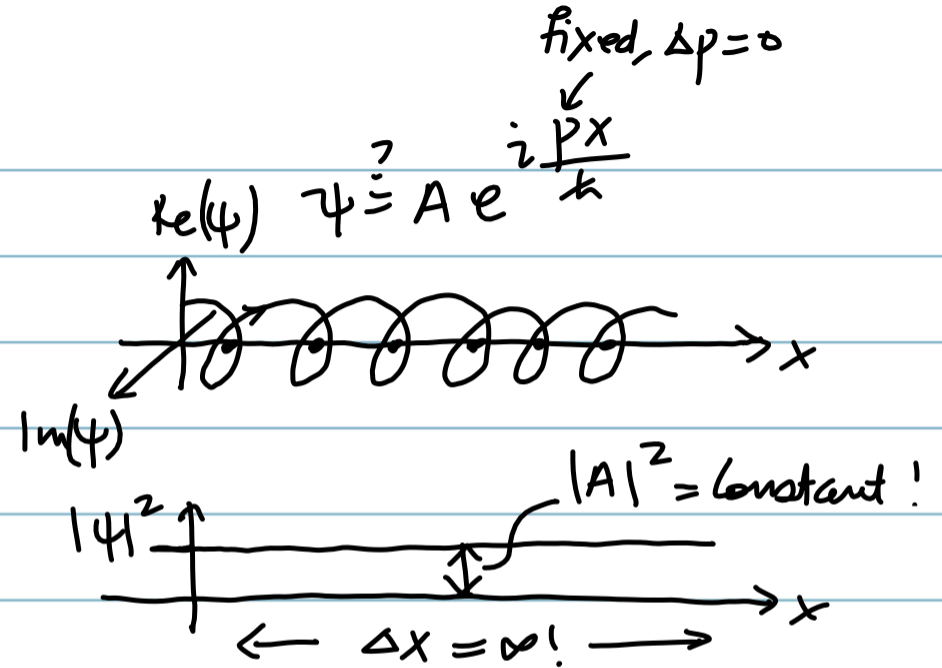
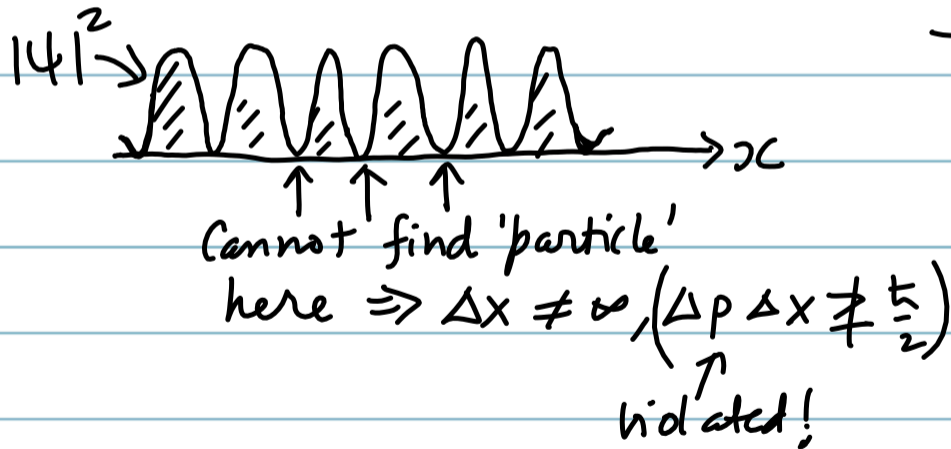
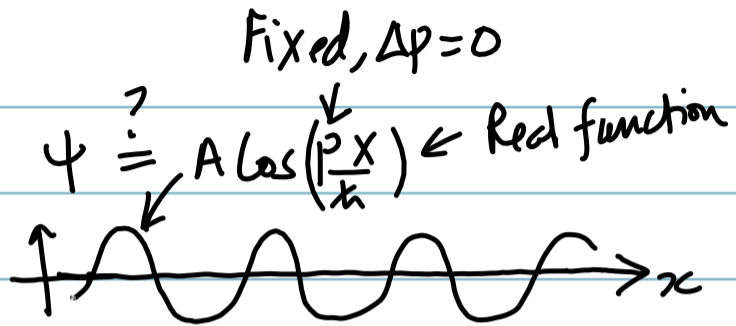


Figure 2.7: RHEED patterns of (a) smooth surface and (b) crystalline but rough of GaN surface.

Electron diffraction pattern on a screen

Wave and particle \rightarrow need for a wavefunction

Quantum states (electrons, photons) behave as waves AND particles. How do we describe them quantitatively?

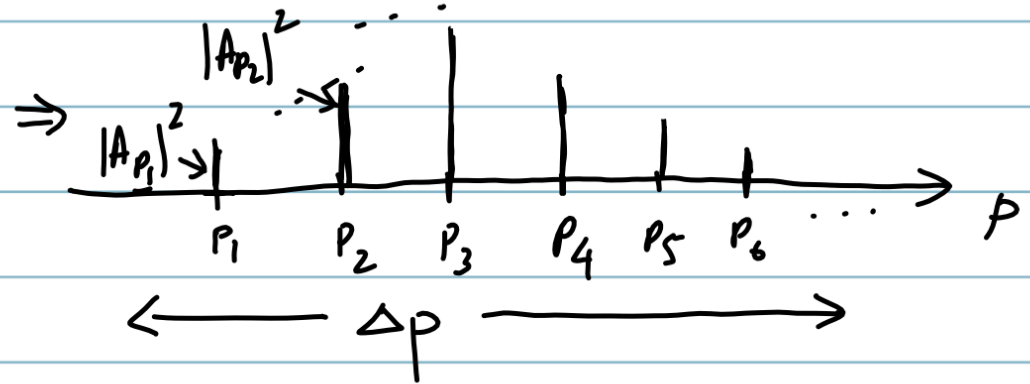
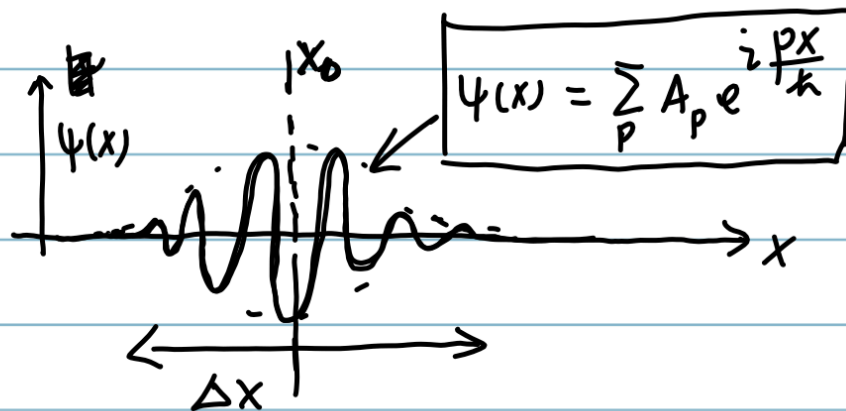


The complex exponential $e^{i \frac{p x}{\hbar}} = \psi$ oscillates with x , yet $|\psi|^2 = \text{constant!}$
 \Rightarrow good candidate for a wavefunction that respects $\Delta x \Delta p \geq \frac{\hbar}{2}$.

- The state of the free quantum particle cannot be represented by independent 'numbers' (x, p_x).
- We need a function whose amplitude oscillates in space, yet its magnitude never goes to zero.
- The complex exponential $e^{i k x}$ satisfies these requirements, and respects the uncertainty relation.

Constructing wavefunctions: superposition

By linear superposition of complex exponentials, we can create 'particle' like or 'wave' like states as desired for the problem.



$A_1 \left(e^{i \frac{p_1 x}{\hbar}} \right)$

λ_1

x

$A_2 \left(e^{i \frac{p_2 x}{\hbar}} \right)$

λ_2

x

$A_3 \left(e^{i \frac{p_3 x}{\hbar}} \right)$

λ_3

x

⋮

\Rightarrow $\psi(x) = \sum_p A_p e^{i \frac{p x}{\hbar}}$ is an allowed "wavefunction".

The best we can do to locate a "particle" \Rightarrow a 'wave packet'.

- Drawing on Fourier series, we realize that we can create any wavefunction shape to capture the correct physics of the problem. Note the corresponding reciprocal space weight distribution.

Math preliminaries before the physics...

$$\psi_p(x) = Ae^{ipx/\hbar}$$

Wavefunction ties x and p together.
Must respect the uncertainty principle.

$$\hat{p} = -i\hbar\partial/\partial x$$

Observables are mathematical operators.
They act on the wavefunction to extract info.

$$\hat{p}\psi_p(x) = (\hbar k)\psi_p(x)$$

The states of definite value of an operator are called the eigenstates of that operator.

$$x\hat{p} - \hat{p}x = [x, \hat{p}] = i\hbar.$$

Unlike classical mechanics, some operators fail to commute!



THE EXCHANGE RELATION⁸⁸
 $PQ - QP = h/2\pi i$

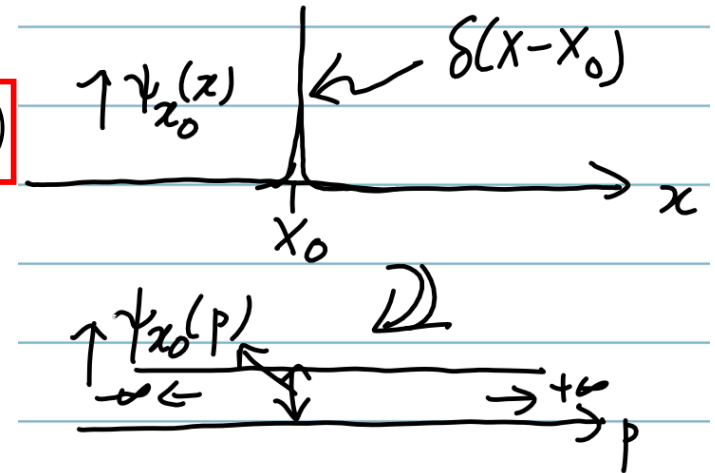
Non-commuting actions...

Ref: Gamow, *Thirty years that shook physics*.

Definite momentum, and definite location states

A state of definite location x_0 :
 Must be an eigenstate of operator x , with eigenvalue x_0 :

$$x\psi_{x_0}(x) = x_0\psi_{x_0}(x) \implies \psi_{x_0}(x) = \delta(x - x_0)$$

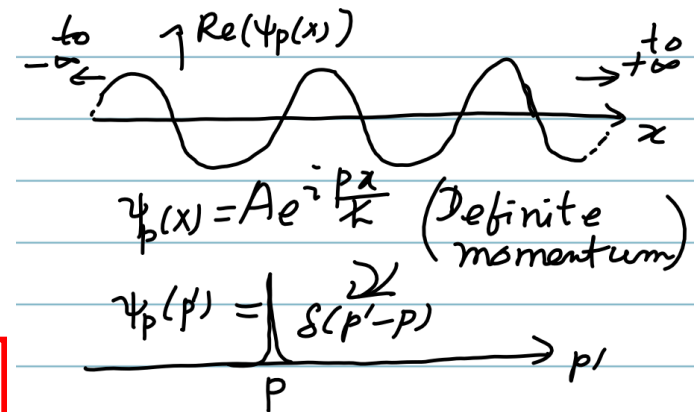


Definite in real space \rightarrow spread out in momentum

A state of definite momentum p :
 Must be an eigenstate of operator $-i\hbar(d/dx)$, with eigenvalue p :

$$\hat{p}_x\psi_p(x) = p_x\psi_p(x) \implies -i\hbar\frac{d}{dx}\psi_p(x) = p_x\psi_p(x)$$

$$\psi_p(x) = Ae^{i\frac{p_x x}{\hbar}} = Ae^{ik_x x}$$



Definite in momentum \rightarrow spread out in real space

States of definite location and definite momentum are unique in quantum mechanics.

States of definite energy: Schrodinger equation

States of definite energy are not unique, because they depend on the 'potential' $V(x)$

In classical mechanics, the energy of a particle is:

$$E_{cl} = \frac{p^2}{2m} + V(r)$$

In quantum mechanics, r & p cannot be simultaneously determined because $[x,p]=i\hbar$. Thus, we must solve an equation to obtain the energy.



Schrodinger

$$\left[-\frac{\hbar^2}{2m} \frac{\partial^2}{\partial x^2} + V(x) \right] \psi_E(x) = E \psi_E(x).$$

The Schrodinger equation gives us the prescription to find the states of definite energy.

$$\underbrace{\left[\frac{\hat{p}^2}{2m} + V(r) \right]}_{\hat{H}} |\psi\rangle = E |\psi\rangle$$

The Postulates of Quantum Mechanics

The five basic postulates of quantum mechanics are:

- (1) The state of any physical system at a given time t is completely represented by a state vector $|\Psi\rangle = |\Psi(\mathbf{r}, t)\rangle$.
- (2) For an observable quantity A there is an operator $\hat{\mathbf{A}}$. The eigenvalues of $\hat{\mathbf{A}}$ are the possible results of the measurements of A , that is, denoting the eigenvalues of $\hat{\mathbf{A}}$ by a ,

$$\hat{\mathbf{A}}|a\rangle = a|a\rangle, \quad (2.23)$$

and the probability of a measurement of A yielding the value a at time t is $|\langle a|\Psi(t)\rangle|^2$. The a 's, which are the results of possible measurements, must be real. This implies that $\hat{\mathbf{A}}$ must be a linear hermitian operator.

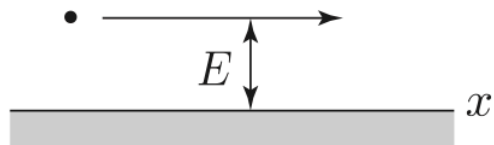
- (3) A measurement of $|\Psi\rangle$ that leads to an eigenvalue a_i leads the quantum mechanical system to *collapse* into the eigenstate $|\Psi_i\rangle$, which is the eigenstate corresponding to the eigenvalue a_i . So a measurement affects the state of the quantum system.
- (4) There exists a hermitian operator $\hat{\mathbf{H}}$ such that

$$i\hbar \frac{\partial |\Psi(\mathbf{r}, t)\rangle}{\partial t} = \hat{\mathbf{H}}|\Psi(\mathbf{r}, t)\rangle. \quad (2.24)$$

- (5) Two classical dynamical variables a, b , which are conjugate in the Hamiltonian sense, are represented by Schrodinger operators $\hat{\mathbf{A}}, \hat{\mathbf{B}}$, which obey

$$\hat{\mathbf{A}}_i \hat{\mathbf{B}}_j - \hat{\mathbf{B}}_j \hat{\mathbf{A}}_i = i\hbar \delta_{ij}. \quad (2.25)$$

The free electron



$$V(x) = 0$$

Free Electron

$$-\frac{\hbar^2}{2m_e} \frac{d^2}{dx^2} \psi(x) = E\psi(x)$$

$$\psi(x) = Ae^{ikx} + Be^{-ikx}$$

$$k = \sqrt{\frac{2m_e E}{\hbar^2}} = \frac{2\pi}{\lambda}$$

$$E = \frac{\hbar^2 k^2}{2m_e}$$

$$V(x) = 0$$

Allowed momenta are continuous

Energy spectrum is continuous

$$\hat{p}_x \psi(x) = -i\hbar \frac{d}{dx} \psi(x) = -i\hbar(ikAe^{ikx} - ikBe^{-ikx}) = \hbar k(Ae^{ikx} - Be^{-ikx}) \neq p\psi(x)$$

Not a momentum eigenstate

but... for $\psi_{\rightarrow}(x) = Ae^{ikx}$,

$$\hat{p}_x \psi_{\rightarrow}(x) = -i\hbar \frac{d}{dx} \psi_{\rightarrow}(x) = -i\hbar(ikAe^{ikx}) = \hbar k \psi_{\rightarrow}(x) = p\psi_{\rightarrow}(x) \text{ momentum eigenstate}$$

Restrict particle in space \rightarrow Quantization

If we restrict the 'particle' in one space, it quantizes the allowed 'vectors' in the reciprocal space.

$$\psi_p(x + L) = \psi_p(x)$$



$$e^{ikL} = 1 = e^{i2\pi n}, \text{ and } k_n = n \times (2\pi/L). \text{ Here } n = 0, \pm 1, \pm 2, \dots$$

Particle on a 'RING'



$$\psi_n(x) = \frac{1}{\sqrt{L}} e^{ik_n x}$$

$$k_n = \frac{2\pi}{L} \cdot n \quad n = 0, \pm 1, \pm 2, \dots$$

Call this 'state vector' $|n\rangle$.

The state functions form a 'set'

$$\{ \dots \psi_{-3}(x), \psi_{-2}(x), \psi_{-1}(x), \psi_0(x), \psi_1(x), \psi_2(x), \dots \}$$

Note: $\int_0^L \psi_n^*(x) \psi_m(x) dx = \delta_{nm} \Rightarrow$ functions are ORTHOGONAL!

$$\langle n | m \rangle = \delta_{nm} \Leftarrow \text{Vectors are "perpendicular"}$$

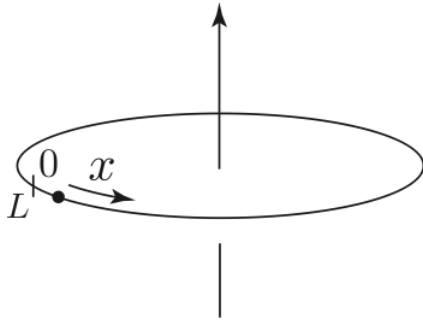
The set of wave functions $[\dots \psi_{-2}(x), \psi_{-1}(x), \psi_0(x), \psi_1(x), \psi_2(x), \dots] = [\psi_n(x)]$ are special. We note that $\int_0^L dx \psi_m^*(x) \psi_n(x) = \delta_{nm}$, i.e., the functions are orthogonal. Any general wavefunction representing the particle $\psi(x)$ can be expressed as a linear combination of this set. This is the principle of superposition, and a basic mathematical result from Fourier theory. Thus the quantum mechanical state of a particle may be represented as $\psi(x) = \sum_n A_n \psi_n(x)$. Clearly, $A_n = \int dx \psi_n^*(x) \psi(x)$. Every wavefunction constructed in this fashion represents a permitted state of the particle, as long as $\sum_n |A_n|^2 = 1$.

- The set of states $\{\dots |-1\rangle, |0\rangle, |+1\rangle, \dots\}$ is an orthogonal basis for constructing the wavefunction.
- One can draw an analogy to vector spaces, and use the tools of linear algebra on states.

The particle on a ring

3.4 Not so free: particle in a ring

$$\psi(x + L) = \psi(x) \rightarrow e^{ik(x+L)} = e^{ikx} \rightarrow e^{ikL} = 1 \rightarrow kL = 2n\pi$$



Particle on a ring

Momentum is quantized

$$k_n = \frac{2\pi}{L}n, n = 0, \pm 1, \pm 2, \dots$$

$$\psi(n, x) = Ae^{ik_n x}.$$

$$\int_0^L dx |\psi(n, x)|^2 = 1 \rightarrow |A|^2 \times L = 1 \rightarrow A = \frac{1}{\sqrt{L}} \rightarrow \psi(n, x) = \frac{1}{\sqrt{L}} e^{ik_n x}$$

Note that $n = 0$ is *allowed* as a result of the periodic boundary condition.

Energy spectrum is discrete,
Zero energy is allowed

$$E_n = \frac{\hbar^2 k_n^2}{2m_e} = n^2 \frac{(2\pi\hbar)^2}{2m_e L^2} = n^2 \frac{h^2}{2m_e L^2}$$

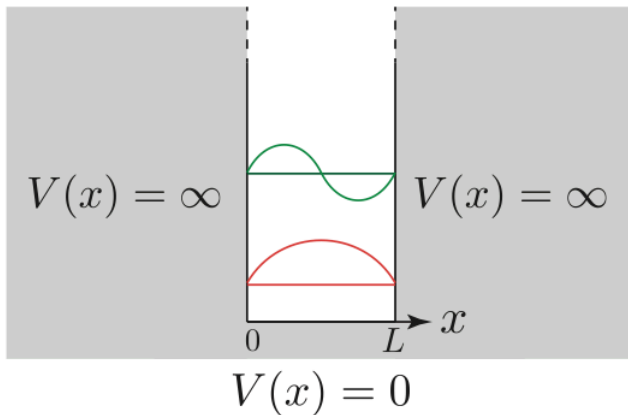
Angular momentum is quantized

$$L = p \times r = \hbar k_n \times \frac{L}{2\pi} = \frac{2\pi\hbar}{L} n \times \frac{L}{2\pi} = n\hbar$$

The particle in a box

$$V(x) = 0, \quad 0 \leq x \leq L$$

$$V(x) = \infty, \quad x < 0, x > L$$



Particle in a box

The major change is that $\psi(x) = 0$ in regions where $V(x) = \infty$.

$$\psi(x) = Ae^{ikx} + Be^{-ikx} \rightarrow \psi(0) = 0 = A + B, \psi(L) = Ae^{ikL} + Be^{-ikL} = 0$$

$$\frac{A}{B} = -e^{-i2kL} = -1 \rightarrow 2kL = 2n\pi \rightarrow k_n = n\frac{\pi}{L}, n = \pm 1, \pm 2, \pm 3, \dots$$

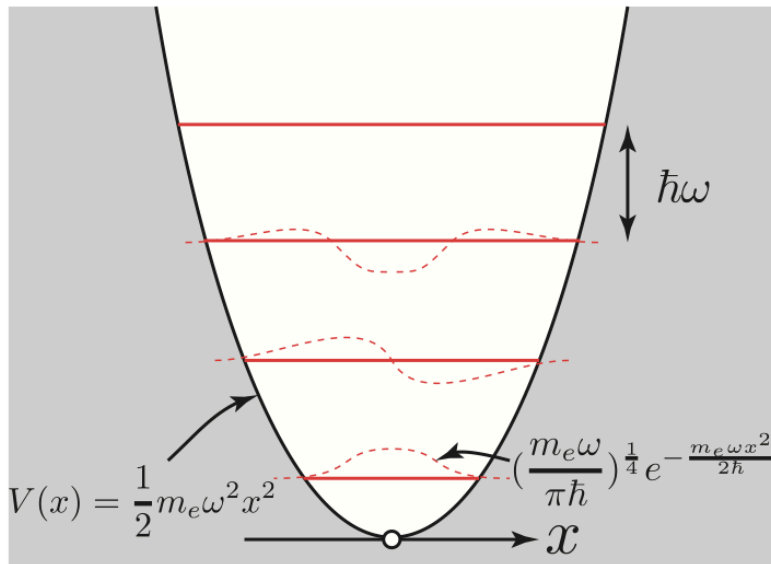
Note that $n = 0$ is *not allowed*, because then $\psi(x) = 0$ and there is no particle wavefunction after normalization over the length L is

$$\psi(n, x) = \sqrt{\frac{2}{L}} \sin\left(n\frac{\pi}{L}x\right) = \sqrt{\frac{2}{L}} \sin(k_n x)$$

Energy spectrum is discrete,
zero energy NOT allowed!

$$E_n = n^2 \frac{(\pi\hbar)^2}{2m_e L^2} = n^2 \frac{h^2}{8m_e L^2}$$

The harmonic oscillator



$$V(x) = \frac{1}{2} m_e \omega^2 x^2$$

Harmonic Oscillator

$$\psi_n(x) = \frac{1}{\sqrt{2^n n!}} \cdot \left(\frac{m\omega}{\pi\hbar}\right)^{1/4} \cdot e^{-\frac{m\omega x^2}{2\hbar}} \cdot H_n\left(\sqrt{\frac{m\omega}{\hbar}}x\right),$$

$n = 0, 1, 2, \dots$

The functions H_n are the **Hermite polynomials**,

$$H_n(x) = (-1)^n e^{x^2} \frac{d^n}{dx^n} (e^{-x^2}).$$

The corresponding energy levels are

$$E_n = \hbar\omega \left(n + \frac{1}{2}\right).$$

*Energy levels equally spaced
Zero energy NOT allowed!*

$$a = \sqrt{\frac{m\omega}{2\hbar}} \left(\hat{x} + \frac{i}{m\omega} \hat{p}\right)$$

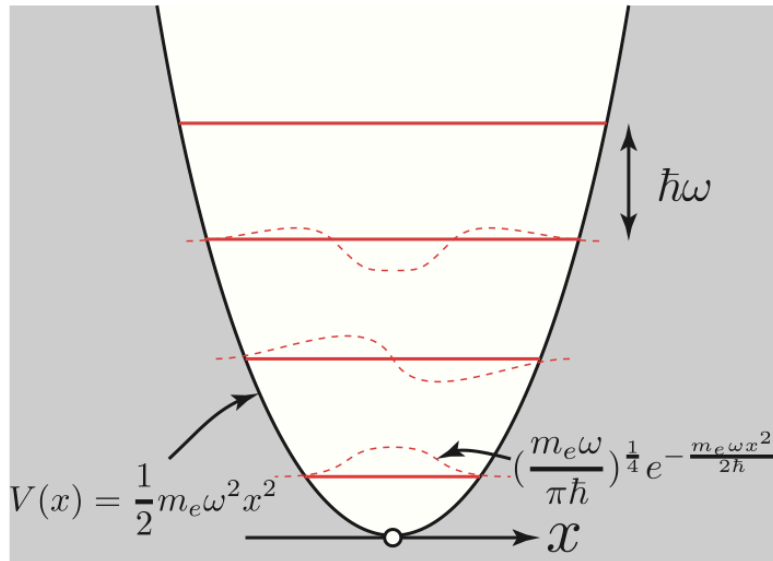
$$a^\dagger = \sqrt{\frac{m\omega}{2\hbar}} \left(\hat{x} - \frac{i}{m\omega} \hat{p}\right)$$

$$\hat{x} = \sqrt{\frac{\hbar}{2m\omega}} (a^\dagger + a)$$

$$\hat{p} = i\sqrt{\frac{m\omega\hbar}{2}} (a^\dagger - a)$$

Can solve the problem using raising and lowering operators

The harmonic oscillator



$$V(x) = \frac{1}{2} m_e \omega^2 x^2$$

$$E_n = \left(n + \frac{1}{2}\right) \hbar \omega$$

$$a = \sqrt{\frac{m\omega}{2\hbar}} \left(\hat{x} + \frac{i}{m\omega} \hat{p}\right)$$

$$a^\dagger = \sqrt{\frac{m\omega}{2\hbar}} \left(\hat{x} - \frac{i}{m\omega} \hat{p}\right)$$

$$\hat{n} = a^\dagger a$$

$$\hat{x} = \sqrt{\frac{\hbar}{2m\omega}} (a^\dagger + a)$$

$$\hat{p} = i \sqrt{\frac{m\omega\hbar}{2}} (a^\dagger - a)$$

$$[a, a^\dagger] = 1$$

Annihilation operator

$$a|n\rangle = \sqrt{n}|n-1\rangle$$

Creation operator

$$a^\dagger|n\rangle = \sqrt{n+1}|n+1\rangle$$

$$\hat{H} = \hbar \omega \left(a^\dagger a + \frac{1}{2}\right)$$

The creation/annihilation operator formalism will be key in the 'second quantization' methods to be developed later in the course!

The hydrogen atom

Energy levels [\[edit source | edit beta \]](#)

The energy levels of hydrogen, including [fine structure](#), are given by the Sommerfeld expression:

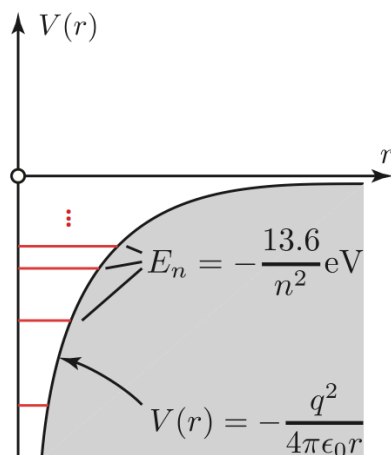
$$E_{jn} = -m_e c^2 \left[\left(1 + \left[\frac{\alpha}{n - j - \frac{1}{2} + \sqrt{(j + \frac{1}{2})^2 - \alpha^2}} \right]^2 \right)^{-1/2} - 1 \right]$$

$$\approx -\frac{m_e c^2 \alpha^2}{2n^2} \left[1 + \frac{\alpha^2}{n^2} \left(\frac{n}{j + \frac{1}{2}} - \frac{3}{4} \right) \right],$$

where α is the [fine-structure constant](#) and j is the "total angular momentum" [quantum number](#), which is equal to $|\ell \pm 1/2|$ depending on the direction of the electron spin. The factor in square brackets in the last expression is nearly one; the extra term arises from relativistic effects (for details, see [#Features going beyond the Schrödinger solution](#)).

The value

$$\frac{m_e c^2 \alpha^2}{2} = \frac{0.51 \text{ MeV}}{2 \cdot 137^2} = 13.6 \text{ eV}$$



Hydrogen Atom

Wavefunction [\[edit source | edit beta \]](#)

The normalized position [wavefunctions](#), given in [spherical coordinates](#) are:

$$\psi_{n\ell m}(r, \vartheta, \varphi) = \sqrt{\left(\frac{2}{na_0}\right)^3 \frac{(n-\ell-1)!}{2n(n+\ell)!}} e^{-\rho/2} \rho^\ell L_{n-\ell-1}^{2\ell+1}(\rho) Y_\ell^m(\vartheta, \varphi)$$

where:

$$\rho = \frac{2r}{na_0},$$

a_0 is the [Bohr radius](#),

$L_{n-\ell-1}^{2\ell+1}(\rho)$ is a [generalized Laguerre polynomial](#) of degree $n - \ell - 1$, and

$Y_\ell^m(\vartheta, \varphi)$ is a [spherical harmonic](#) function of degree ℓ and order m . Note that the [generalized Laguerre polynomials](#) are defined differently by different authors. The usage here is consistent with the definitions used by Messiah,^[8] and Mathematica.^[9] In other places, the Laguerre polynomial includes a factor of $(n + \ell)!$,^[10] or the generalized Laguerre polynomial appearing in the hydrogen wave function is $L_{n+\ell}^{2\ell+1}(\rho)$ instead.^[11]

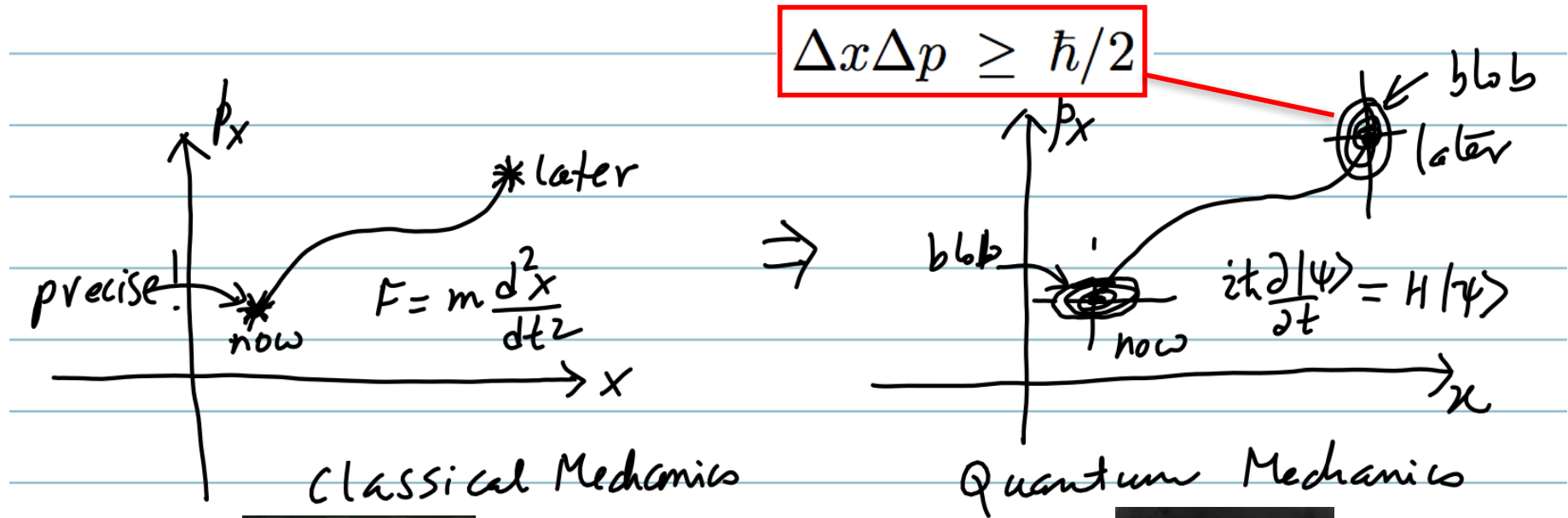
The quantum numbers can take the following values:

$$n = 1, 2, 3, \dots$$

$$\ell = 0, 1, 2, \dots, n - 1$$

$$m = -\ell, \dots, \ell.$$

Time-evolution of states: Time-dep. Schr. Eqn.



Newton



Schrodinger

$$\mathbf{F} = -\nabla V(\mathbf{r}) = \frac{d\mathbf{p}}{dt}$$

Path is deterministic

$$i\hbar \frac{\partial |\psi\rangle}{\partial t} = \left[\frac{\hat{\mathbf{p}}^2}{2m} + V(\mathbf{r}, t) \right] |\psi\rangle$$

Path respects uncertainty relation

States of definite energy are stationary states

$$i\hbar \frac{\partial \Psi(x, t)}{\partial t} = \underbrace{\left[-\frac{\hbar^2}{2m} \frac{\partial^2}{\partial x^2} + V(x) \right]}_{\hat{H}} \Psi(x, t).$$

$$\Psi(x, t) = \chi(t)\psi(x)$$

Try set of solutions that allow the separation of x and t .

$$i\hbar \frac{\dot{\chi}(t)}{\chi(t)} = \frac{\hat{H}\psi(x)}{\psi(x)} = E.$$

$$\Psi_E(x, t) = \psi_E(x) e^{-i\frac{E}{\hbar}t}$$

This means that the **amplitude** of states of definite energy oscillate with time with frequency E/\hbar

$$|\Psi_E(x, t)|^2 = |\psi_E(x)|^2$$

But observables relate to the probability, which is time independent \rightarrow this is why they are called **stationary states**.

$$\frac{d\langle \hat{A} \rangle}{dt} = -\frac{i}{\hbar} \langle [\hat{A}, \hat{H}] \rangle$$

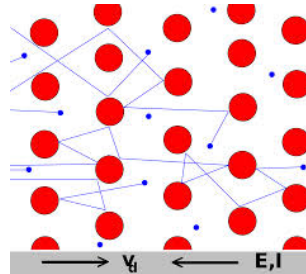
Ehrenfest's theorem for the time evolution of an operator.

- The energy eigenvalues of the time-independent Schrodinger equation are states of definite energy.
- Their probability density does not change with time \rightarrow they are called stationary states.
- This is analogous to the 1st law of classical mechanics: quantum states of definite energy will continue to remain in those states unless perturbed by a potential.

The classical Drude model



Paul Drude
(1900)



Electrons move and scatter every tau seconds

dc field:

$$m \frac{dv}{dt} = qE - \frac{mv}{\tau} \quad \text{steady state: } \frac{d}{dt}(\dots) \rightarrow 0 \quad v = \frac{q\tau}{m} E = \mu E$$

$$J = qnv = \frac{nq^2\tau}{m} E = \sigma E \implies \sigma_0 = \frac{nq^2\tau}{m}$$

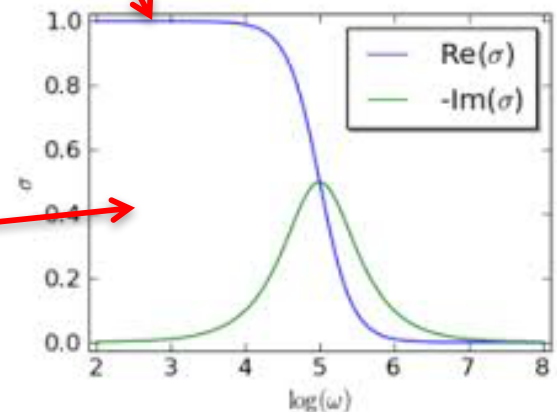
dc conductivity

Oscillating field:

$$E(t) = Ee^{i\omega t} \quad m \frac{dv}{dt} = qEe^{i\omega t} - \frac{mv}{\tau} \quad v(t) = v(0)e^{i\omega t}$$

$$\sigma(\omega) = \frac{\sigma_0}{1 + i\omega\tau} = \underbrace{\frac{\sigma_0}{1 + (\omega\tau)^2}}_{\text{Re}(\sigma(\omega))} - i \underbrace{\frac{\omega\tau\sigma_0}{1 + (\omega\tau)^2}}_{\text{Im}(\sigma(\omega))}$$

ac conductivity



Quantum mechanical current

$$|\Psi(x, t)|^2 = \Psi^* \Psi$$

Probability density in space and time

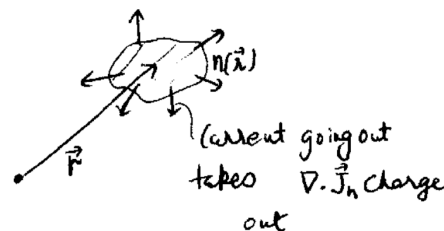
$$\frac{\partial |\Psi(x, t)|^2}{\partial t} = \Psi^* \frac{\partial \Psi}{\partial t} + \frac{\partial \Psi^*}{\partial t} \Psi$$

Change in probability density with time

$$\frac{\partial |\Psi(x, t)|^2}{\partial t} = \Psi^* \frac{(\hat{p}^2/2m + V)\Psi}{i\hbar} + \Psi \frac{(\hat{p}^2/2m + V)\Psi^*}{-i\hbar}$$

Use time-dependent Schrodinger equation

$$\frac{\partial |\Psi(x, t)|^2}{\partial t} = \frac{1}{2mi\hbar} (\Psi^* \hat{p}^2 \Psi - \Psi \hat{p}^2 \Psi^*)$$



Since $\hat{p} = -i\hbar \nabla_{\mathbf{r}}$

$$\frac{\partial |\Psi(x, t)|^2}{\partial t} = -\nabla_{\mathbf{r}} \cdot \left[\frac{1}{2m} (\Psi^* \hat{p} \Psi - \Psi \hat{p} \Psi^*) \right]$$

In the form of a continuity equation \rightarrow read off the current density!

Continuity equation

$$\partial \rho / \partial t = -\nabla_{\mathbf{r}} \cdot \mathbf{j}$$

$$\mathbf{j} = \frac{1}{2m} (\Psi^* \hat{p} \Psi - \Psi \hat{p} \Psi^*)$$

Quantum mechanical probability current density

$$\frac{d}{dt} \left(\int_{space} d^3r |\Psi|^2 \right) = - \int_{space} d^3r \nabla \cdot \mathbf{j} = - \oint \mathbf{j} \cdot d\mathbf{S} = 0$$

Satisfies the conservation of number of particles

Electric current of quantum states

$$\mathbf{J} = \frac{q}{2m_e} (\Psi^* \hat{\mathbf{p}} \Psi - \Psi \hat{\mathbf{p}} \Psi^*)$$

For most semiconductors we know the bandstructure, but not the Bloch functions. Go through the derivation to recast the current in terms of the bandstructure, or the group-velocity (see notes).

$$\mathbf{v}_g(\mathbf{k}) = \nabla_{\mathbf{k}} E(\mathbf{k}) / \hbar$$

$$\mathbf{J}_d = \frac{q}{L^d} \sum_{\mathbf{k}} \mathbf{v}_g(\mathbf{k}) f(\mathbf{k})$$

• Group velocity of electron in state $|\mathbf{k}\rangle$

VERY useful result: current in d -dimensions!

$$\mathbf{J}_d = \frac{q g_s g_v}{L^d} \sum_{\mathbf{k}} \mathbf{v}_g(\mathbf{k}) T(\mathbf{k}) [f_L(\mathbf{k}) - f_R(\mathbf{k})]$$

General expression for charge current density in d -dimensions

$$\mathbf{J}_d = \frac{q g_s g_v}{(2\pi)^d} \int d^d \mathbf{k} \times \mathbf{v}_g(\mathbf{k}) T(\mathbf{k}) [f_L(\mathbf{k}) - f_R(\mathbf{k})]$$

Quantum states are vectors in the Hilbert space

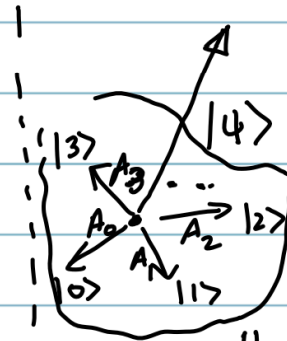
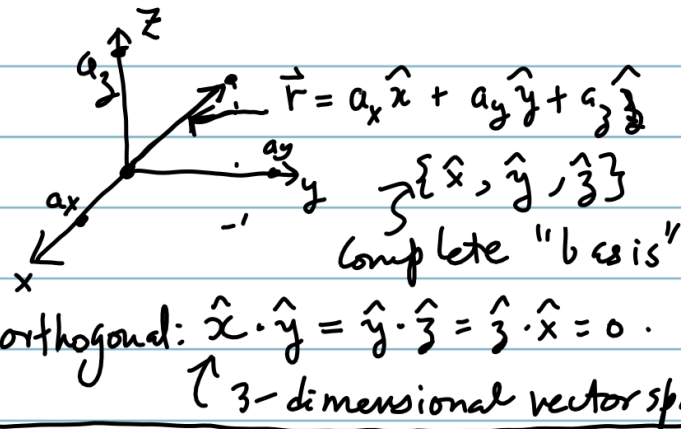
Any wavefunction

$$\psi(x) = \sum_n A_n \psi_n(x)$$

is an allowed state.

vector picture \Rightarrow

$$|\psi\rangle = \sum_n A_n |n\rangle$$



$$|\psi\rangle = \sum_n A_n |n\rangle$$

complete "basis"

$\{\dots, | -2\rangle, | -1\rangle, | 0\rangle, | 1\rangle, | 2\rangle, \dots\}$

$|\psi\rangle$ is an abstract "State Vector".
 - it lives in the Hilbert Space.

$\{\dots, |n-1\rangle, |n\rangle, |n+1\rangle, \dots\}$
 is an ∞ -dimensional vector space,
 or a **Hilbert Space!**

It is useful here to draw an analogy to the decomposition of a vector into specific coordinates. The 'hybrid' state function $\psi(x)$ is pictured as a vector $|\psi\rangle$ in an abstract space. The definite momentum wavefunctions $\psi_n(x)$ are pictured as the 'coordinate' vectors $|n\rangle$ in that space of vectors. This set of vectors is called the basis. Since there are an infinite set of integers $n = 0, \pm 1, \pm 2, \dots$, the vector space is infinite dimensional. It is called the Hilbert space. One may then consider the coefficients A_n as the length of the projections of the state on the basis states. The abstract picture allows great economy of expression by writing $|\psi\rangle = \sum_n A_n |n\rangle$. The orthogonality of the basis states

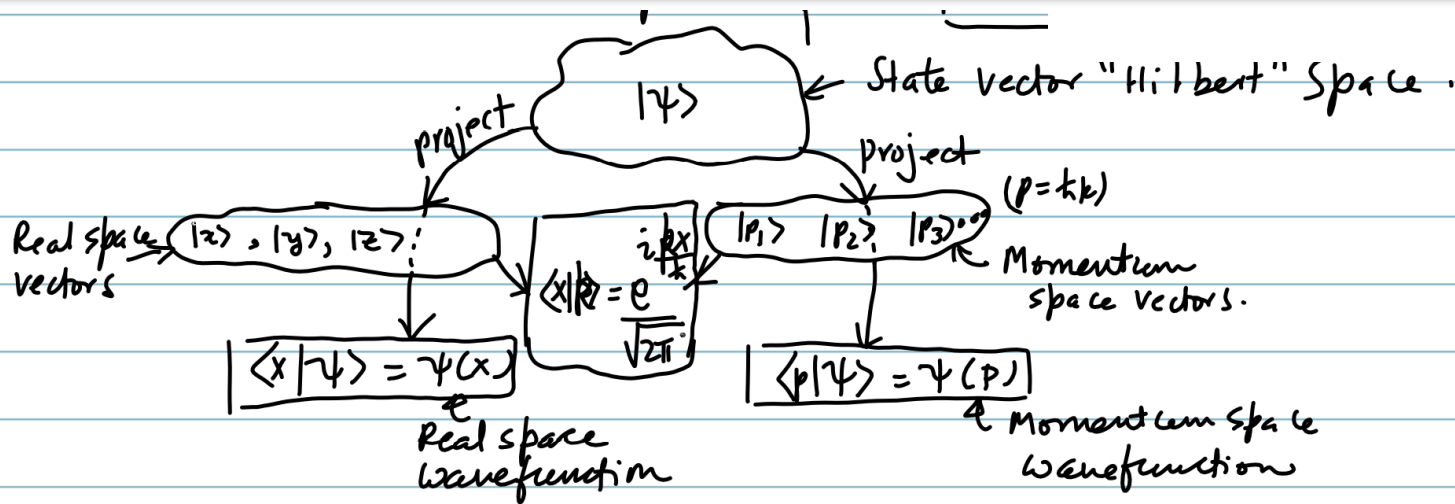
$$|\psi\rangle = \sum_n A_n |n\rangle \quad \langle m|n\rangle = \delta_{mn}$$

$$A_n = \langle n|\psi\rangle$$

$$|\psi\rangle = \sum_n \langle n|\psi\rangle |n\rangle = \sum_n |n\rangle \langle n|\psi\rangle$$

$$\sum_n |n\rangle \langle n| = 1$$

By projecting states, get various representations



$$|\psi\rangle = \sum_n A_n |n\rangle \Rightarrow A_n = \langle n|\psi\rangle$$

↑
a number

$$\Rightarrow |\psi\rangle = \sum_n \langle n|\psi\rangle |n\rangle = \left[\sum_n |n\rangle \langle n|\psi\rangle \right] \text{ Same as LHS!}$$

$$\Rightarrow \boxed{\sum_n |n\rangle \langle n| = 1} \quad \text{Similarly, } \boxed{\int d^3x |x\rangle \langle x| = 1}$$

"outer product"

$$\langle x|\psi\rangle = \psi(x)$$

$$\langle k|\psi\rangle = \psi(k)$$

$$\langle x|k_x\rangle = \frac{e^{ik_x x}}{\sqrt{2\pi}}$$

$$\langle \psi_2|\psi_1\rangle = \int_{-\infty}^{\infty} dx \langle \psi_2|x\rangle \langle x|\psi_1\rangle = \int_{-\infty}^{\infty} dx \psi_2^*(x) \psi_1(x)$$

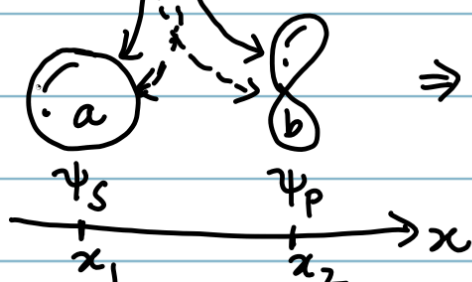
- We can think of the states as vectors.
- The 'inner product' is a complex number generated by projection to the appropriate space.
- This number is the wavefunction – it can be found in real space, momentum space, etc...

Identity crisis: Indistinguishable particles

2 particles: total energy = $E_1 + E_2 \Rightarrow$ time evolution $\sim e^{i \frac{(E_1 + E_2)t}{\hbar}}$

Since $i\hbar \frac{\partial}{\partial t} \psi = E \psi$, $\psi \sim \psi_1 \cdot \psi_2$

indistinguishable! $\psi_1 \sim e^{-i \frac{E_1}{\hbar} t}$ (2 electrons)
 distinguishable! $\psi_2 \sim e^{-i \frac{E_2}{\hbar} t}$ (electron & proton)



$\Rightarrow \psi(x_1, x_2) = \psi_a(x_1) \psi_b(x_2)$

OK for distinguishable
 but WRONG for indistinguishable!

indistinguishable $\Rightarrow x_1 \leftrightarrow x_2$ should NOT change the observables!

$$\psi(x_1, x_2) = \psi_a(x_1) \psi_b(x_2)$$

This is OK for distinguishable particles such as a proton and an electron. But NOT OK for **indistinguishable particles** such as two electrons! For example, $|\psi|^2$ should not change on swapping $x_1 \leftrightarrow x_2$. How must we then write the wavefunction for two identical particles?

Resolution of identity crisis: Bosons & Fermions

This is necessary for indistinguishable particles.

$$P(x_2, x_1) = P(x_1, x_2) \rightarrow |\psi(x_2, x_1)|^2 = |\psi(x_1, x_2)|^2.$$

$$\psi(x_1, x_2) = \psi_a(x_1)\psi_b(x_2)$$

$$\psi(x_1, x_2) = \psi_a(x_1)\psi_b(x_2) \boxed{+} \psi_a(x_2)\psi_b(x_1)$$

$$\psi(x_2, x_1) = \boxed{+} \psi(x_1, x_2)$$

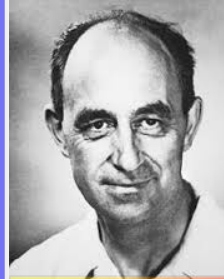
$$\psi(x_1, x_1) = +\psi(x_1, x_1)$$

$$f_{BE}(E) = \frac{1}{e^{\frac{E-\mu}{kT}} \boxed{-} 1}$$

The Bose-Einstein distribution!
Particles are called **Bosons**.
Examples: Photons, Phonons



Bose



Fermi

$$\psi(x_1, x_2) = \psi_a(x_1)\psi_b(x_2) \boxed{-} \psi_a(x_2)\psi_b(x_1)$$

$$\psi(x_2, x_1) = \boxed{-} \psi(x_1, x_2),$$

$$\psi(x_1, x_1) = -\psi(x_1, x_1) \rightarrow \psi(x_1, x_1) = 0.$$

The Pauli exclusion principle!

$$f_{FD}(E) = \frac{1}{1 \boxed{+} e^{\frac{E-E_F}{kT}}}$$

The Fermi-Dirac distribution!
Particles are called **Fermions**.
Examples: Electrons, Protons

- Note: Why not $\psi(x_2, x_1) = e^{i\phi}\psi(x_1, x_2)$? Majorana particles \rightarrow later...

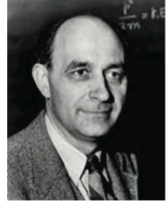
Quantum Statistical Mechanics in 1 slide



Boltzmann



Maxwell

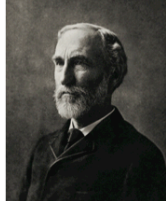


Fermi



Dirac

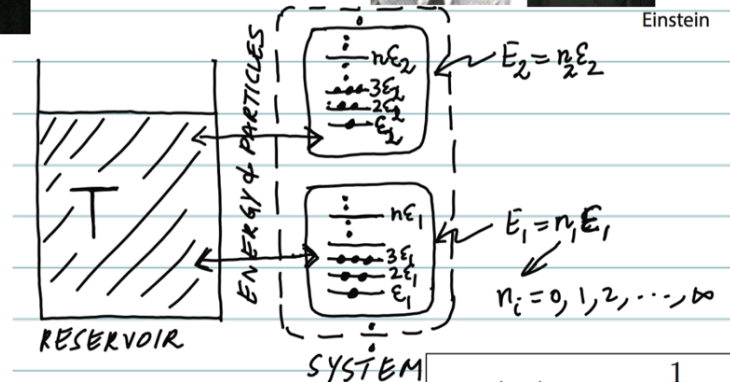
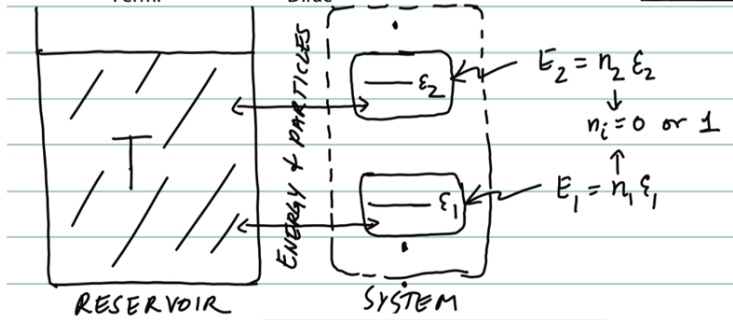
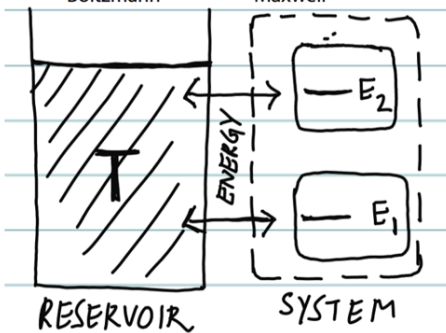
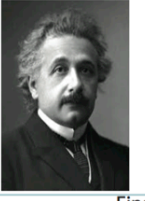
Gibbs



Bose



Einstein



$$\frac{P(E_1)}{P(E_2)} = \frac{e^{-\beta E_1}}{e^{-\beta E_2}}$$

Boltzmann

$$f_{FD}(E_i) = \frac{1}{1 + e^{\beta(\epsilon_i - \mu)}}$$

$$\frac{P(E_1)}{P(E_2)} = \frac{e^{-\beta(E_1 - n_1\mu)}}{e^{-\beta(E_2 - n_2\mu)}} \stackrel{\text{non-interacting}}{=} \frac{e^{n_1\beta(\mu - \epsilon_1)}}{e^{n_2\beta(\mu - \epsilon_2)}}$$

Fundamental law of quantum statistical mechanics

$$P(E_i) = \frac{e^{\beta(n_i\mu - E_i)}}{Z} = \frac{e^{\beta n_i(\mu - \epsilon_i)}}{Z} = \frac{e^{\beta n_i(\mu - \epsilon_i)}}{\sum_{n_i=0}^{n_i=n_{max}} e^{\beta n_i(\mu - \epsilon_i)}}$$

$$f_{BE}(E_i) = \frac{1}{e^{\beta(\epsilon_i - \mu)} - 1}$$

$$\langle n_i \rangle = f(\epsilon_i) = \frac{0 \cdot e^0 + 1 \cdot e^{\beta(1 \cdot \mu - 1 \cdot \epsilon_i)}}{1 + e^{\beta(\mu - \epsilon_i)}}$$

$$f_{FD}(\epsilon_i) = \frac{1}{1 + e^{\beta(\epsilon_i - \mu)}}$$

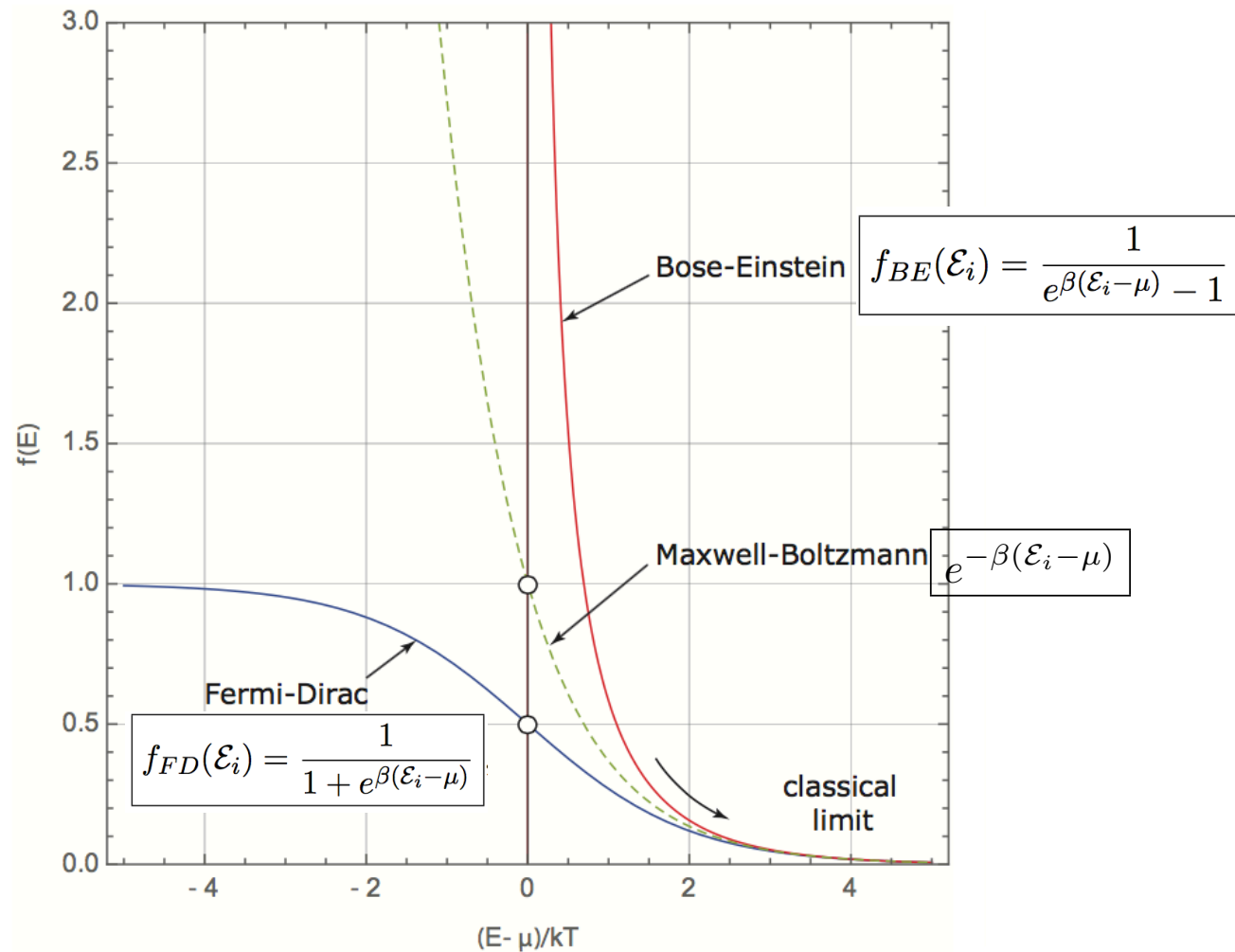
Partition function

$$\langle n_i \rangle = f(\epsilon_i) = \frac{0 \cdot u^0 + 1 \cdot u^1 + 2 \cdot u^2 + 3 \cdot u^3 + \dots}{(1 - u)^{-1}}$$

$$f_{BE}(\epsilon_i) = \frac{1}{e^{\beta(\epsilon_i - \mu)} - 1} \quad u = e^{\beta(\mu - \epsilon_i)}$$

- Boltzmann equilibrium allows energy exchange without particles between reservoir and system
- Gibb's equilibrium allows energy and particle exchange between the reservoir and the system
- The chemical potential is a measure of the number of particles

Fermi-Dirac and Bose-Einstein Distributions



- Both the Fermi-Dirac and Bose-Einstein distributions are for non-interacting particles
- In the limit of high energies, they merge to the classical Boltzmann limit

Fermi-Difference function and its integrals

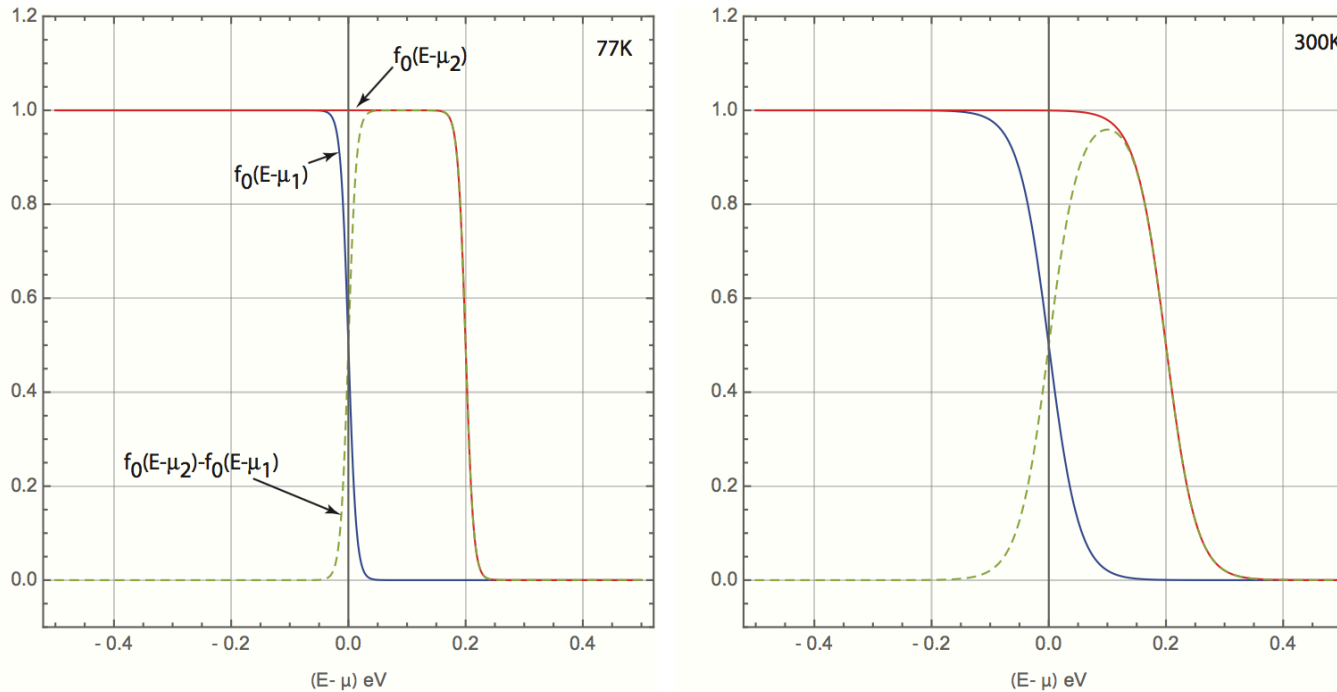


FIGURE 6.4: Illustration of the temperature dependence of the Fermi-difference distribution. The difference is a window between $\mu_2 - \mu_1$ that becomes increasingly rectangular as the temperature drops.

$$f(u) = 1/(1 + e^u) \text{ and } f(v) = 1/(1 + e^v)$$

$$f(u) - f(v) = \underbrace{[f(u) + f(v) - 2f(u)f(v)]}_{\geq 0} \times \tanh\left(\frac{v - u}{2}\right)$$

$$\int_0^\infty dE f_0(E - \mu) = \int_0^\infty \frac{dE}{1 + e^{\beta(E - \mu)}} = \frac{1}{\beta} \ln(1 + e^{\beta\mu}),$$

$$\int_0^\infty dE [f_0(E - \mu_1) - f_0(E - \mu_2)] = \frac{1}{\beta} \ln\left[\frac{1 + e^{\beta\mu_1}}{1 + e^{\beta\mu_2}}\right] = (\mu_1 - \mu_2) + \frac{1}{\beta} \ln\left[\frac{1 + e^{-\beta\mu_1}}{1 + e^{-\beta\mu_2}}\right].$$

$$\xrightarrow{\mu_1, \mu_2 \gg kT} \int_0^\infty dE [f_0(\mu_1) - f_0(\mu_2)] \approx (\mu_1 - \mu_2).$$

- The Fermi difference function will dominate our treatment of electron transport.
- The Fermi difference function looks like a box function with edges smeared with temperature.

Fermi-Dirac Integrals

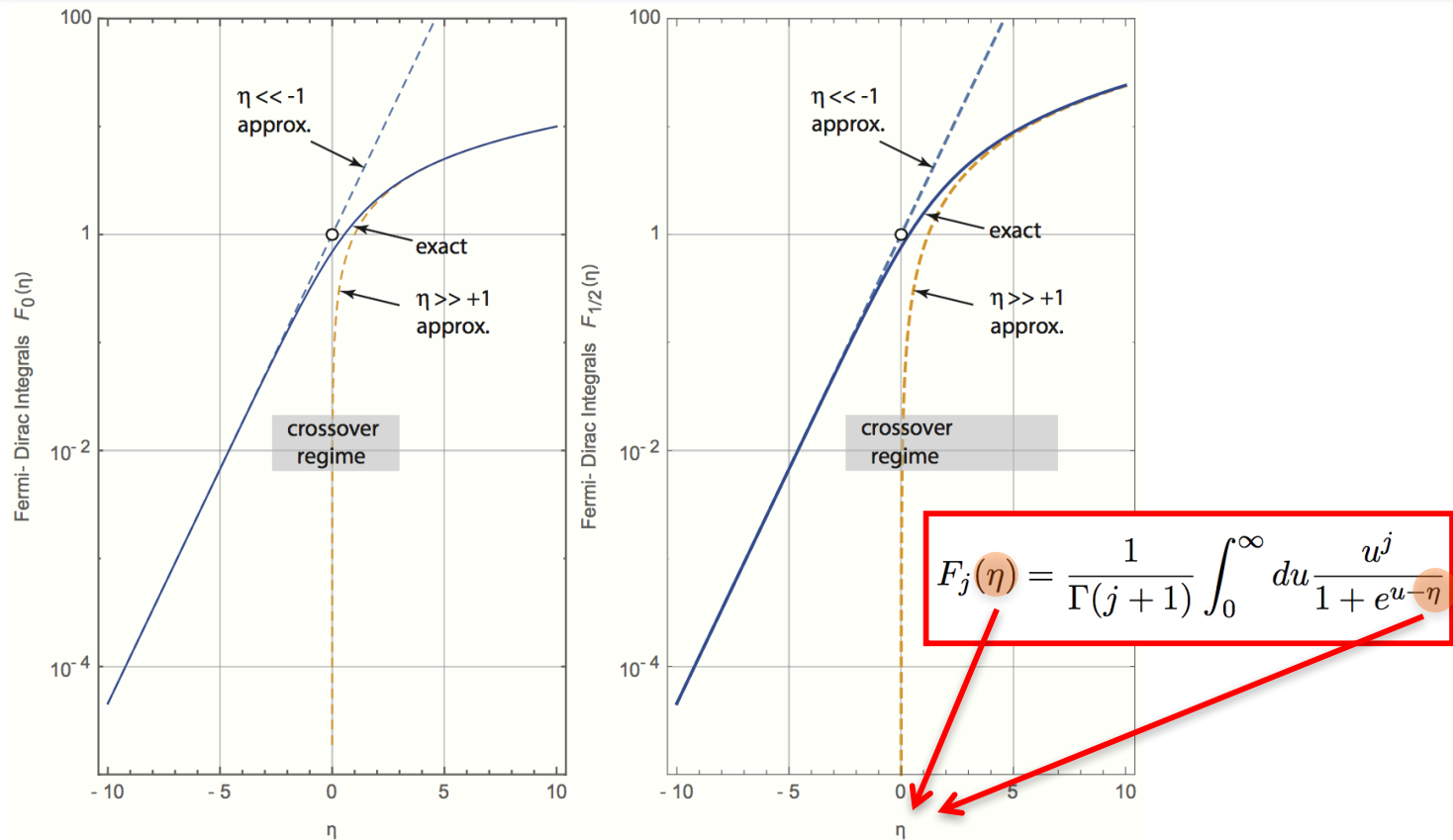


FIGURE 6.5: Fermi-Dirac integrals and their non-degenerate ($\eta \ll -1$) and degenerate ($\eta \gg 1$) approximations, illustrating Equation 6.20.

$$F_j(\eta) = \frac{1}{\Gamma(j+1)} \int_0^\infty du \frac{u^j}{1+e^{u-\eta}}, \quad F_j(\eta) \underset{\eta \ll -1}{\approx} e^\eta, \quad F_j(\eta) \underset{\eta \gg 1}{\approx} \frac{\eta^{j+1}}{\Gamma(j+2)}$$

- The Fermi-Dirac Integrals (are moments) appear when we sum over states to calculate current
- The “order” of the integral is dependent on the dimensionality of the problem

Equilibrium at contacts

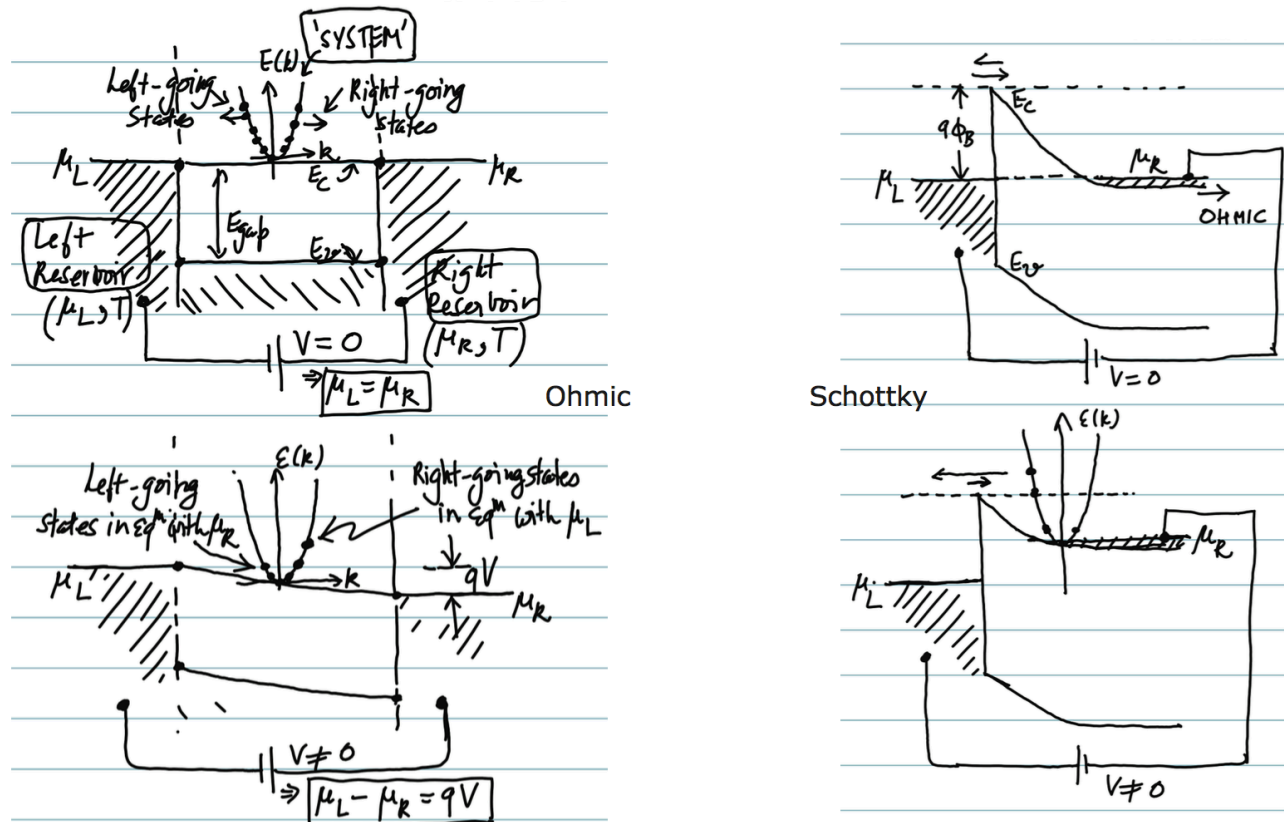


FIGURE 6.6: Illustration of the concept of equilibrium for Ohmic and Schottky contacts between metals and semiconductors.

- Electrons states in the metal contact reservoirs try bringing the “semiconductor” channel electron states in equilibrium with them by particle (or energy) transfer
- States in equilibrium share the same chemical potential, and their $f(k)$ is thus known
- Multiple contacts with different chemical potentials bring parts of channel states to equilibrium with themselves; the net current flows if there is an imbalance in current carrying states

Equilibrium at multicarrier junctions

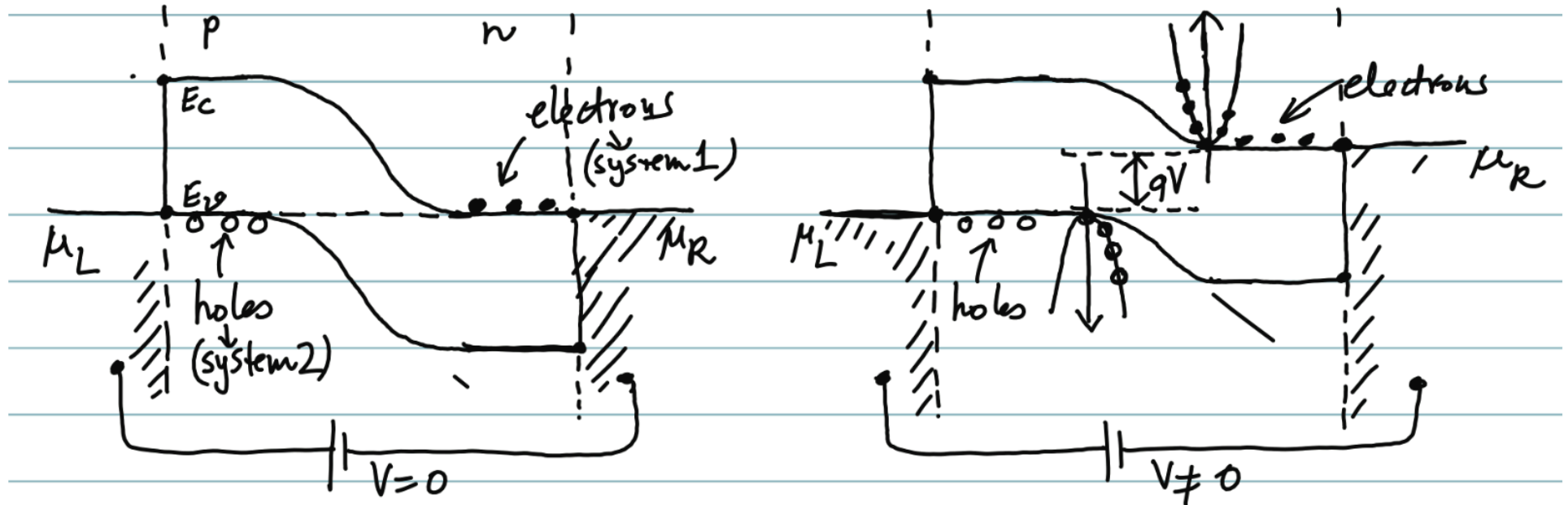


FIGURE 6.7: Illustration of the concept of equilibrium for p-n junctions.

- Electrons states in the metal contact reservoirs try bringing the “semiconductor” channel electron states in equilibrium with them by particle (or energy) transfer
- States in equilibrium share the same chemical potential, and their $f(k)$ is thus known
- Multiple contacts with different chemical potentials bring parts of channel states to equilibrium with themselves; the net current flows if there is an imbalance in current carrying states

Equilibrium in Transistors

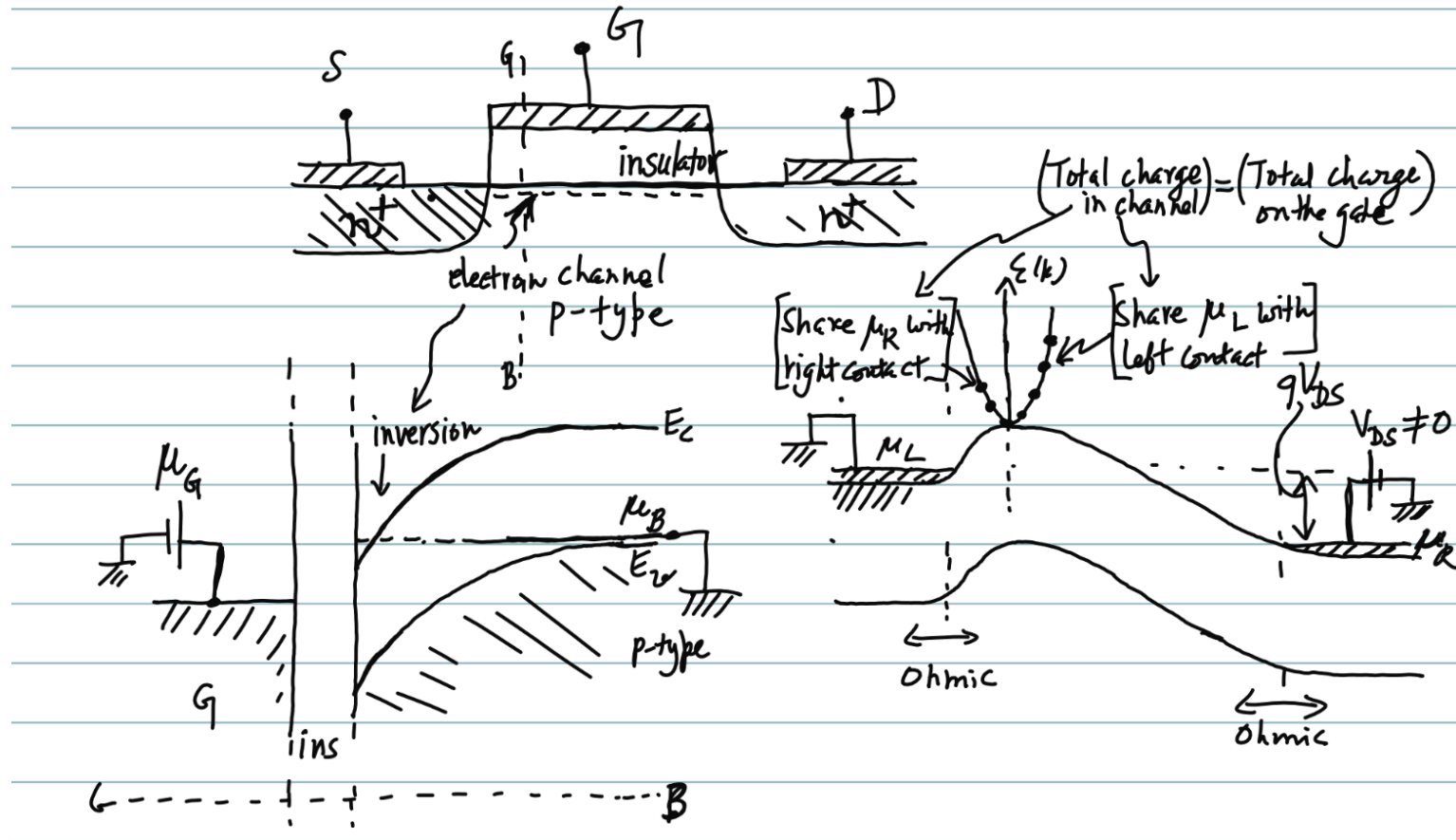


FIGURE 6.8: Illustration of the concept of equilibrium for a 3-terminal MOSFET

- Electrons states in the metal contact reservoirs try bringing the “semiconductor” channel electron states in equilibrium with them by particle (or energy) transfer
- States in equilibrium share the same chemical potential, and their $f(k)$ is thus known
- Multiple contacts with different chemical potentials bring parts of channel states to equilibrium with themselves; the net current flows if there is an imbalance in current carrying states

Perfect Crystal: 'Bloch' single electron transport

PERFECT
CRYSTALLINE
MATERIALS



- Bloch oscillations

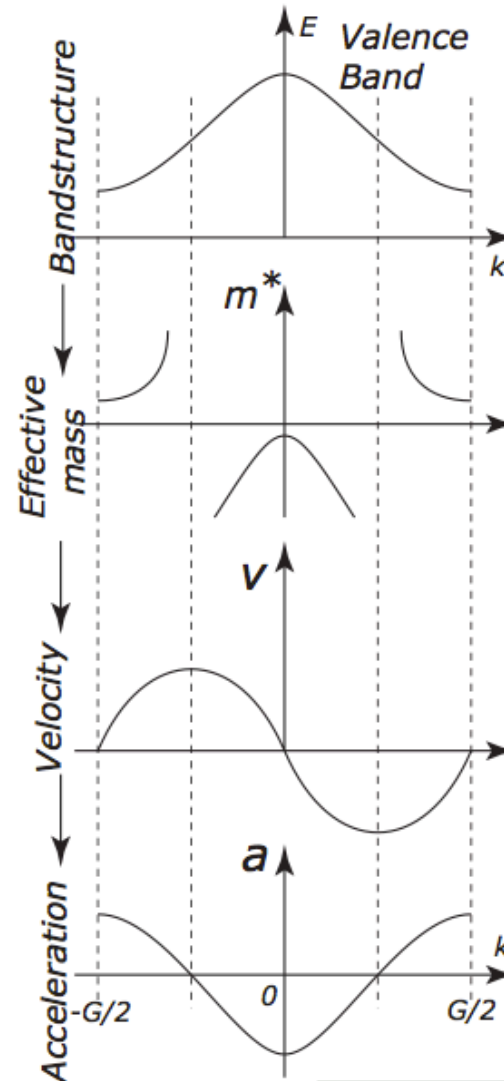
A static periodic potential causes no scattering.

$$\mathbf{F} = (-e) \cdot [\mathbf{E} + \mathbf{v} \times \mathbf{B}] = \hbar \frac{d\mathbf{k}}{dt}$$

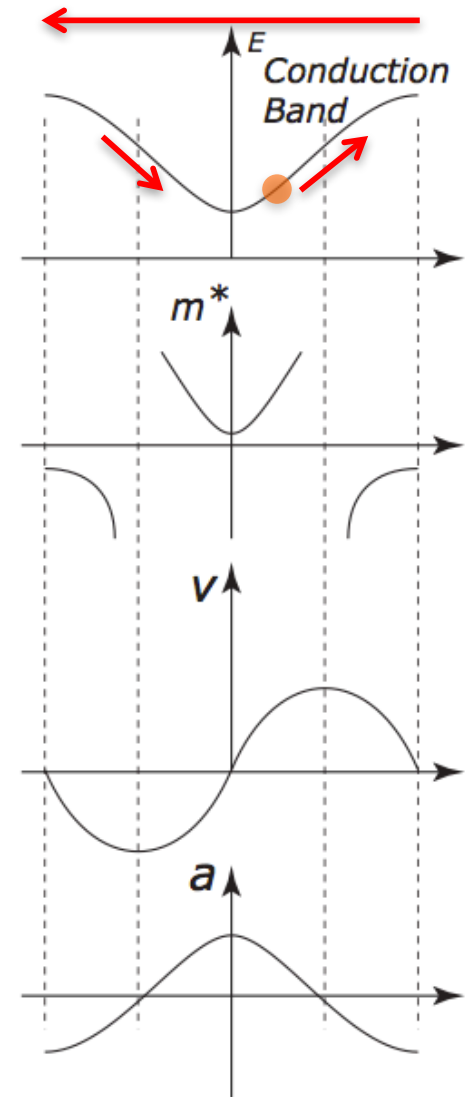
$$\mathbf{v} = \frac{1}{\hbar} \frac{\partial E(k)}{\partial k} = \frac{1}{\hbar} \nabla_k E(k)$$

$$\mathbf{a} = \frac{\mathbf{F}}{m^*} \quad \mathbf{v} = \frac{d\mathbf{r}}{dt}$$

Can easily transform to real space.



Umklapp process



'One' electron: Bloch oscillations

Electron in a periodic potential (no analytic soln!)

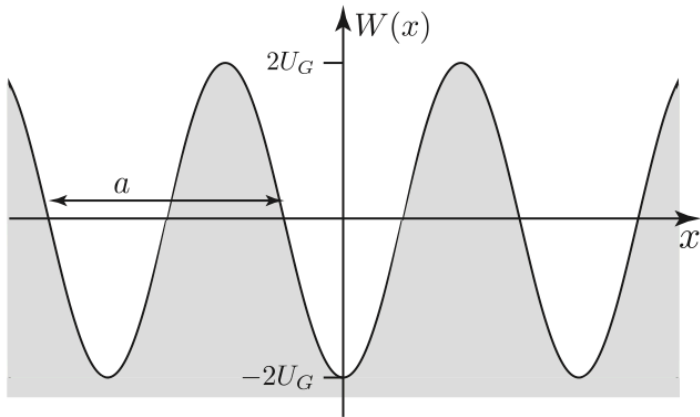


FIGURE 13.1: A periodic potential $W(x) = -2U_G \cos(Gx)$ acts as a perturbation to the free electron.

We know the bandstructure, or $E(k)$ eigenvalues of the electron in the crystal.

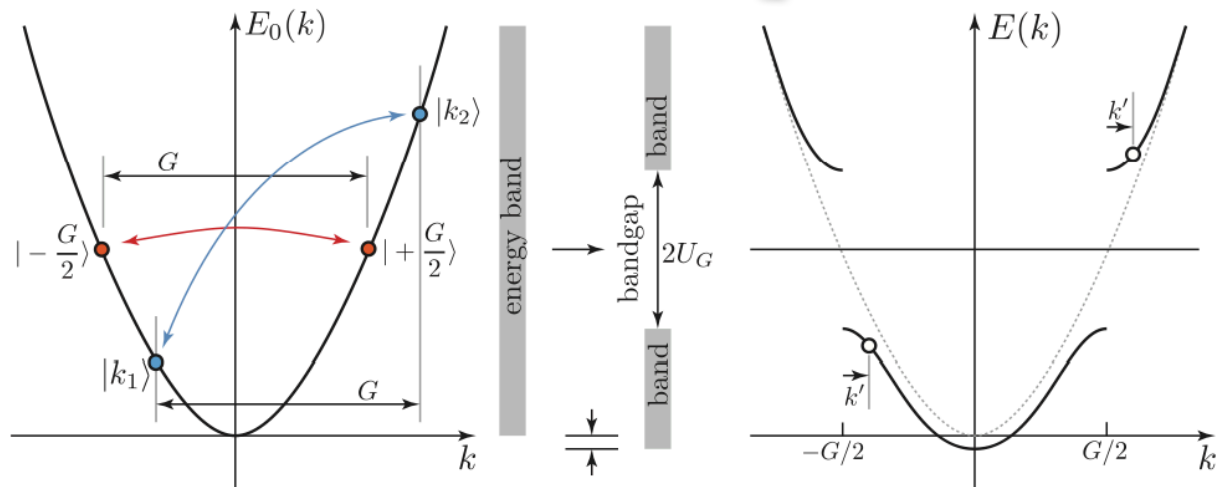


FIGURE 13.2: Bandgap opening in the energy spectrum of a free electron upon perturbation by a periodic potential.

Effective Mass Approximation

- *Effective Mass Approximation MAPS the complicated problem of*
- ***Electrons in a complicated crystal + heterostructure potential ... to ... the simplest of all quantum mech problems: The particle in a box***

PHYSICAL REVIEW

VOLUME 97, NUMBER 4

FEBRUARY 15, 1955

Motion of Electrons and Holes in Perturbed Periodic Fields

J. M. LUTTINGER* AND W. KOHN†
Bell Telephone Laboratories, Murray Hill, New Jersey
(Received October 13, 1954)

A new method of developing an “effective-mass” equation for electrons moving in a perturbed periodic structure is discussed. This method is particularly adapted to such problems as arise in connection with impurity states and cyclotron resonance in semiconductors such as Si and Ge. The resulting theory generalizes the usual effective-mass treatment to the case where a band minimum is not at the center of the Brillouin zone, and also to the case where the band is degenerate. The latter is particularly striking, the usual Wannier equation being replaced by a set of coupled differential equations.



The Nobel Prize in Chemistry 1998

Walter Kohn

1/2 of the prize

USA

University of California
Santa Barbara, CA, USA



JOAQUIN M. LUTTINGER

- *Developed by Luttinger & Kohn and refined since then...*
- *Real power of the EMA is exercised in understanding the electronic properties of Quantum Heterostructures.*

Effective Mass Approximation

$$E_n(k) \approx E_c(r) + \frac{\hbar^2 k^2}{2m^*} \rightarrow E_n(-i\nabla) \approx E_c(r) - \frac{\hbar^2}{2m^*} \nabla^2$$

$$\left[-\frac{\hbar^2}{2m^*} \nabla^2 + V_{imp}(r)\right] C(r) = [E - E_c(r)] C(r)$$

Central Result of Effective Mass Approximation

“Particle-in-a-box” problem with:
Real mass \rightarrow Effective mass,
Real wavefunction \rightarrow Envelope function
Crystal potential \rightarrow Band-edge potential + Impurity potentials, etc

Example: Shallow donor states

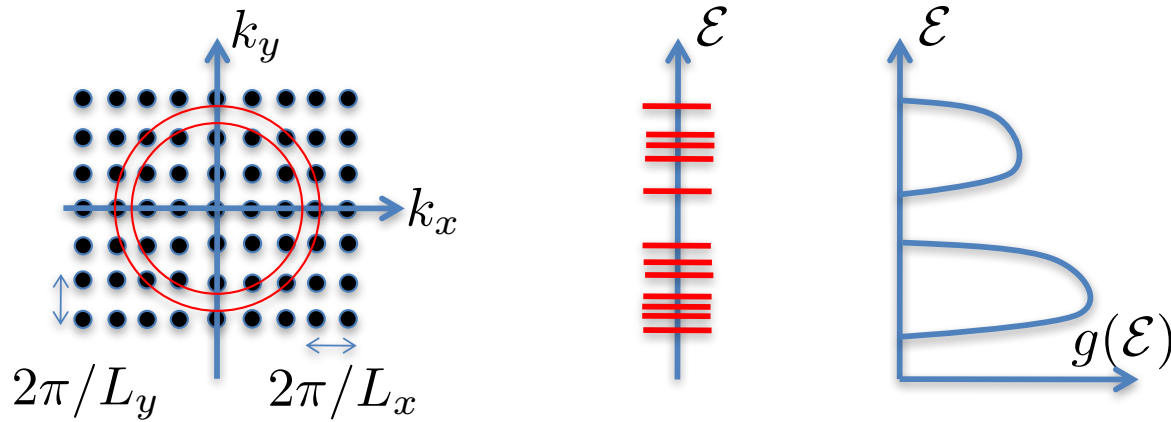
$$\left[-\frac{\hbar^2}{2m^*} \nabla^2 - \frac{e^2}{4\pi\epsilon r}\right] C(r) = (E - E_c) C(r)$$

$$E - E_c = E_\infty \frac{m^*}{\epsilon_r^2}$$

$$a_B^* = a_B \frac{\epsilon_r}{m^*}$$

$$C(r) \sim e^{-r/r_0}$$

Density of States



$$\text{DOS: } g(\mathcal{E}) = g_s \cdot \sum_{\mathbf{k}} \delta[\mathcal{E} - \mathcal{E}(\mathbf{k})]$$

Valid for electrons, photons, phonons...

$$\text{Important result: } \sum_{\mathbf{k}} (\dots) \rightarrow \int \frac{d^d \mathbf{k}}{(2\pi)^d} (\dots)$$

If we know the energy dispersion $\mathcal{E}(\mathbf{k})$, we can find the DOS using this prescription.

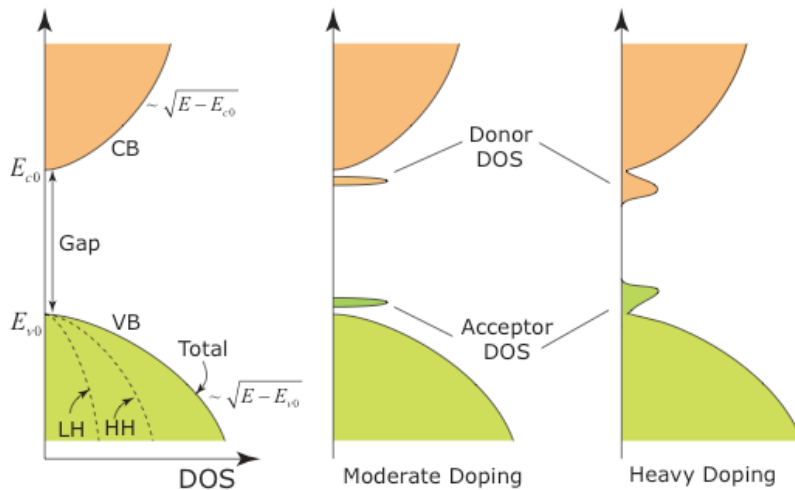
$$\text{Free Electron: } \mathcal{E}(\mathbf{k}) = \frac{\hbar^2 |\mathbf{k}|^2}{2m_0}$$

$$\text{Free electron in 3D: } g(\mathcal{E}) = g_s \cdot \frac{1}{(2\pi)^2} \left(\frac{2m_0}{\hbar^2} \right)^{\frac{3}{2}} \sqrt{\mathcal{E}}$$

Effective Mass Approximation

Application: Bulk Semiconductors

• 3D (Bulk)



$$\left[-\frac{\hbar^2}{2m^*} \nabla^2 + V_{\text{imp}}(r) \right] C(r) = [E - E_c(r)] C(r)$$

$$C(r) = \frac{1}{\sqrt{V}} e^{i\vec{k} \cdot \vec{r}}$$

$$E(k) = E_{c0}(r) + \frac{\hbar^2 k^2}{2m^*} = E_{c0}(r) + \frac{\hbar^2}{2} \left(\frac{k_x^2}{m_{xx}^*} + \frac{k_y^2}{m_{yy}^*} + \frac{k_z^2}{m_{zz}^*} \right)$$

$$g_{3D}(E) = \frac{1}{2\pi^2} \left(\frac{2m^*}{\hbar^2} \right)^{3/2} \sqrt{E - E_{c0}}$$

$$n = \int_0^\infty dE f_{FD}(E) g_{3D}(E) = N_C^{3D} F_{1/2} \left(\frac{E_C - E_F}{k_B T} \right) \approx N_C^{3D} e^{-\frac{E_C - E_F}{k_B T}}$$

Effective Mass Approximation

• 2D (Quantum Wells)

$$\begin{aligned}
 V(x, y, z) &= 0, z < 0 \\
 V(x, y, z) &= 0, z > W \\
 V(x, y, z) &= -\Delta E_c, 0 \leq z \leq W.
 \end{aligned}$$

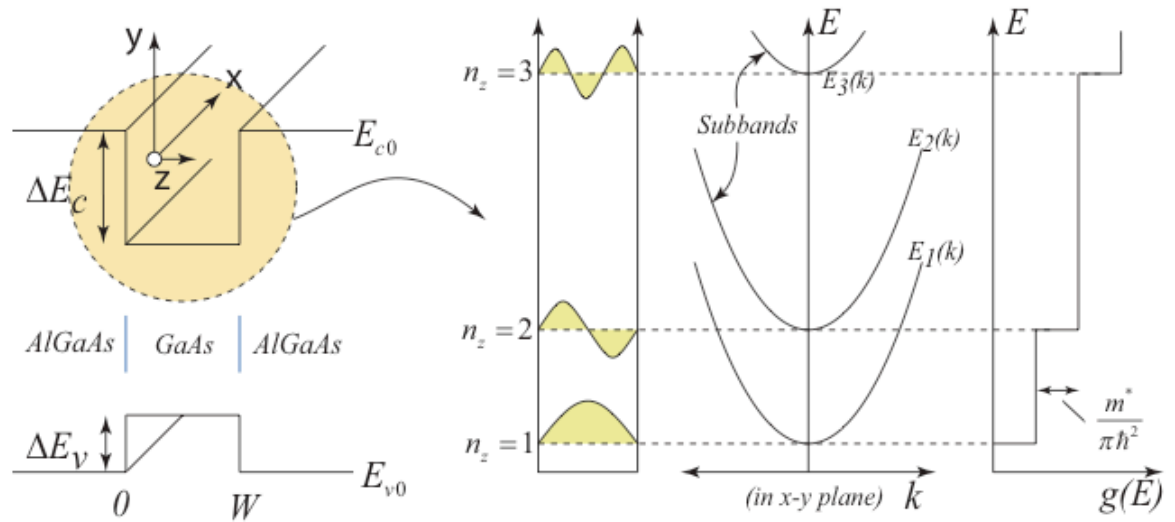


Figure 2: Bandstructure, and DOS of realistic heterostructure quantum wells

$$k_{n_z} = \frac{\pi}{W} n_z$$

$$C_{n_z}(x, y, z) = \phi(x, y) \chi_{n_z}(z) = \left[\frac{1}{\sqrt{A}} e^{i(k_x x + k_y y)} \right] \cdot [\chi_{n_z}(z)]$$

$$\chi_{n_z}(z) = \sqrt{\frac{2}{W}} \sin \frac{\pi n_z z}{W}$$

$$E(k) = E_{c0} + \underbrace{\frac{\hbar^2}{2} \left(\frac{k_x^2}{m_{xx}^*} + \frac{k_y^2}{m_{yy}^*} \right)}_{E_{2D}(k_x, k_y)} + \underbrace{\frac{\hbar^2}{2m_{zz}^*} \left(\frac{\pi n_z}{W} \right)^2}_{E_{1D}(n_z)}$$

$$n_{2D} = \int_0^\infty dE f_{FD}(E) g_{2D}(E) = \frac{m^* k_B T}{\pi \hbar^2} \ln \left(1 + e^{\frac{E_F - E_1}{k_B T}} \right)$$

$$g_{QW}(E) = \frac{m^*}{\pi \hbar^2} \sum_{n_z} \theta(E - E_{n_z})$$

$$n_{2D} = \sum_j n_j = N_c^{2D} \sum_j \ln \left(1 + e^{\frac{E_F - E_j}{k_B T}} \right)$$

Effective Mass Approximation

• 1D (Quantum Wires)

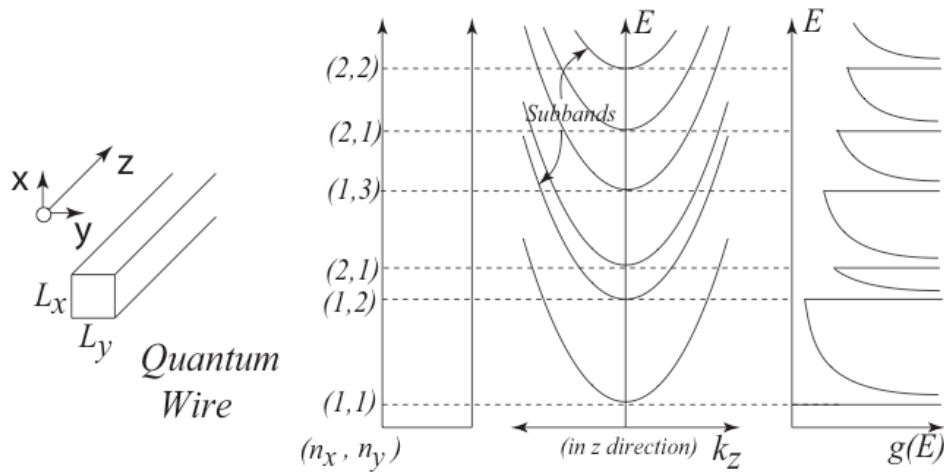


Figure 3: Bandstructure, and DOS of realistic quantum wires.

$$C_{n_x, n_y}(x, y, z) = \left[\sqrt{\frac{2}{L_x}} \sin\left(\frac{\pi n_x}{L_x} x\right) \right] \cdot \left[\sqrt{\frac{2}{L_y}} \sin\left(\frac{\pi n_y}{L_y} y\right) \right] \cdot \left[\frac{1}{\sqrt{L_z}} e^{ik_x x} \right]$$

$$E(n_x, n_y, k_z) = \underbrace{\left[\frac{\hbar^2}{2m_{xx}} \left(\frac{\pi n_x}{L_x}\right)^2 \right] + \left[\frac{\hbar^2}{2m_{yy}} \left(\frac{\pi n_y}{L_y}\right)^2 \right]}_{E(n_x, n_y)} + \frac{\hbar^2 k_z^2}{2m_{zz}^*}$$

$$g_{1D}(E) = \frac{1}{\pi} \sqrt{\frac{2m^*}{\hbar^2}} \frac{1}{\sqrt{E - E_1}}$$

$$g_{QWire}(E) = \frac{1}{\pi} \sqrt{\frac{2m^*}{\hbar^2}} \sum_{n_x, n_y} \frac{1}{\sqrt{E - E(n_x, n_y)}}$$

$$k_{n_x} = \frac{\pi}{L_x} n_x,$$

$$k_{n_y} = \frac{\pi}{L_y} n_y,$$

$$C(x, y, z) = \chi_{n_x}(x) \cdot \chi_{n_y}(y) \cdot \left(\frac{1}{\sqrt{L_z}} e^{ik_x x} \right)$$

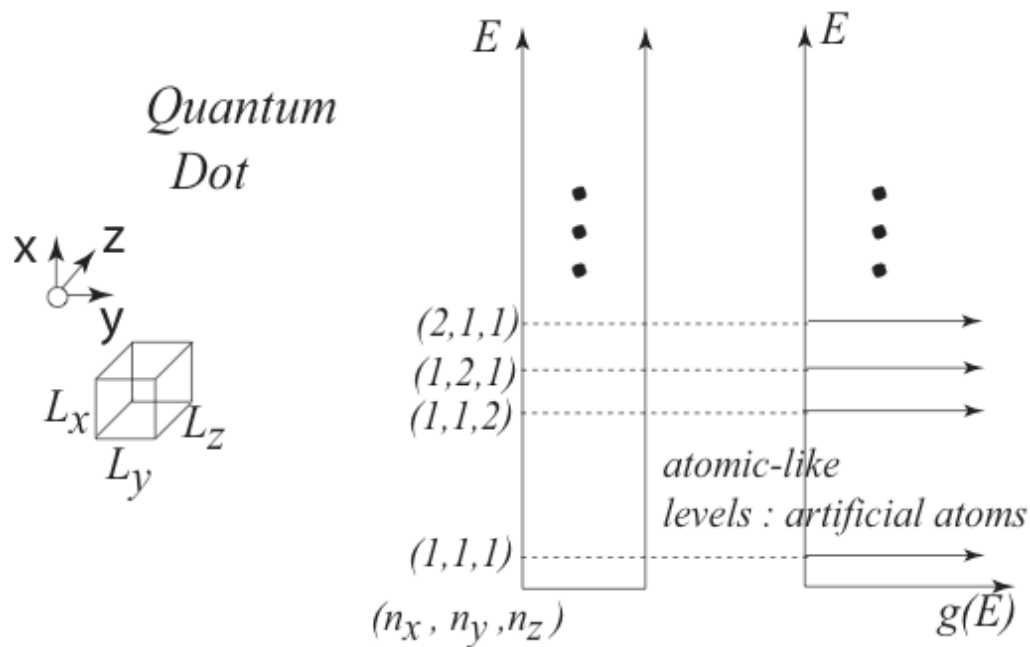
$$E(n_x, n_y, k_z) = E(n_x, n_y) + \frac{\hbar^2 k_k^2}{2m_{zz}^*}$$

Effective Mass Approximation

• 0D (Quantum Dots)

$$C(x, y, z) = \left[\sqrt{\frac{2}{L_x}} \sin\left(\frac{\pi n_x}{L_x}\right) \right] \cdot \left[\sqrt{\frac{2}{L_y}} \sin\left(\frac{\pi n_y}{L_y}\right) \right] \cdot \left[\sqrt{\frac{2}{L_z}} \sin\left(\frac{\pi n_z}{L_z}\right) \right]$$

$$E(n_x, n_y, n_z) = \frac{\hbar^2}{2m_{xx}} \left(\frac{\pi n_x}{L_x}\right)^2 + \frac{\hbar^2}{2m_{yy}} \left(\frac{\pi n_y}{L_y}\right)^2 + \frac{\hbar^2}{2m_{zz}} \left(\frac{\pi n_z}{L_z}\right)^2$$



$$g_{QDot} = \sum_{n_x, n_y, n_z} \delta(E - E_{n_x, n_y, n_z})$$

Figure 4: Energy levels and DOS of quantum dots.

Effective Mass Approximation @ Heterojunctions

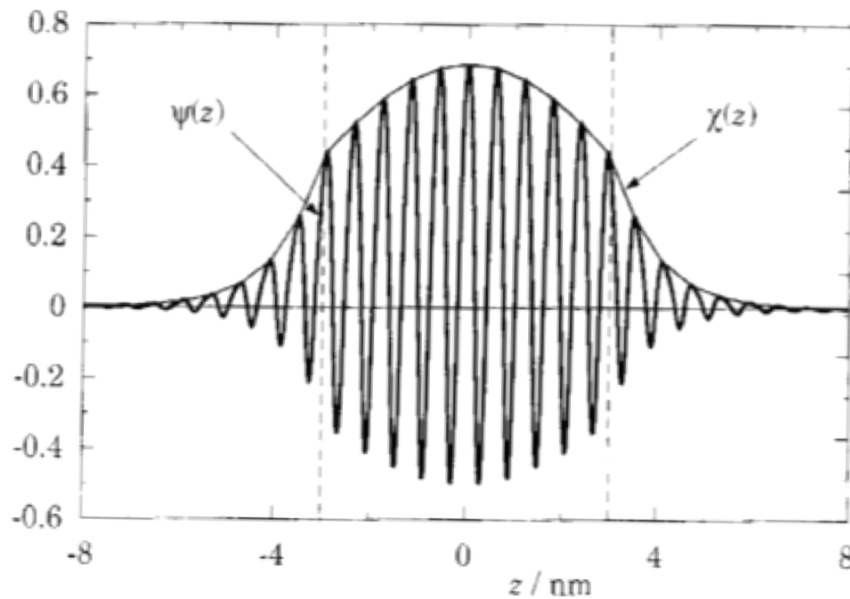


FIGURE 3.22. Wave function for the lowest state in a 6 nm quantum well in a heterostructure, including the Bloch functions. The thin curve is an approximate envelope function joining the peaks of the full wave function. [Redrawn from Burt (1994).]

- *Effective Mass Theory works even at sharp heterojunctions, and it works amazingly well! Quantum cascade lasers are designed using this theory.*

*Proof presented in:
Burt, APL 65 717 (1994)*

On the validity and range of applicability of the particle in a box model

M. G. Burt

BT Laboratories, Martlesham Heath, Ipswich IP5 7RE, United Kingdom

(Received 24 February 1994; accepted for publication 27 May 1994)

$$\left(E_c^A - \frac{\hbar^2}{2m_A m_0} \frac{d^2}{dz^2}\right) \chi(z) = E \chi(z), \quad (3.16)$$

$$\left(E_c^B - \frac{\hbar^2}{2m_B m_0} \frac{d^2}{dz^2}\right) \chi(z) = E \chi(z). \quad (3.17)$$

The difference in the bottoms of the conduction bands behaves like a step potential with material B higher by $\Delta E_c = E_c^B - E_c^A$. If the materials were the same we would simply match the value and derivative of the wave function at the interface, giving the usual conditions

$$\chi(0_A) = \chi(0_B), \quad \left. \frac{d\chi(z)}{dz} \right|_{z=0_A} = \left. \frac{d\chi(z)}{dz} \right|_{z=0_B}, \quad (3.18)$$

where 0_A means the side of the interface in material A and so on. This simple condition is not correct for a heterojunction where the two effective masses are different, and we shall see in Section 5.8 that equation (3.18) does not conserve current. A correct set of matching conditions is

$$\chi(0_A) = \chi(0_B), \quad \left. \frac{1}{m_A} \frac{d\chi(z)}{dz} \right|_{z=0_A} = \left. \frac{1}{m_B} \frac{d\chi(z)}{dz} \right|_{z=0_B}. \quad (3.19)$$

The condition for matching the derivative now includes the effective mass. Since the derivative is essentially the momentum operator, equation (3.19) requires the velocity to be the same on both sides to conserve current. The envelope function gains a kink at the interface if $m_A \neq m_B$.

Example: Exciton in an InN Nanowire

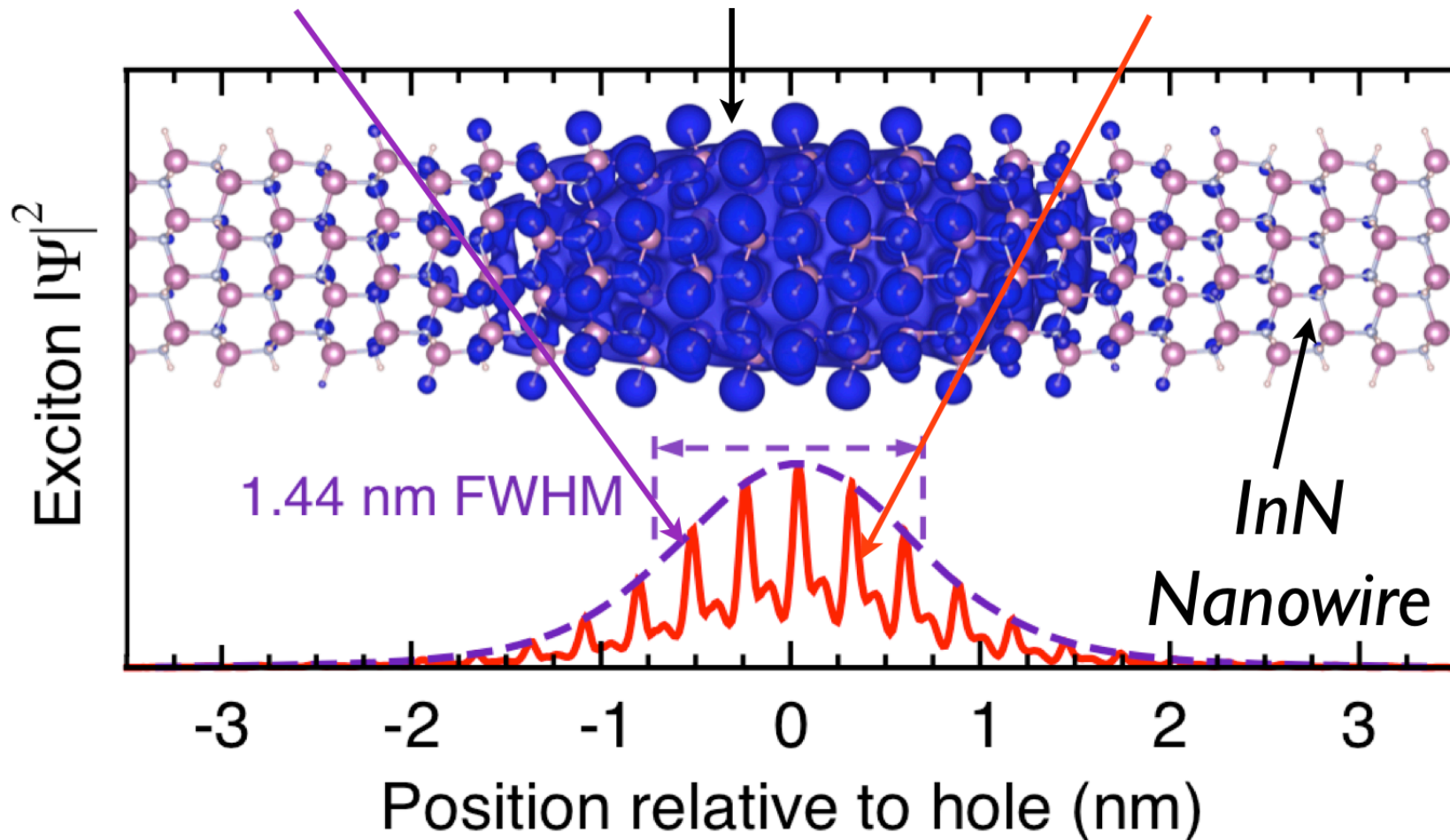
$$|C(r)|^2$$

envelope function

$$|\Psi(r)|^2 = |C(r)|^2 \times |u(r)|^2$$

exciton

Bloch function



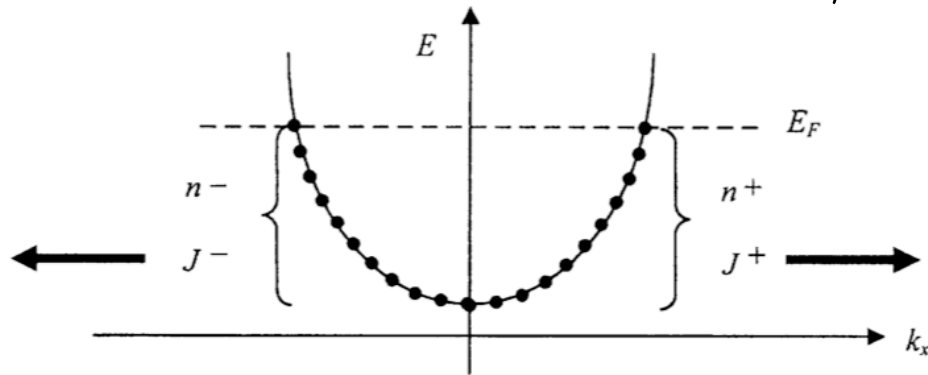
Nano Letters (2014)

E. Kioupakis et al. (Michigan)

“Ballistic” Transport & Quantized Conductance

Many electrons:

$$\mathbf{F} = \hbar d\mathbf{k}/dt$$



Most general expression for ‘Current Density’ in ‘d’ dimensions:

$$\mathbf{J}_d = q \times \frac{g_s g_v}{L^d} \sum_k \mathbf{v}_g(k) f(k), \text{ where}$$

g_s = spin degeneracy

g_v = valley degeneracy

$\mathbf{v}_g = \frac{1}{\hbar} \nabla \mathcal{E}(\mathbf{k})$ is the group velocity

$f(k)$ is the Fermi-Dirac function

Example: 1D current flow at $T = 0$ K :

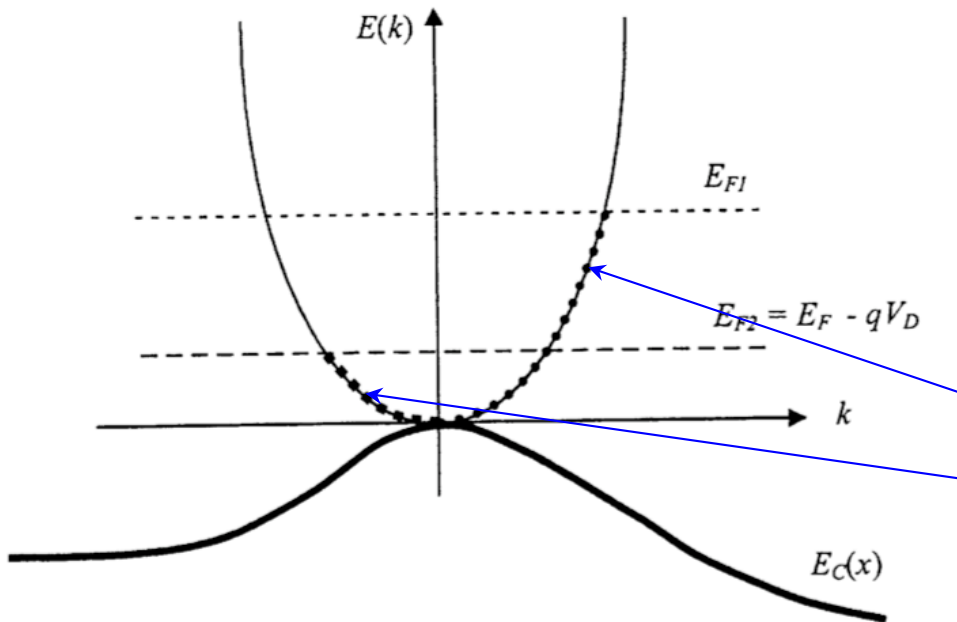
$$J_1 = I = I^{\rightarrow} - I^{\leftarrow}$$

$$I^{\rightarrow} = \frac{2q}{h} E_{F1}$$

$$I^{\leftarrow} = \frac{2q}{h} E_{F2}$$

$$\rightarrow I = I^{\rightarrow} - I^{\leftarrow} = \frac{2q^2}{h} V_D$$

Quantum of conductance



“Ballistic” Transport & Quantized Conductance

Experiments:

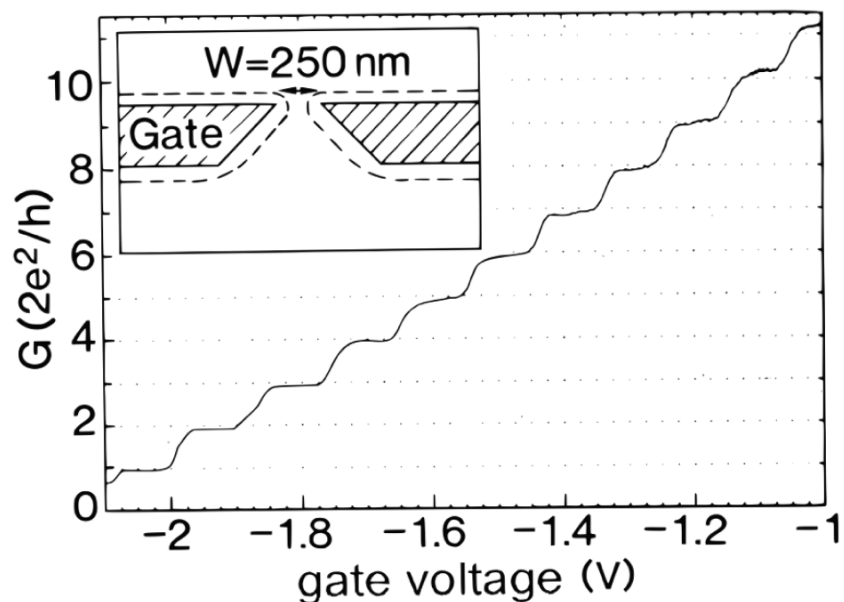


FIG. 44 Point contact conductance as a function of gate voltage at 0.6 K, demonstrating the conductance quantization in units of $2e^2/h$. The data are obtained from the two-terminal resistance after subtraction of a background resistance. The constriction width increases with increasing voltage on the gate (see inset). Taken from B. J. van Wees et al., Phys. Rev. Lett. **60**, 848 (1988).

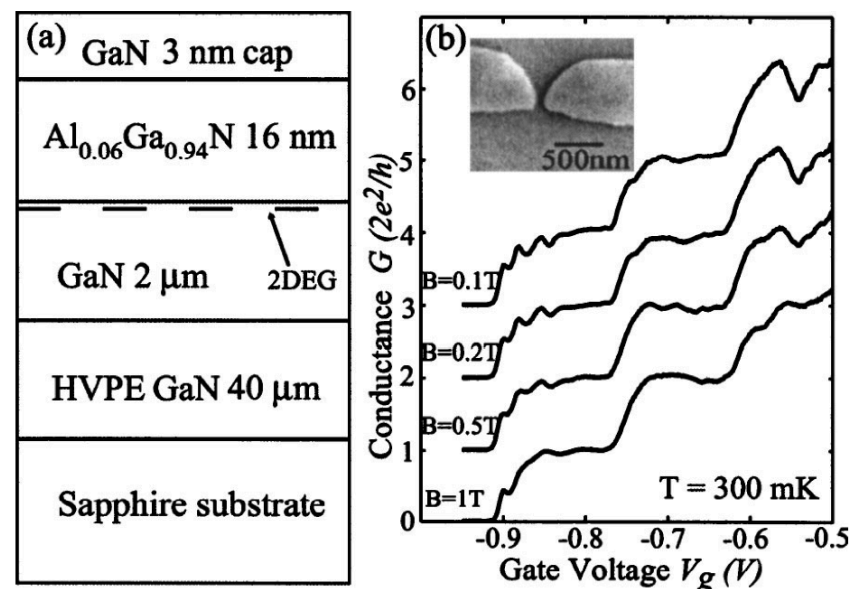
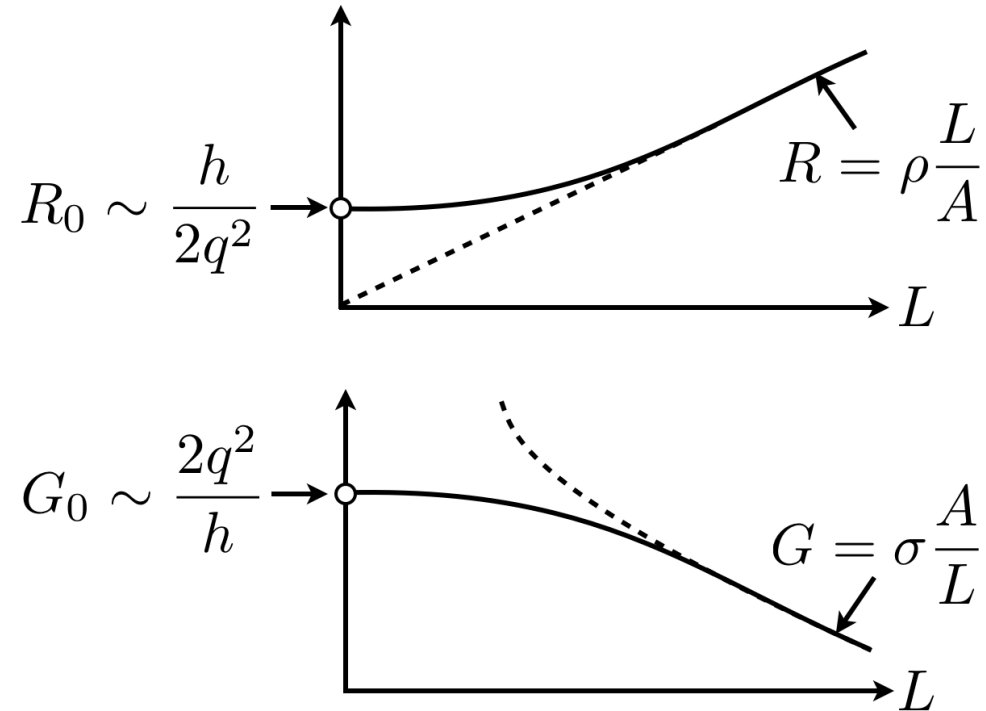
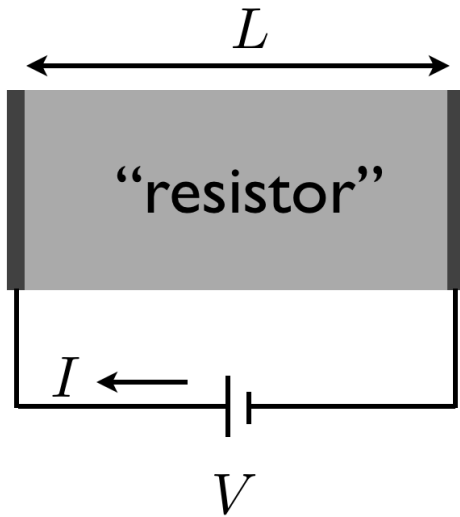


FIG. 1. (a) Schematic layer structure of the heterostructure. (b) improvement of plateau quantization with the application of a small magnetic field. Linear conductance $G(V_g)$ is plotted at magnetic field $B=0.1$ T, 0.2 T, 0.5 T, and 1 T. Traces are shifted vertically for clarity. Inset: micrograph of the QPC. The gap between the two split gates is 80 nm at its narrowest point. All experimental data shown in this letter were measured at 300 mK.

Appl. Phys. Lett. **86**, 073108 (2005);

From Ballistic conductance to Ohm's Law



$$R = \frac{h}{2q^2} \cdot \frac{1}{M} \cdot \left(1 + \frac{L}{\lambda_{mfp}}\right)$$

For $L \gg \lambda_{mfp}$ and 3D: $M \sim k_F^2 A$
 $\rightarrow R \sim \frac{h}{2q^2} \cdot \frac{1}{k_F^2 A} \cdot \frac{L}{\lambda_{mfp}}$ (Ohm's Law)

For $L \ll \lambda_{mfp}$ and 3D: $M \sim k_F^2 A$
 $\rightarrow R \sim \frac{h}{2q^2} \cdot \frac{1}{k_F^2 A}$ (Sharvin resistance)

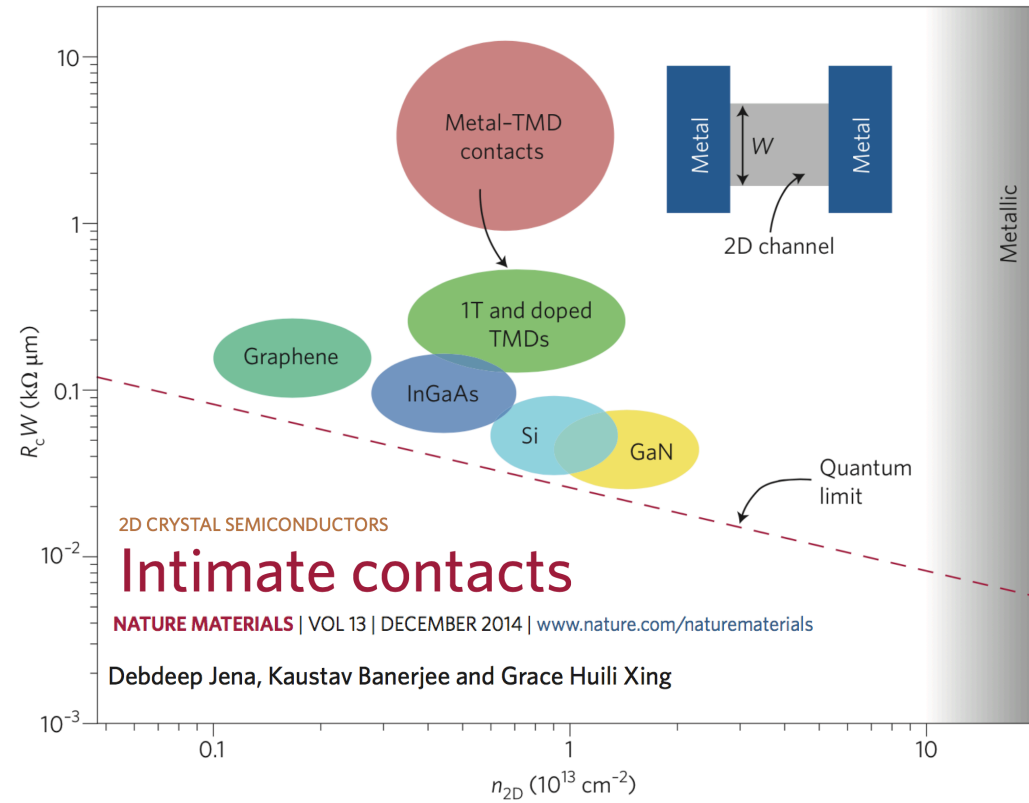
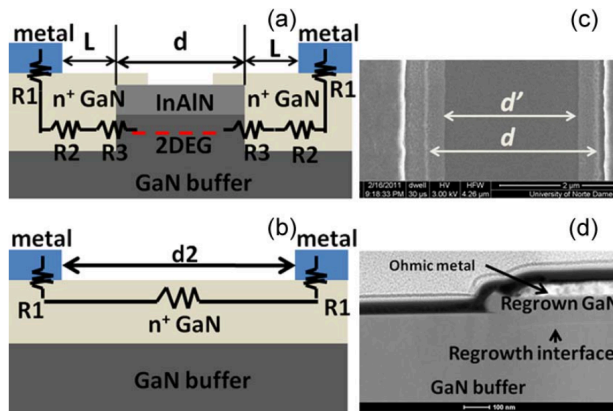
Contact resistances are at the quantum limit!

IEEE ELECTRON DEVICE LETTERS, VOL. 33, NO. 4, APRIL 2012

525

MBE-Regrown Ohmics in InAlN HEMTs With a Regrowth Interface Resistance of $0.05 \Omega \cdot \text{mm}$

Jia Guo, *Student Member, IEEE*, Guowang Li, *Student Member, IEEE*, Faiza Faria, Yu Cao, Ronghua Wang, Jai Verma, Xiang Gao, Shiping Guo, *Member, IEEE*, Edward Beam, Andrew Ketterson, Michael Schuette, *Member, IEEE*, Paul Saunier, *Senior Member, IEEE*, Mark Wistey, *Member, IEEE*, Debdeep Jena, *Member, IEEE*, and Huili Xing, *Member, IEEE*



$$R_c = \frac{\pi \hbar}{q^2} \sqrt{\frac{\pi}{2n_s}} = (0.026 \Omega \cdot \text{mm}) \sqrt{\frac{10^{13} / \text{cm}^2}{n_s}}$$

- MBE grown ohmic contacts are a key enabler of high RF performance
- Various groups (e.g. HRL) have adopted AlN/GaN MBE HEMT technology

Ballistic Field-Effect Transistor

Ballistic metal-oxide-semiconductor field effect transistor

Kenji Natori

Institute of Applied Physics, University of Tsukuba, Tsukuba, Ibaraki 305, Japan

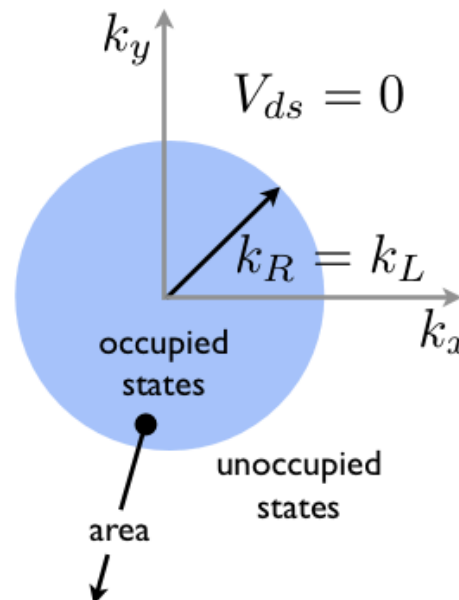
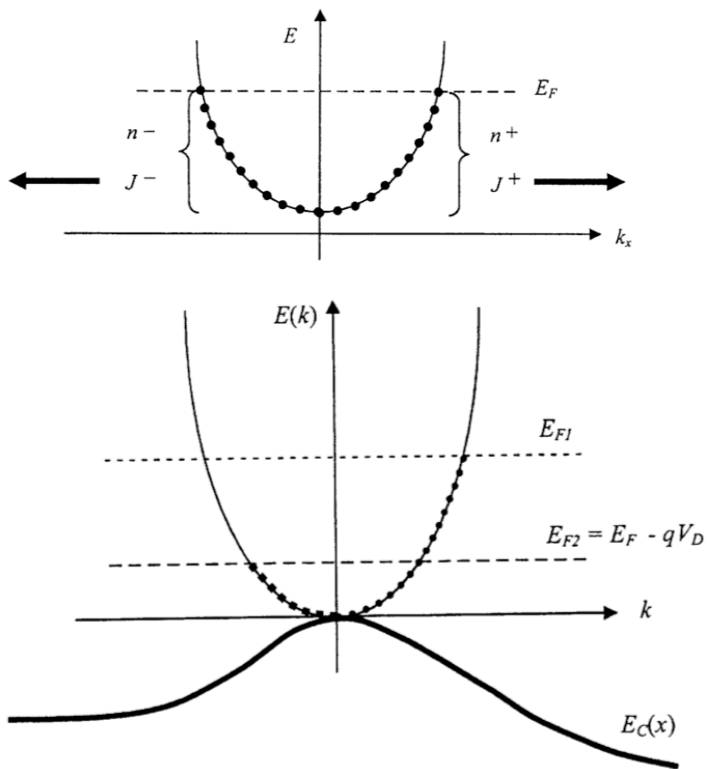
(Received 14 March 1994; accepted for publication 6 July 1994)

J. Appl. Phys. 76 (8), 15 October 1994

0021-8979/94/76(8)/4879/12/\$6.00

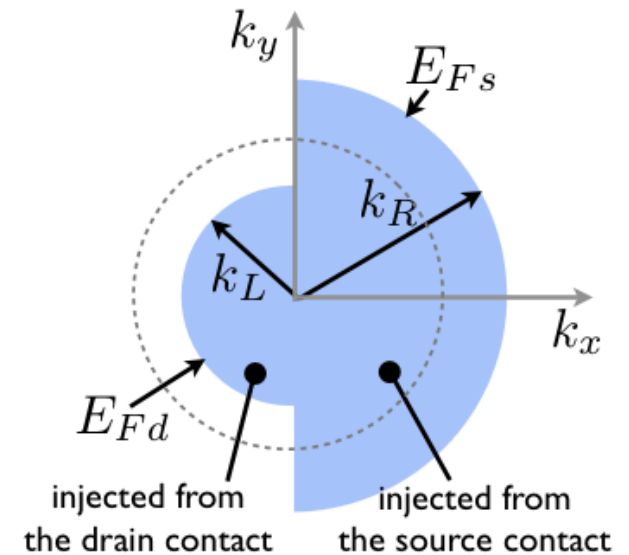
© 1994 American Institute of Physics

4879



$$n_{2d} = C_{gs}(V_g - V_t)/q$$

On-state approximation



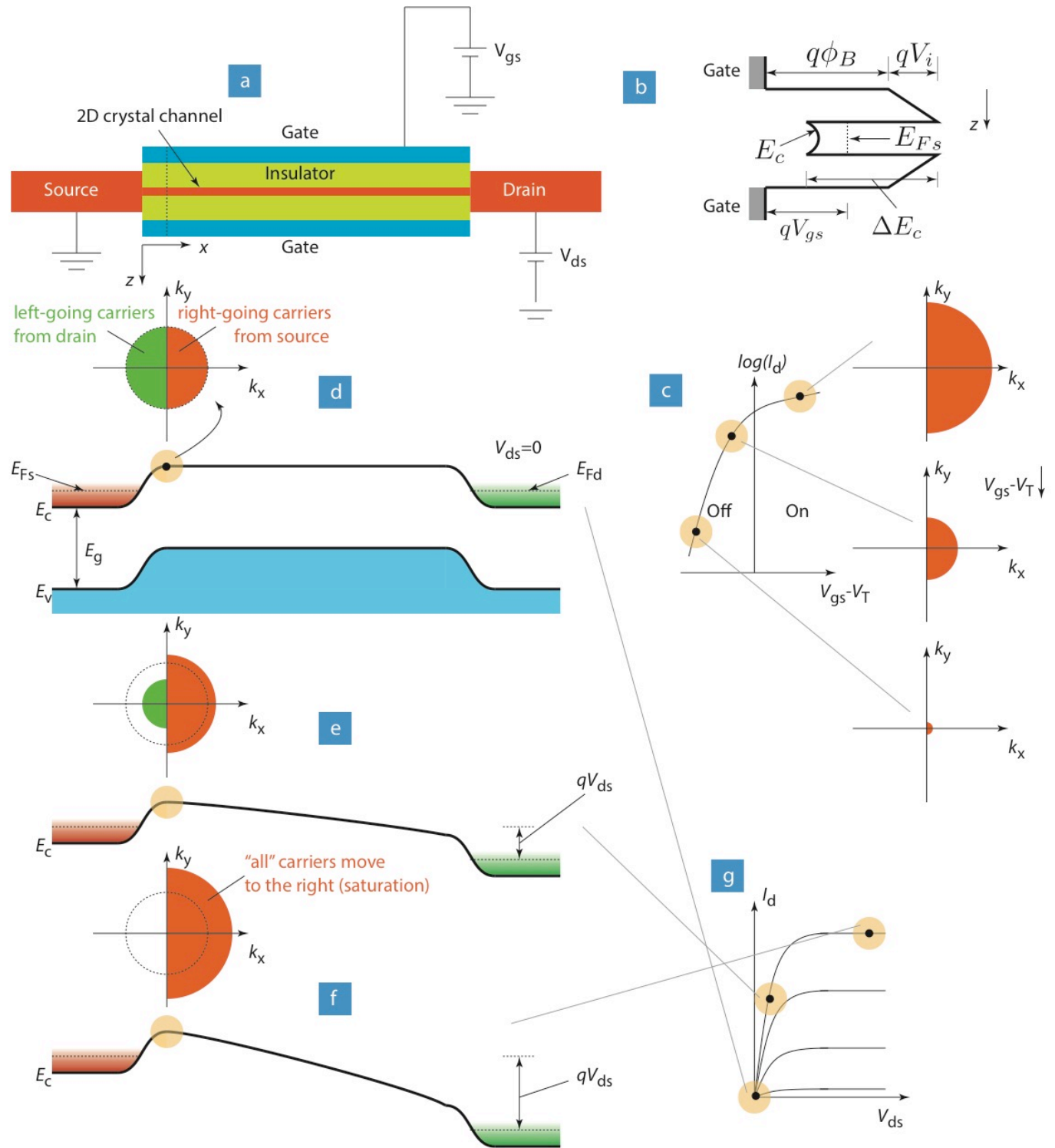
$$E_{F_s} - E_{F_d} = qV_{ds}$$

- The physics of a Ballistic FET can be understood by inspecting the carrier distribution in k -space at the source-injection Point.

Ballistic FET

$$\frac{q^2 n_s}{C_b} + kT \ln \left(e^{\frac{qn_s}{C_b V_{th}}} - 1 \right) = q(V_{gs} - V_T)$$

$$\Rightarrow \boxed{e^{\frac{qn_s}{C_b V_{th}}} \left(e^{\frac{qn_s}{C_b V_{th}}} - 1 \right) = e^{\frac{V_{gs} - V_T}{V_{th}}}}$$



Ballistic Field-Effect Transistor

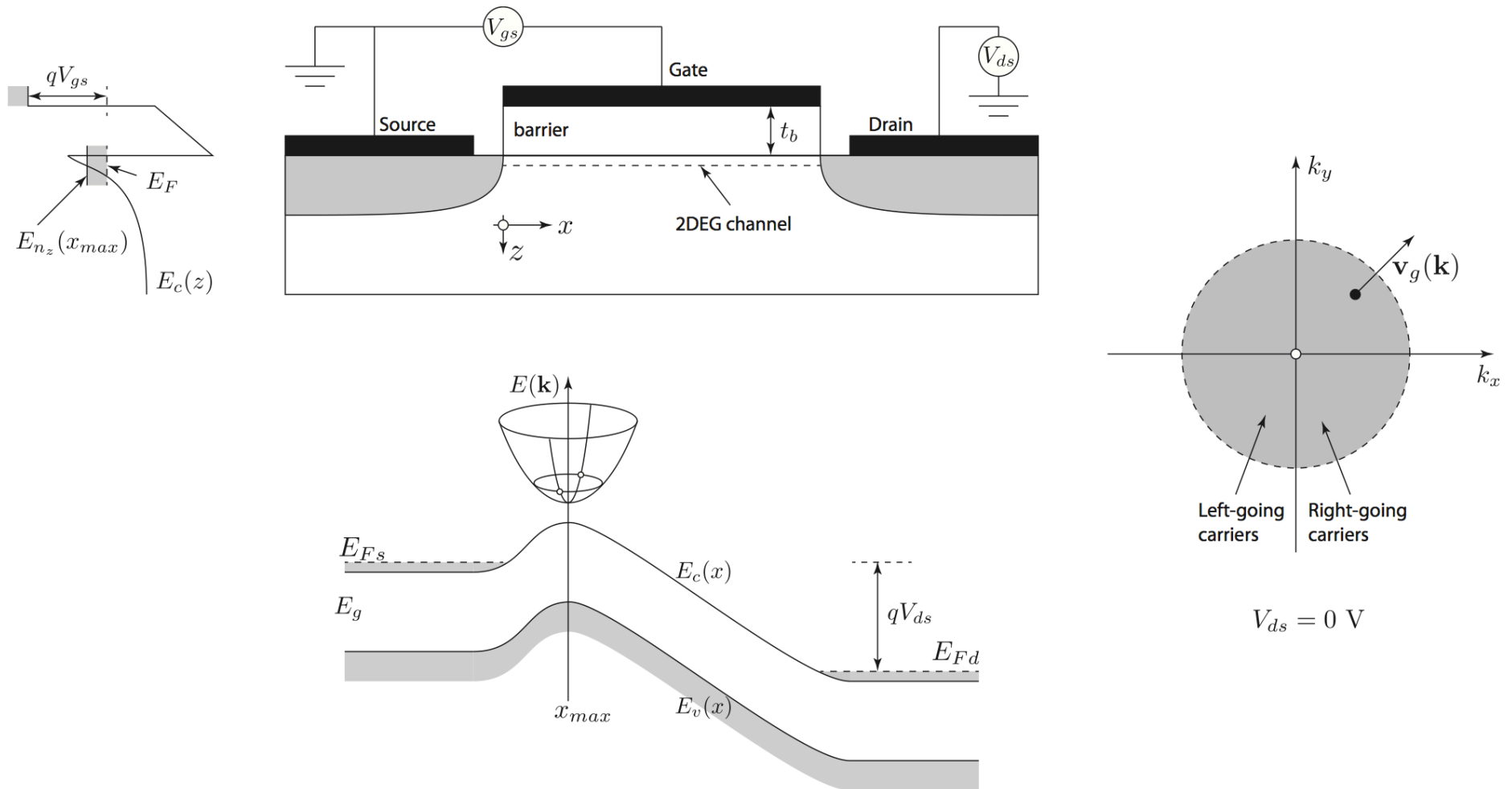


Figure 1: Field effect transistor, energy band diagram, and \mathbf{k} -space occupation of states.

Ballistic Field-Effect Transistor

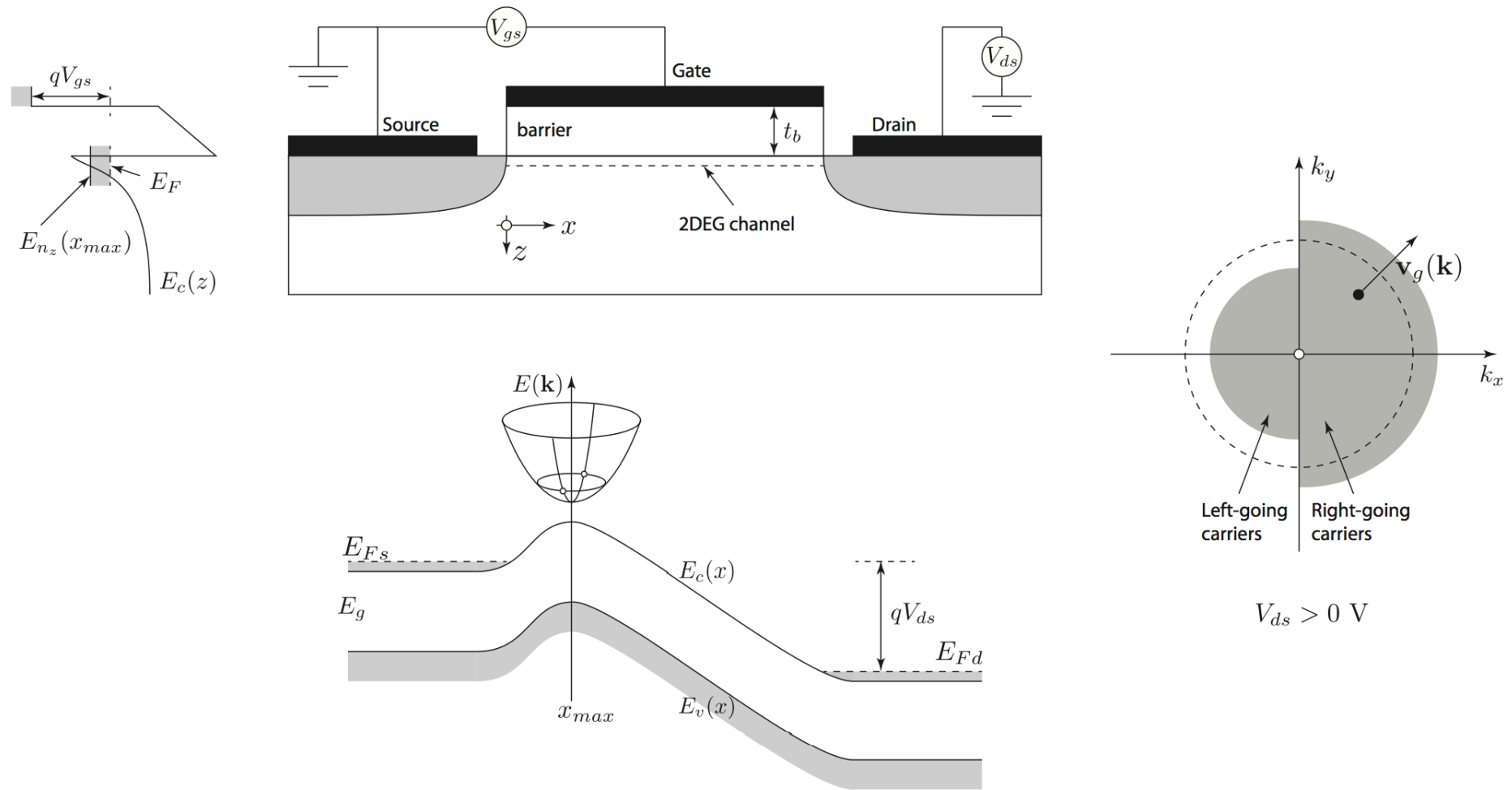
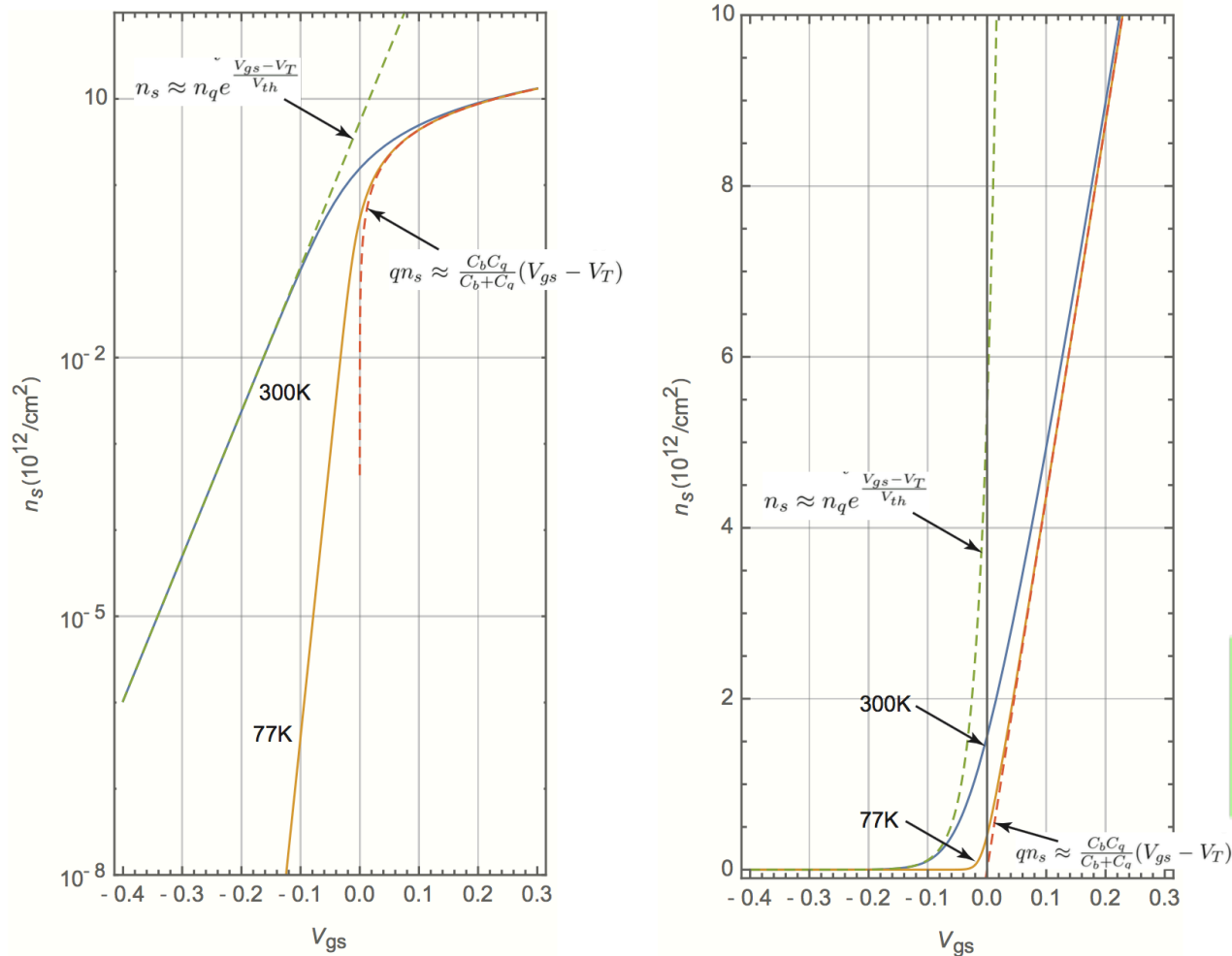


Figure 2: Field effect transistor, energy band diagram, and \mathbf{k} -space occupation of states.

Ballistic Field-Effect Transistor

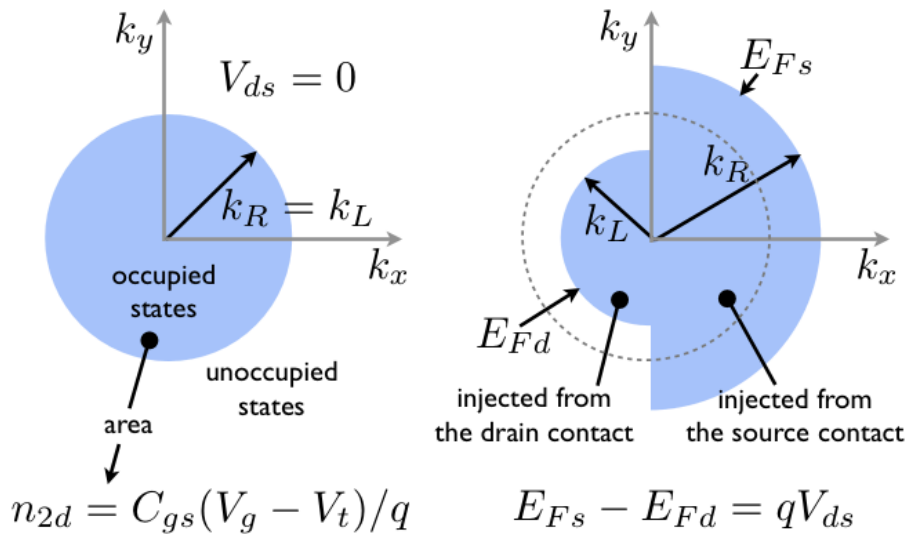
$$\frac{q^2 n_s}{C_b} + kT \ln \left(e^{\frac{q n_s}{C_q V_{th}}} - 1 \right) = q(V_{gs} - V_T) \implies e^{\frac{q n_s}{C_b V_{th}}} \left(e^{\frac{q n_s}{C_q V_{th}}} - 1 \right) = e^{\frac{V_{gs} - V_T}{V_{th}}}$$



2D electron gas density at the injection point of a FET as a function of the gate voltage

FIGURE 10.2: Illustrating the dependence of the 2DEG sheet density at the injection point on the gate voltage.

Ballistic Field-Effect Transistor



- Ballistic FETs are much simpler to understand than long-channel devices based on drift/diffusion.

- 2DEG electron density dependence on V_{ds} & V_g

$$n_{inj} = n_R + n_L = \frac{g_s g_v m^* kT}{4\pi \hbar^2} \left[\ln\left(1 + e^{\frac{E_{fs}}{kT}}\right) + \ln\left(1 + e^{\frac{E_{fd}}{kT}}\right) \right]$$



Thus, $qn_{inj} = C_{gs}(V_{gs} - V_t)$, and $E_{fs} - E_{fd} = qV_{ds}$. Solve these two equations and show that the source quasi-Fermi-level is related to the gate and drain biases through the relation

$$v_s = \frac{E_{fs}}{kT} = \ln\left[\sqrt{(1 + e^{v_d})^2 + 4e^{v_d}(e^\rho - 1)} - (1 + e^{v_d})\right] - \ln[2], \quad (4)$$

where $v_d = V_{ds}/kT$ and $\rho = 4\pi \hbar^2 C_{gs}(V_{gs} - V_t)/qg_s g_v m^* kT$.

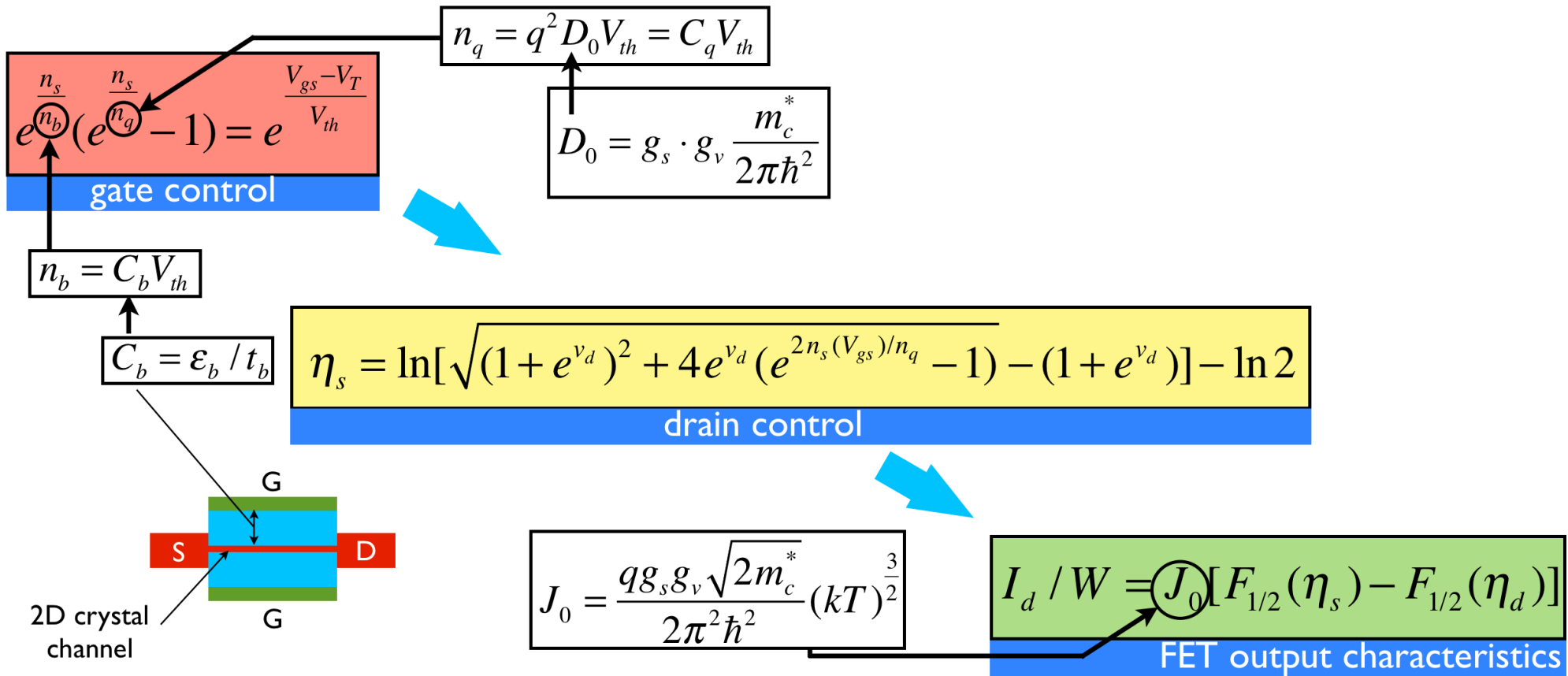


$$\frac{I_d}{W} = q \frac{g_s g_v}{(2\pi)^2} \frac{\hbar}{m^*} \left(\frac{2m^* kT}{\hbar^2}\right)^{\frac{3}{2}} [F_{1/2}(v_s) - F_{1/2}(v_s - v_d)], \quad (5)$$

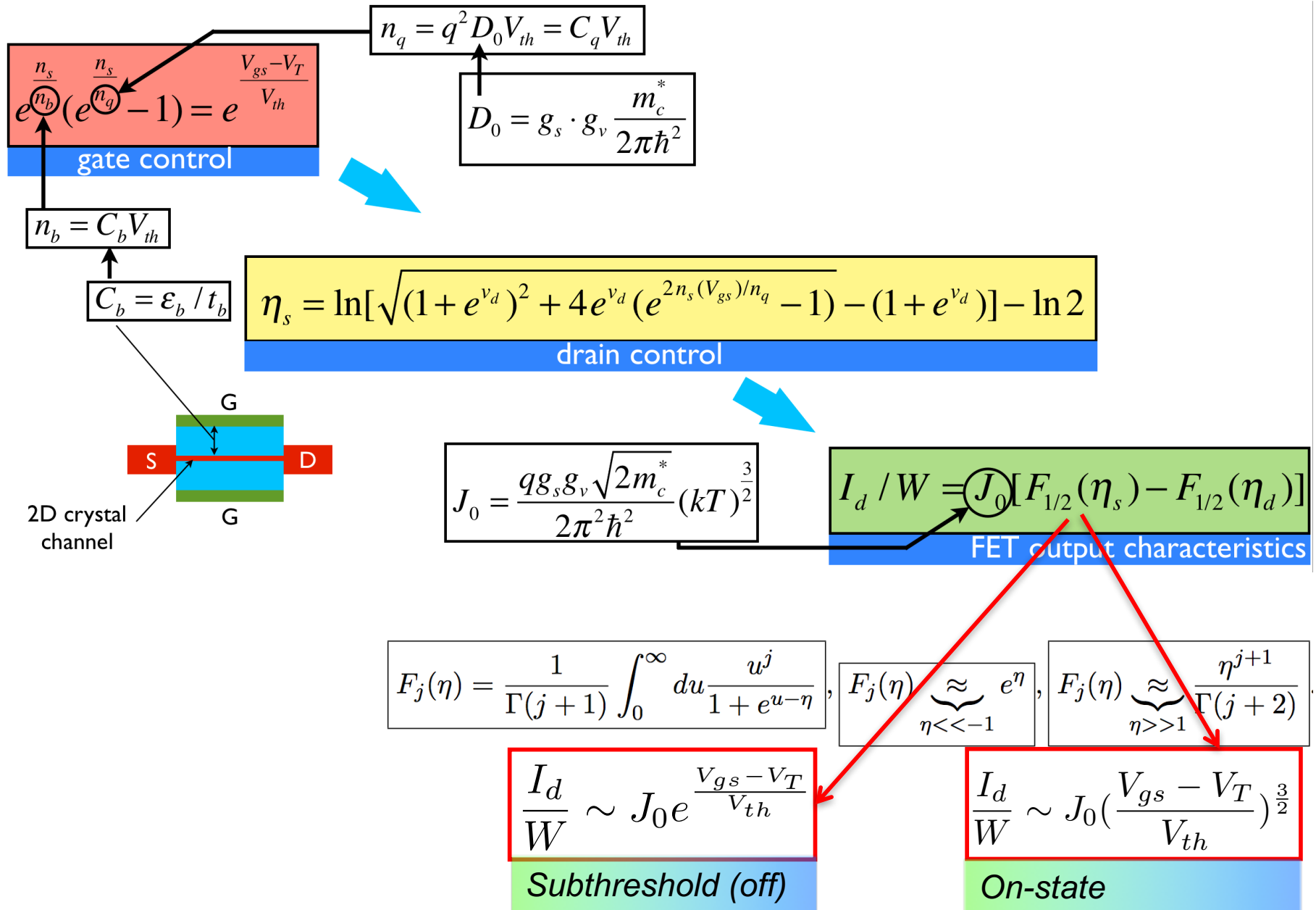
- Ballistic FET current!

where $F_j(x) = 1/\Gamma(j + 1) \int_0^\infty y^j (1 + \exp[y - x])^{-1} dy$ is the Fermi-Dirac integral of order j .

Ballistic Field-Effect Transistor



Ballistic Field-Effect Transistor



Silicon Ballistic Field-Effect Transistor

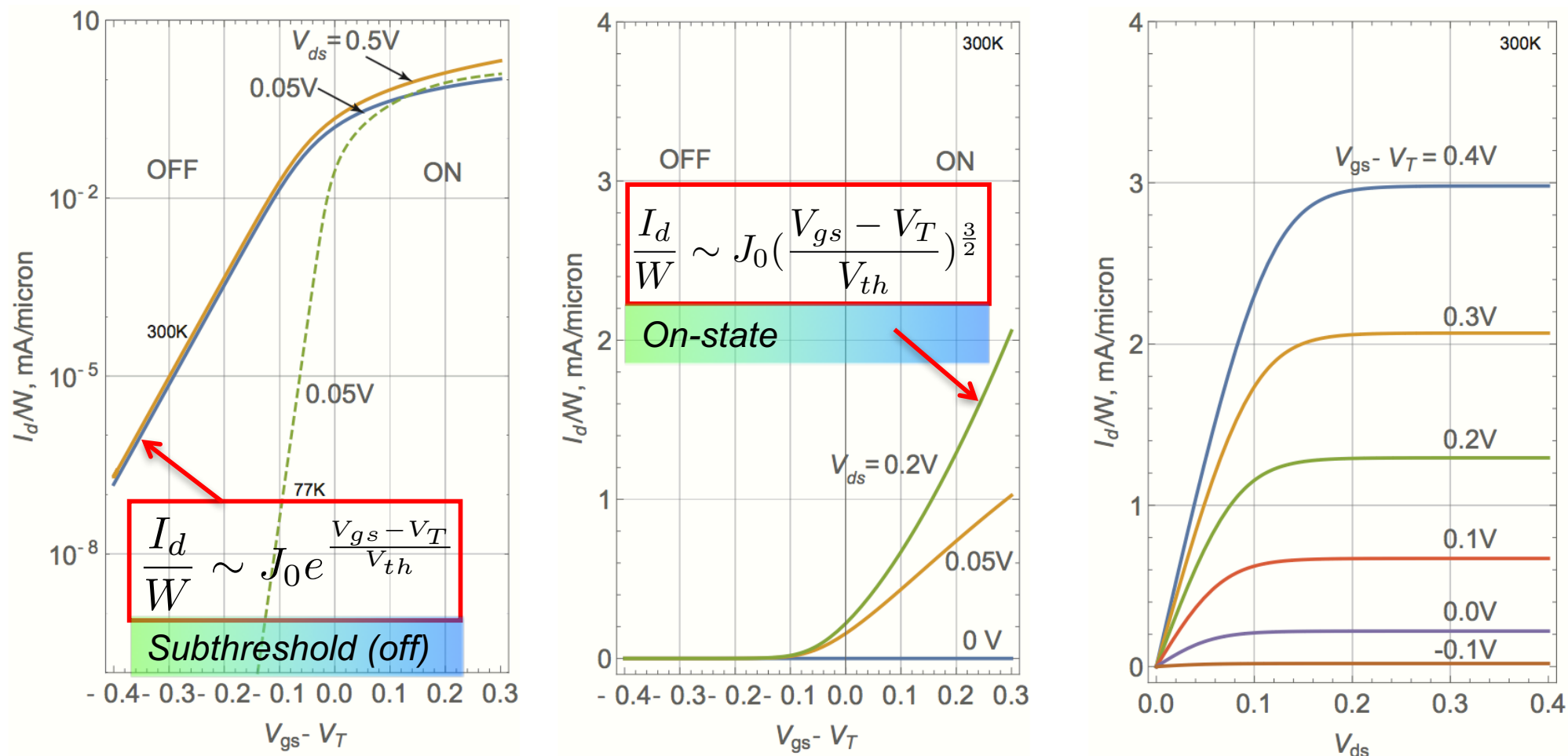


FIGURE 10.4: Ballistic Silicon FET. The device dimensions are $t_b = 1$ nm, $\epsilon_b = 10\epsilon_0$, and for Silicon, $m^* = 0.2m_0$ and $g_v = 2.5$ are used.

- Note the on-off ratio, and the sharper switching at low temperatures. The subthreshold slope is $\sim(kT/q)\ln(10)$.
- This calculation neglects the contact resistance incurred in injecting carriers from 3D source to 2D channel.

Silicon Ballistic Field-Effect Transistor

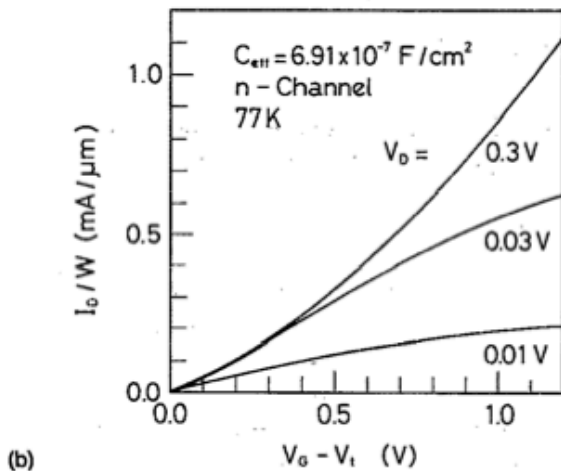
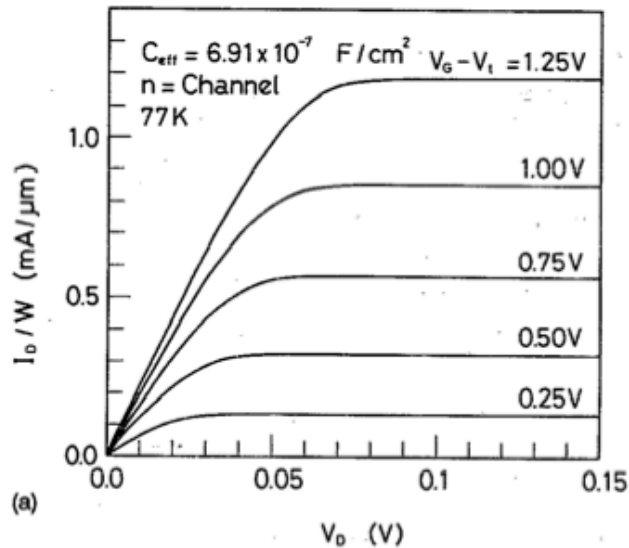


FIG. 5. Calculated examples of I - V characteristics of an n MOSFET on (100) plane. C_{eff} corresponds to effective 5 nm oxide thickness: (a) channel current per unit width vs drain voltage, parameter is the gate voltage; (b) channel current per unit width versus gate voltage, parameter is the drain voltage.

• injection velocity (ensemble averaged)

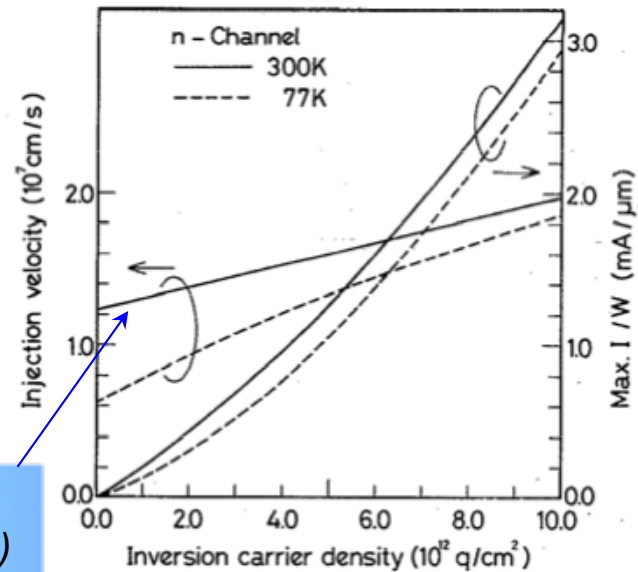


FIG. 8. Saturation current per unit width and the injection velocity of a n MOSFET on (100) plane as functions of inversion carrier density. The current value gives the maximum limit of the MOSFET current.

$$v_{\text{inj}} = \frac{I_{\text{sat}}}{WC_{\text{eff}}(V_G - V_t)}, \quad (31)$$

v_{inj} gives the mean carrier velocity injected from the source to the channel in ballistic MOSFETs, and we will call it the injection velocity. With use of Eq. (24),

$$v_{\text{inj}} = \frac{8\hbar\sqrt{|Q|}}{3m_t\sqrt{q\pi M_v}} = \frac{8\hbar\sqrt{C_{\text{eff}}(V_G - V_t)}}{3m_t\sqrt{q\pi M_v}} \quad (32)$$

when the carriers towards the drain are degenerate. This value is consistent with the fact that the propagating state towards the drain is occupied at x_{max} up to those with the velocity v_f

Ballistic FET vs Vacuum Tube Transport

Space-charge transport of electrons

The saturated current, Eq. (24), is proportional to $(V_G - V_t)^{3/2}$ since the carrier mean velocity is proportional to $\sqrt{|Q|}$, as is the Fermi velocity. The fact that carriers are degenerate Fermi particles plays an important role here. This is in contrast with the classical MOSFET where the saturated current is proportional to $(V_G - V_t)^2$ or $(V_G - V_t)$.

The ballistic current in the bulk material reminds us of the space charge limited current expressed by the 3/2 power law¹⁹ of Langmuir's equation. The geometry of the MOSFET is different from those that are assumed in these bulk type current structures, but a similar simple discussion is attempted so that we may be able to gain some insight into the resultant potential variation along the channel. Suppose that the carrier transport is ballistic and the channel length is not as short. The channel potential variation along the x axis measured from the value at the source edge is denoted by $\Delta\phi(x)$ [$\Delta\phi(0)=0$]. The carrier mean velocity at $x, v(x)$, is related to $\Delta\phi(x)$ as

$$\frac{1}{2}mv(0)^2 = \frac{1}{2}mv(x)^2 + \Delta\phi(x), \quad (34)$$

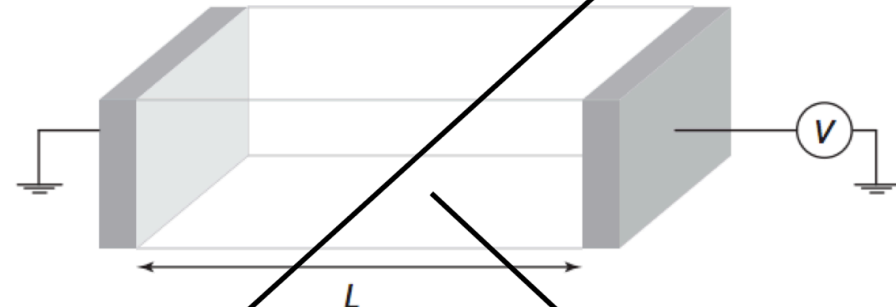
where m is the carrier effective mass. The current continuity condition requires that

$$I = qWn(x)v(x). \quad (35)$$

Ballistic metal-oxide-semiconductor field effect transistor

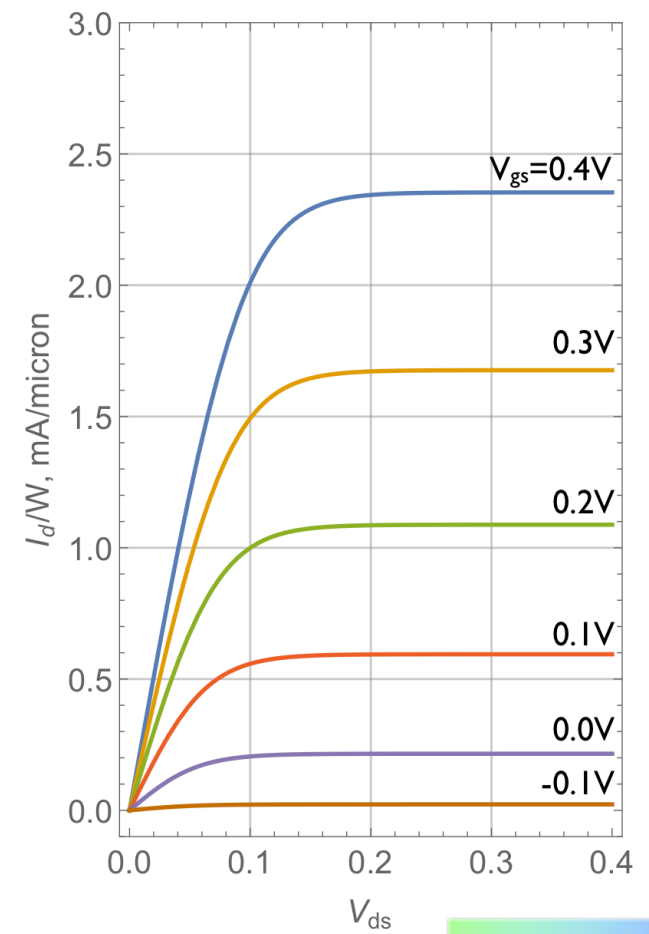
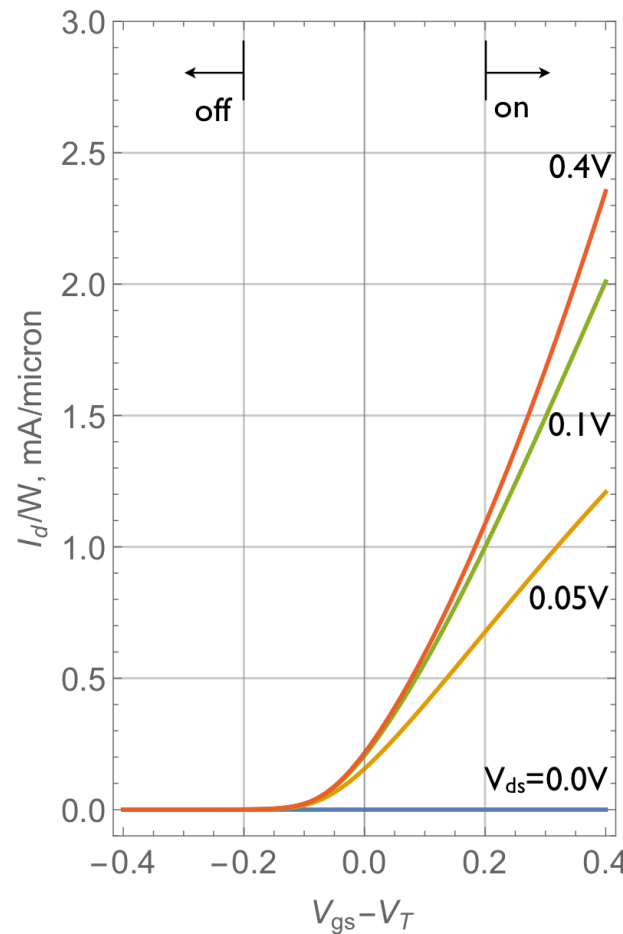
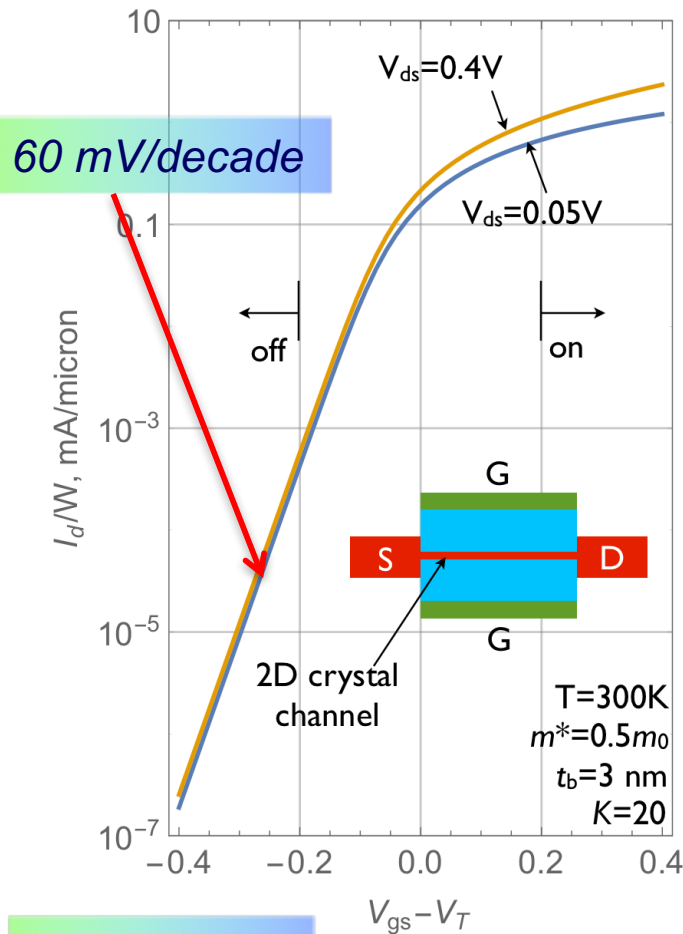
Kenji Natori
Institute of Applied Physics, University of Tsukuba, Tsukuba, Ibaraki 305, Japan
(Received 14 March 1994; accepted for publication 6 July 1994)

$$I_{\text{sat}} = W \frac{8\hbar|Q|^{3/2}}{3m_t\sqrt{q\pi M_v}} = W \frac{8\hbar[C_{\text{eff}}(V_G - V_t)]^{3/2}}{3m_t\sqrt{q\pi M_v}}. \quad (24)$$



- 1) Ballistic Limit: $J_{\text{ballistic}}^{sc} \propto V^{3/2}$ ← vacuum
- 2) Mott-Gurney, diffusive limit: $J_{\text{diff}}^{sc} \propto V^2$ ← insulator, low field
- 3) Saturated diffusive limit: $J_{\text{sat}}^{sc} \propto V$ ← insulator, high field

A 2D Crystal Channel Ballistic FET



subthreshold

$$n_s \approx \left(\frac{C_q V_{th}}{q} \right) \cdot e^{\frac{V_{gs}-V_T}{V_{th}}}$$

$$\frac{V_{gs}-V_T}{V_{th}} \ll -1$$

$$e^{\frac{qn_s}{C_b V_{th}}} \left(e^{\frac{qn_s}{C_q V_{th}}} - 1 \right) = e^{\frac{V_{gs}-V_T}{V_{th}}}$$

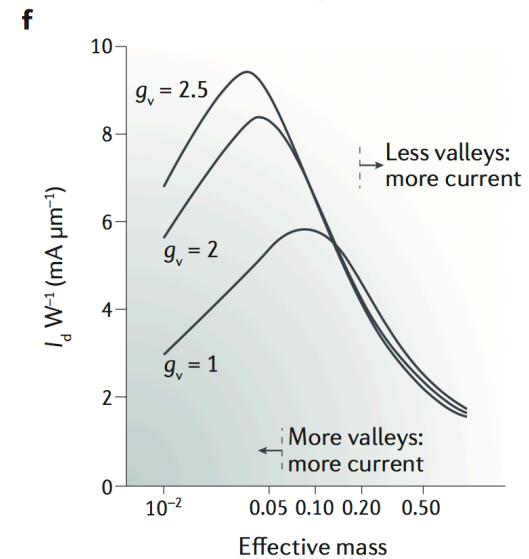
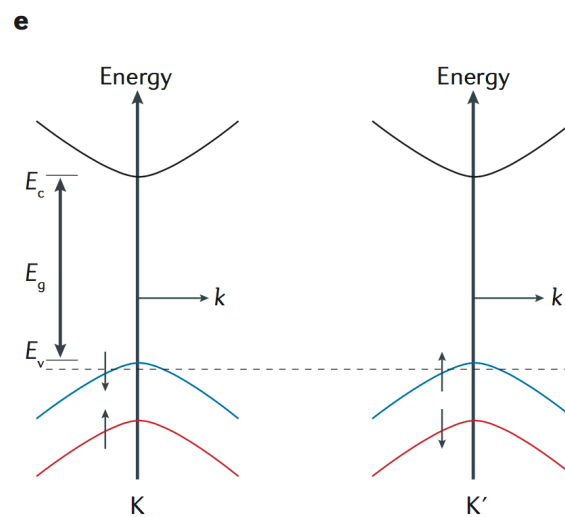
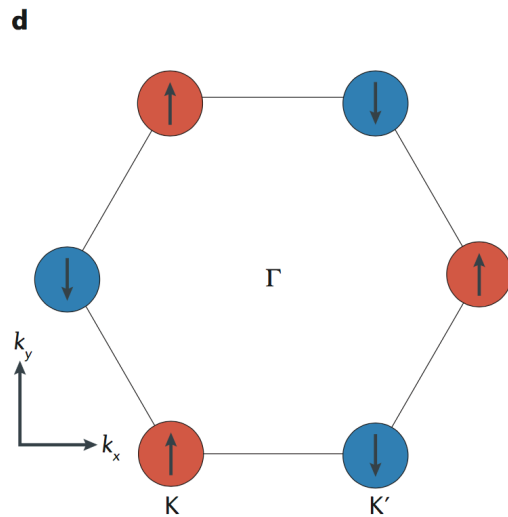
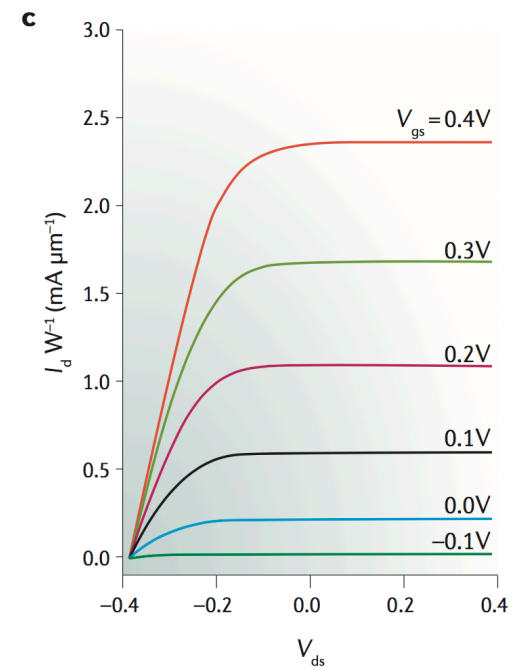
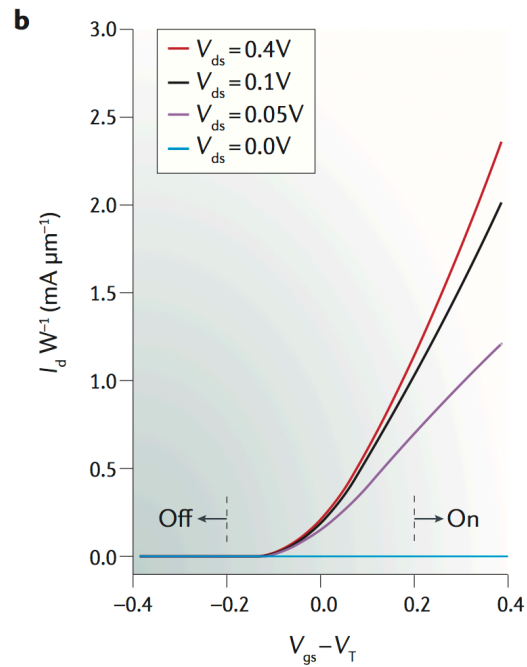
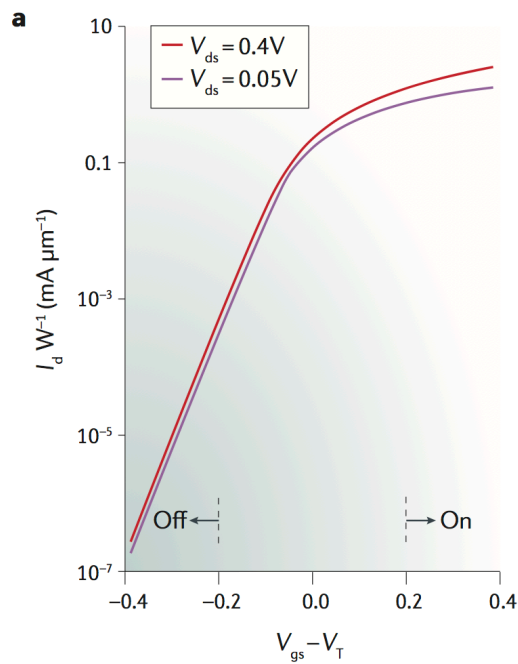
$$\frac{V_{gs}-V_T}{V_{th}} \gg +1$$

On-state

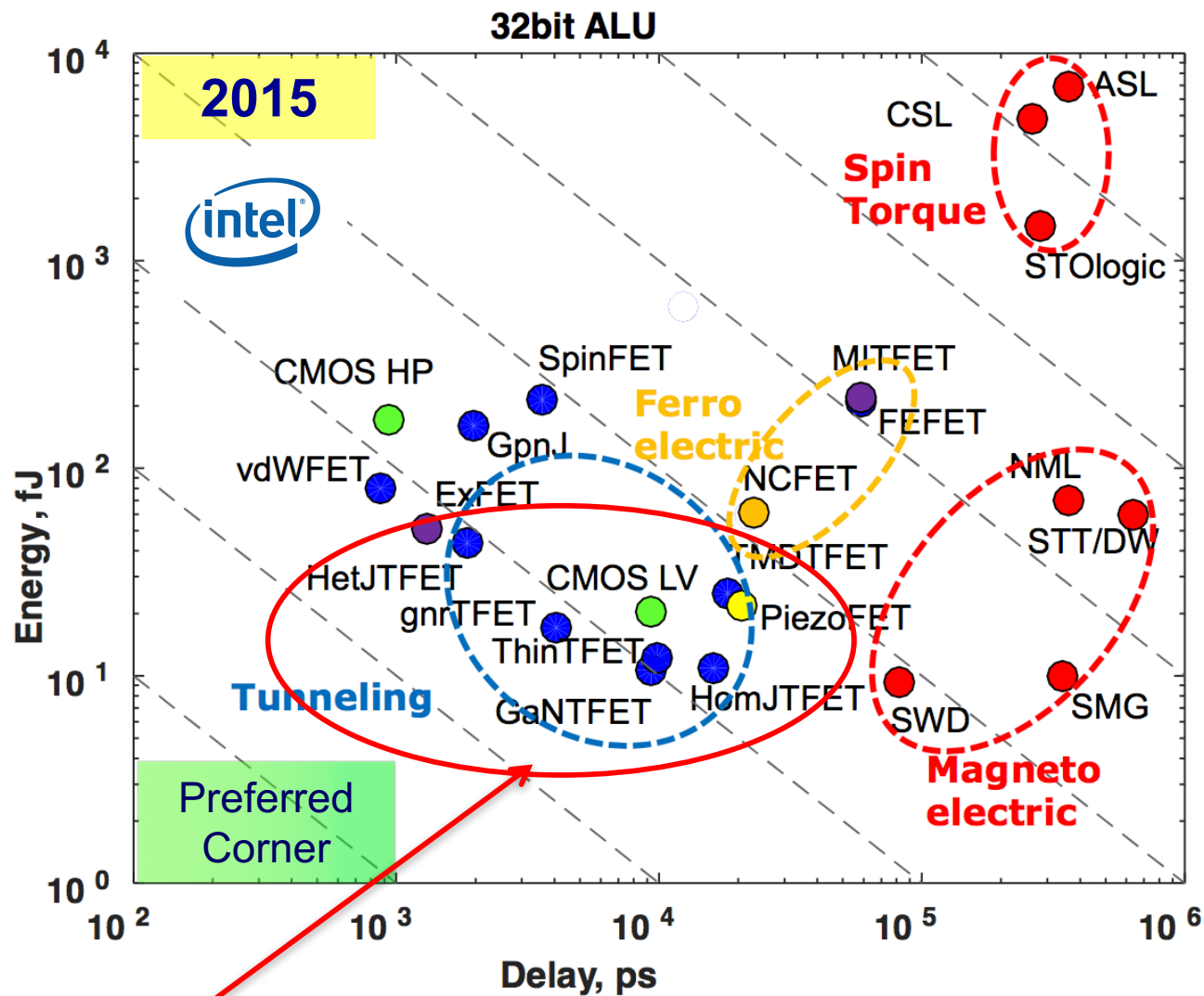
$$n_s \approx \frac{1}{q} \frac{C_b C_q}{C_b + C_q} (V_{gs} - V_T)$$

- Note the on-off ratio, and the sharper switching at low temperatures. The subthreshold slope is $\sim (kT/q)\ln(10)$.
- This calculation neglects the contact resistance incurred in injecting carriers from 3D source to 2D channel.

Ballistic FET limits



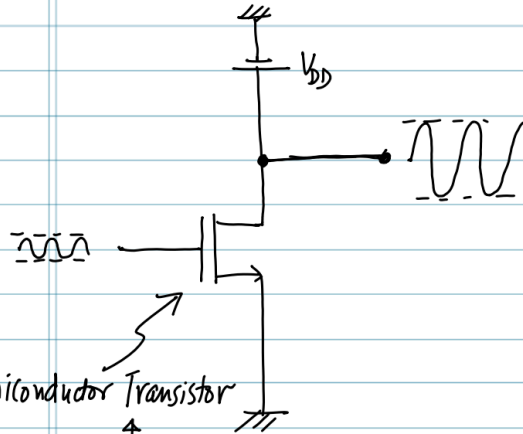
How good can GaN TFETs be?



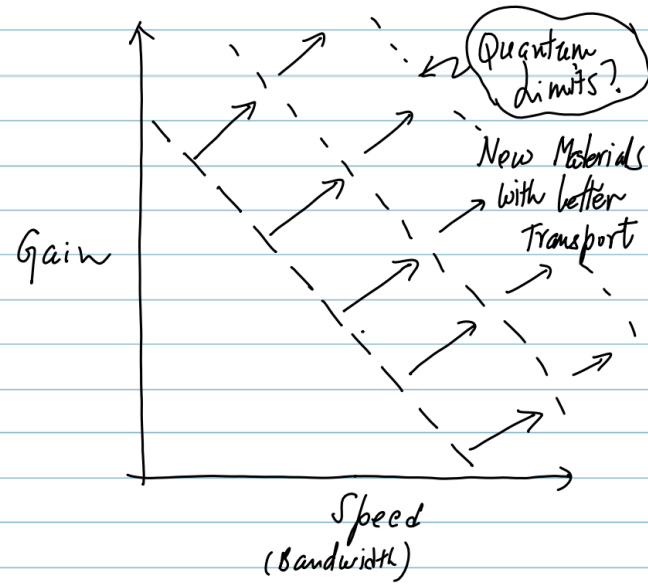
- Tunnel-FETs have the potential to beat the 60 mV/decade limit in switching

How can one go below the 60 mV/decade limit?

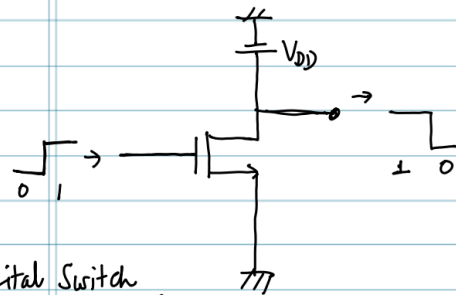
Communication Devices



- Semiconductor Transistor
- Vacuum tube

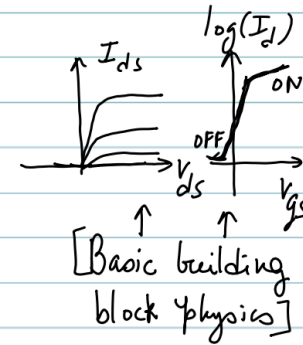
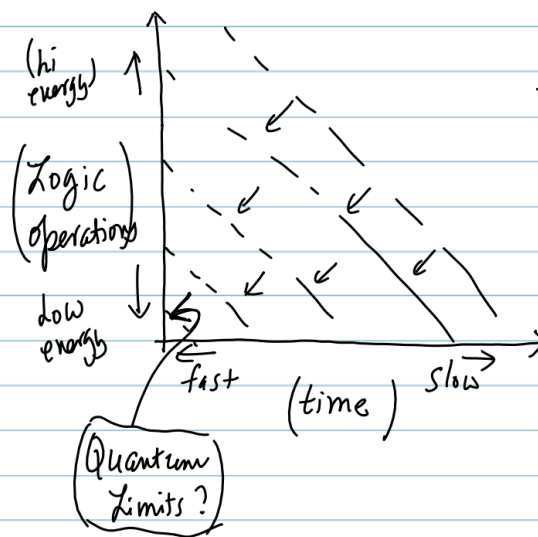


Logic Devices

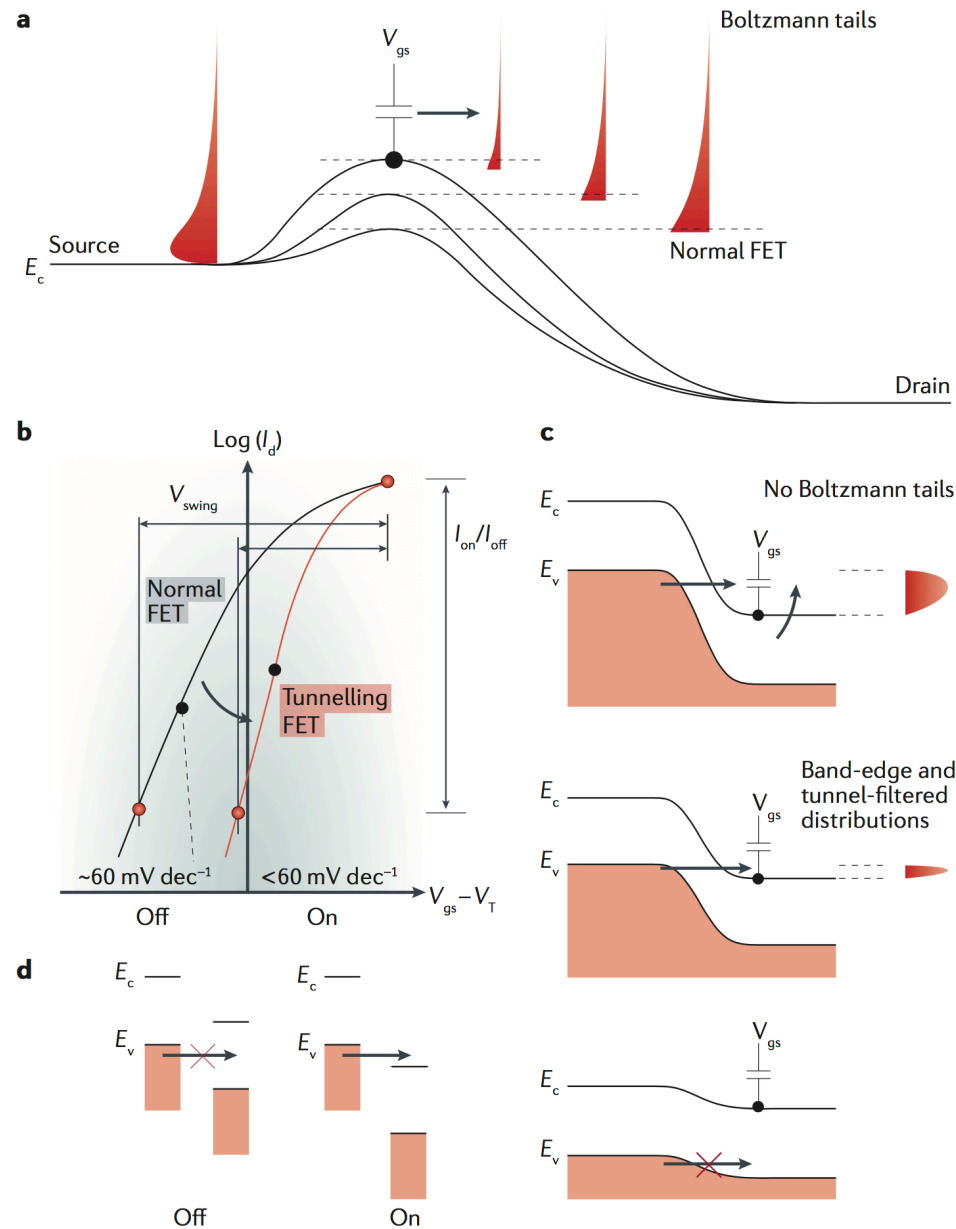


- Digital Switch
- Mechanical relay

- Charge-based
- Spin-based
- Correlated / Phase Transitions.



How can go below the 60 mV/decade limit?



Equilibrium at contacts

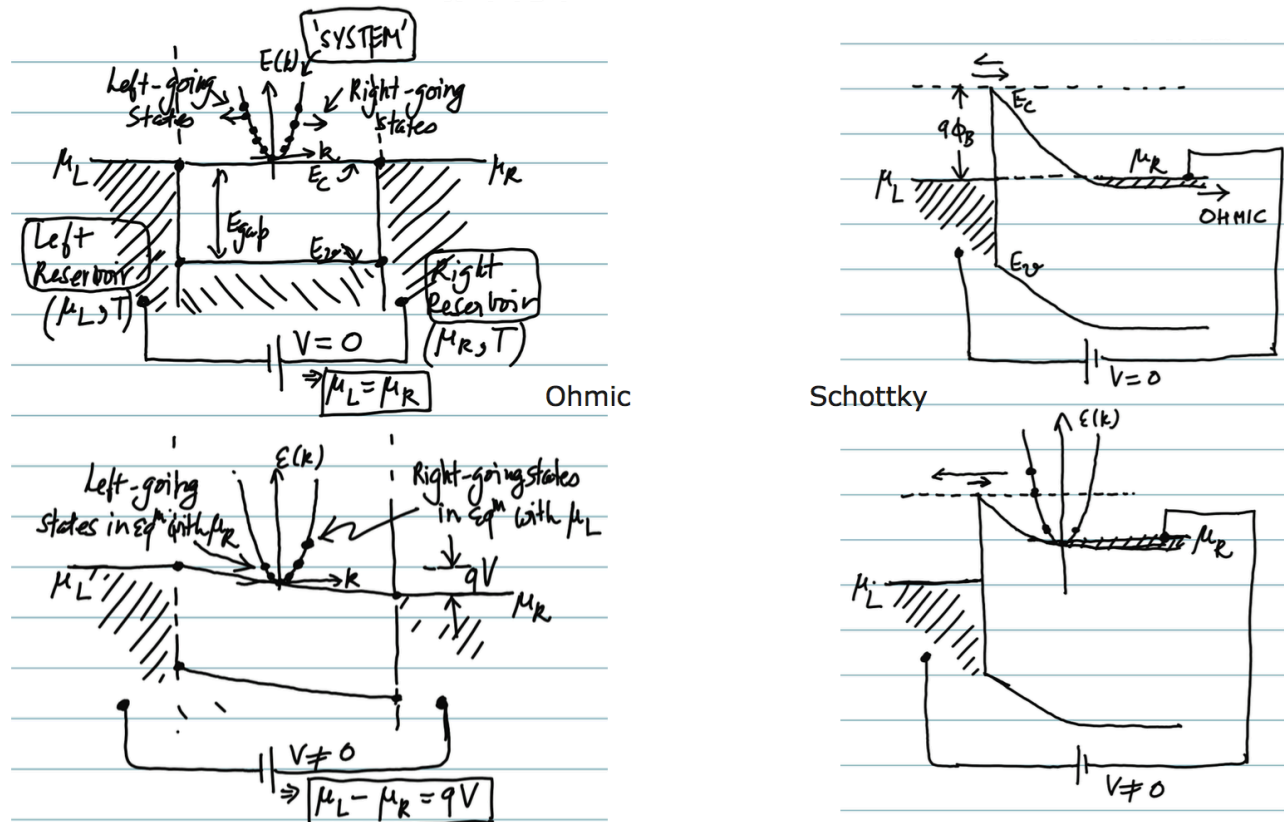


FIGURE 6.6: Illustration of the concept of equilibrium for Ohmic and Schottky contacts between metals and semiconductors.

- Electrons states in the metal contact reservoirs try bringing the “semiconductor” channel electron states in equilibrium with them by particle (or energy) transfer
- States in equilibrium share the same chemical potential, and their $f(k)$ is thus known
- Multiple contacts with different chemical potentials bring parts of channel states to equilibrium with themselves; the net current flows if there is an imbalance in current carrying states

Equilibrium at multicarrier junctions

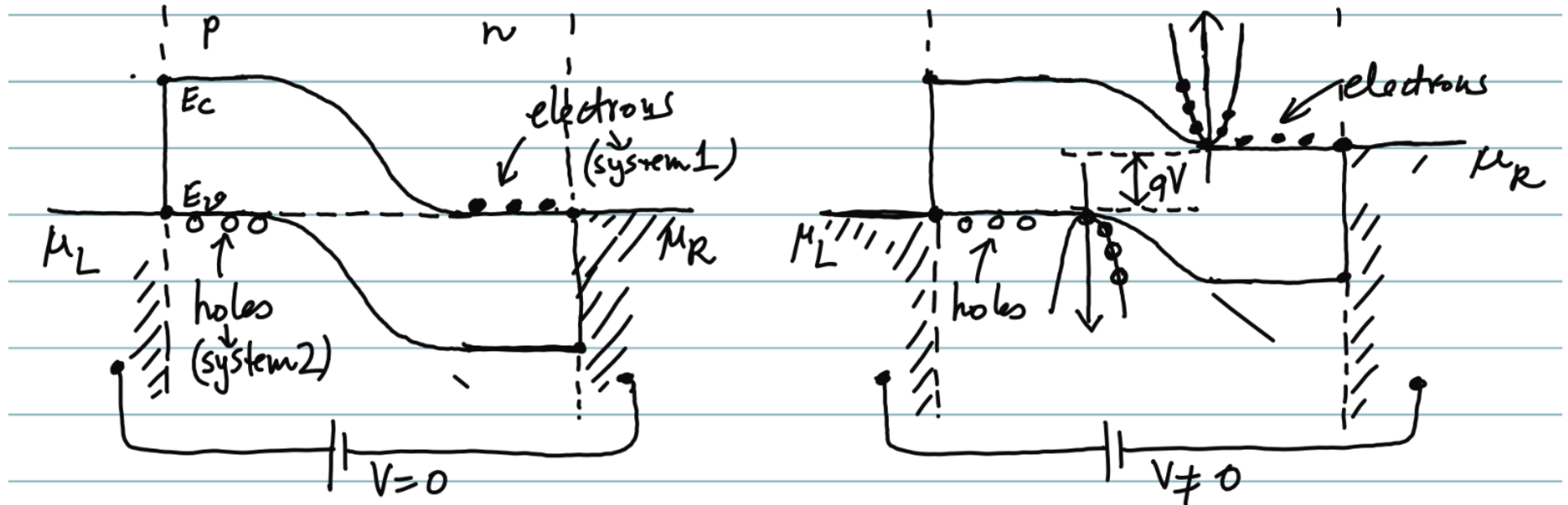


FIGURE 6.7: Illustration of the concept of equilibrium for p-n junctions.

- Electrons states in the metal contact reservoirs try bringing the “semiconductor” channel electron states in equilibrium with them by particle (or energy) transfer
- States in equilibrium share the same chemical potential, and their $f(k)$ is thus known
- Multiple contacts with different chemical potentials bring parts of channel states to equilibrium with themselves; the net current flows if there is an imbalance in current carrying states

Equilibrium in Transistors

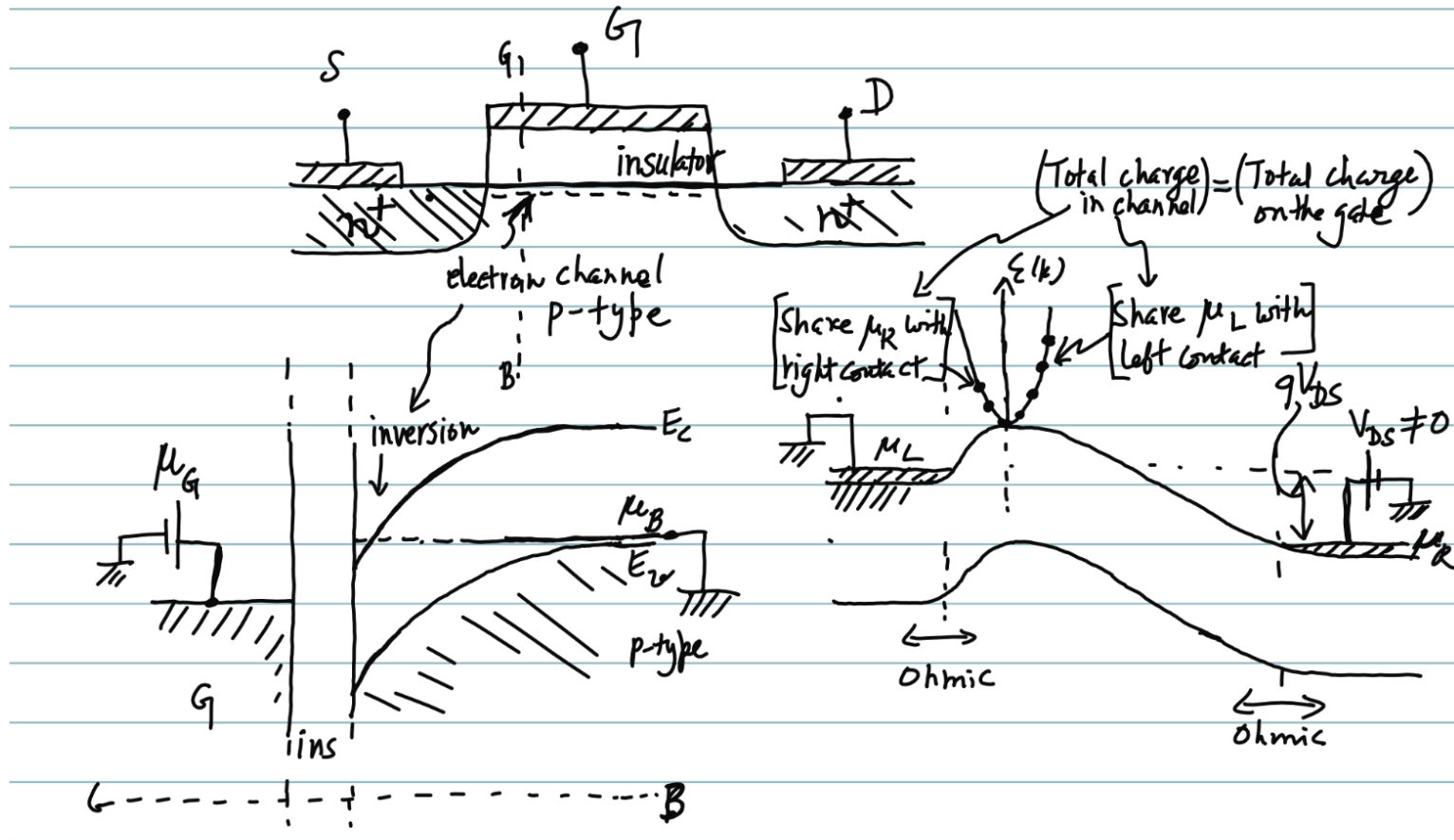


FIGURE 6.8: Illustration of the concept of equilibrium for a 3-terminal MOSFET

- Electrons states in the metal contact reservoirs try bringing the “semiconductor” channel electron states in equilibrium with them by particle (or energy) transfer
- States in equilibrium share the same chemical potential, and their $f(k)$ is thus known
- Multiple contacts with different chemical potentials bring parts of channel states to equilibrium with themselves; the net current flows if there is an imbalance in current carrying states

Outline

- *Part I: Review of fundamentals*

- 1: Review of classical and quantum mechanics

- 2: Current flow in quantum mechanics

- 3: Quantum statistics, quest for equilibrium as the driver for transport

- *Part II: Single-particle transport*

- 4: Ballistic transport: Quantized conductance, Ballistic MOSFETs

- 5: Transmission and tunneling, Tunneling FETs

- 6. Closed vs. open systems, the Non-Equilibrium Green's Function approach to transport

- 7. Diffusive transport: Boltzmann transport equation, scattering, electron-phonon interactions

- 8. High-field effects, Gunn diodes and oscillators for high-frequency power

- 9. Feynman path integrals, Aharonov-Bohm effect, Weak Localization

- *Part III: Geometrical and topological quantum mechanics, unification with relativity*

- 10: Spin, transport in a magnetic field, Quantum Hall effect, Berry phase in quantum mechanics

- 11: Chern numbers, Edge/Topological states, Topological insulators and Majorana Fermions

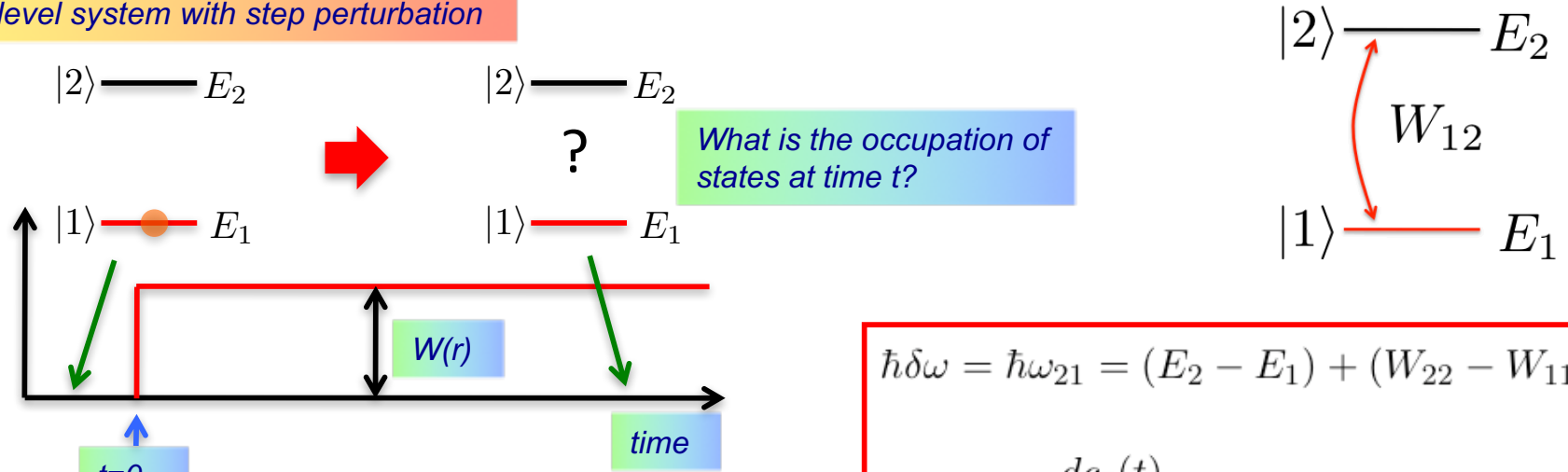
- *Part IV: Many-particle correlated transport*

- 12: Fock-space way of thinking transport, second quantization, conductance anomalies

- 13: BCS theory of superconductivity, Josephson junctions, Phase transitions and broken symmetries

Example: Exactly solvable 2-state problem

Simplest case: A 2-level system with step perturbation



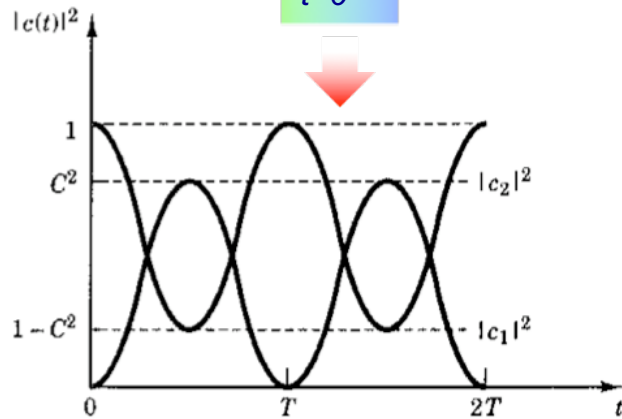
Perturbation: $W(r,t)$

What is the occupation of states at time t ?

$$\hbar\delta\omega = \hbar\omega_{21} = (E_2 - E_1) + (W_{22} - W_{11})$$

$$i\hbar \frac{dc_2(t)}{dt} = c_1(t)e^{i\delta\omega t}W_{21}$$

$$i\hbar \frac{dc_1(t)}{dt} = c_2(t)e^{-i\delta\omega t}W_{12}$$



$$|c_1(t)|^2 = 1 - C^2 \sin^2 \Omega t$$

$$|c_2(t)|^2 = C^2 \sin^2 \Omega t$$

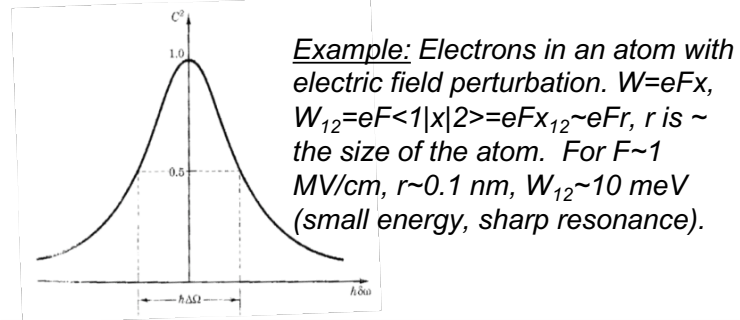
$$C^2 = \frac{|W_{12}|^2}{(\frac{1}{2}\hbar\delta\omega)^2 + |W_{12}|^2}$$

$$\omega = \pm\Omega = \pm\sqrt{\frac{|W_{12}|^2}{\hbar^2} + (\frac{1}{2}\delta\omega)^2}$$

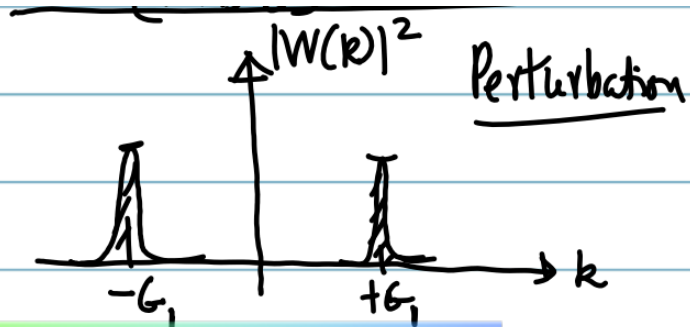
setting $c_1(t) = b_1 e^{i(\omega - \frac{1}{2}\delta\omega)t}$ and $c_2(t) = b_2 e^{i(\omega + \frac{1}{2}\delta\omega)t}$ to get

$$b_1\hbar(\omega - \frac{1}{2}\delta\omega) + b_2W_{21} = 0$$

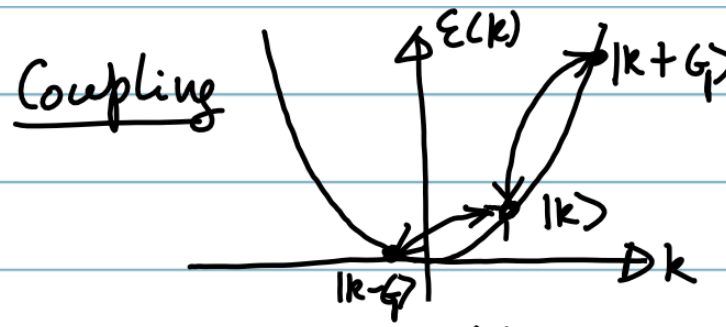
$$b_1W_{12} + b_2\hbar(\omega + \frac{1}{2}\delta\omega) = 0$$



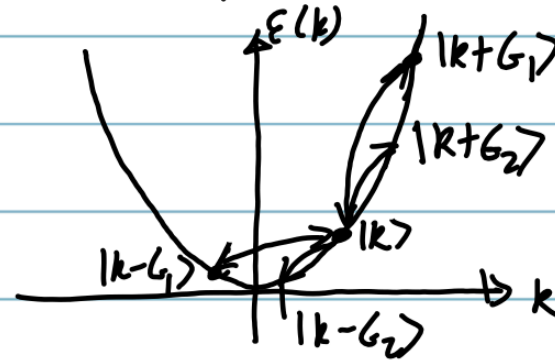
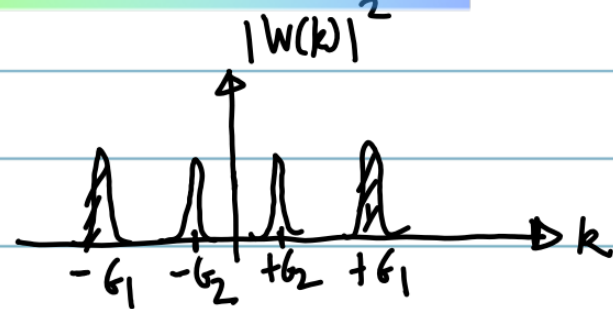
The idea behind "Scattering"



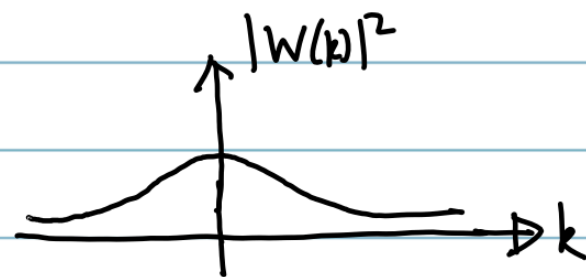
Discrete, specific frequencies



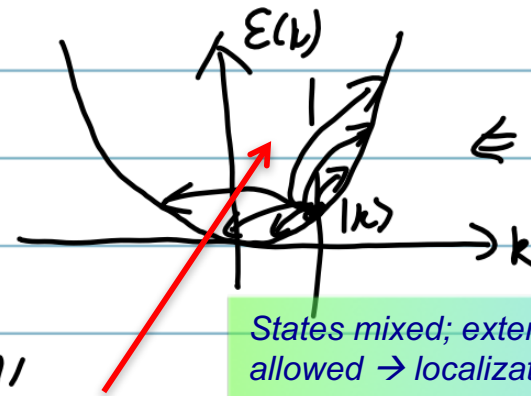
$|k\rangle$ couples to only $|k+G\rangle$ & $|k-G\rangle$..



"Bands" and "Gaps"



Continuous, all weights



$|k\rangle$ couples to all states

States mixed; extended states may not be allowed \rightarrow localization, but gaps still possible

"SCATTERING"

Time-dependent perturbation theory

$$i\hbar \frac{\partial}{\partial t} |\Psi_t\rangle = H_0 |\Psi_t\rangle$$

Unperturbed problem

$$i\hbar \frac{\partial}{\partial t} |\Psi_t\rangle = [H_0 + W_t] |\Psi_t\rangle$$

Time-dependent perturbation

Perturbation

transformation

$$|\Psi_t\rangle = e^{-i\frac{H_0}{\hbar}t} |\Psi(t)\rangle$$

H_0 is the Hamiltonian operator.

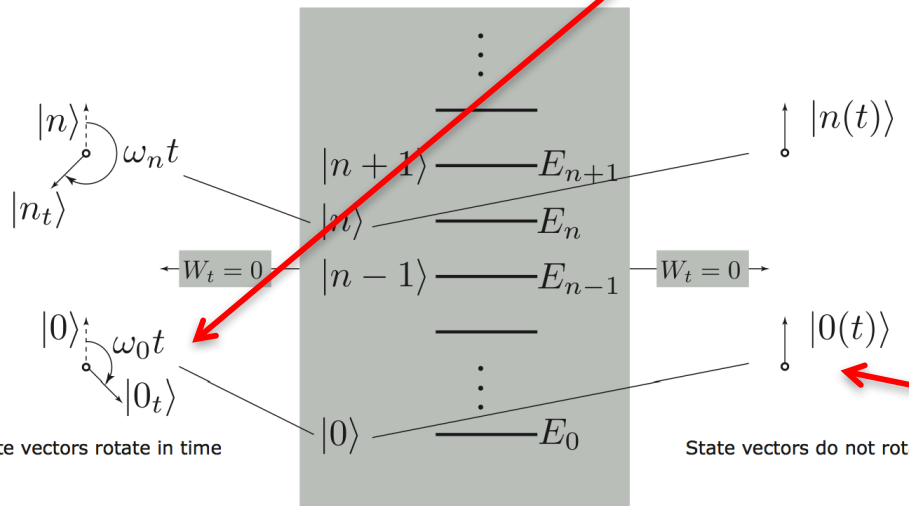
If the system was in an eigenstate $|\Psi_{t_0}\rangle = |0\rangle$ of energy E_0 at time t_0 , then the state at a future time differs from the initial state by a phase factor

$$H_0 |\Psi_{t_0}\rangle = E_0 |\Psi_{t_0}\rangle \implies |\Psi_t\rangle = e^{-i\frac{E_0}{\hbar}(t-t_0)} |\Psi_{t_0}\rangle.$$

$$i\hbar \left(-\frac{i}{\hbar} H_0 e^{-i\frac{H_0}{\hbar}t} |\Psi(t)\rangle + e^{-i\frac{H_0}{\hbar}t} \frac{\partial}{\partial t} |\Psi(t)\rangle \right) = [H_0 + W_t] e^{-i\frac{H_0}{\hbar}t} |\Psi(t)\rangle$$

$$i\hbar \frac{\partial}{\partial t} |\Psi(t)\rangle = [e^{+i\frac{H_0}{\hbar}t} W_t e^{-i\frac{H_0}{\hbar}t}] |\Psi(t)\rangle = W(t) |\Psi(t)\rangle$$

Time-dependent evolution in the Interaction picture



$$W_t = 0 \implies W(t) = 0 \implies i\hbar \frac{\partial |\Psi(t)\rangle}{\partial t} = 0$$

$$|\Psi(t)\rangle = |\Psi(t_0)\rangle$$

If $W=0$, the state vector does not rotate in time in the interaction picture.

$ \Psi_t\rangle$	$ \Psi(t)\rangle$
$ \Psi_t\rangle = e^{-i\frac{H_0}{\hbar}t} \Psi(t)\rangle$ Transformation	
$i\hbar \frac{\partial}{\partial t} \Psi_t\rangle = [H_0 + W_t] \Psi_t\rangle$	$i\hbar \frac{\partial}{\partial t} \Psi(t)\rangle = \underbrace{[e^{-i\frac{H_0}{\hbar}t} W_t e^{-i\frac{H_0}{\hbar}t}]}_{W(t)} \Psi(t)\rangle$
Schrodinger picture	Interaction picture

$$i\hbar \frac{\partial}{\partial t} |\Psi(t)\rangle = W(t) |\Psi(t)\rangle$$

$$|\Psi(t)\rangle = |\Psi(t_0)\rangle + \frac{1}{i\hbar} \int_{t_0}^t dt' W(t') |\Psi(t')\rangle$$

Starting point for time-dependent perturbation theory

FIGURE 24.1: Schrodinger vs. Interaction pictures of time-evolution of quantum state.

Time-dependent perturbation theory

$$|\Psi(t)\rangle = |\Psi(t_0)\rangle + \frac{1}{i\hbar} \int_{t_0}^t dt' W(t') \left[|\Psi(t_0)\rangle + \frac{1}{i\hbar} \int_{t_0}^{t'} dt'' W(t'') |\Psi(t'')\rangle \right]$$

$$|\Psi(t)\rangle = |\Psi(t_0)\rangle + \frac{1}{i\hbar} \int_{t_0}^t dt' W(t') |\Psi(t')\rangle$$

Starting point for time-dependent perturbation theory

$$|\Psi(t)\rangle = \underbrace{|\Psi(t_0)\rangle}_{\sim W^0} + \underbrace{\frac{1}{i\hbar} \int_{t_0}^t dt' W(t') |\Psi(t_0)\rangle}_{\sim W^1} + \underbrace{\frac{1}{(i\hbar)^2} \int_{t_0}^t dt' W(t') \int_{t_0}^{t'} dt'' W(t'') |\Psi(t_0)\rangle}_{\sim W^2} + \dots$$

$$W(t) = e^{+i\frac{H_0}{\hbar}t} W_t e^{-i\frac{H_0}{\hbar}t}$$

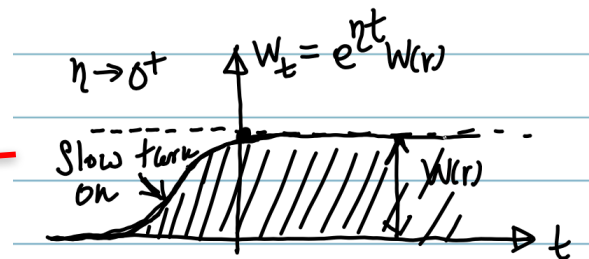
Approximation: retain terms to 1st order in perturbation W

Let $|\Psi(t_0)\rangle = |0\rangle$ be the initial state of the quantum system.

$$\langle n|\Psi(t)\rangle \approx \underbrace{\langle n|0\rangle}_{=0} + \frac{1}{i\hbar} \int_{t_0}^t dt' \langle n|W(t')|0\rangle = \frac{1}{i\hbar} \int_{t_0}^t dt' \langle n|e^{+i\frac{H_0}{\hbar}t'} W_t e^{-i\frac{H_0}{\hbar}t'} |0\rangle$$

Assume that the perturbation is turned on 'slowly'

$$W_t = e^{\eta t} W \quad \eta = 0^+, \text{ and } W = W(r)$$



$$\langle n|\Psi(t)\rangle \approx \frac{1}{i\hbar} \int_{t_0}^t dt' \underbrace{\langle n|e^{+i\frac{H_0}{\hbar}t'}}_{e^{+i\frac{E_n}{\hbar}t'} \langle n|} e^{\eta t'} W \underbrace{e^{-i\frac{H_0}{\hbar}t'} |0\rangle}_{e^{-i\frac{E_0}{\hbar}t'} |0\rangle} = \frac{\langle n|W|0\rangle}{i\hbar} \int_{t_0}^t dt' e^{i\left(\frac{E_n - E_0}{\hbar}\right)t'} e^{\eta t'}$$

$$\int_{t_0}^t dt' e^{i\left(\frac{E_n - E_0}{\hbar}\right)t'} e^{\eta t'} = \frac{e^{i\left(\frac{E_n - E_0}{\hbar}\right)t} e^{\eta t} - e^{i\left(\frac{E_n - E_0}{\hbar}\right)t_0} e^{\eta t_0}}{i\left(\frac{E_n - E_0}{\hbar}\right) + \eta} \underset{t_0 \rightarrow -\infty}{=} \frac{e^{i\left(\frac{E_n - E_0}{\hbar}\right)t} e^{\eta t}}{i\left(\frac{E_n - E_0}{\hbar}\right) + \eta}$$

Probability that the system is in state n at time t

$$\langle n|\Psi(t)\rangle \approx \frac{\langle n|W|0\rangle}{i\hbar} \cdot \frac{e^{i\left(\frac{E_n - E_0}{\hbar}\right)t} e^{\eta t}}{i\left(\frac{E_n - E_0}{\hbar}\right) + \eta} = \langle n|W|0\rangle \cdot \frac{e^{i\left(\frac{E_n - E_0}{\hbar}\right)t} e^{\eta t}}{(E_0 - E_n) + i\hbar\eta}$$

$$|\langle n|\Psi_t\rangle|^2 = |\langle n|\Psi(t)\rangle|^2 \approx |\langle n|W|0\rangle|^2 \frac{e^{2\eta t}}{(E_0 - E_n)^2 + (\hbar\eta)^2}$$

Time-dependent perturbation theory

The *probability* of the state making a transition from $|0\rangle$ to $|n\rangle$ at time t is

$$|\langle n|\Psi_t\rangle|^2 = |\langle n|\Psi(t)\rangle|^2 \approx |\langle n|W|0\rangle|^2 \frac{e^{2\eta t}}{(E_0 - E_n)^2 + (\hbar\eta)^2}.$$

The *rate* of transitions from state $|0\rangle \rightarrow |n\rangle$ is

$$\frac{1}{\tau_{|0\rangle \rightarrow |n\rangle}} = \frac{d}{dt} |\langle n|\Psi(t)\rangle|^2 \approx |\langle n|W|0\rangle|^2 \left(\frac{2\eta}{(E_0 - E_n)^2 + (\hbar\eta)^2} \right) e^{2\eta t}.$$

$$\lim_{\eta \rightarrow 0^+} \frac{2\eta}{x^2 + \eta^2} = \lim_{\eta \rightarrow 0^+} \frac{1}{i} \left[\frac{1}{x - i\eta} - \frac{1}{x + i\eta} \right] = 2\pi\delta(x)$$

$$\delta(ax) = \delta(x)/|a|$$

$$\frac{1}{\tau_{|0\rangle \rightarrow |n\rangle}} \approx \frac{2\pi}{\hbar} |\langle n|W|0\rangle|^2 \delta(E_0 - E_n),$$

Fermi's golden rule for time-varying potentials

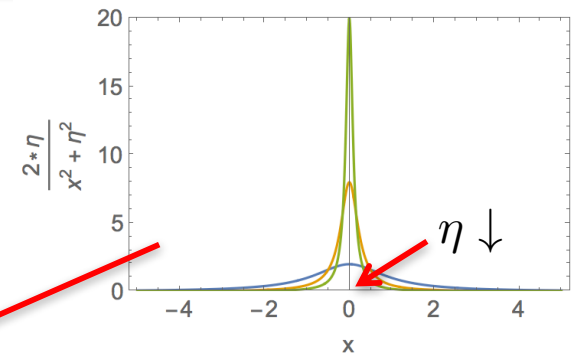
Perturbations oscillating in time

$$W_t = 2W e^{i\omega t} \cos(\omega t) = e^{\eta t} W (e^{i\omega t} + e^{-i\omega t})$$

$$\langle n|\Psi(t)\rangle \approx \frac{\langle n|W|0\rangle}{i\hbar} \left(\int_{t_0}^t dt' e^{i\left(\frac{E_n - E_0 + \hbar\omega}{\hbar}\right)t'} e^{\eta t'} + \int_{t_0}^t dt' e^{i\left(\frac{E_n - E_0 - \hbar\omega}{\hbar}\right)t'} e^{\eta t'} \right)$$

$$\frac{1}{\tau_{|0\rangle \rightarrow |n\rangle}} \approx \frac{2\pi}{\hbar} \times |\langle n|W|0\rangle|^2 \times \left[\underbrace{\delta(E_0 - E_n + \hbar\omega)}_{\text{absorption}} + \underbrace{\delta(E_0 - E_n - \hbar\omega)}_{\text{emission}} \right].$$

Fermi's golden rule for oscillating potentials



$$\begin{aligned} \theta(\omega) &= \int_0^{\infty} dt e^{i\omega t} = \lim_{\eta \rightarrow 0^+} \int_0^{\infty} dt e^{-\eta t} e^{i\omega t} \\ &= \lim_{\eta \rightarrow 0^+} \frac{i}{\omega + i\eta} = \frac{i}{\omega^+} \end{aligned}$$

Two useful results to be used extensively later!

$$\begin{aligned} \frac{1}{\omega^+} &= P\left[\frac{1}{\omega}\right] - i\pi\delta(\omega) \rightarrow \\ \int_{-\infty}^{+\infty} d\omega \frac{f(\omega)}{\omega^+} &= P\left[\int_{-\infty}^{+\infty} d\omega \frac{f(\omega)}{\omega}\right] - i\pi f(0) \end{aligned}$$

Here $P[...]$ is the "principal part" of a function

Higher order perturbation theory

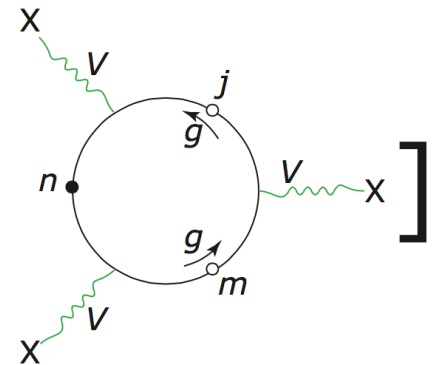
$$\begin{aligned}
 |\psi(t)\rangle = & \underbrace{|0\rangle}_{|\psi(t)\rangle^{(0)}} + \underbrace{\frac{1}{i\hbar} \int_{t_0}^t dt' V(t') |0\rangle}_{|\psi(t)\rangle^{(1)}} + \underbrace{\frac{1}{(i\hbar)^2} \int_{t_0}^t dt' \int_{t_0}^{t'} dt'' V(t') V(t'') |0\rangle}_{|\psi(t)\rangle^{(2)}} \\
 & + \underbrace{\frac{1}{(i\hbar)^3} \int_{t_0}^t dt' \int_{t_0}^{t'} dt'' \int_{t_0}^{t''} dt''' V(t') V(t'') V(t''') |0\rangle}_{|\psi(t)\rangle^{(3)}} + \dots,
 \end{aligned}$$

$$\Gamma_{0 \rightarrow n} = \frac{2\pi}{\hbar} |\langle n|V|0\rangle + \sum_m \frac{\langle n|V|m\rangle \langle m|V|0\rangle}{\epsilon_0 - \epsilon_m + i\eta\hbar} + \sum_{k,l} \frac{\langle n|V|k\rangle \langle k|V|l\rangle \langle l|V|0\rangle}{(\epsilon_0 - \epsilon_k + 2i\eta\hbar)(\epsilon_0 - \epsilon_l + i\eta\hbar)} + \dots|^2 \delta(\epsilon_0 - \epsilon_n)$$

$$G = \sum_m \frac{|m\rangle \langle m|}{\epsilon_0 - \epsilon_m + i\eta\hbar}$$

$$\Gamma_{0 \rightarrow n} = \frac{2\pi}{\hbar} |\langle n|V + VGV + \boxed{VGVG}V + \dots|0\rangle|^2 \delta(\epsilon_0 - \epsilon_n)$$

$$\langle n|VgVgV|n\rangle = \sum_{mj}$$



Scattering events in semiconductors

Scattering processes

Elastic

Inelastic

Coulombic

Remote impurities
Background impurity
Charged dislocations
Strain field of dislocations
Dipoles in alloy

Isotropic

Alloy disorder
Interface roughness
Acoustic phonon

Optical phonon

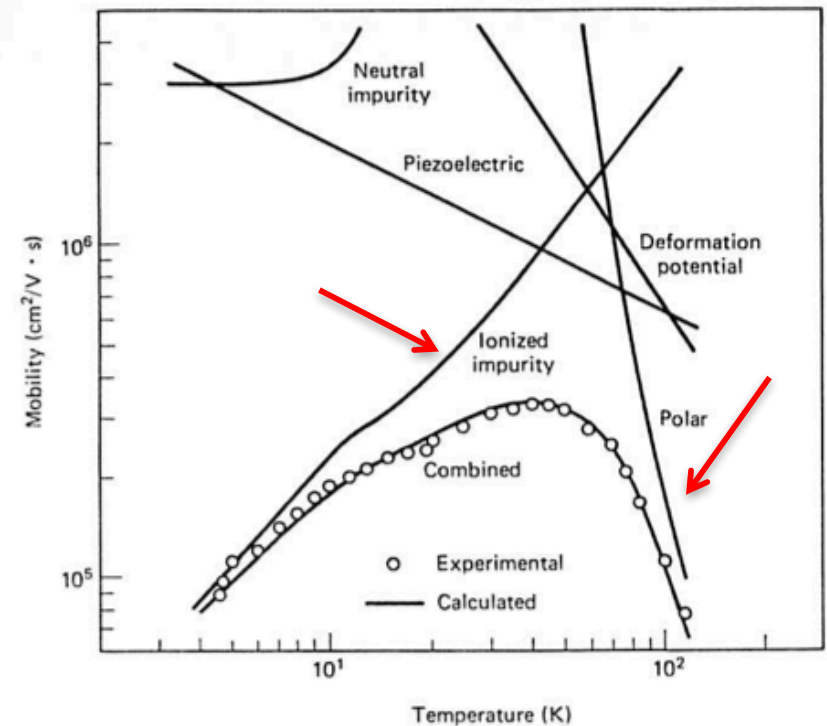
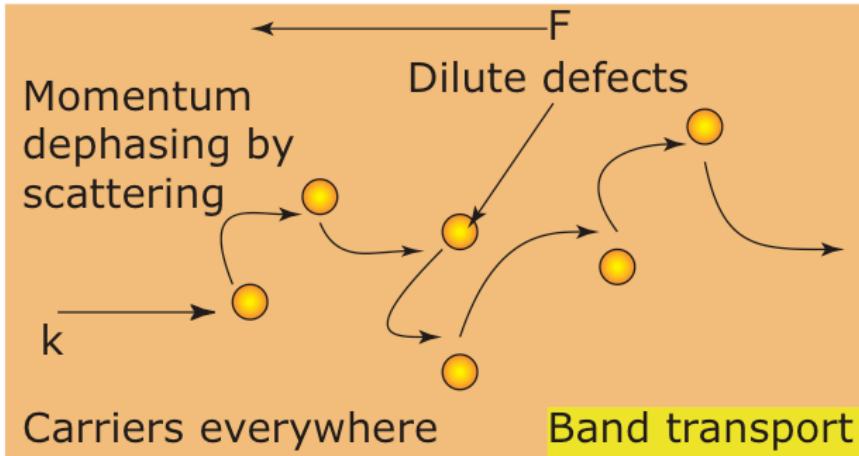


Figure 6.7 Temperature dependence of the mobility for *n*-type GaAs showing the separate and combined scattering processes. [From C. M. Wolfe, G. E. Stillman, and W. T. Lindley, *J. Appl. Phys.* 41, 3088 (1970).]

Scattering by each type of impurity affects the net electron mobility.

- Mobility in a ultra-clean (defect-free) semiconductor is limited by phonon (optical+acoustic) scattering.
- If the scattering rate of defects/impurities exceed that of phonons, then they determine the mobility.
- Method: find the scattering rate due to each type of defect. The total scattering rate is the sum of all.

Scattering of Bloch Electron States



Fermi's Golden Rule tells us that the scattering potential is the SUM of ALL the scatterers in the macroscopic crystal.

How do multiple scattering centers add up and contribute to the total scattering rate?

$$\frac{1}{\tau_{\mathbf{k}\mathbf{k}'}} = \frac{2\pi}{\hbar} |V(\mathbf{q})|^2 \delta[E_{\mathbf{k}'} - (E_{\mathbf{k}} \pm \hbar\omega)]$$

$$\mathbf{q} = \mathbf{k} - \mathbf{k}'$$

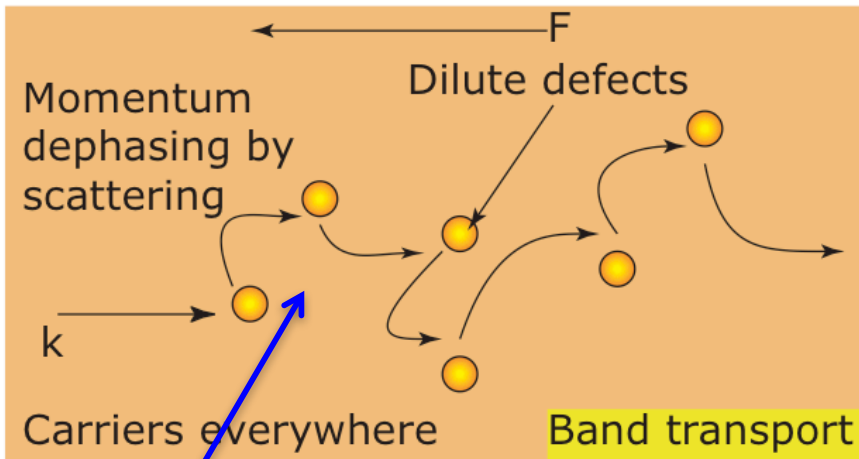
$$V(\mathbf{q}) = \langle \mathbf{k}' | W(\mathbf{r}) | \mathbf{k} \rangle$$

$$\begin{aligned} &= \int_V \left[\frac{e^{-i\mathbf{k}' \cdot \mathbf{r}}}{\sqrt{V}} u_{\mathbf{K}'}^*(\mathbf{r}) \right] \times W(\mathbf{r}) \times \left[\frac{e^{+i\mathbf{k} \cdot \mathbf{r}}}{\sqrt{V}} u_{\mathbf{K}}(\mathbf{r}) \right] d^3\mathbf{r} \\ &= \int_V \left[\frac{e^{i(\mathbf{k}-\mathbf{k}') \cdot \mathbf{r}}}{V} \right] W(\mathbf{r}) \times [u_{\mathbf{K}'}^*(\mathbf{r}) u_{\mathbf{K}}(\mathbf{r})] d^3\mathbf{r} \\ &\approx \underbrace{\left(\int_V e^{i\mathbf{q} \cdot \mathbf{r}} W(\mathbf{r}) \frac{d^3\mathbf{r}}{V} \right)}_{\text{crystal}} \times \underbrace{\left(\int_{\Omega} u_{\mathbf{K}'}^*(\mathbf{r}) u_{\mathbf{K}}(\mathbf{r}) \frac{d^3\mathbf{r}}{\Omega} \right)}_{=1} \end{aligned}$$

Fourier Transform of real-space scattering potential!

$$V(\mathbf{q}) \approx \int_V e^{i\mathbf{q} \cdot \mathbf{r}} W(\mathbf{r}) \frac{d^3\mathbf{r}}{V}$$

Scattering by many impurities



Impurity locations are R_1, R_2, \dots
They are "uncorrelated"

$$W_{total}(\mathbf{r}) = \underbrace{W(\mathbf{r}) + W(\mathbf{r} - \mathbf{R}_1) + W(\mathbf{r} - \mathbf{R}_2) + \dots}_{\text{'N' impurities}}$$

$$V_0(\mathbf{q}) \approx \int_V e^{i\mathbf{q}\cdot\mathbf{r}} W(\mathbf{r}) \frac{d^3\mathbf{r}}{V}$$

$$V_{total}(\mathbf{q}) = V_0(\mathbf{q}) + \int_V e^{i\mathbf{q}\cdot\mathbf{r}} W(\mathbf{r} - \mathbf{R}_1) \frac{d^3\mathbf{r}}{V} + \dots$$

$$V_{total}(\mathbf{q}) = V_0(\mathbf{q}) + V_0(\mathbf{q})e^{i\mathbf{q}\cdot\mathbf{R}_1} + V_0(\mathbf{q})e^{i\mathbf{q}\cdot\mathbf{R}_2} \dots$$

$$V_{total}(\mathbf{q}) = V_0(\mathbf{q}) \underbrace{[1 + e^{i\mathbf{q}\cdot\mathbf{R}_1} + e^{i\mathbf{q}\cdot\mathbf{R}_2} \dots]}_{\text{'N' terms}}$$

$$|V_{total}(\mathbf{q})|^2 = |V_0(\mathbf{q})|^2 \underbrace{[(1 + e^{i\mathbf{q}\cdot\mathbf{R}_1} + e^{i\mathbf{q}\cdot\mathbf{R}_2} \dots)]}_{\text{'N' imp terms}} \times \underbrace{(1 + e^{-i\mathbf{q}\cdot\mathbf{R}_1} + e^{-i\mathbf{q}\cdot\mathbf{R}_2} \dots)}_{\text{'N' imp terms}}$$

$$|V_{total}(\mathbf{q})|^2 = |V_0(\mathbf{q})|^2 [N_{imp} + \underbrace{(e^{i\mathbf{q}\cdot(\mathbf{R}_1 - \mathbf{R}_2)} + e^{i\mathbf{q}\cdot(\mathbf{R}_1 - \mathbf{R}_3)} \dots)}_{\approx 0 (RPA)}]$$

Fourier Transform property:

$$\int e^{iqx} f(x) dx \leftrightarrow F(q)$$

$$\int e^{iqx} f(x + a) dx \leftrightarrow F(q) \times e^{iqa}$$

Effect of multiple scattering

$$|V_{total}(\mathbf{q})|^2 = N_{imp} |V_0(\mathbf{q})|^2$$

$$\frac{1}{\tau_{\mathbf{k}\mathbf{k}'}(total)} = \frac{2\pi}{\hbar} N_{imp} \times |V_0(\mathbf{q})|^2 \delta[E_{\mathbf{k}'} - (E_{\mathbf{k}} \pm \hbar\omega)]$$

Scattering rate is linearly proportional to impurity density in the dilute uncorrelated limit!

Scattering rate due to point scatterers

$$W(\mathbf{r}) = V_0 \delta(\mathbf{r})$$

$$\langle \mathbf{k}' | V_0 \delta(\mathbf{r}) | \mathbf{k} \rangle = \int d^3 \mathbf{r} \left(\frac{e^{-i\mathbf{k}' \cdot \mathbf{r}}}{\sqrt{V}} \right) V_0 \delta(\mathbf{r}) \left(\frac{e^{+i\mathbf{k} \cdot \mathbf{r}}}{\sqrt{V}} \right) = \frac{V_0}{V}$$

$$\frac{1}{\tau(|\mathbf{k}\rangle \rightarrow |\mathbf{k}'\rangle)} = \frac{2\pi}{\hbar} \left(\frac{V_0}{V} \right)^2 \delta(E_{\mathbf{k}} - E_{\mathbf{k}'})$$

$$\frac{1}{\tau(|\mathbf{k}\rangle)} = \sum_{\mathbf{k}'} \frac{1}{\tau(|\mathbf{k}\rangle \rightarrow |\mathbf{k}'\rangle)} = \frac{2\pi}{\hbar} \left(\frac{V_0}{V} \right)^2 \underbrace{\sum_{\mathbf{k}'} \delta(E_{\mathbf{k}} - E_{\mathbf{k}'})}_{D(E_{\mathbf{k}})}$$

$$\frac{1}{\tau(E_{\mathbf{k}})} = \frac{2\pi}{\hbar} \left(\frac{V_0}{V} \right)^2 n_{sc} V \int \frac{d^3 \mathbf{k}'}{(2\pi)^3} \delta(E_{\mathbf{k}} - E_{\mathbf{k}'}) = \frac{2\pi}{\hbar} V_0^2 n_{sc} g(E_{\mathbf{k}})$$

The Boltzmann Transport Equation

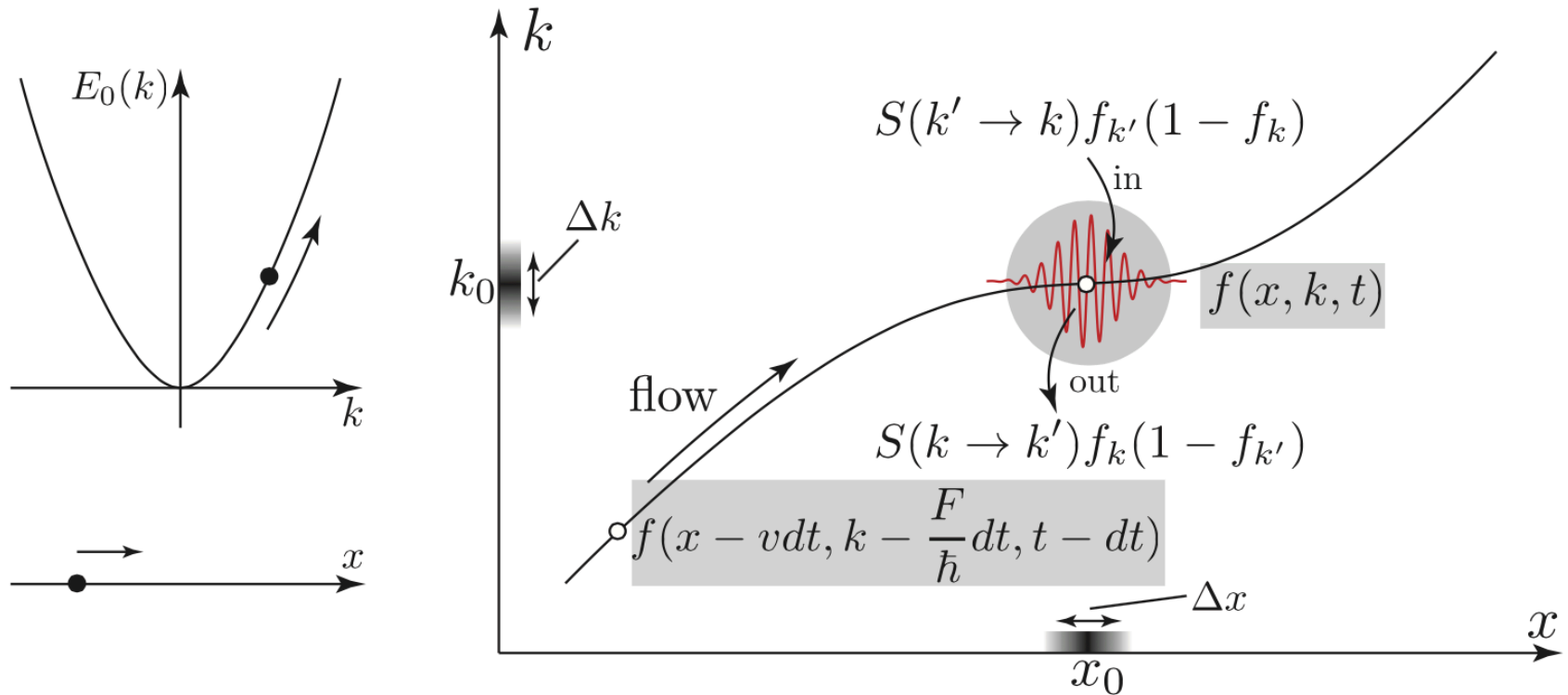


FIGURE 30.1: Scattering term of Boltzmann transport equation depicting the inflow and outflow of the distribution function.

$$f = f(x, k, t) = f(x - vdt, k - \frac{F}{\hbar} dt, t - dt) + (S_{in} - S_{out})dt$$

The Boltzmann Transport Equation

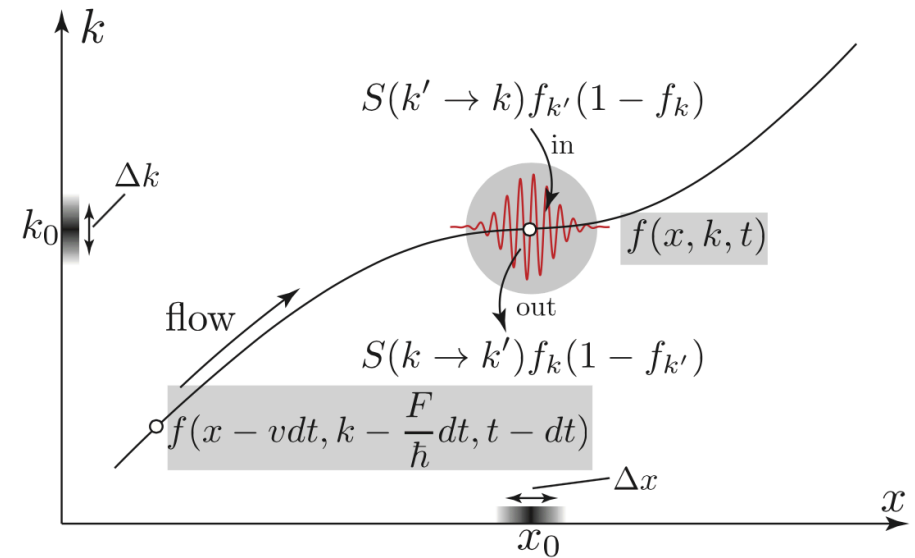
$$f = f(x, k, t) = f\left(x - vdt, k - \frac{F}{\hbar}dt, t - dt\right) + (S_{in} - S_{out})dt$$

$$\frac{\partial f}{\partial t} + v \frac{\partial f}{\partial x} + \frac{F}{\hbar} \frac{\partial f}{\partial k} = S_{in} - S_{out}$$

$$\frac{\partial f}{\partial t} + \mathbf{v}_k \cdot \nabla_r f + \frac{\mathbf{F}}{\hbar} \cdot \nabla_k f = S_{in} - S_{out}$$

$$S_{in} = S(k' \rightarrow k) f_{k'} (1 - f_k),$$

$$S_{out} = S(k \rightarrow k') f_k (1 - f_{k'}).$$



$$\frac{\partial f_k}{\partial t} + \mathbf{v}_k \cdot \nabla_r f_k + \frac{\mathbf{F}}{\hbar} \cdot \nabla_k f_k = \underbrace{\sum_{k'} [S(k' \rightarrow k) f_{k'} (1 - f_k) - S(k \rightarrow k') f_k (1 - f_{k'})]}_{\text{scattering term, } \hat{C} f_k}.$$

The Boltzmann Transport Equation

$$\frac{\partial f_k}{\partial t} + \mathbf{v}_k \cdot \nabla_r f_k + \frac{\mathbf{F}}{\hbar} \cdot \nabla_k f_k = \underbrace{\sum_{k'} [S(k' \rightarrow k) f_{k'} (1 - f_k) - S(k \rightarrow k') f_k (1 - f_{k'})]}_{\text{scattering term, } \hat{C}f_k}.$$

$$S(k \rightarrow k') = \frac{2\pi}{\hbar} |W_{k,k'}|^2 \delta(E_k - E_{k'} \pm \hbar\omega)$$

$$S(k' \rightarrow k) f_{0k'} (1 - f_{0k}) = S(k \rightarrow k') f_{0k} (1 - f_{0k'})$$

$$\frac{S(k' \rightarrow k)}{S(k \rightarrow k')} = \frac{1 - f_{0k'}}{f_{0k'}} \cdot \frac{f_{0k}}{1 - f_{0k}} = e^{\frac{E_{k'} - E_k}{kT}}$$

The Boltzmann Transport Equation

Microscopic nature of the collision term

$$\left. \frac{\partial f(\mathbf{k})}{\partial t} \right|_{coll} = \sum_{\mathbf{k}'} [S(\mathbf{k}', \mathbf{k}) f(\mathbf{k}') [1 - f(\mathbf{k})] - S(\mathbf{k}, \mathbf{k}') f(\mathbf{k}) [1 - f(\mathbf{k}')]]. \quad (85)$$

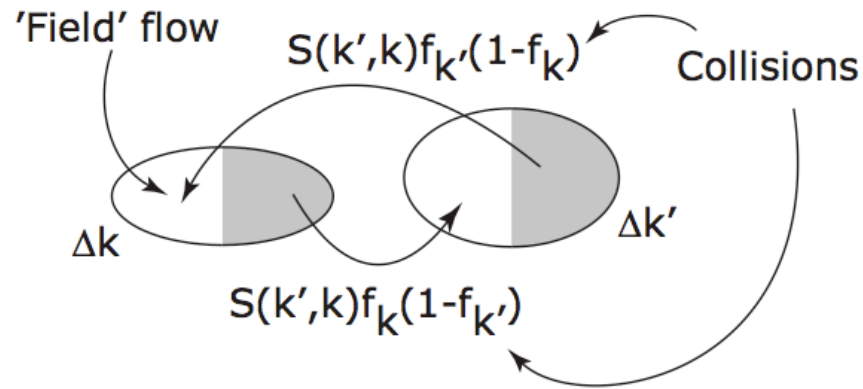


Figure 11: Scattering term of Boltzmann transport equation depicting the inflow and outflow of the distribution function.

At equilibrium ($f = f_0$), the 'principle of detailed balance' enforces the condition

$$S(\mathbf{k}', \mathbf{k}) f_0(\mathbf{k}') [1 - f_0(\mathbf{k})] = S(\mathbf{k}, \mathbf{k}') f_0(\mathbf{k}) [1 - f_0(\mathbf{k}')],$$

which translates to

$$S(\mathbf{k}', \mathbf{k}) e^{\frac{\varepsilon_{\mathbf{k}}}{k_B T}} = S(\mathbf{k}, \mathbf{k}') e^{\frac{\varepsilon_{\mathbf{k}'}}{k_B T}}.$$

In the special case of *elastic* scattering, $\varepsilon_{\mathbf{k}} = \varepsilon_{\mathbf{k}'}$, and as a result, $S(\mathbf{k}', \mathbf{k}) = S(\mathbf{k}, \mathbf{k}')$

Absorption, Spontaneous and Stimulated Emission

Enforcing the principle of detailed balance is telling us that for electrons, the scattering rate from state $|k\rangle \rightarrow |k'\rangle$ is *not the same* as for the reverse process, *unless* the energies of the two states are the same. For *elastic* scattering events $E_k = E_{k'}$ for which the energy of the electron is unchanged, the scattering rate $S(k \rightarrow k') = S(k' \rightarrow k)$ is the same for a process and its reverse. But for inelastic scattering events with $E_{k'} - E_k = \hbar\omega$, the scattering rate going uphill in energy is slower: $S(k \rightarrow k') = S(k' \rightarrow k)e^{-\hbar\omega/kT}$. The scattering rates $S(\dots)$ remain the same whether electrons are in equilibrium or not, the occupation functions f are what change.

Consider for example, the electron scattering rate due to either the absorption or emission of phonons of energy $\hbar\omega$. The rate of phonon absorption must be proportional to the number of phonons already present, i.e., $S_{abs} \propto n_{ph}$. The rate of phonon emission by an electron requires it to go downhill in energy, thus $S_{em} = S_{abs}e^{\hbar\omega/kT} \propto e^{\hbar\omega/kT} n_{ph}$.

Since the number of phonons in mode ω is given by the Bose-Einstein function $n_{ph} = 1/(e^{\hbar\omega/kT} - 1)$, we note that $e^{\hbar\omega/kT} n_{ph} = 1 + n_{ph}$. Thus, $S_{abs} \propto n_{ph}$, but $S_{em} \propto (1 + n_{ph})$.

Electrons are free to 'emit' phonons even when there are no phonons present - thus, the '1' represents *spontaneous* emission. But if there already are phonons present, the emission rate is enhanced, or *stimulated*; this is the reason for the $1 + n_{ph}$ proportionality of the net emission rate.

The Collision Integral

$$\hat{C}f_k = \sum_{k'} S(k \rightarrow k') (e^{\frac{E_{k'} - E_k}{kT}} f_{k'} (1 - f_k) - f_k (1 - f_{k'}))$$

$$E_{k'} - E_k = \hbar\omega_0 \gg kT.$$

$$f_k f_{k'} \ll f_{k'}$$

$$\hat{C}f_k \approx e^{\frac{\hbar\omega_0}{kT}} \sum_{k'} S(k \rightarrow k') f_{k'}$$

Inelastic Scattering

$$E_{k'} = E_k.$$

$$\hat{C}f_k = \sum_{k'} S(k \rightarrow k') (f_{k'} - f_k) = \sum_{k'} S(k \rightarrow k') f_{k'} - \frac{f_k}{\tau(k)}$$

Elastic Scattering

Quantum and Momentum Scattering Rates

$$\left. \frac{\partial f(\mathbf{k})}{\partial t} \right|_{coll} = \sum_{\mathbf{k}'} S(\mathbf{k}, \mathbf{k}') (f(\mathbf{k}') - f(\mathbf{k})).$$

One can rewrite this collision equation as

$$\frac{df(\mathbf{k})}{dt} + \frac{f(\mathbf{k})}{\tau_q(\mathbf{k})} = \sum_{\mathbf{k}'} S(\mathbf{k}, \mathbf{k}') f(\mathbf{k}'),$$

where the *quantum scattering time* is defined as

$$\frac{1}{\tau_q(\mathbf{k})} = \sum_{\mathbf{k}'} S(\mathbf{k}, \mathbf{k}').$$

quantum scattering rate (dephasing)

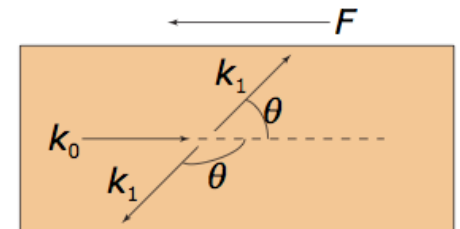
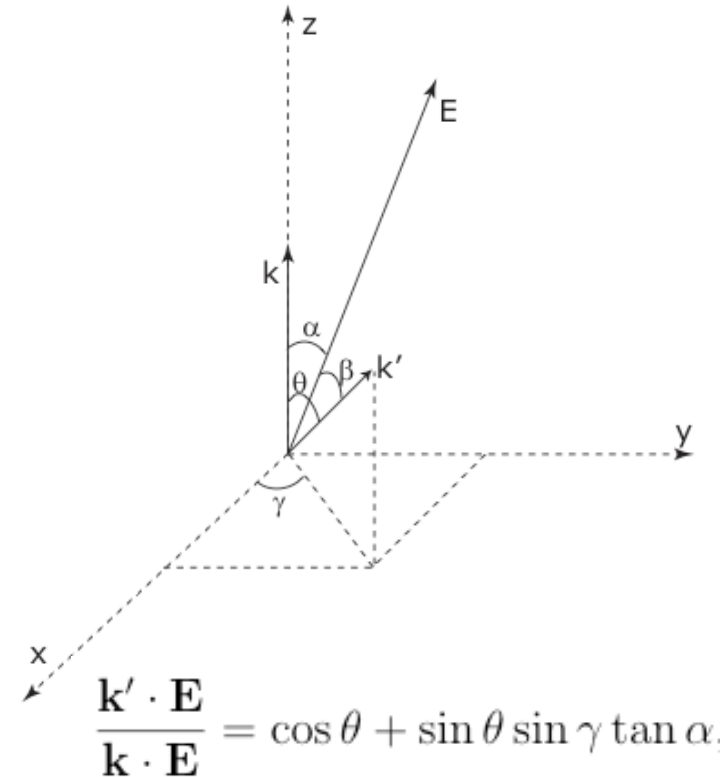
$$f(\mathbf{k}) = f_0(\mathbf{k}) - \tau \mathbf{F}_t \cdot \mathbf{v} \frac{\partial f_0(\mathbf{k})}{\partial \varepsilon}$$

$$f(\mathbf{k}') - f(\mathbf{k}) = e\tau \underbrace{\frac{\partial f_0}{\partial \varepsilon} \mathbf{E} \cdot \mathbf{v}}_{f(\mathbf{k}) - f_0(\mathbf{k})} (1 - \frac{\mathbf{E} \cdot \mathbf{v}'}{\mathbf{E} \cdot \mathbf{v}})$$

$$\frac{1}{\tau_m(\mathbf{k})} = \sum_{\mathbf{k}'} S(\mathbf{k}, \mathbf{k}') (1 - \frac{\mathbf{E} \cdot \mathbf{k}'}{\mathbf{E} \cdot \mathbf{k}})$$

$$\frac{1}{\tau_m(\mathbf{k})} = \sum_{\mathbf{k}'} S(\mathbf{k}, \mathbf{k}') (1 - \cos \theta)$$

momentum scattering rate (mobility, conductivity)



$$\frac{1}{\tau_m} = \frac{1}{\tau_q} [1 - \cos(\theta)]$$

Fermi level and temperature at equilibrium

$$\frac{\partial f_k}{\partial t} + \mathbf{v}_k \cdot \nabla_r f_k + \frac{\mathbf{F}}{\hbar} \cdot \nabla_k f_k = \underbrace{\sum_{k'} [S(k' \rightarrow k) f_{k'} (1 - f_k) - S(k \rightarrow k') f_k (1 - f_{k'})]}_{\text{scattering term, } \hat{C} f_k}$$

$$g(r, k, T) = \frac{E_c(r) + \mathcal{E}_c(k) - E_F(r)}{kT}$$

$$f_0 = \frac{1}{1 + e^g}$$

$$\frac{\partial f_0}{\partial t} = 0 \text{ at equilibrium, } \hat{C} f_k = 0$$

$$\mathbf{v}_k \cdot \nabla_r f_0 + \frac{\mathbf{F}}{\hbar} \cdot \nabla_k f_0 = 0$$

$$\frac{\partial f_0}{\partial \mathcal{E}} = \frac{\partial g}{\partial \mathcal{E}} \frac{\partial f_0}{\partial g} = -\frac{1}{kT} \frac{e^g}{(1 + e^g)^2} \implies \frac{\partial f_0}{\partial g} = kT \frac{\partial f_0}{\partial \mathcal{E}}$$

$$\nabla_r f_0 = kT \frac{\partial f_0}{\partial \mathcal{E}} \nabla_r g \text{ and } \nabla_k f_0 = kT \frac{\partial f_0}{\partial \mathcal{E}} \nabla_k g$$

$$kT \cdot \frac{\partial f_0}{\partial \mathcal{E}} \cdot \mathbf{v}_k \cdot \left[\frac{\mathbf{F}}{kT} + \nabla_r g \right] = 0 \quad \frac{\mathbf{F}}{kT} + \nabla_r g = 0 \text{ requires}$$

$$\frac{1}{kT} \left(\mathbf{F} + \nabla_r E_c(r) - \nabla_r E_F(r) \right) + [E_c(r) + \mathcal{E}_c(k) - E_F(r)] \nabla_r \left(\frac{1}{kT} \right) = 0.$$

$$\text{since } \mathbf{F} = -\nabla_r E_c(r)$$

$$-\nabla_r E_F(r) + [E_c(r) + \mathcal{E}_c(k) - E_F(r)] T \nabla_r \left(\frac{1}{T} \right) = 0.$$

would imply $\nabla_r E_F(r) = 0$ and $\nabla_r T_L(r) = 0$, implying the Fermi level and the lattice temperature are equal everywhere at equilibrium.

The Boltzmann Transport Equation

equilibrium

$$f_0(\varepsilon) = \frac{1}{1 + e^{\frac{\varepsilon_{\mathbf{k}} - \mu}{k_B T}}}$$

perturbation

$$f(\mathbf{k}, \mathbf{r}, t)$$

Boltzmann Transport Equation

$$\frac{df}{dt} = \frac{\mathbf{F}_t}{\hbar} \cdot \nabla_{\mathbf{k}} f(\mathbf{k}) + \mathbf{v} \cdot \nabla_{\mathbf{r}} f(\mathbf{k}) + \frac{\partial f}{\partial t}$$

Particle number conserved

$$\frac{\partial f}{\partial t} = \frac{\partial f}{\partial t} \Big|_{\text{coll}} - \frac{\mathbf{F}_t}{\hbar} \cdot \nabla_{\mathbf{k}} f(\mathbf{k}) - \mathbf{v} \cdot \nabla_{\mathbf{r}} f(\mathbf{k})$$

$$\frac{\partial f}{\partial t} \Big|_c = \frac{-(f - f_0)}{\tau_m}$$

Relaxation time approximation

equilibrium

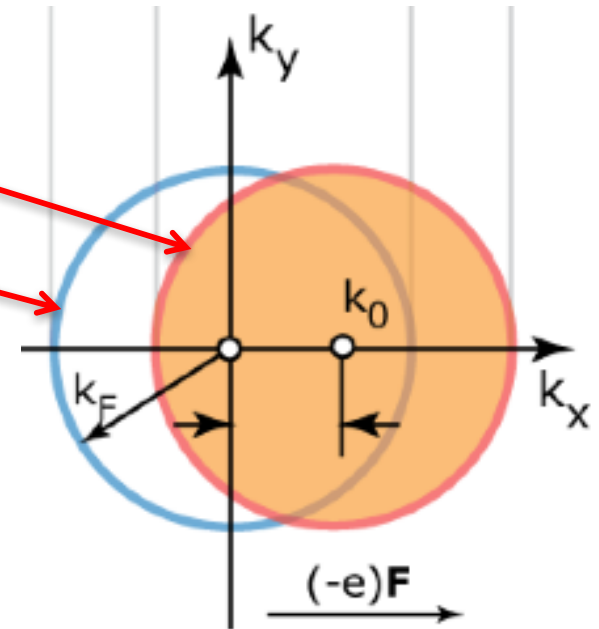
scattering

$$f = f_0 - \frac{\tau_m}{\hbar} \nabla_{\mathbf{k}} \mathcal{E} \cdot \left(\frac{\partial f}{\partial \mathcal{E}} \mathbf{F} + \nabla_{\mathbf{r}} f \right)$$

bandstructure

applied forces

conc. gradients



The Boltzmann transport equation gives a full-blown treatment of transport properties, and can be solved in several levels of approximation.

Many electrons: Model by Distribution Function

$$n = \int \frac{d^d k}{(2\pi)^d} f(\mathbf{k}) = \int d\varepsilon f(\varepsilon) g_d(\varepsilon)$$

$$g_d(\varepsilon) = \frac{1}{2^{d-1} \pi^{\frac{d}{2}} \Gamma(\frac{d}{2})} \left(\frac{2m^*}{\hbar^2} \right)^{\frac{d}{2}} \varepsilon^{\frac{d}{2}-1}$$

$$\mathbf{J} = 2e \int \frac{d^d k}{(2\pi)^d} \mathbf{v} f(\mathbf{k})$$

$$J_i = en \underbrace{\left(-\frac{2e}{dm^*} \frac{\int d\varepsilon \tau_m \varepsilon^{\frac{d}{2}} \frac{\partial f_0}{\partial \varepsilon}}{\int d\varepsilon f_0(\varepsilon) \varepsilon^{\frac{d}{2}-1}} \right)}_{\mu_d} F_i$$

Distribution function: Solution of Boltzmann Transport Equation

$$f(\mathbf{k}) = f_0(\mathbf{k}) + eF_i \tau(\mathbf{k}) v_i \frac{\partial f_0}{\partial \varepsilon}$$

Fermi's Golden Rule

Basic ideas:

- If we know the distribution function and the bandstructure, then the current can be calculated.
- The distribution function changes from the equilibrium Fermi-Dirac form in response to perturbation.

The Boltzmann Transport Equation

Boltzmann equation \rightarrow

$$f(k) = f_0(k) + e\tau_m(k)(\mathbf{F} \cdot \mathbf{v}) \frac{\partial f_0(k)}{\partial \varepsilon}$$

$$\frac{1}{\tau_m(k)} = \sum_{k'} S(k, k')(1 - \cos\theta) - \text{Momentum scattering time} \quad (\mu = \frac{e\langle\tau_m(k)\rangle}{m^*})$$

$$\frac{1}{\tau_q(k)} = \sum_{k'} S(k, k') - \text{Quantum scattering time}$$

$$S(k, k') = \frac{2\pi}{\hbar} |\langle k' | \Delta E_c(r) | k \rangle|^2 \delta(\varepsilon_k - \varepsilon_{k'})$$

Fermi's Golden Rule gives: Scattering rate from state $k \rightarrow k'$ by perturbation ΔE_c



Most general expression for 'Current Density' in 'd' dimensions:

$$\mathbf{J}_d = q \times \frac{g_s g_v}{L^d} \sum_k \mathbf{v}_g(k) f(k), \text{ where}$$

charge current density (general case)

$q\mathbf{v}_g$ may be replaced by other physical quantities:

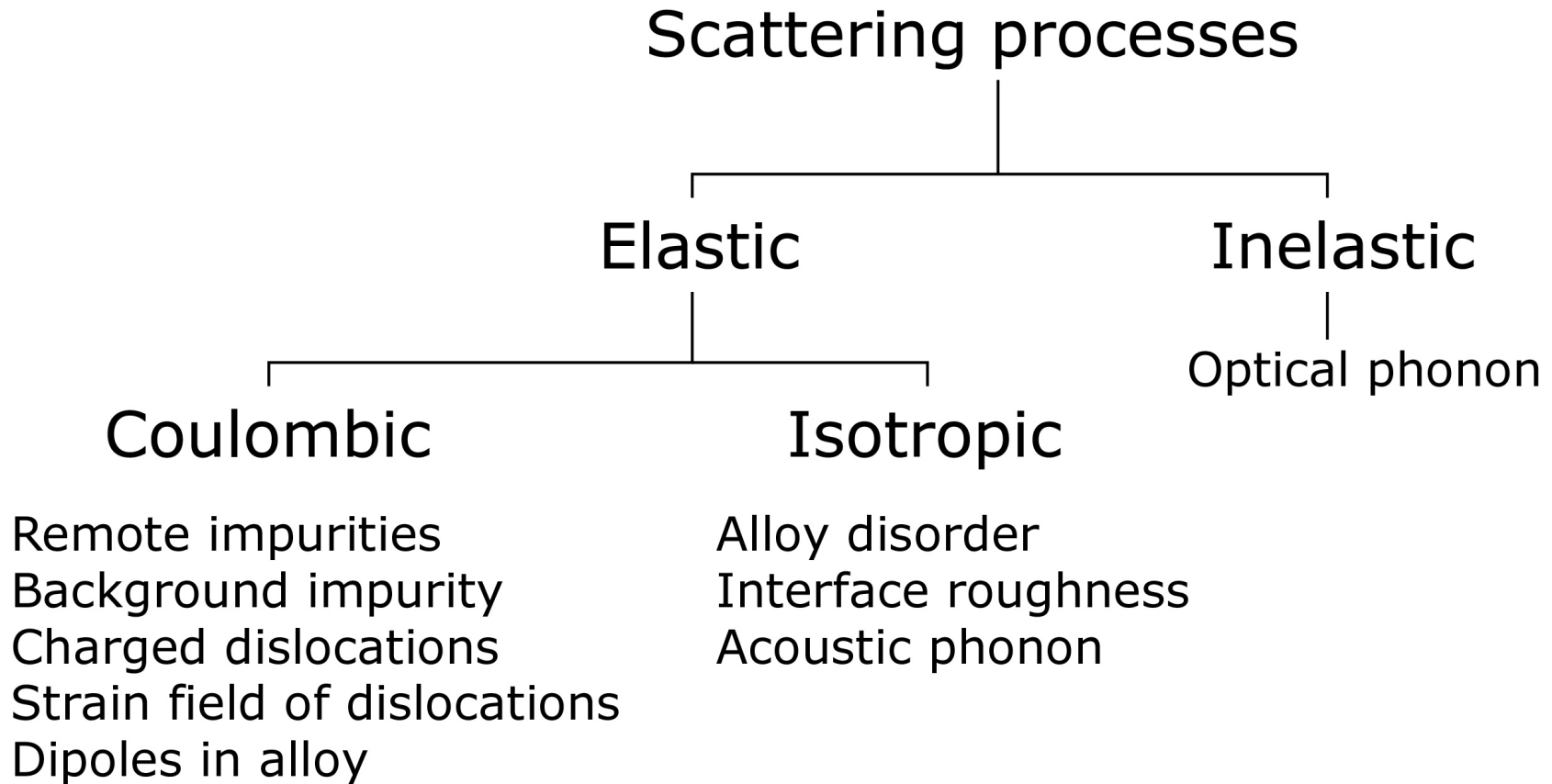
$q\mathbf{v}_g \rightarrow$ charge current density (electrical cond.)

$\mathbf{1} \rightarrow$ carrier density

$\mathbf{E}(k) \rightarrow$ heat current density (thermal cond.)

...

Scattering events in semiconductors



A static periodic potential causes no scattering → every other potential causes scattering!

*Periodic 'non-static' potentials: **Phonons**.*

*Static non-periodic potentials: **Defects & Impurities**.*

Scattering events in semiconductors

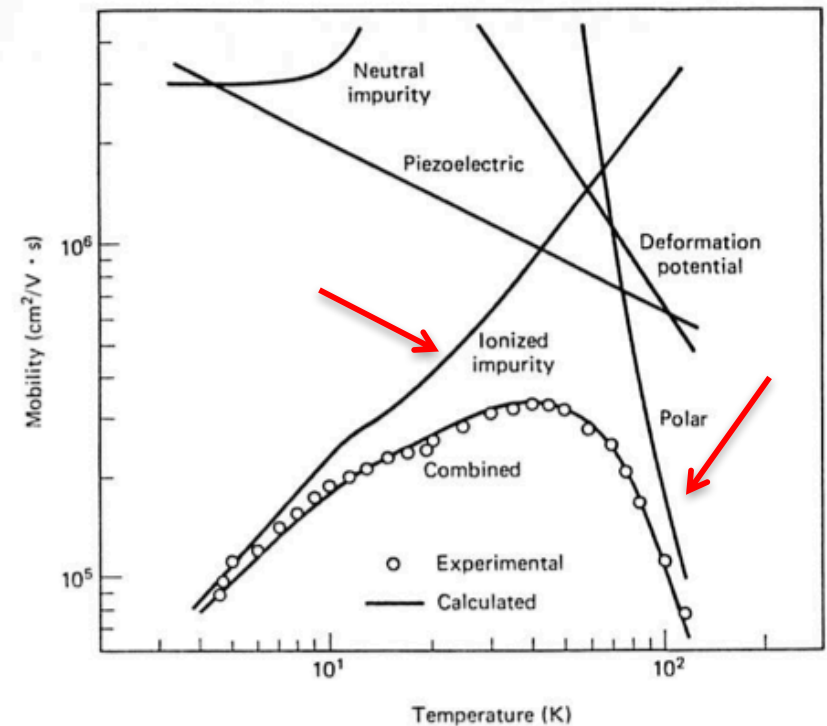
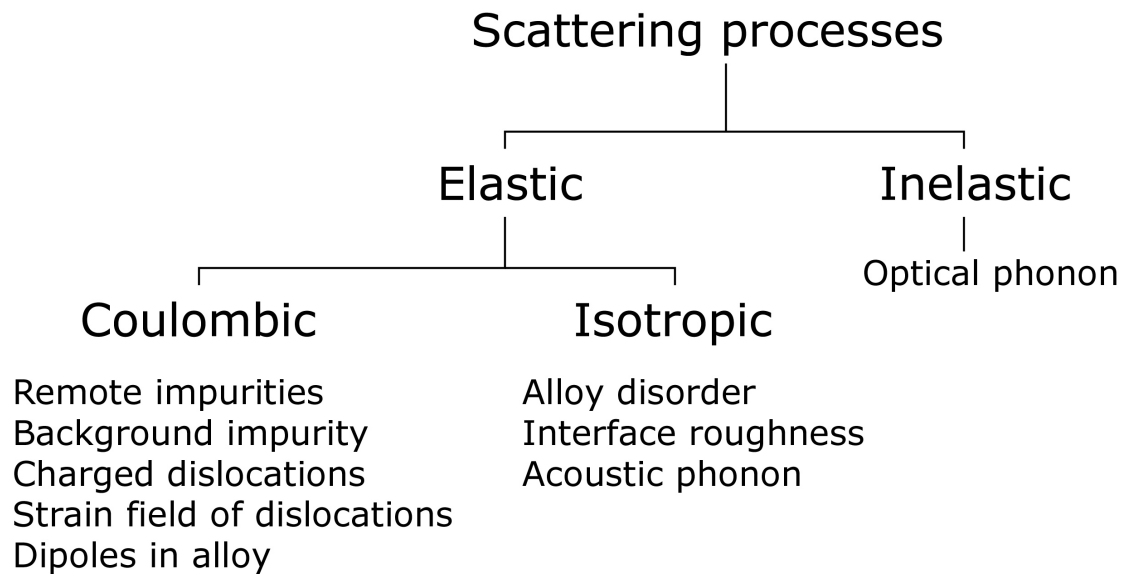


Figure 6.7 Temperature dependence of the mobility for *n*-type GaAs showing the separate and combined scattering processes. [From C. M. Wolfe, G. E. Stillman, and W. T. Lindley, *J. Appl. Phys.* 41, 3088 (1970).]

Scattering by each type of impurity affects the net electron mobility.

- Mobility in a ultra-clean (defect-free) semiconductor is limited by phonon (optical+acoustic) scattering.
- If the scattering rate of defects/impurities exceed that of phonons, then they determine the mobility.
- Method: find the scattering rate due to each type of defect. The total scattering rate is the sum of all.

Calculating the mobility/conductivity

$$f = f_0 + q\tau_m \frac{\partial f_0}{\partial \mathcal{E}} \mathbf{v} \cdot \mathbf{E}$$

$$\langle \mathbf{v} \rangle = \frac{\int_{-\infty}^{\infty} \mathbf{v} f \, d\mathbf{v}}{\int_{-\infty}^{\infty} f \, d\mathbf{v}}$$

$$\langle \mathbf{v} \rangle = \frac{\int_{-\infty}^{\infty} \mathbf{v} f_0 \, d\mathbf{v} + q \int_{-\infty}^{\infty} \tau_m (\partial f_0 / \partial \mathcal{E}) \mathbf{v} (\mathbf{v} \cdot \mathbf{E}) \, d\mathbf{v}}{\int_{-\infty}^{\infty} f_0 \, d\mathbf{v} + q \int_{-\infty}^{\infty} \tau_m (\partial f_0 / \partial \mathcal{E}) (\mathbf{v} \cdot \mathbf{E}) \, d\mathbf{v}}$$

$$\langle \mathbf{v} \rangle = \frac{+ q \int_{-\infty}^{\infty} \tau_m (\partial f_0 / \partial \mathcal{E}) \mathbf{v} (\mathbf{v} \cdot \mathbf{E}) \, d\mathbf{v}}{\int_{-\infty}^{\infty} f_0 \, d\mathbf{v}}$$

$$\mathcal{E} - \mathcal{E}_c = \frac{1}{2} m^* v^2 = \frac{1}{2} m^* v^2$$

$$d\mathbf{v} = 4\pi v^2 \, dv$$

$$\langle \mathbf{v} \rangle = \frac{+ q \int_{\mathcal{E}_c}^{\infty} \tau_m (\partial f_0 / \partial \mathcal{E}) \mathbf{v} (\mathbf{v} \cdot \mathbf{E}) (\mathcal{E} - \mathcal{E}_c)^{1/2} \, d\mathcal{E}}{\int_{\mathcal{E}_c}^{\infty} f_0 (\mathcal{E} - \mathcal{E}_c)^{1/2} \, d\mathcal{E}}$$

$$\mathbf{v} (\mathbf{v} \cdot \mathbf{E}) = + v_x^2 E_x \quad v^2 = v_x^2 + v_y^2 + v_z^2 = 3v_x^2$$

$$\langle v_x \rangle = \frac{2qE_x}{3m^*} \frac{\int_{\mathcal{E}_c}^{\infty} \tau_m (\partial f_0 / \partial \mathcal{E}) (\mathcal{E} - \mathcal{E}_c)^{3/2} \, d\mathcal{E}}{\int_{\mathcal{E}_c}^{\infty} f_0 (\mathcal{E} - \mathcal{E}_c)^{1/2} \, d\mathcal{E}}$$

$$v_{dx} = \frac{-qE_x}{m^*} \langle \tau_m \rangle$$



$$\langle \tau_m \rangle = \frac{2}{3} \frac{\int_0^{\infty} \tau_m (-\partial f_0 / \partial x) x^{3/2} \, dx}{\int_0^{\infty} f_0 x^{1/2} \, dx}$$

$$v_{dx} = -\mu_c E_x \quad \mu_c = \frac{q \langle \tau_m \rangle}{m^*} \quad J_x = \frac{q^2 n \langle \tau_m \rangle}{m^*} E_x \quad \sigma = \frac{q^2 n \langle \tau_m \rangle}{m^*}$$

Thus, for the simple case of a small applied electric field, we can define all the transport parameters in terms of the average momentum relaxation time, $\langle \tau_m \rangle$. Once $\langle \tau_m \rangle$ has been obtained, the transport problem is solved.

Formalism for diffusive charge transport

- Find the perturbation potential due to the defect.
- Use Fermi's Golden rule to evaluate the single-particle scattering rate
- Add up for all allowed states
- Use the solution of Boltzmann equation to find the mobility/conductivity.

$$\mathcal{E}_c(\mathbf{r}) = \mathcal{E}_c^0 + W(\mathbf{r})$$

$$V(\mathbf{q}) = \langle \mathbf{k}' | W(\mathbf{r}) | \mathbf{k} \rangle$$

Fermi's golden rule

$$\frac{1}{\tau_{\mathbf{k}\mathbf{k}'}} = \frac{2\pi}{\hbar} |V(\mathbf{q})|^2 \delta[E_{\mathbf{k}'} - (E_{\mathbf{k}} \pm \hbar\omega)]$$

$$f(\mathbf{k}) = f_0(\mathbf{k}) + eF_i \tau(\mathbf{k}) v_i \frac{\partial f_0}{\partial \epsilon}$$

Distribution function: Solution of Boltzmann Transport Equation

$$\mathbf{J} = 2e \int \frac{d^d k}{(2\pi)^d} \mathbf{v} f(\mathbf{k})$$

Current density: Sum over all group velocities \mathbf{v} in k -space

General Nature of Scattering Rates

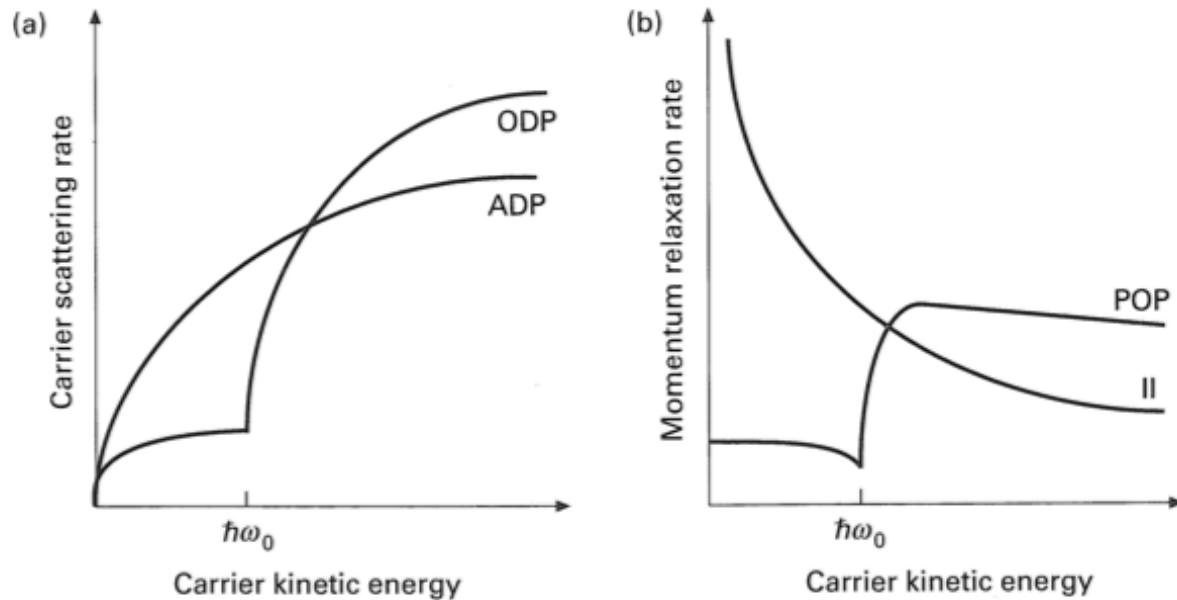
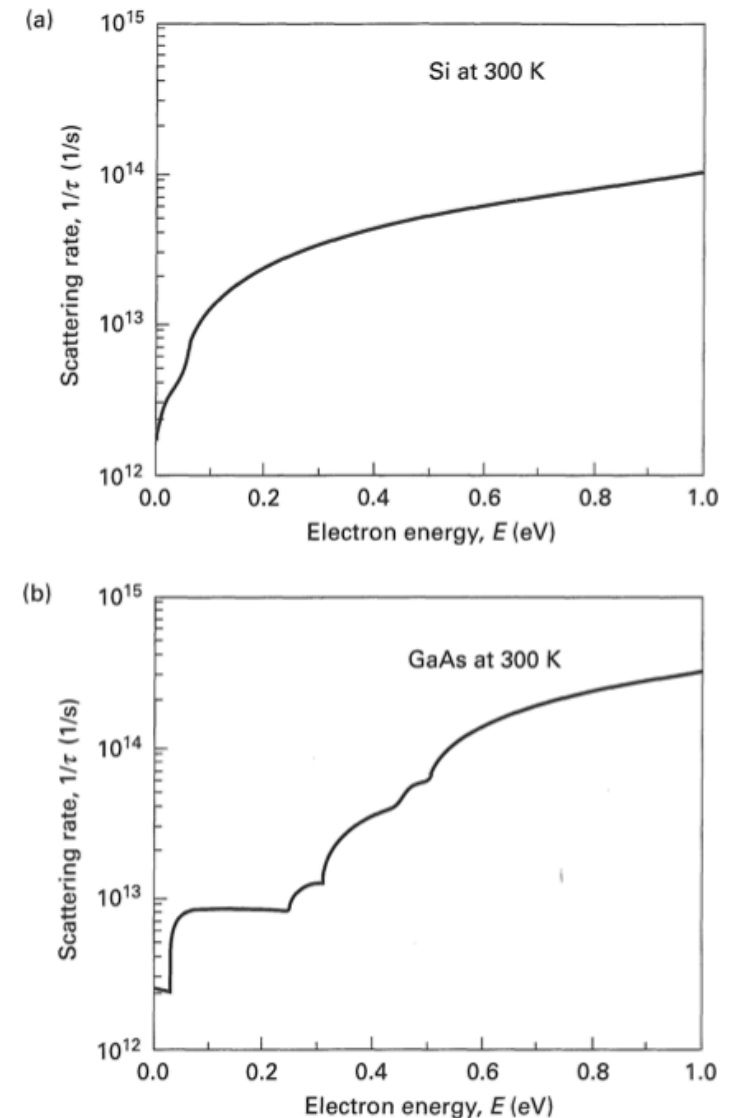


Fig. 2.4 General features of carrier scattering in semiconductors. (a) Nonpolar phonon scattering, acoustic deformation potential (ADP) in the elastic limit and optical deformation potential (ODP). (b) Scattering by electrostatic interactions, ionized impurity (II) and polar optical phonon (POP).

Scattering rates are typically proportional to the density of states



From Lundstrom: Fundamentals of Carrier Transport

Scattering by a neutral impurity

$$\mathcal{E}_c(\mathbf{r}) = \mathcal{E}_c^0 + W(\mathbf{r}) \longleftarrow W(r) = W_0 \Theta(r - r_0)$$

$$V(\mathbf{q}) = \langle \mathbf{k}' | W(\mathbf{r}) | \mathbf{k} \rangle$$

$$\frac{1}{\tau_{\mathbf{k}\mathbf{k}'}} = \frac{2\pi}{\hbar} |V(\mathbf{q})|^2 \delta[E_{\mathbf{k}'} - (E_{\mathbf{k}} \pm \hbar\omega)]$$

$$\langle \tau_m \rangle = \frac{2}{3} \frac{\int_0^\infty \tau_m (-\partial f_0 / \partial x) x^{3/2} dx}{\int_0^\infty f_0 x^{1/2} dx}$$

$$\mu_c = \frac{q \langle \tau_m \rangle}{m^*}$$

This & next few slides: material from
 - Wolfe/Holonyak/Stillman
 - Seeger

From Seeger: Derive your own expression!

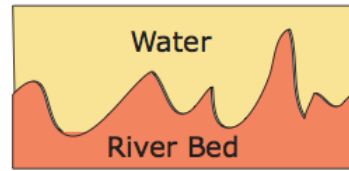
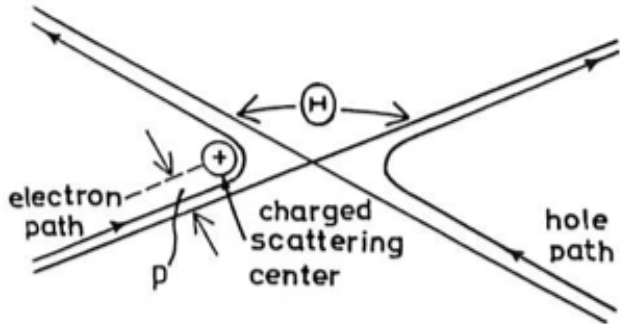
$$\mu = \frac{e}{20 a_B \hbar} \frac{m/m_0}{\kappa N^\kappa}$$

which is independent of temperature.

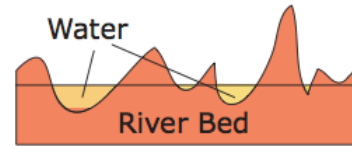
$$\mu = \frac{1.44 \times 10^{22} \text{ cm}^{-3}}{N^\kappa} \frac{m/m_0}{\kappa}$$

For example, for electrons in Ge, where $m/m_0 = 0.12$ and $\kappa = 16$, a mobility of $1.1 \times 10^3 \text{ cm}^2/\text{Vs}$ is obtained assuming, e.g., 10^{17} cm^{-3} neutral impurities.

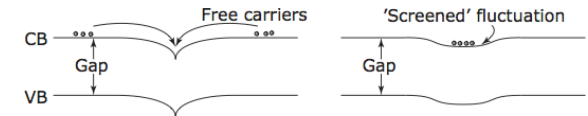
Scattering by charged impurities



River bed fluctuations 'screened' by water



Insufficient water fails to screen fluctuations



Screened coulomb scattering potential

$$V(r) = - (Z |e| / 4 \pi \kappa \epsilon_0 r) \exp(-r/L_D)$$

$$H_{k'k} = - \frac{Z e^2}{V \kappa \epsilon_0 |k - k'|} \int_0^{\infty} \exp(-r/L_D) \sin(|k - k'| r) dr \quad (6.3.13)$$

$$= - \frac{Z e^2}{V \kappa \epsilon_0} \frac{1}{|k - k'|^2 + L_D^{-2}} \approx - \frac{Z e^2}{V \kappa \epsilon_0 4 k^2} \frac{1}{\sin^2(\theta/2) + (2k L_D)^{-2}}$$

$$|k - k'| \approx 2k \sin(\theta/2)$$

$$\beta_{BH} = 2 \frac{m}{\hbar} \left(\frac{2}{m} 3 k_B T \right)^{1/2} L_D$$

$$\beta_{BH} = \left(\frac{\kappa}{16} \right)^{1/2} \frac{T}{100 \text{ K}} \left(\frac{m}{m_0} \right)^{1/2} \left(\frac{2.08 \times 10^{18} \text{ cm}^{-3}}{n} \right)^{1/2}$$

Brooks-Herring dimensionless factor

The mobility $\mu = (e/m) \langle \tau_m \rangle$ is given by

$$\mu = \frac{2^{7/2} (4 \pi \kappa \epsilon_0)^2 (k_B T)^{3/2}}{\pi^{3/2} Z^2 e^3 m^{1/2} N_1 [\ln(1 + \beta_{BH}^2) - \beta_{BH}^2 / (1 + \beta_{BH}^2)]}$$

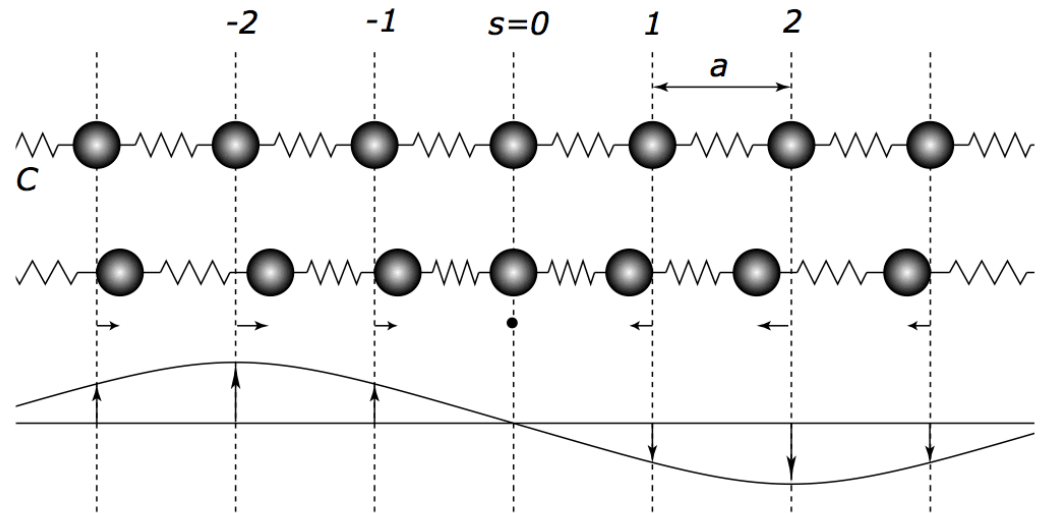
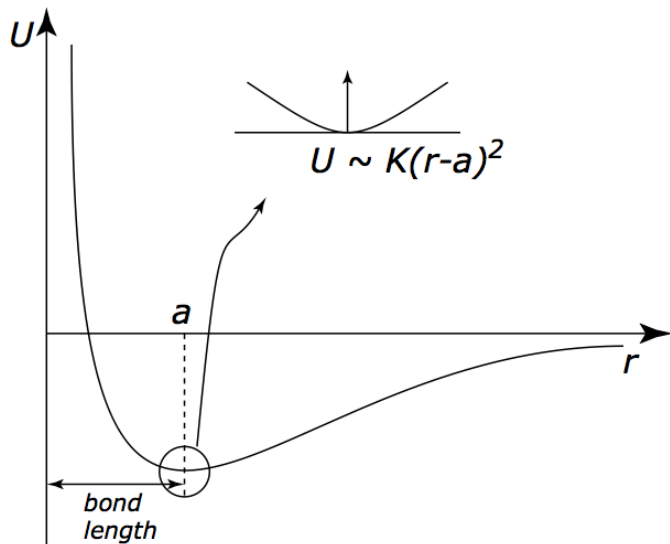
which in units of $\text{cm}^2/\text{V s}$ is

$$\mu = \frac{3.68 \times 10^{20} \text{ cm}^{-3}}{N_1} \frac{1}{Z^2} \left(\frac{\kappa}{16} \right)^2 \left(\frac{T}{100 \text{ K}} \right)^{1.5}$$

$$\frac{1}{(m/m_0)^{1/2} [\log(1 + \beta_{BH}^2) - 0.434 \beta_{BH}^2 / (1 + \beta_{BH}^2)]}$$

and the log is to the base 10.

Phonons in Semiconductors



Newton's law for mass-spring chain

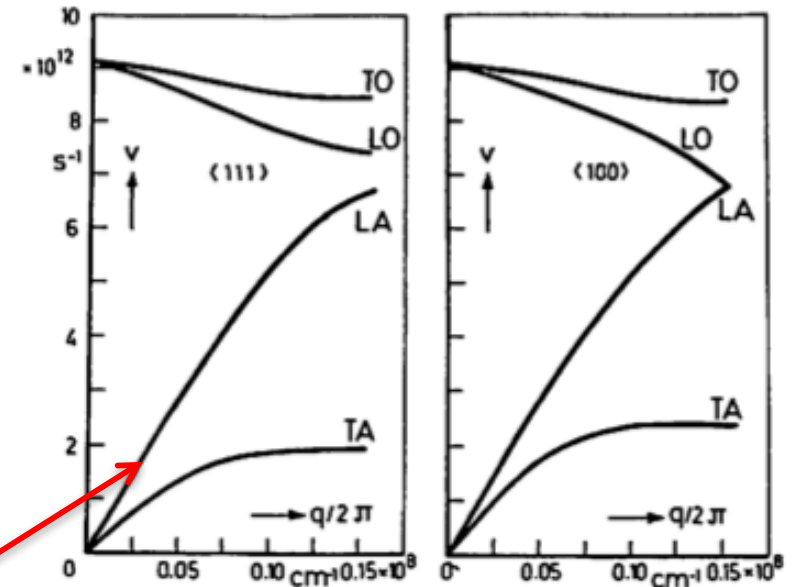
$$F = M \frac{d^2 u_s}{dt^2} = C(u_{s+1} - u_s) + C(u_{s-1} - u_s)$$

$$u_s = u_0 e^{i(qsa - \omega t)}$$

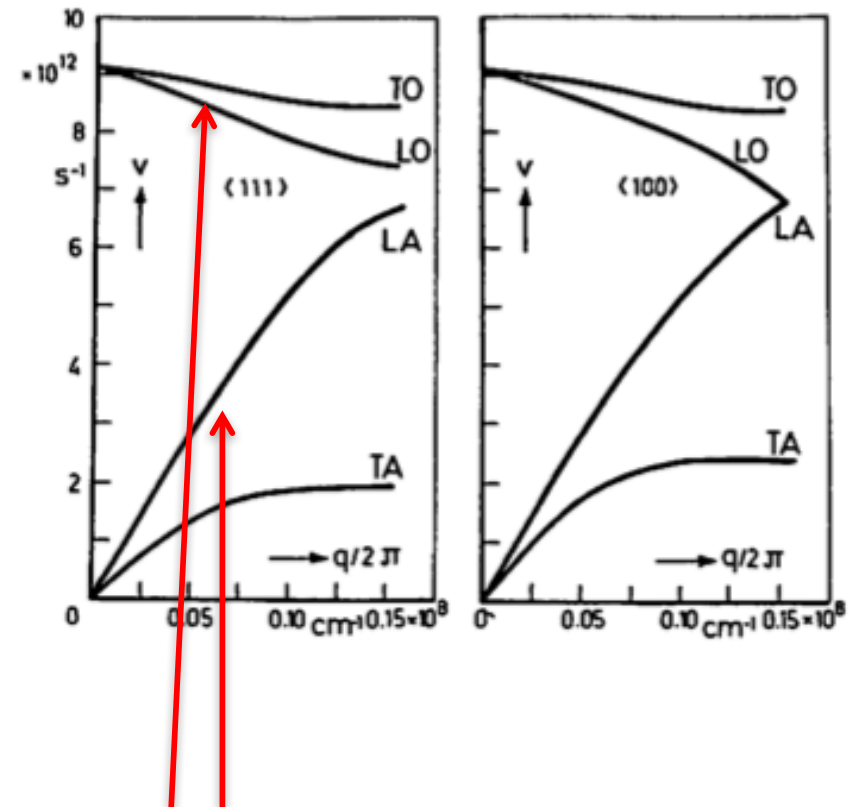
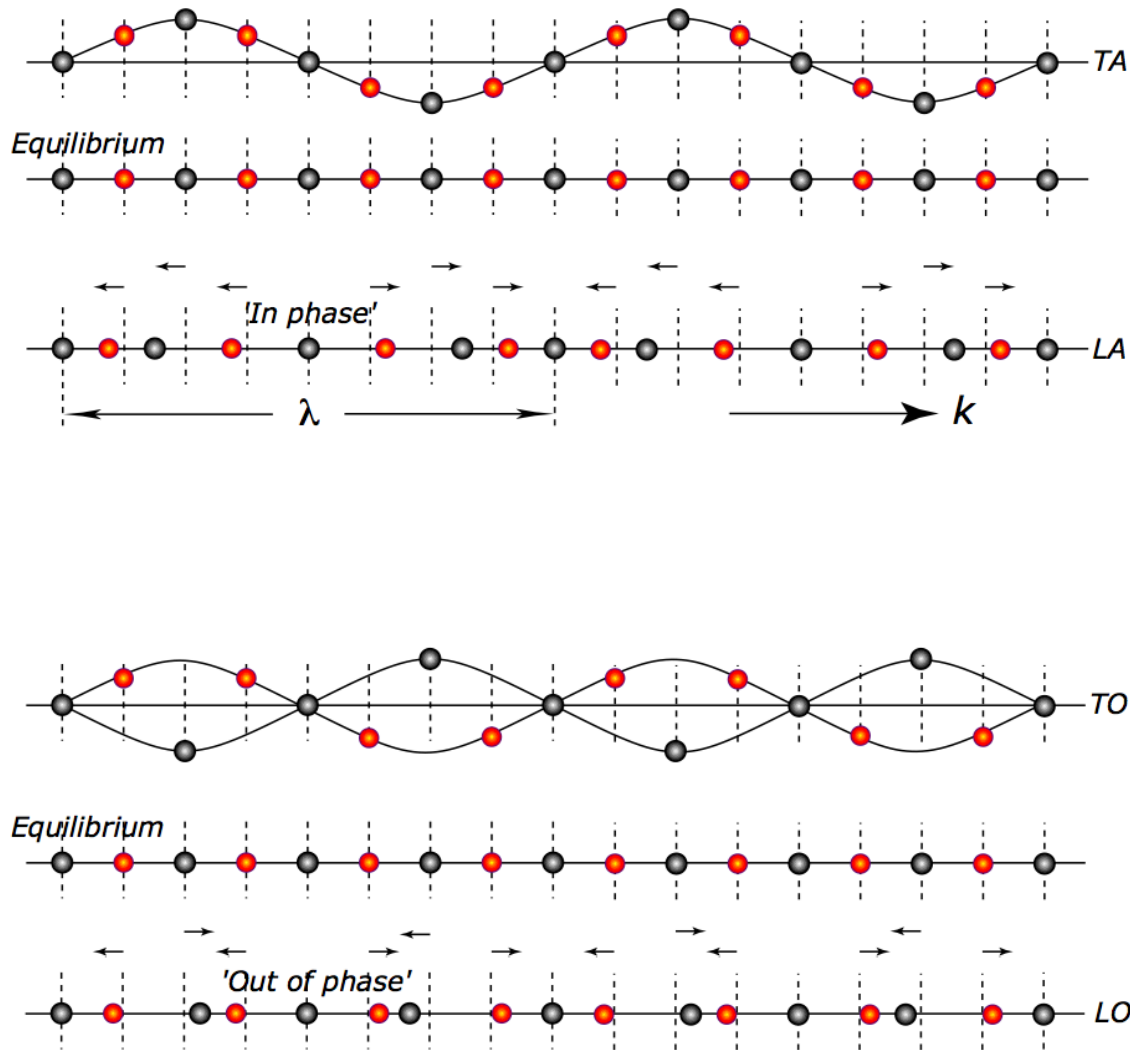
Vibrations form a wave

$$\omega^2(q) = \frac{2C}{M} (1 - \cos qa)$$

Acoustic phonon dispersion



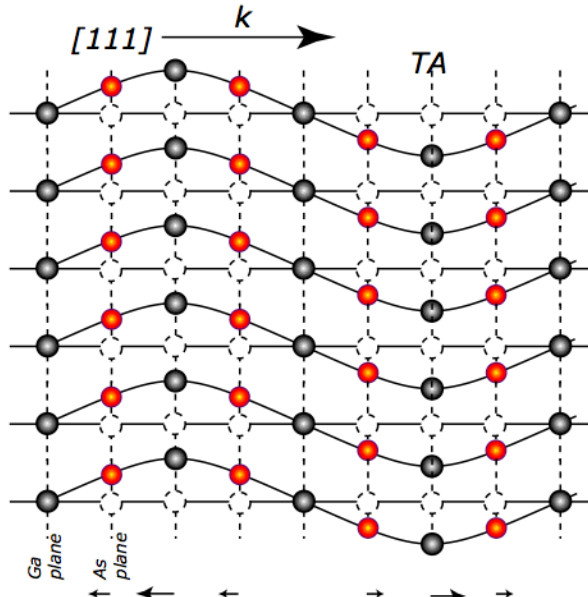
Phonons in Semiconductors



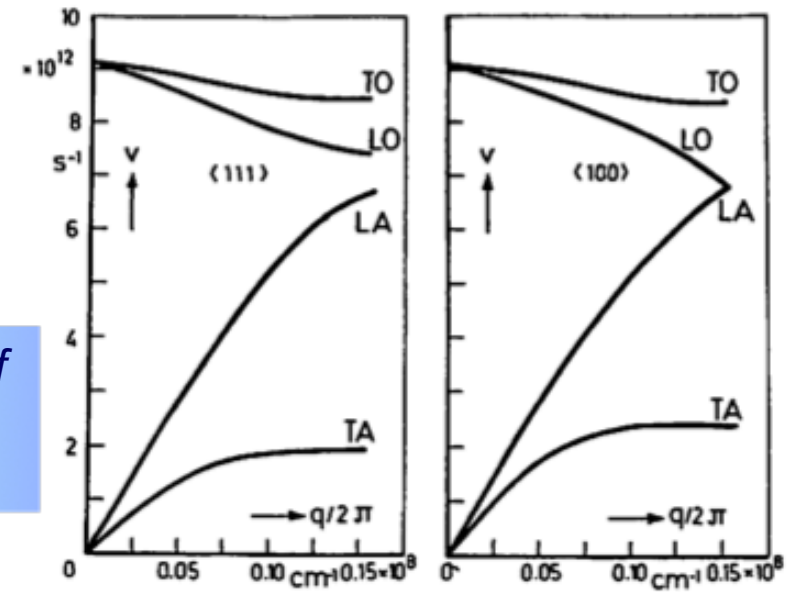
Acoustic and optical phonon dispersion

$$\omega_{\pm}^2(k) = \frac{C}{M_r} \left[1 \pm \sqrt{1 - \frac{2M_r}{M_1 + M_2} (1 - \cos ka)} \right]$$

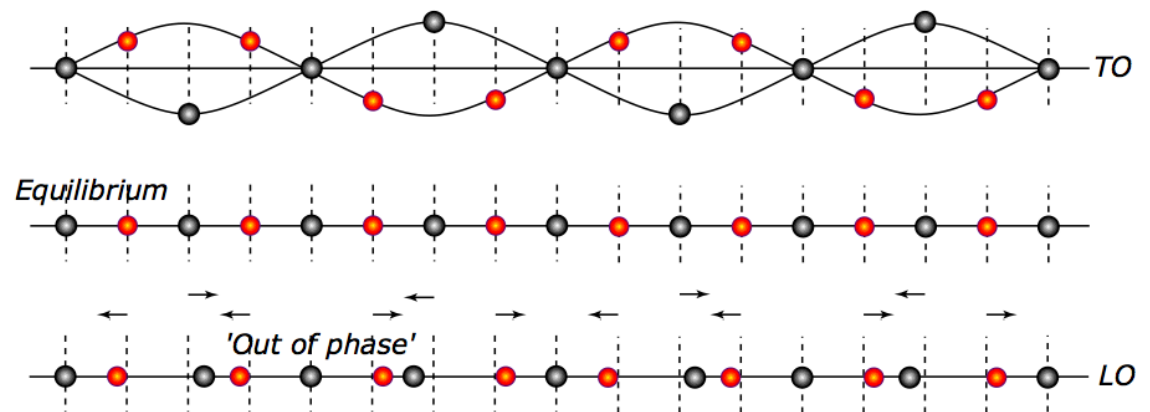
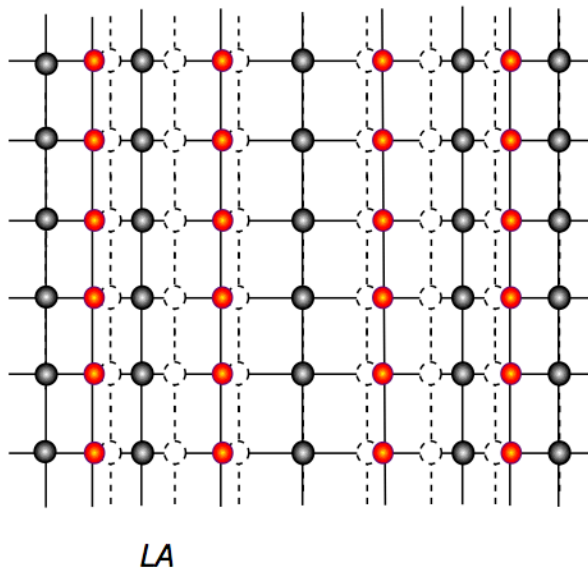
Phonons in Semiconductors



Difference in energies of longitudinal and optical acoustic phonons



Typical phonon spectra of semiconductors



Electron-Def. Pot. Acoustic Phonon interaction

Deformation Potential Acoustic Phonon Scattering Potential

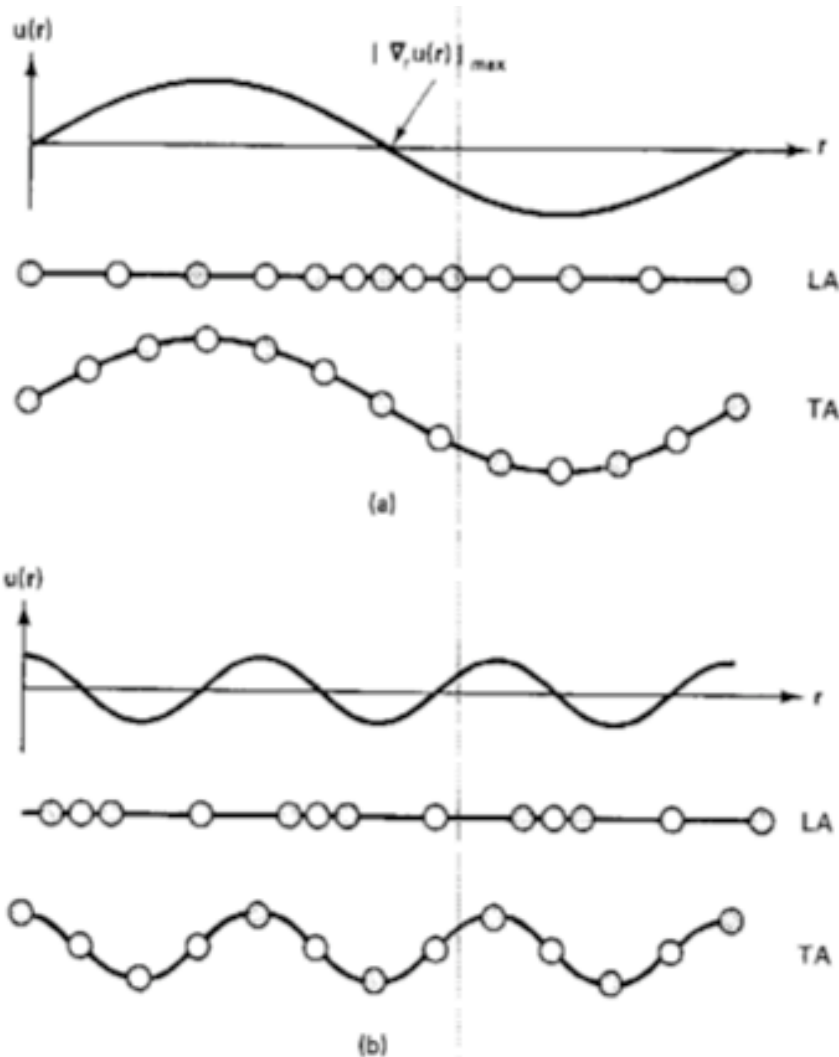


Figure 6.2 Displacements of a diatomic chain for LA and TA phonons at (a) the center and (b) the edge of the Brillouin zone. The lighter mass atoms are indicated by open circles. For zone edge acoustic phonons only the heavier atoms are displaced.

$$\mathbf{u}(\mathbf{r}, t) = \mathbf{a}u(\mathbf{r}, t) \quad (6.4)$$

where

$$u(\mathbf{r}, t) = u \exp [i(\mathbf{q}_s \cdot \mathbf{r} - \omega_s t)] \quad (6.5)$$

In these equations \mathbf{a} is the displacement direction, and u is the amplitude. The strain associated with the displacement is

$$\nabla \cdot \mathbf{u}(\mathbf{r}, t) = \mathbf{a} \cdot \nabla u(\mathbf{r}, t) \quad (6.6)$$

$$\nabla \cdot \mathbf{u}(\mathbf{r}, t) = i\mathbf{q}_s \cdot \mathbf{a}u(\mathbf{r}, t) \quad (6.7)$$

Equation (6.7) indicates that for the transverse components of a phonon where the displacement and the wavevector are orthogonal, $\mathbf{q}_s \cdot \mathbf{a} = 0$, and no strain is produced. The scattering potential for the longitudinal component is, therefore,

$$\Delta U(\mathbf{r}, t) = \mathcal{E}_A \nabla \cdot \mathbf{u}(\mathbf{r}, t) \quad (6.8)$$

where the *deformation potential*, \mathcal{E}_A , in units of energy, is defined as the proportionality constant between the scattering potential (units of energy) and the strain.

Electron-Piezoelectric Acoustic Phonon interaction

Piezoelectric Acoustic Phonon Scattering Potential

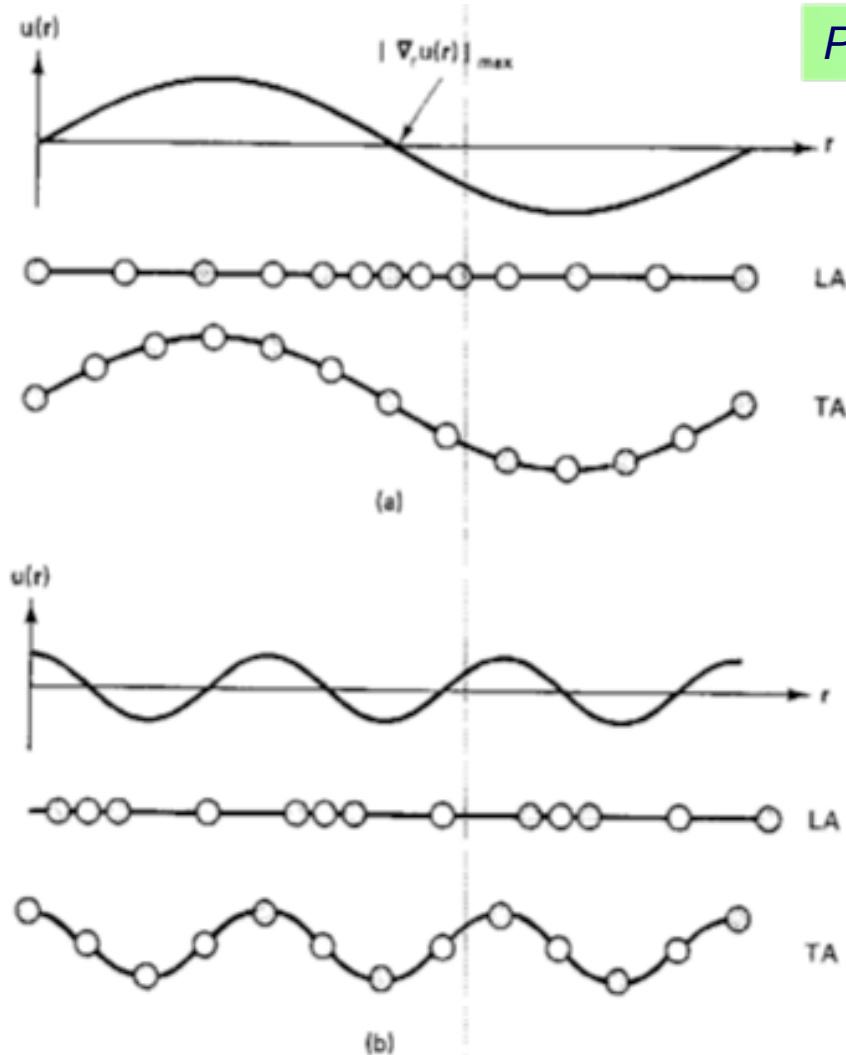


Figure 6.2 Displacements of a diatomic chain for LA and TA phonons at (a) the center and (b) the edge of the Brillouin zone. The lighter mass atoms are indicated by open circles. For zone edge acoustic phonons only the heavier atoms are displaced.

$$\Delta U(\mathbf{r}, t) = -q\psi(\mathbf{r}, t)$$

$$\psi(\mathbf{r}, t) = - \int \mathbf{E}(\mathbf{r}, t) \cdot d\mathbf{r}$$

$$\mathbf{D}(\omega) = \epsilon(\omega)\mathbf{E} = \epsilon_0\mathbf{E} + \mathbf{P}(\omega)$$

$$\mathbf{D}(0) = \epsilon(0)\mathbf{E} = \epsilon_0\mathbf{E} + \mathbf{P}(0)$$

Piezo charge

$$\mathbf{D}(0) = \epsilon(0)\mathbf{E}(\mathbf{r}, t) + e_{pz} \nabla u(\mathbf{r}, t)$$

$$\mathbf{E}(\mathbf{r}, t) = - \frac{e_{pz}}{\epsilon(0)} \nabla u(\mathbf{r}, t)$$

$$\Delta U(\mathbf{r}, t) = \frac{-qe_{pz}}{\epsilon(0)} u(\mathbf{r}, t)$$

$$\Delta U(\mathbf{r}, t) = \frac{iqe_{pz}}{\epsilon(0)q_s} \nabla \cdot \mathbf{u}(\mathbf{r}, t)$$

Electron-Def. Pot. Optical Phonon interaction

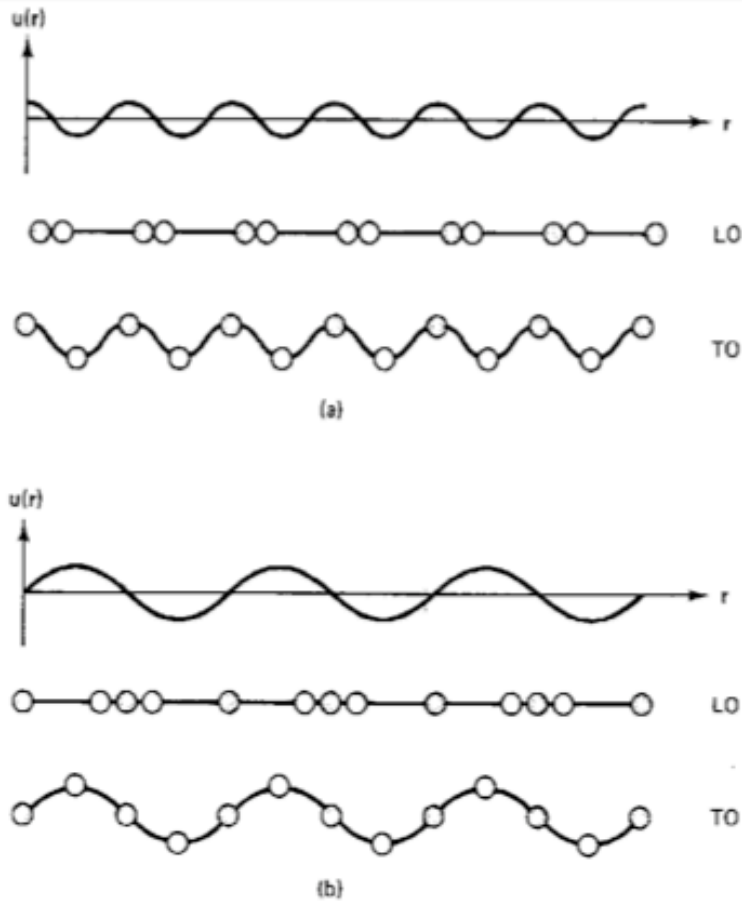
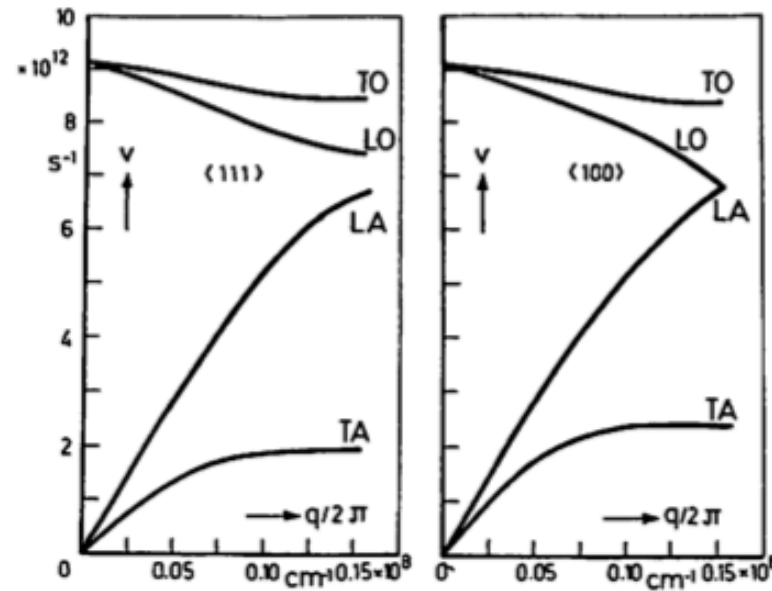


Figure 6.3 Displacements of a diatomic chain for LO and TO phonons at (a) the center and (b) the edge of the Brillouin zone. The lighter mass atoms are indicated by open circles. For zone edge optical phonons only the lighter atoms are displaced.



Typical phonon spectra of semiconductors

$$\delta u(\mathbf{r}, t) \equiv u_1(\mathbf{r}, t) - u_2(\mathbf{r}, t) \quad (6.17)$$

where $u_1(\mathbf{r}, t)$ and $u_2(\mathbf{r}, t)$ have the form given by (6.4) and (6.5). The scattering potential due to modulation of the conduction and valence edges must then be proportional to this relative displacement and

$$\Delta U(\mathbf{r}, t) = D \delta u(\mathbf{r}, t) \quad (6.18)$$

where

$$\delta u(\mathbf{r}, t) = a \delta u(\mathbf{r}, t) \quad (6.19)$$

Optical Deformation Potential scattering potential $D \sim 10^8$ eV/cm

Electron-Polar Optical Phonon interaction

$$\mathbf{D}(0) = \epsilon(0)\mathbf{E} = \epsilon_0\mathbf{E} + \mathbf{P}(0)$$

$$\mathbf{D}(\infty) = \epsilon(\infty)\mathbf{E} = \epsilon_0\mathbf{E} + \mathbf{P}(\infty)$$

$$\mathbf{P}(0) = \mathbf{P}(\infty) + \mathbf{P}_i$$

Using (6.22) in (6.20) and subtracting (6.21), we obtain

$$\epsilon(0)\mathbf{E} = \epsilon(\infty)\mathbf{E} + \mathbf{P}_i$$

or

$$\mathbf{D}(0) = \epsilon(\infty)\mathbf{E} + \mathbf{P}_i$$

From (6.24) we can determine the internal fields induced by the optical phonon polarization of the unit cell.

The polarization of a unit cell, $\mathbf{P}_i(\mathbf{r}, t)$, is determined by the relative displacement of the ions in a unit cell, $\delta\mathbf{u}(\mathbf{r}, t)$, and the effective ionic charge, e^* , such that

$$\mathbf{P}_i(\mathbf{r}, t) = \frac{e^*}{\Omega} \delta\mathbf{u}(\mathbf{r}, t) \quad (6.25)$$

In this equation $\Omega = V/N$ is the volume of the N primitive or Wigner-Seitz unit cells and e^* is the Born effective charge given by

$$e^* = \Omega\omega_{LO}\epsilon(\infty)\rho^{1/2} \left[\frac{1}{\epsilon(\infty)} - \frac{1}{\epsilon(0)} \right]^{1/2} \quad (7.174)$$

where ρ is the mass density. This equation is derived in Chapter 7. Assuming no space or surface charges, (6.24) and (6.25) give an internal field,

$$\mathbf{E}(\mathbf{r}, t) = -\frac{e^*}{\Omega\epsilon(\infty)} \delta\mathbf{u}(\mathbf{r}, t) \quad (6.26)$$

Frohlich interaction

$$\frac{\epsilon_r(0)}{\epsilon_r(\infty)} = \left(\frac{\omega_{LO}}{\omega_{TO}} \right)^2$$

as the Lyddane-Sachs-Teller relation

Using (6.9), (6.10), and (6.26), the scattering potential for polar mode scattering is

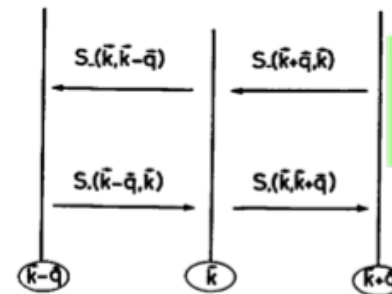
$$\Delta U(\mathbf{r}, t) = \frac{-qe^*}{\Omega\epsilon(\infty)} \int \delta\mathbf{u}(\mathbf{r}, t) \cdot d\mathbf{r} \quad (6.27)$$

or with (6.5) and (6.19),

$$\Delta U(\mathbf{r}, t) = \frac{iqe^*}{\Omega\epsilon(\infty)q_s} \delta u(\mathbf{r}, t) \quad (6.28)$$

A comparison of (6.18) and (6.28) shows that the scattering potentials for deformation potential and polar mode scattering by optical phonons are out of phase by 90° and are thus independent.

Polar optical phonon scattering potential



Optical phonon absorption and emission processes

Fig. 6.12. Schematic representation of electron transitions involving phonon emission and phonon absorption

$$\begin{aligned} [-\partial f(k)/\partial t]_{\text{coll}} = & V(2\pi)^{-3} \int d^3q \{ S_-(k, k-q) f(k) [1 - f(k-q)] \\ & + S_+(k, k+q) f(k) [1 - f(k+q)] - S_-(k+q, k) f(k+q) [1 - f(k)] \\ & - S_+(k-q, k) f(k-q) [1 - f(k)] \}. \end{aligned} \quad (6.9.1)$$

Amplitude of Phonon Vibrations

$$u_s(x, t) = u_0 e^{i(\beta x - \omega t)} + u_0 e^{-i(\beta x - \omega t)}$$

$$|u_s|^2 = 4u_0^2 \cos^2(\beta x - \omega t)$$

$$\text{KE} = \frac{1}{2} M \left(\frac{du_s}{dt} \right)^2 = 2M\omega^2 u_0^2 \sin^2(\beta x - \omega t)$$

$$\text{PE} = \frac{1}{2} K u_s^2 = 2K u_0^2 \cos^2(\beta x - \omega t)$$

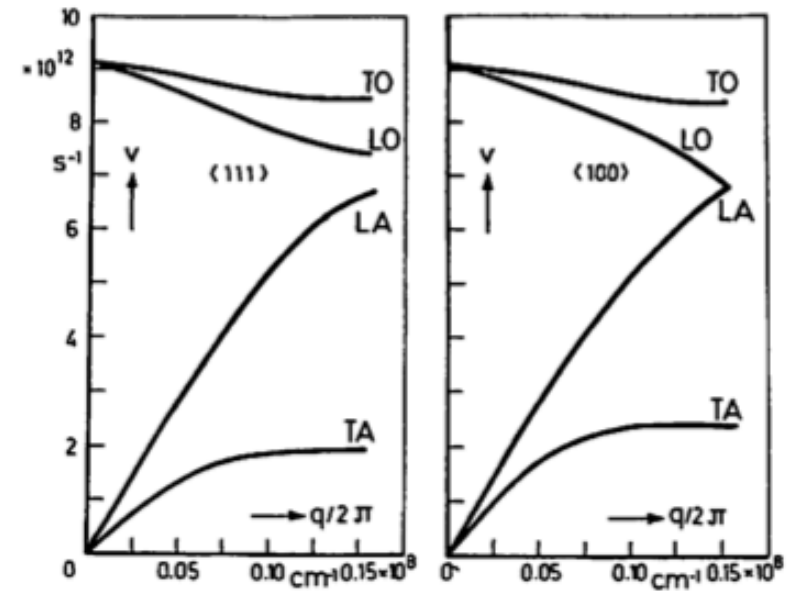
$$\text{but... } \omega^2 = \frac{K}{M} \rightarrow$$

$$\text{KE} + \text{PE} = 2M\omega^2 u_0^2 = N_\omega \cdot \hbar\omega \rightarrow$$

$$\text{since... } M = \rho V,$$

$$u_0^2 = \frac{\hbar}{2\omega\rho V} \cdot N_\omega$$

$$N_\omega(T) = \frac{1}{e^{\frac{\hbar\omega}{kT}} - 1}$$



Typical phonon spectra of semiconductors

Vibration amplitude as a function of the temperature: Quantum-Classical connection of the phonon harmonic oscillator

Electron-Phonon Scattering Rates

Polar optical phonon

$$D = \epsilon_0 E + \frac{q^* u}{\Omega}$$

$$E(x, t) = -\frac{q q^* u}{\epsilon_0 \Omega}$$

$$W(r, t) = -q \int dx E(x, t) = \frac{q}{i\beta \epsilon_0} \cdot \frac{q^*}{\Omega} \cdot u_0 e^{i(\beta \cdot r - \omega t)}$$

$$\left(\frac{q^*}{\Omega}\right)^2 = \rho \epsilon_0 \omega_0^2 \left(\frac{1}{\epsilon_s^\infty} - \frac{1}{\epsilon_s^0}\right)$$

$$W(r, t) = -q \int dx E(x, t) = \frac{q \omega_0 \sqrt{\rho}}{i\beta} \sqrt{\frac{1}{\epsilon_s^\infty} - \frac{1}{\epsilon_s^0}} \cdot u_0 e^{i(\beta \cdot r - \omega t)}$$

$$S(k \rightarrow k') = \frac{2\pi}{\hbar} |W(q_s)|^2 \frac{\hbar}{2\rho\Omega\omega_{q_s}} \left[N(\omega_{q_s}) + \frac{1}{2} \mp \frac{1}{2} \right] \delta\left[\pm \cos(\theta) + \frac{q_s}{2k} \mp \frac{\omega_{q_s}}{v_{q_s}}\right]$$

Deformation potential acoustic phonon

$$W(x, t) = D_{ac} \frac{\partial u}{\partial x}$$

$$W(r, t) = D_{ac} (\nabla \cdot \mathbf{u}) = i D_{ac} \beta u_0 e^{i(\beta \cdot r - \omega t)}$$

Momentum conservation

$$\hbar \mathbf{k}' = \hbar \mathbf{k} \pm \hbar \beta$$

Energy conservation

$$E_{\mathbf{k}'} = E_{\mathbf{k}} \pm \hbar \omega_\beta$$

Deformation potential optical phonon

$$W(r, t) = D_{op} u = D_{op} u_0 e^{i(\beta \cdot r - \omega t)}$$

$$k'^2 = k^2 + \beta^2 \pm 2k\beta \cos \theta$$

Energy conservation

$$\beta^2 \pm 2\beta k \cos \theta \mp \frac{2m^* \hbar \omega_\beta}{\hbar^2} = 0$$

For acoustic phonons, $\hbar \omega_\beta = \hbar v_s \beta$, and we get

Allowed angles for acoustic phonon scattering events

$$\beta = 2k(\mp \cos \theta \pm \frac{m^* v_s}{\hbar k}) = 2k(\mp \cos \theta \pm \frac{v_s}{v_k})$$

For optical phonons, we get

Allowed angles for optical phonon scattering events

$$\beta = \mp k \cos \theta \pm \sqrt{k^2 \cos^2 \theta \pm \frac{2m^* \hbar \omega_\beta}{\hbar^2}}$$

Piezoelectric acoustic phonon

$$D = \epsilon_0 \epsilon_s E + e_{pz} \frac{\partial u}{\partial x}$$

$$E(x, t) = -\frac{e_{pz}}{\epsilon_0 \epsilon_s} \frac{\partial u}{\partial x}$$

$$W(r, t) = -q \int dx E(x, t) = \frac{q e_{pz}}{\epsilon_0 \epsilon_s} u_0 e^{i(\beta \cdot r - \omega t)}$$

$$\frac{K^2}{1 - K^2} = \frac{e_{pz}^2}{\epsilon_0 \epsilon_s v_s}$$

Electron-Acoustic Phonon interaction: Mobility

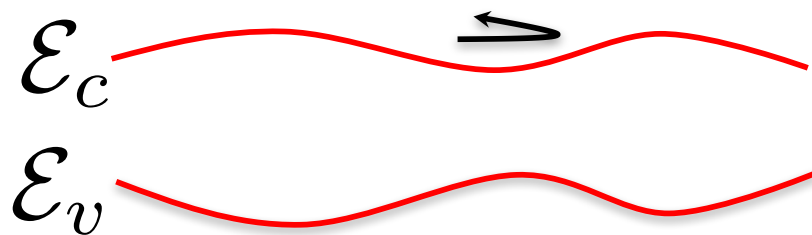
$\delta \mathbf{r} = A_l \exp [\pm i (\mathbf{q}_l \cdot \mathbf{r})]$, Acoustic phonon scattering

$$|H_{k'k}| = \frac{\epsilon_{ac} q_l A_l}{V} \left| \int \exp [i (\mathbf{k} - \mathbf{k}' \pm \mathbf{q}_l) \cdot \mathbf{r}] d^3 r \right|$$

$$\mathbf{k}' = \mathbf{k} \pm \mathbf{q}_l$$

$$2M\omega^2 u_0^2 \approx N_{ph} \times \hbar \omega$$

$$|H_{k'k}| = \epsilon_{ac} q_l A_l$$



$$A_l \rightarrow \left| \int \psi_{N \pm 1}^* x \psi_N d^3 r \right| = \begin{cases} (N \hbar / 2 M \omega_l)^{1/2} & \text{for } N \rightarrow N - 1 \\ ((N + 1) \hbar / 2 M \omega_l)^{1/2} & \text{for } N \rightarrow N + 1 \end{cases}$$

SHO: |amplitude|² ~ number of phonons

$$N \rightarrow N_q = [\exp(\hbar \omega_l / k_B T) - 1]$$

$$S \approx \frac{2\pi}{\hbar} |H_{k'k}|^2 [\delta(\epsilon(k') - \epsilon(k) + \hbar \omega_l) + \delta(\epsilon(k') - \epsilon(k) - \hbar \omega_l)]$$

$$|H_{k \pm q, k}| = \epsilon_{ac} q_l [(N_q + 1/2 \mp 1/2) \hbar / 2 \rho V \omega_l]^{1/2}$$

$$c_l = \rho v_s^2$$

$$\approx 2 \frac{2\pi}{\hbar} |H_{k'k}|^2 \delta[\epsilon(k') - \epsilon(k)]$$

absorption ~ emission

$$|H_{k'k}| = \epsilon_{ac} q_l [k_B T / 2 \rho V \omega_l^2]^{1/2} = \epsilon_{ac} [k_B T / 2 V c_l]^{1/2}$$

Deformation potential

Piezoelectric

$$\Delta U(\mathbf{r}, t) = \mathcal{E}_A \nabla \cdot \mathbf{u}(\mathbf{r}, t)$$

$$\Delta U(\mathbf{r}, t) = \frac{i q e_{pz}}{\epsilon(0) q_s} \nabla \cdot \mathbf{u}(\mathbf{r}, t)$$

$$\mu = \frac{2 \sqrt{2\pi}}{3} \frac{e \hbar^4 c_l}{m^{5/2} (k_B)^{3/2} \epsilon_{ac}^2} T^{-3/2}$$

$$K^2 = \frac{e_{pz}^2 / c_l}{\chi \chi_0 + e_{pz}^2 / c_l}$$

$$\mu = \frac{16 \sqrt{2\pi}}{3} \frac{\hbar^2 \chi \chi_0}{m^{3/2} e K^2 (k_B T)^{1/2}} \propto T^{-1/2}$$

which in units of cm²/V s is given by

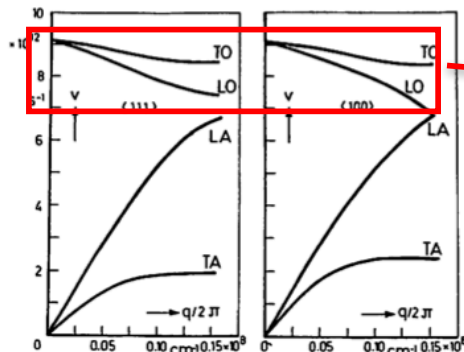
and in units of cm²/V s

$$\mu = 3.06 \times 10^4 \frac{c_l / 10^{12} \text{ dyn cm}^{-2}}{(m/m_0)^{5/2} (T/100 \text{ K})^{3/2} (\epsilon_{ac} / \text{eV})^2} \propto T^{-3/2}$$

$$\mu = 2.6 \frac{\chi}{(m/m_0)^{3/2} K^2 (T/100 \text{ K})^{1/2}}$$

Coupling $K \sim 10^{-3}$

Electron-Optical Phonon Scattering Rates, Mobility



$$\hbar \omega_0 = k_B \Theta .$$

Θ is known as the *Debye temperature*

Deformation potential Optical Phonon

$$\mu_0 = \frac{4 \sqrt{2\pi} e \hbar^2 \rho (k_B \Theta)^{1/2}}{3 m^{5/2} D^2} f(T/\Theta) .$$

The function $f(T/\Theta)$ is given by

$$f(T/\Theta) = (2z)^{5/2} (e^{2z} - 1) \int_0^\infty \frac{y^{3/2} e^{-2zy} dy}{\sqrt{y+1} + e^{2z} \operatorname{Re}\{\sqrt{y-1}\}} ,$$

where $z = \Theta/2T$ and $y = \epsilon/k_B \Theta$. The function is shown

Its numerical value in units of $\text{cm}^2/\text{V s}$ is given by

$$\mu = 2.04 \times 10^3 \frac{(\rho/g \text{ cm}^{-3}) (\Theta/400 \text{ K})^{1/2}}{(m/m_0)^{5/2} (D/10^8 \text{ eV cm}^{-1})^2} f(T/\Theta)$$

Polar Optical Phonon Scattering

$$\begin{aligned} \alpha &= \frac{\hbar |e| E_0}{2^{1/2} m^{1/2} (\hbar \omega_0)^{3/2}} = \frac{1}{137} \sqrt{\frac{m c^2}{2 k_B \Theta}} \left(\frac{1}{\kappa_{\text{opt}}} - \frac{1}{\kappa} \right) \\ &= 397.4 \sqrt{\frac{m/m_0}{\Theta/\text{K}}} \left(\frac{1}{\kappa_{\text{opt}}} - \frac{1}{\kappa} \right) \end{aligned}$$

The mobility is simply $(e/m) \tau_m$:

$$\mu = [|e|/(2m \alpha \omega_0)] \exp(\Theta/T)$$

which in units of $\text{cm}^2/\text{V s}$ is given by

$$\mu = 2.6 \times 10^5 \frac{\exp(\Theta/T)}{\alpha (m/m_0) (\Theta/\text{K})} \quad \text{for } T \ll \Theta$$

For example, in n-type GaAs where $\Theta = 417 \text{ K}$, $m/m_0 = 0.072$, $\alpha = 0.067$, we calculate a mobility at 100 K of $2.2 \times 10^5 \text{ cm}^2/\text{V s}$. This is of the order of magnitude of the highest mobilities observed in this material. At this and

All Scattering Matrix Elements

TABLE 6.1 Scattering Potentials and Matrix Elements for Various Scattering Mechanisms^a

Scattering Mechanisms	Scattering Potential	Matrix Element
Impurities		
Ionized	$\frac{Zq^2}{4\pi\epsilon(0)r}$	$\frac{Zq^2}{\epsilon(0)V k - k' ^2}$
Neutral	$\frac{\hbar^2}{m^*} \left(\frac{r_B}{r^5}\right)^{1/2}$	$\frac{2\pi\hbar^2}{m^*V} \left(\frac{20r_B}{k}\right)^{1/2}$
Acoustic phonons		
Deformation potential	$\mathcal{E}_A \nabla \cdot \mathbf{u}$	$\mathcal{E}_A \left(\frac{\hbar}{2V\rho\omega_s}\right)^{1/2} (\mathbf{a} \cdot \mathbf{q}_s) \left(n_q + \frac{1}{2} \pm \frac{1}{2}\right)^{1/2}$
Piezoelectric	$\frac{iqe_{pz}}{\epsilon(0)q_s} \nabla \cdot \mathbf{u}$	$\frac{qe_{pz}}{\epsilon(0)} \left(\frac{\hbar}{2V\rho\omega_s}\right)^{1/2} \left(n_q + \frac{1}{2} \pm \frac{1}{2}\right)^{1/2}$
Optical phonons		
Deformation potential	$D\delta u$	$D \left(\frac{\hbar}{2V\rho\omega_{LO}}\right)^{1/2} \left(n_q + \frac{1}{2} \pm \frac{1}{2}\right)^{1/2}$
Polar	$\frac{iqe^*}{\omega\epsilon(\infty)q_s} \delta u$	$\frac{qe^*}{\Omega\epsilon(\infty)q_s} \left(\frac{\hbar}{2V\rho\omega_{LO}}\right)^{1/2} \left(n_q + \frac{1}{2} \pm \frac{1}{2}\right)^{1/2}$

^a r_B = Bohr radius; n_q = phonon occupation number; $e^* = \Omega\omega_{LO}\epsilon(\infty)\rho^{1/2}[1/\epsilon(\infty) - 1/\epsilon(0)]^{1/2}$.

All Momentum Relaxation Times

TABLE 6.2 Momentum Relaxation Times and Reduced Energy Dependence for Materials with Isotropic Parabolic Bands^a

Scattering Mechanisms	τ_i (sec)	r_i
Impurities		
Ionized	$\frac{0.414\epsilon_r^2(0)T^{3/2}}{Z^2N_I(\text{cm}^{-3})g(n^*, T, x)} \left(\frac{m^*}{m}\right)^{1/2}$	$\frac{3}{2}$
Neutral	$\frac{8.16 \times 10^6}{\epsilon_r(0)N_N(\text{cm}^{-3})} \left(\frac{m^*}{m}\right)^2$	0
Acoustic phonons		
Deformation potential	$\frac{2.40 \times 10^{-20}C_I(\text{dyn/cm}^2)}{\mathcal{E}_A^2(\text{eV})T^{3/2}} \left(\frac{m}{m^*}\right)^{3/2}$	$-\frac{1}{2}$
Piezoelectric	$\frac{9.54 \times 10^{-8}}{h_{14}^2(\text{V/cm})(3/C_I + 4/C_I)T^{1/2}} \left(\frac{m}{m^*}\right)^{1/2}$	$\frac{1}{2}$
Optical phonons		
Deformation potential	$\frac{4.83 \times 10^{-20}C_I(\text{dyn/cm}^2)[\exp(\theta/T) - 1]}{\mathcal{E}_A^2(\text{eV})T^{1/2}\theta} \left(\frac{m}{m^*}\right)^{3/2}$	$\cong -\frac{1}{2}$
Polar	$\frac{9.61 \times 10^{-15}\epsilon_r(0)\epsilon_r(\infty)[\exp(\theta/T) - 1]}{[\epsilon_r(0) - \epsilon_r(\infty)]\theta^{1/2}(\theta/T)^r} \left(\frac{m}{m^*}\right)^{1/2}$	$r \left(\frac{\theta}{T}\right)$

^a N_I = concentration of ionized impurities; $g(n^*, T, x) = \ln(1+b) - b/(1+b)$; $b = 4.31 \times 10^{13}[\epsilon_r(0)T^2/n^*(\text{cm}^{-3})](m^*/m)x$; N_N = concentration of neutral impurities; $C_I = \frac{1}{2}(3C_{11} + 2C_{12} + 4C_{44})$; $C_I = \frac{1}{2}(C_{11} - C_{12} + 3C_{44})$; $\theta = h\omega_{LO}/k$.

Material Properties relevant for Transport

TABLE 6.3 Parameters for Calculating the Transport Properties of *n*-Type Semiconductors with Isotropic Parabolic Bands

Material	$\frac{m^*}{m}$	$\epsilon_r(0)$	$\epsilon_r(\infty)$	θ (K)	ϵ_A (eV)	C_l (10^{12} dyn/cm ²)	$h_{i4}^2 \left(\frac{3}{C_l} + \frac{4}{C_t} \right)$ (10^3 V ² /dyn)
→ GaN	0.218	9.87	5.80	1044	8.4	2.65	18.32
GaP	0.13	11.10	9.11	580	13.0	1.66	1.15
→ GaAs	0.067	12.53	10.90	423	6.3	1.44	2.04
GaSb	0.042	15.69	14.44	346	8.3	1.04	
InP	0.082	12.38	9.55	497	6.8	1.21	0.137
InAs	0.025	14.54	11.74	337	5.8	1.0	0.192
InSb	0.0125	17.64	15.75	274	7.2	0.79	0.409
ZnS	0.312	8.32	5.13	506	4.9	1.28	6.87
ZnSe	0.183	9.20	6.20	360	4.2	1.03	0.620
ZnTe	0.159	9.67	7.28	297	3.5	0.84	0.218
CdS	0.208	8.58	5.26	428	3.3	0.85	32.5
CdSe	0.130	9.40	6.10	303	3.7	0.74	16.7
CdTe	0.096	10.76	7.21	246	4.0	0.70	0.445
HgSe	0.0265	25.6	12.0	268	4	0.80	0.445
HgTe	0.0244	20.0	14.0	199	4	0.61	0.445
PbS		175	17	300	20		
PbSe		250	24	190	24	0.71	
PbTe		400	33	160	25		

Note relative Strengths!

Scattering events in semiconductors

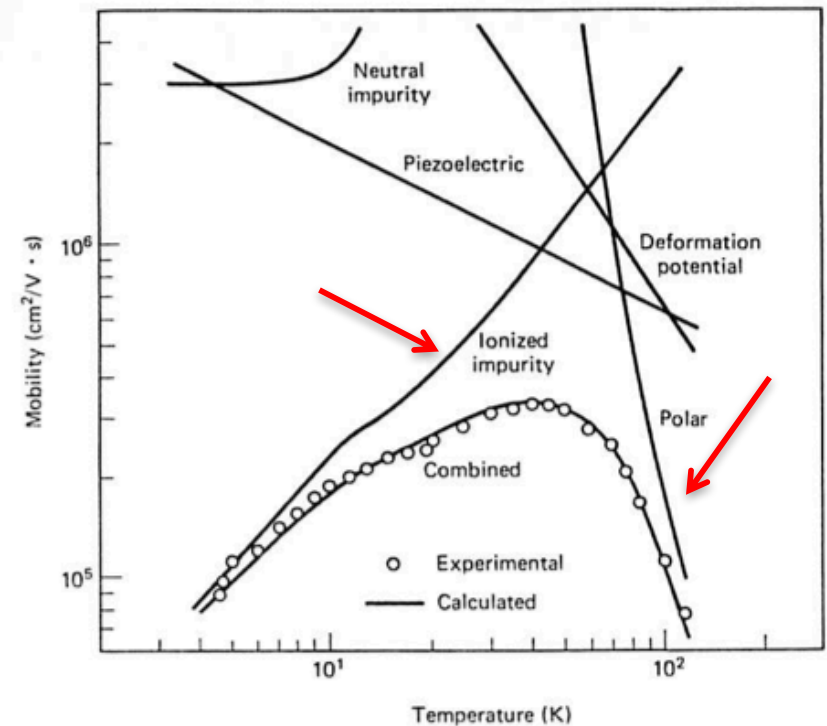
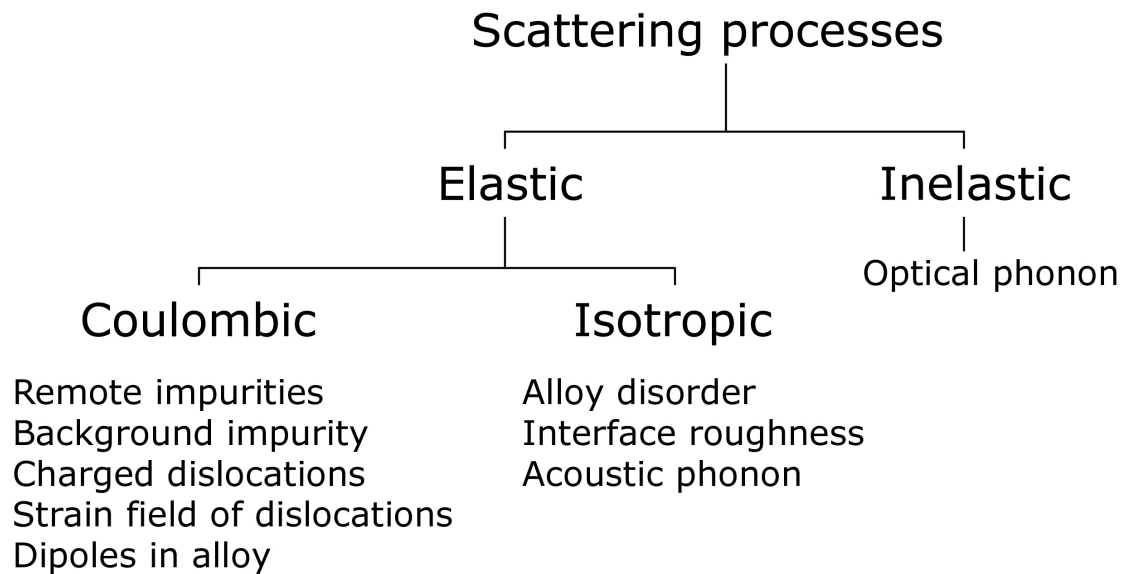


Figure 6.7 Temperature dependence of the mobility for *n*-type GaAs showing the separate and combined scattering processes. [From C. M. Wolfe, G. E. Stillman, and W. T. Lindley, *J. Appl. Phys.* 41, 3088 (1970).]

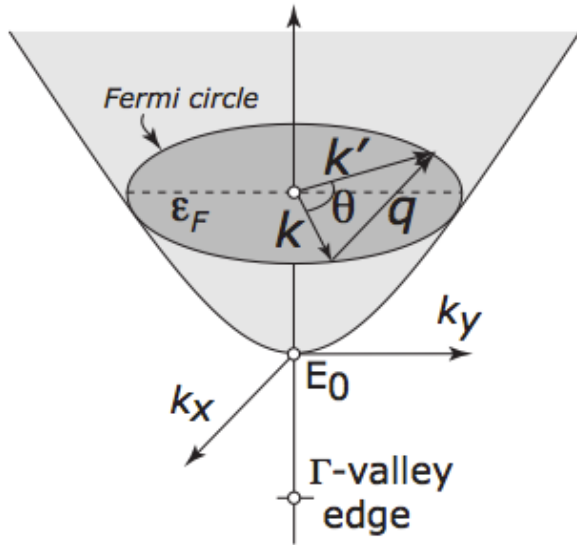
Scattering by each type of impurity affects the net electron mobility.

- Mobility in a ultra-clean (defect-free) semiconductor is limited by phonon (optical+acoustic) scattering.
- If the scattering rate of defects/impurities exceed that of phonons, then they determine the mobility.
- Method: find the scattering rate due to each type of defect. The total scattering rate is the sum of all.

Handling Diffusive Transport in Low-Dimensions

Example: Transport in 2DEGs

2DEG electron wavefunction (note: \mathbf{k} , \mathbf{r} are in the 2D plane!)



$$\frac{1}{\sqrt{A}} e^{i\mathbf{k}\cdot\mathbf{r}} \chi(z) u_{n\mathbf{k}}(\mathbf{r}) \rightarrow S(\mathbf{k}, \mathbf{k}') = \frac{2\pi}{\hbar} |H_{\mathbf{k}, \mathbf{k}'}|^2 \delta(\epsilon_{\mathbf{k}} - \epsilon_{\mathbf{k}'})$$

envelope fn.

$$H_{\mathbf{k}, \mathbf{k}'} = \langle \mathbf{k}' | V(\mathbf{r}, z) | \mathbf{k} \rangle \cdot I_{\mathbf{k}, \mathbf{k}'}$$

$$I_{\mathbf{k}, \mathbf{k}'} \approx 1$$

$$\frac{1}{\tau_m(\mathbf{k})} = N_{2D} \sum_{k'} S(k', k) (1 - \cos \theta)$$

$$\frac{1}{\langle \tau_m \rangle} = n_{2D}^{imp} \frac{m^*}{2\pi \hbar^3 k_F^3} \int_0^{2k_F} |V(q)|^2 \frac{q^2}{\sqrt{1 - (q/2k_F)^2}} dq$$

$$1 - \cos \theta = q^2 / 2k_F^2$$

In general, scattering can lead to intersubband transitions...

$$V_{nm}(q) = \frac{1}{A} \int dz \left(\chi_n^*(z) \chi_m(z) \int d^2\mathbf{r} V(\mathbf{r}, z) e^{i\mathbf{q}\cdot\mathbf{r}} \right)$$

n, m are the subband indices.

Within the same subband: 'Electric quantum limit'

$$V(q) = V_{00}(q) = \frac{1}{A} F(q) V(q, z_0)$$

Screening in 2D

$$\epsilon_{2d}(q) = \epsilon(0) \left(1 + \frac{q_{TF}}{q} \right)$$

2D screening function

$$q_{TF} = \frac{m^* e^2}{2\pi \epsilon(0) \epsilon_0 \hbar^2} = \frac{2}{a_B^*}$$

Thomas-Fermi wavevector

$$V(q, z_0) = \frac{V_{uns}(q, z_0)}{\epsilon_{2d}(q)}$$

Screened 2D potential

Handling Diffusive Transport in Low-Dimensions

$$\rho(z) \rightarrow en_s \delta(z)$$

'perfect' 2D: Graphene, BN

$$\rho(r, z) = \rho(z) = en_s |\chi(z)|^2$$

Quasi-2D: MOSFETs/HEMTs

$$\chi_{n_z}(z) = \sqrt{\frac{2}{L_z}} \sin\left(\frac{n_z \pi}{L_z} z\right)$$

'Infinitely' deep square QW

$$\chi(z) = 0, z < 0$$

$$\chi(z) = \sqrt{\frac{b^3}{2}} z e^{-\frac{bz}{2}}, z \geq 0,$$

$$b = \left(33m^*e^2n_s/8\hbar^2\epsilon_0\epsilon_b\right)^{1/3}$$

Triangular QW:
Variational Wavefunction
(Fang-Howard)
Can handle multiple
subband occupation...

$$V(q) = \frac{1}{A} F(q) V(q, z_0)$$

$$F(q) = \eta^3 = \left(\frac{b}{b+q}\right)^3$$

Form factor

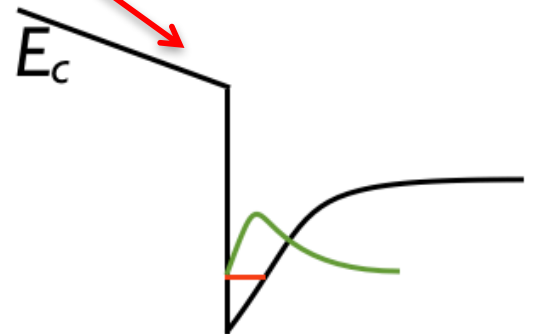
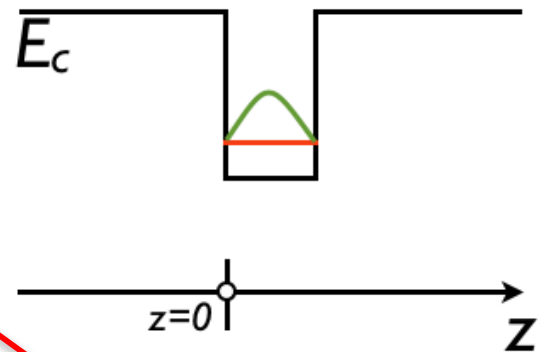
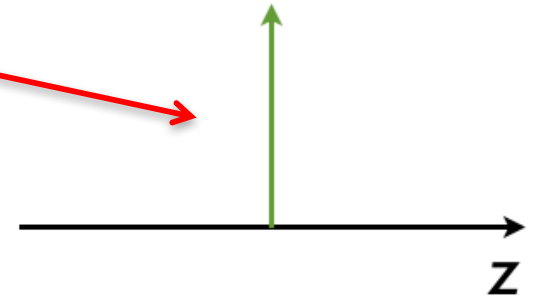
$$V(q, z_0) = \frac{V_{uns}(q, z_0)}{\epsilon_{2d}(q)}$$

Screened scattering potential

$$\epsilon_{2d}(q) = \epsilon(0) \left(1 + \frac{q_{TF}}{q} G(q)\right)$$

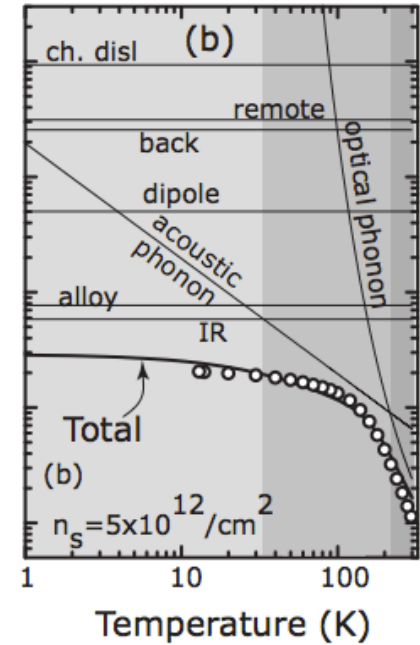
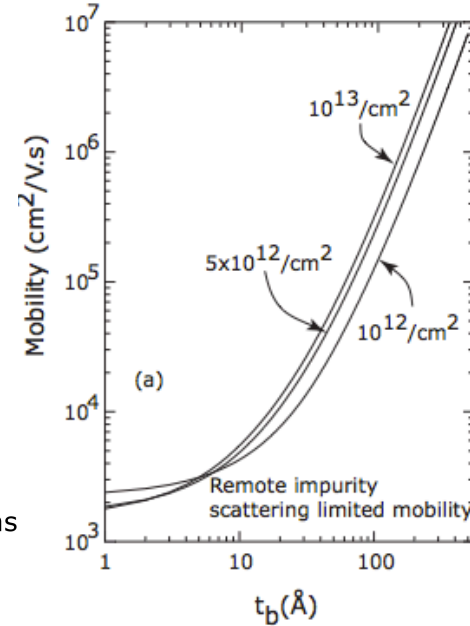
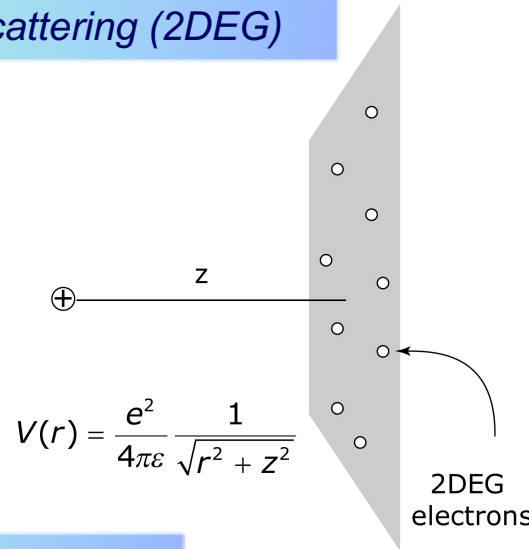
$$G(q) = \frac{1}{8} (2\eta^3 + 3\eta^2 + 3\eta)$$

Screening form factor



Handling Diffusive Transport in Low-Dimensions

Example: Remote Impurity Scattering (2DEG)



Screened remote Coulomb potential

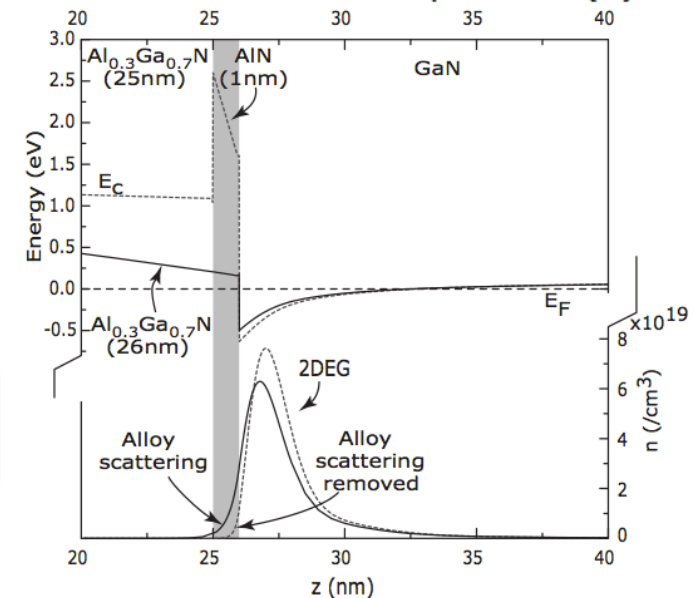
$$V(q) = \frac{V(q, z_0)}{\epsilon_{2d}(q)} = \int_0^\infty r dr \int_0^{2\pi} d\theta \frac{e^2}{4\pi\epsilon(q)\sqrt{r^2 + z_0^2}} e^{iqr \cos\theta} = \frac{e^2}{2\epsilon_0\epsilon(0)} \frac{e^{-qz_0}}{q + q_{TF}}$$

Scattering rate (note dependence on k_F)

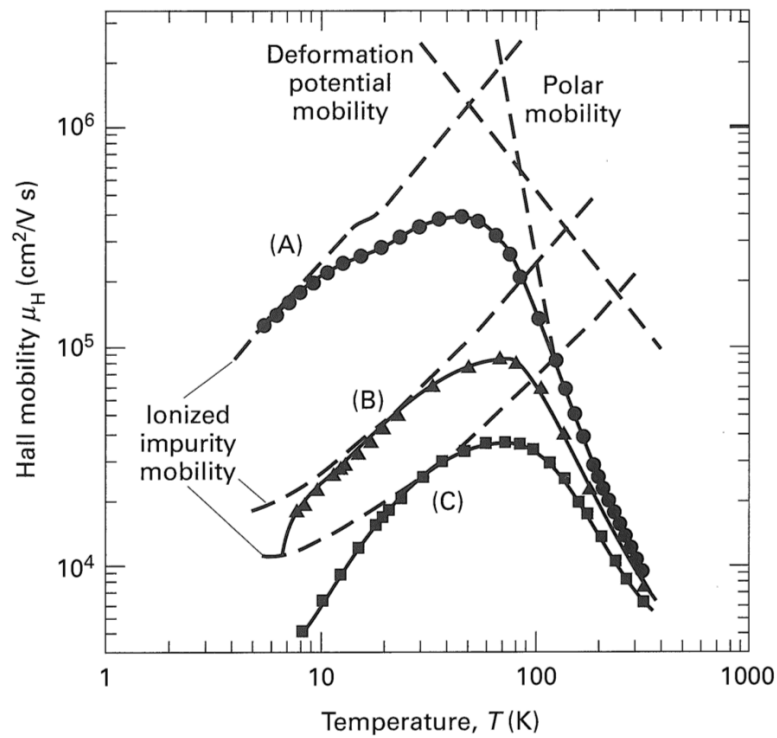
$$\frac{1}{\tau_{rem}(k_F)} = N_s \frac{m^*}{2\pi\hbar^3 k_F^3} \left(\frac{e^2}{2\epsilon_0\epsilon(0)} \right)^2 \int_0^{2k_F} dq \frac{F(q)e^{-2qt_b}}{(q + q_{TF}G(q))^2} \frac{q^2}{\sqrt{1 - \left(\frac{q}{2k_F}\right)^2}}$$

Averaging over distribution: No averaging necessary for degenerate 2DEGs because transport occurs by electrons at the Fermi energy!

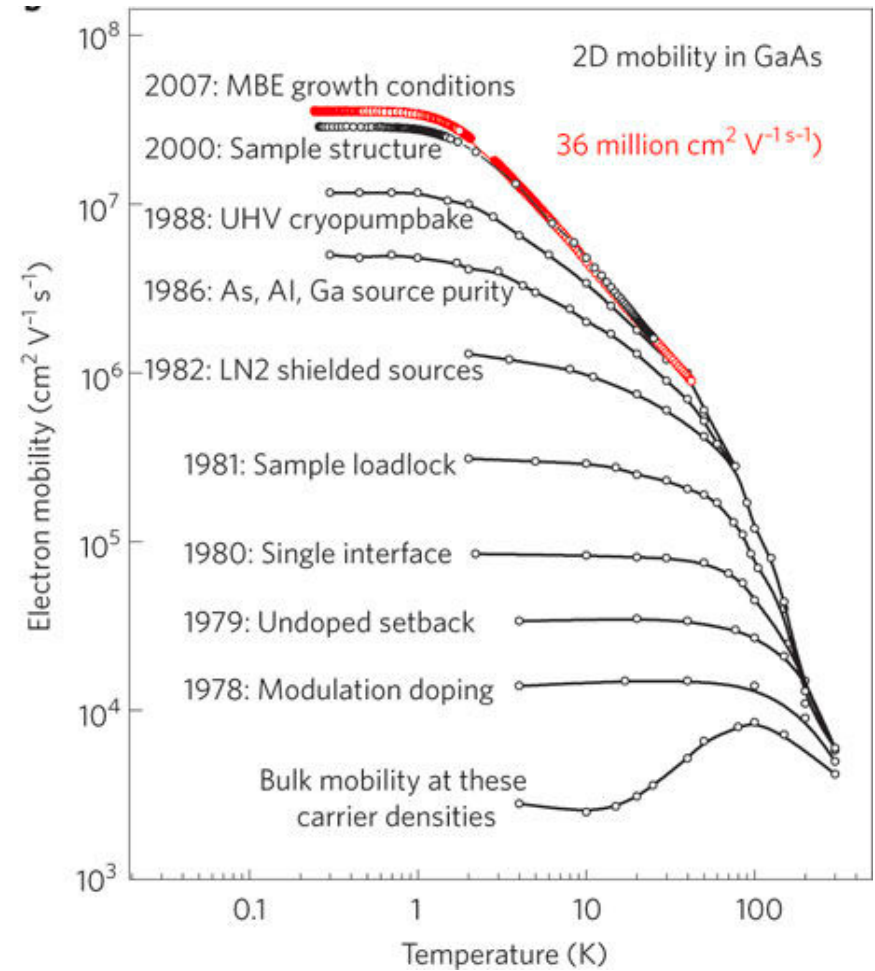
$$\frac{\partial f_0(E)}{\partial E} \approx \delta(E - E_F) \rightarrow \mu_{2DEG} \approx \frac{q\tau_m(k_F)}{m^*}$$



Transport in 3D vs 2D

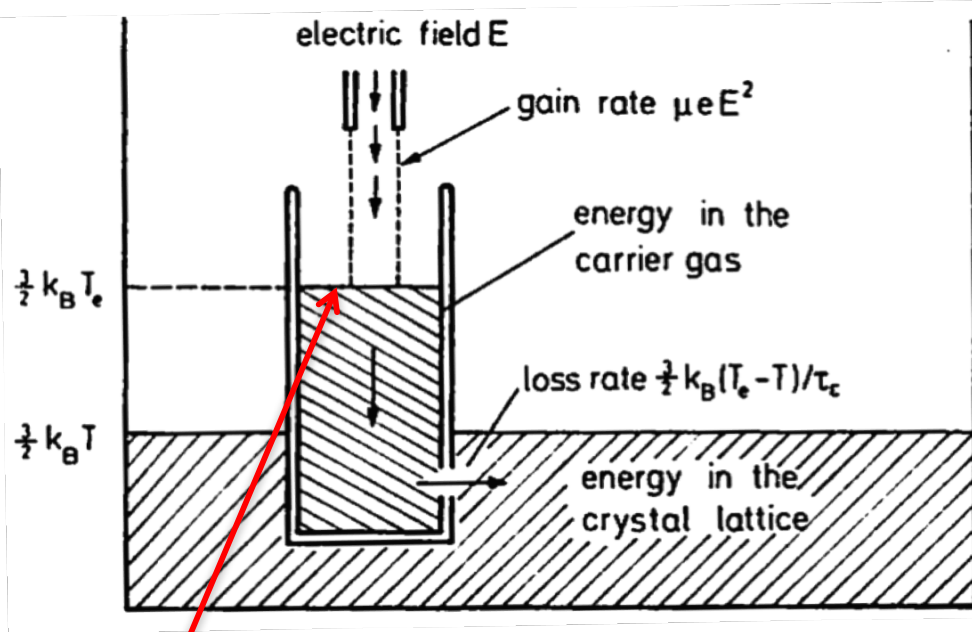


3D (Doped GaAs)



Modulation Doped GaAs

High Field Transport: Current/velocity Saturation



Hot-electron temperature: models non-equilibrium

$$v_d = v_0 \sqrt{\tau_m / \tau_E}$$

$$v_0 = \sqrt{\hbar \omega_{LO} / m_e}$$

Ensemble saturation velocity $\sim (E_{op} / m^*)^{1/2}$

$$f = \frac{1}{1 + \exp[(\mathcal{E} - \zeta) / kT_e]}$$

Hot-electron temperature

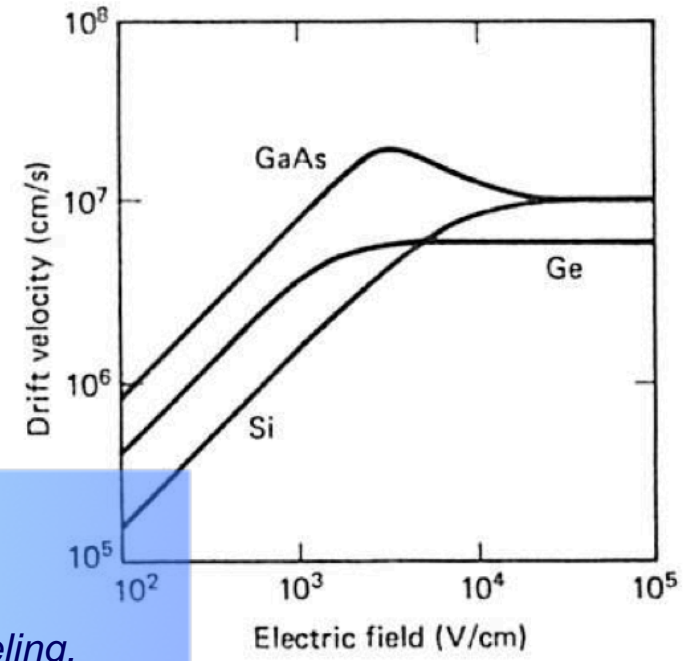
$$\frac{\partial E}{\partial t} = (-eF)v_d - \frac{\hbar \omega_{LO}}{\tau_E(T_e)}$$

Energy balance eqn.

$$\frac{\partial v_d}{\partial t} = \frac{-eF}{m_e} - \frac{v_d}{\tau_m(T_e)}$$

Momentum balance eqn.

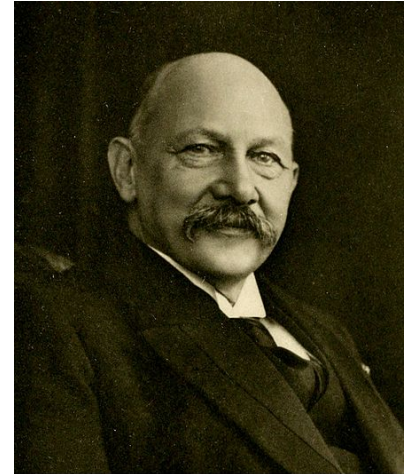
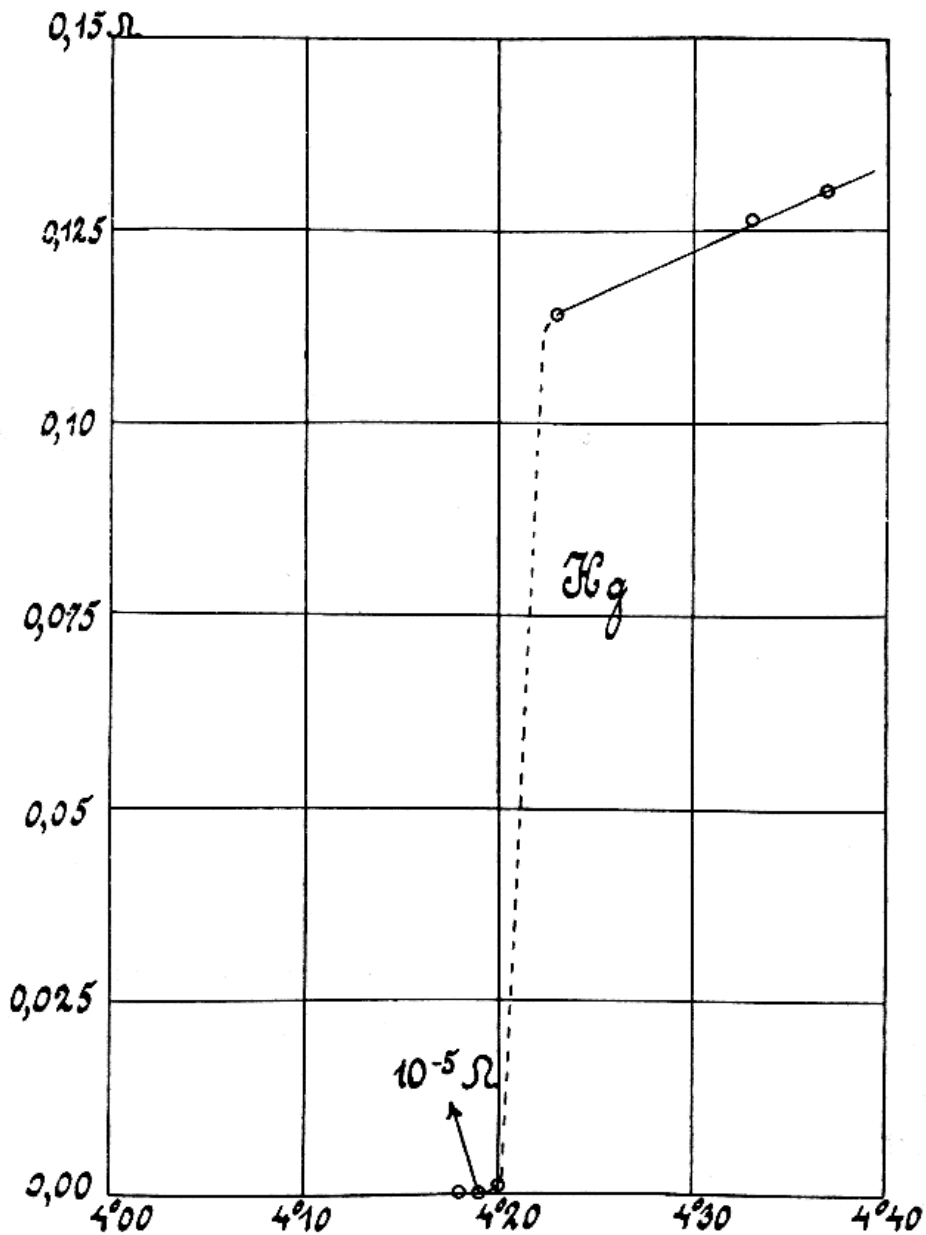
Steady state



However(!): Unanswered questions -

- Story not complete yet...
- Is saturation velocity independent of carrier concentrations? Not clear...
- Monte-Carlo simulations necessary for accurate high-field transport modeling.

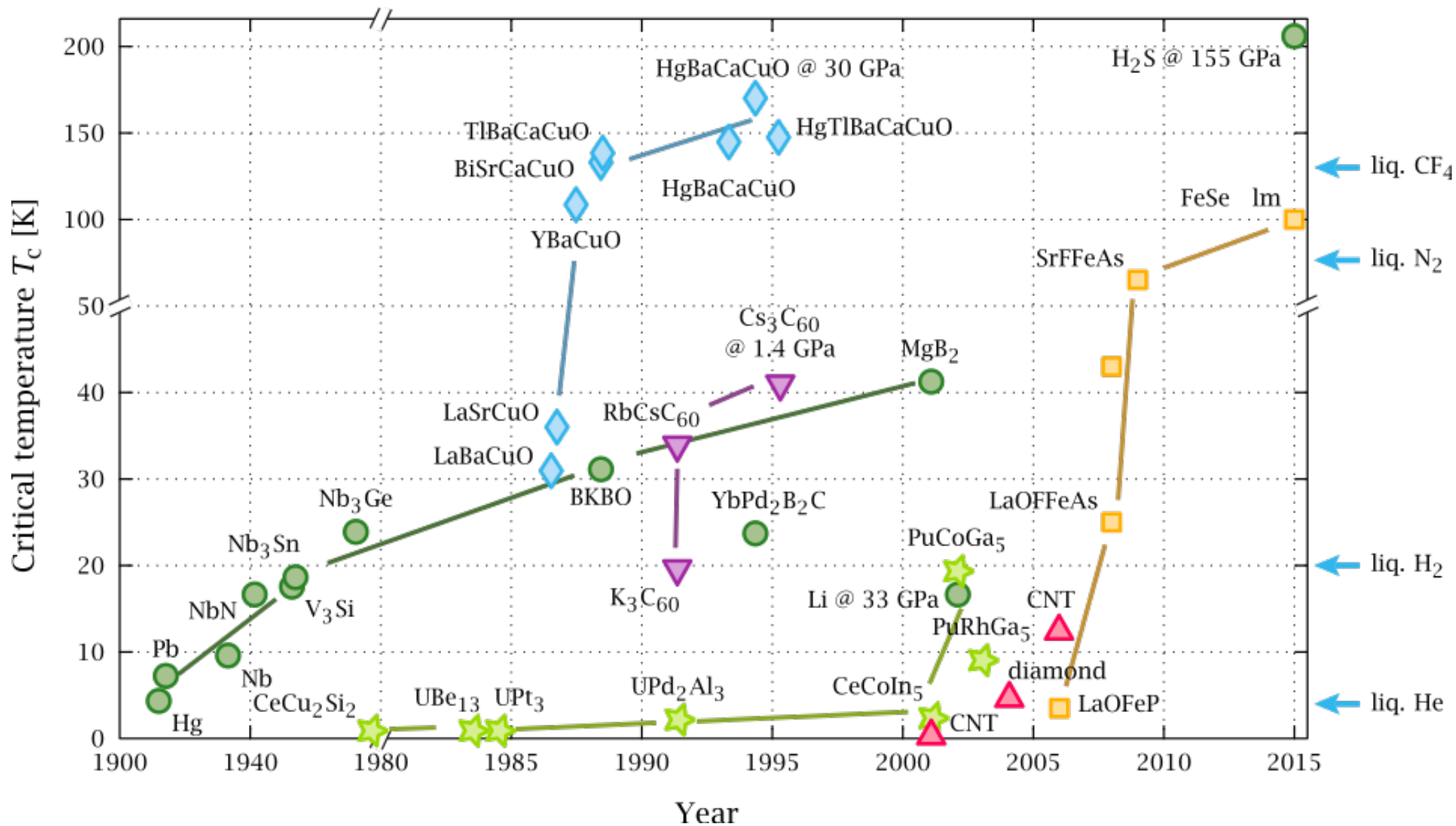
Superconductivity



Heike Kamerlingh Onnes

Kammerligh Onnes

Superconductivity



Superconductivity

1911: Liquefaction of Helium

1912: Discovery of Superconductivity

1913: Discovery of Persistent Supercurrents

1920: Electronic Specific Heat of Superconductivity

1933: Discovery of Meissner Effect

1935: London theory of Meissner Effect

1950: Landau Ginzburg Theory of Superconductivity

1951: Frohlich theory of electron-phonon interactions

1953: Isotope Effect in Superconductors

1956: BCS Microscopic Theory of Superconductivity

1960: Giaever Measurement of Superconductor gap

1962: Josephson Tunneling Effect

1987: High-temperature superconductivity in cuprates

200x: Topological superconductivity

Superconductivity

1911: Liquefaction of Helium

1912: Discovery of Superconductivity

1913: Discovery of Persistent Supercurrents

1920: Electronic Specific Heat of Superconductivity

1933: Discovery of Meissner Effect

1935: London theory of Meissner Effect

1950: Landau Ginzburg Theory of Superconductivity

1951: Frohlich theory of electron-phonon interactions

1953: Isotope Effect in Superconductors

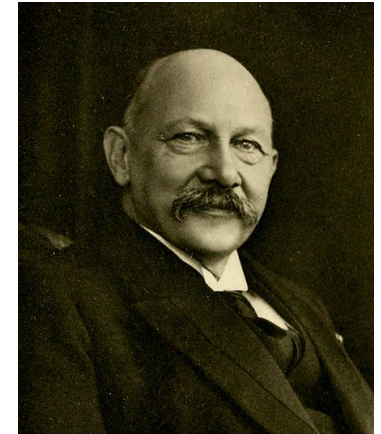
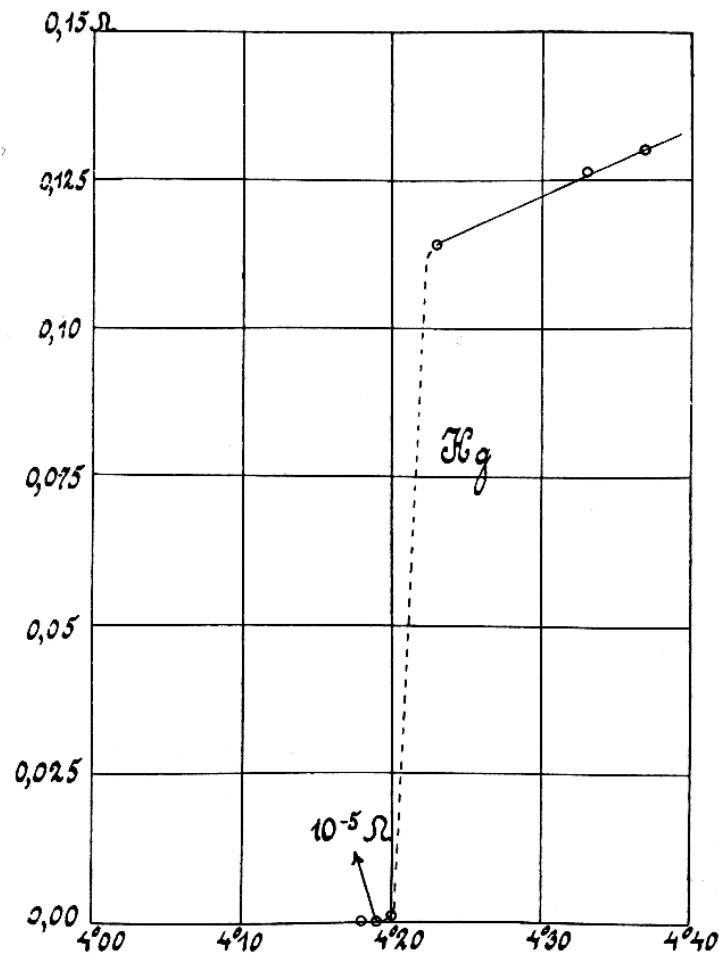
1956: BCS Microscopic Theory of Superconductivity

1960: Giaever Measurement of Superconductor gap

1962: Josephson Tunneling Effect

1987: High-temperature superconductivity in cuprates

200x: Topological superconductivity



Heike Kamerlingh Onnes

Kammerligh Onnes

Superconductivity

1911: Liquefaction of Helium

1912: Discovery of Superconductivity

1913: Discovery of Persistent Supercurrents

1920: Electronic Specific Heat of Superconductivity

1933: Discovery of Meissner Effect

1935: London theory of Meissner Effect

1950: Landau Ginzburg Theory of Superconductivity

1951: Frohlich theory of electron-phonon interactions

1953: Isotope Effect in Superconductors

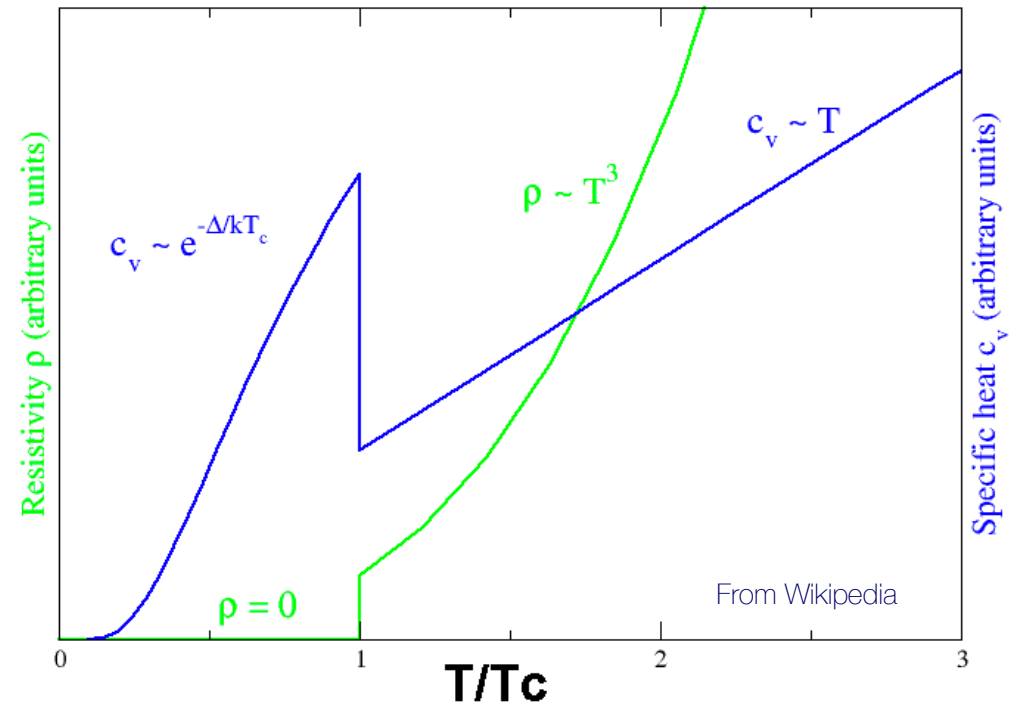
1956: BCS Microscopic Theory of Superconductivity

1960: Giaever Measurement of Superconductor gap

1962: Josephson Tunneling Effect

1987: High-temperature superconductivity in cuprates

200x: Topological superconductivity



Superconductivity

1911: Liquefaction of Helium

1912: Discovery of Superconductivity

1913: Discovery of Persistent Supercurrents

1920: Electronic Specific Heat of Superconductivity

1933: Discovery of Meissner Effect

1935: London theory of Meissner Effect

1950: Landau Ginzburg Theory of Superconductivity

1951: Frohlich theory of electron-phonon interactions

1953: Isotope Effect in Superconductors

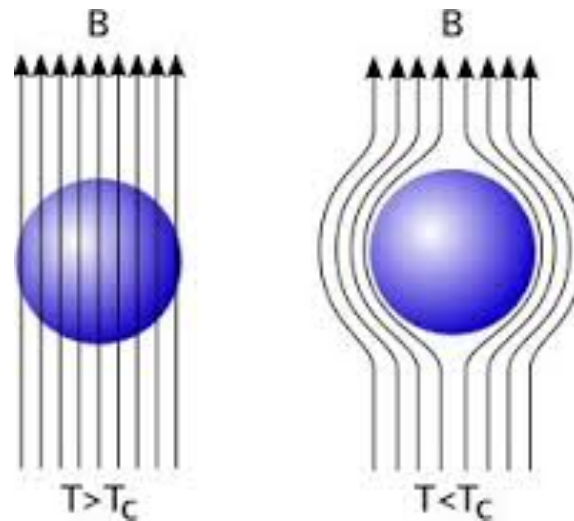
1956: BCS Microscopic Theory of Superconductivity

1960: Giaever Measurement of Superconductor gap

1962: Josephson Tunneling Effect

1987: High-temperature superconductivity in cuprates

200x: Topological superconductivity



The Meissner Effect



Meissner

Superconductivity

1911: Liquefaction of Helium

1912: Discovery of Superconductivity

1913: Discovery of Persistent Supercurrents

1920: Electronic Specific Heat of Superconductivity

1933: Discovery of Meissner Effect

1935: London theory of Meissner Effect

1950: Landau Ginzburg Theory of Superconductivity

1951: Frohlich theory of electron-phonon interactions

1953: Isotope Effect in Superconductors

1956: BCS Microscopic Theory of Superconductivity

1960: Giaever Measurement of Superconductor gap

1962: Josephson Tunneling Effect

1987: High-temperature superconductivity in cuprates

200x: Topological superconductivity

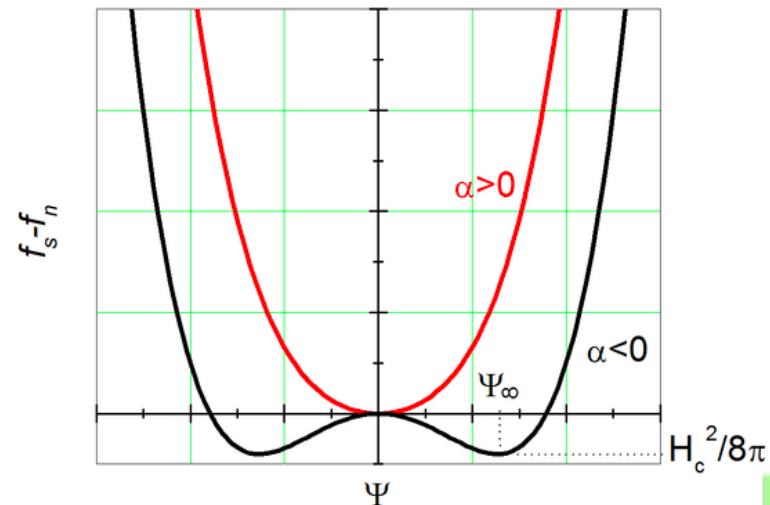
Free energy of a superconductor:

$$F = F_n + \alpha|\psi|^2 + \frac{\beta}{2}|\psi|^4 + \frac{1}{2m}|(-i\hbar\nabla - 2e\mathbf{A})\psi|^2 + \frac{|\mathbf{B}|^2}{2\mu_0}$$

Minimization of the free energy

$$\alpha\psi + \beta|\psi|^2\psi + \frac{1}{2m}(-i\hbar\nabla - 2e\mathbf{A})^2\psi = 0$$

$$\nabla \times \mathbf{B} = \mu_0\mathbf{j} ; \mathbf{j} = \frac{2e}{m}\text{Re}\{\psi^*(-i\hbar\nabla - 2e\mathbf{A})\psi\}$$



$$\alpha\psi + \beta|\psi|^2\psi = 0.$$

$$|\psi|^2 = -\frac{\alpha}{\beta}.$$

$$|\psi|^2 = -\frac{\alpha_0(T - T_c)}{\beta},$$

$$\lambda = \sqrt{\frac{m}{4\mu_0 e^2 \psi_0^2}}, \quad \xi = \sqrt{\frac{\hbar^2}{4m|\alpha|}}.$$

Type-I and Type II Superconductors

From Wikipedia

Superconductivity

1911: Liquefaction of Helium

1912: Discovery of Superconductivity

1913: Discovery of Persistent Supercurrents

1920: Electronic Specific Heat of Superconductivity

1933: Discovery of Meissner Effect

1935: London theory of Meissner Effect

1950: Landau Ginzburg Theory of Superconductivity

1951: Frohlich theory of electron-phonon interactions

1953: Isotope Effect in Superconductors

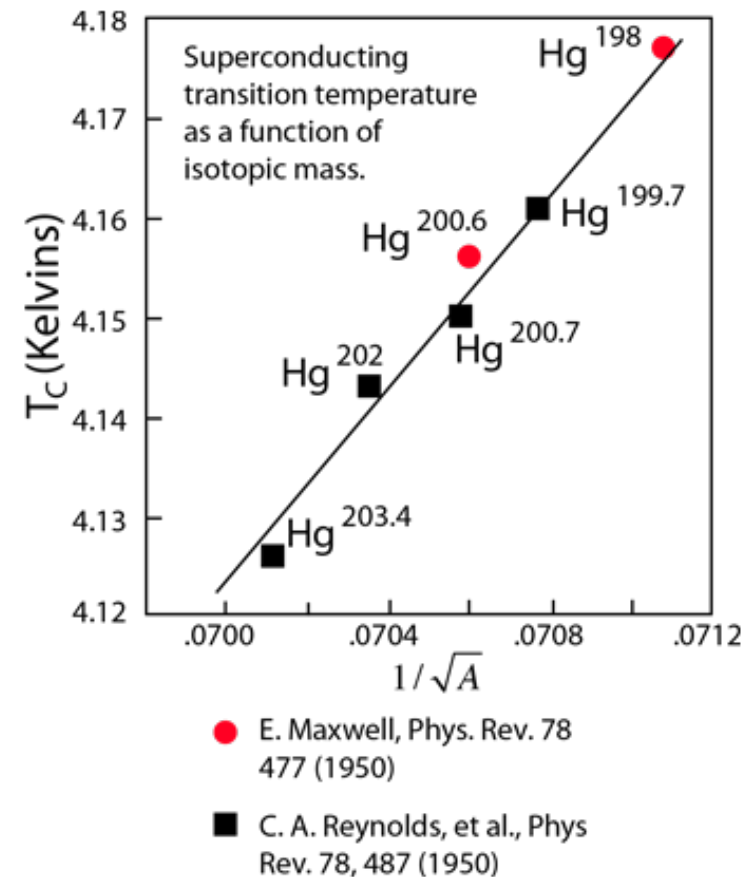
1956: BCS Microscopic Theory of Superconductivity

1960: Giaever Measurement of Superconductor gap

1962: Josephson Tunneling Effect

1987: High-temperature superconductivity in cuprates

200x: Topological superconductivity



From Hyperphysics

Superconductivity

- 1911: Liquefaction of Helium
- 1912: Discovery of Superconductivity
- 1913: Discovery of Persistent Supercurrents
- 1920: Electronic Specific Heat of Superconductivity
- 1933: Discovery of Meissner Effect
- 1935: London theory of Meissner Effect
- 1950: Landau Ginzburg Theory of Superconductivity
- 1951: Frohlich theory of electron-phonon interactions
- 1953: Isotope Effect in Superconductors
- 1956: BCS Microscopic Theory of Superconductivity
- 1960: Giaever Measurement of Superconductor gap
- 1962: Josephson Tunneling Effect
- 1987: High-temperature superconductivity in cuprates
- 200x: Topological superconductivity

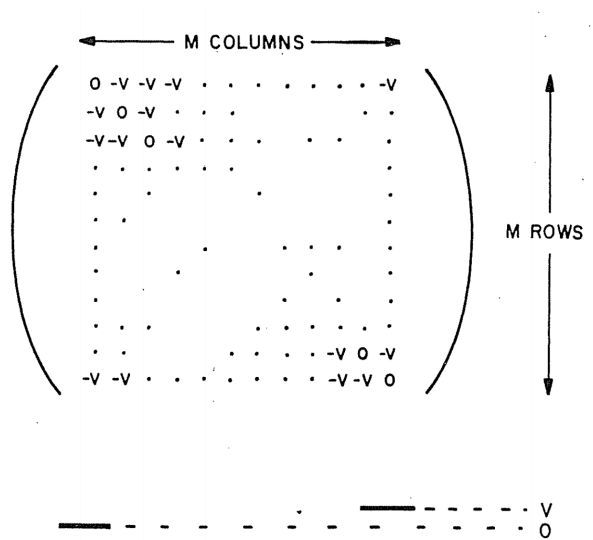
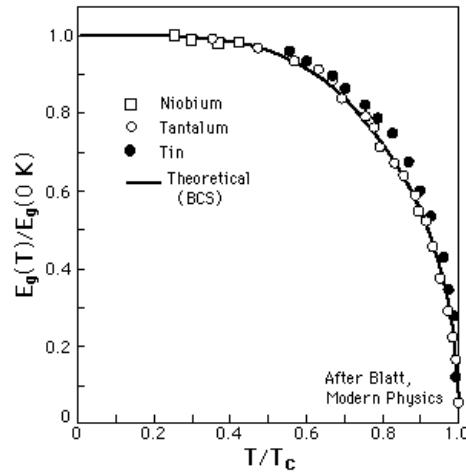


Fig. 3.

The Nobel Prize in Physics 1972



John Bardeen
Prize share: 1/3



Leon Neil Cooper
Prize share: 1/3



John Robert Schrieffer
Prize share: 1/3

The Nobel Prize in Physics 1972 was awarded jointly to John Bardeen, Leon Neil Cooper and John Robert Schrieffer "for their jointly developed theory of superconductivity, usually called the

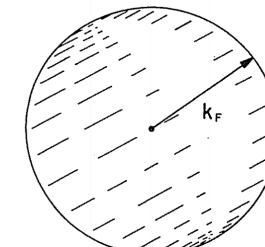


Fig. 1. The normal ground state wavefunction, Φ_0 , is a filled Fermi sphere for both spin directions.

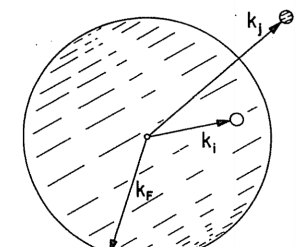


Fig. 2. An excitation of the normal system.

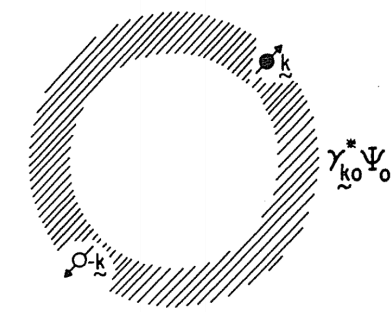


Fig. 6. A single paricle excitation of the superconduc or in one-to-one correspondenc with an excitation of the normal fermion system.

From Wikipedia

Superconductivity: Reason for Cooper Pairing

1911: Liquefaction of Helium

1912: Discovery of Superconductivity

1913: Discovery of Persistent Supercurrents

1920: Electronic Specific Heat of Superconductivity

1933: Discovery of Meissner Effect

1935: London theory of Meissner Effect

1950: Landau Ginzburg Theory of Superconductivity

1951: Frohlich theory of electron-phonon interactions

1953: Isotope Effect in Superconductors

1956: BCS Microscopic Theory of Superconductivity

1960: Giaever Measurement of Superconductor gap

1962: Josephson Tunneling Effect

1987: High-temperature superconductivity in cuprates

200x: Topological superconductivity

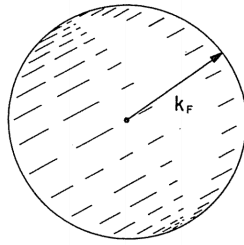


Fig. 1. The normal ground state wavefunction, Φ_0 , is a filled Fermi sphere for both spin directions.

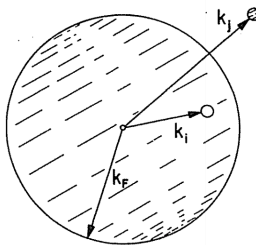


Fig. 2. An excitation of the normal system.

$$\Psi(\mathbf{r}_1, \mathbf{r}_2) = \sum_{\mathbf{k}} g_{\mathbf{k}} e^{i\mathbf{k} \cdot (\mathbf{r}_1 - \mathbf{r}_2)} (|\uparrow\downarrow\rangle - |\downarrow\uparrow\rangle)$$

$$\left(\frac{p_1^2}{2m} + \frac{p_2^2}{2m} + V(\mathbf{r}_1 - \mathbf{r}_2) \right) \Psi = E \Psi$$

$$\sum_{\mathbf{k}} g_{\mathbf{k}} \left(2 \frac{\hbar^2 k^2}{2m} \right) e^{i\mathbf{k} \cdot (\mathbf{r}_1 - \mathbf{r}_2)} + \sum_{\mathbf{k}} g_{\mathbf{k}} V(\mathbf{r}_1 - \mathbf{r}_2) e^{i\mathbf{k} \cdot (\mathbf{r}_1 - \mathbf{r}_2)} = E \sum_{\mathbf{k}} g_{\mathbf{k}} e^{i\mathbf{k} \cdot (\mathbf{r}_1 - \mathbf{r}_2)}$$

writing $\mathbf{r} = \mathbf{r}_1 - \mathbf{r}_2$, multiplying by $e^{-i\mathbf{k}' \cdot \mathbf{r}}$ and integrating both sides $\int \frac{d^3\mathbf{r}}{\Omega} e^{-i\mathbf{k}' \cdot \mathbf{r}} (\dots)$

re-indexing $\mathbf{k} \leftrightarrow \mathbf{k}'$

$$2E_0(\mathbf{k})g_{\mathbf{k}} + \sum_{\mathbf{k}'} g_{\mathbf{k}'} \int \frac{d^3\mathbf{r}}{\Omega} V(\mathbf{r}) e^{-i(\mathbf{k}-\mathbf{k}') \cdot \mathbf{r}} = E g_{\mathbf{k}} \Rightarrow g_{\mathbf{k}} = \sum_{\mathbf{k}'} \frac{-V_{\mathbf{k}\mathbf{k}'} g_{\mathbf{k}'}}{2E_0(\mathbf{k}) - E}$$

$$V_{\mathbf{k},\mathbf{k}'} = \int \frac{d^3\mathbf{r}}{\Omega} V(\mathbf{r}) e^{-i(\mathbf{k}-\mathbf{k}') \cdot \mathbf{r}}$$

Simplified pairing potential

$$V_{\mathbf{k},\mathbf{k}'} = -V_0 \quad E_{\mathbf{k},\mathbf{k}'} \in (E_F, E_F + \hbar\omega_D), \text{ and } V_0 = 0 \text{ otherwise}$$

$$g_{\mathbf{k}} = V_0 \left(\sum_{\mathbf{k}'} g_{\mathbf{k}'} \right) \frac{1}{2E_0(\mathbf{k}) - E} \Rightarrow \left(\sum_{\mathbf{k}} g_{\mathbf{k}} \right) = V_0 \left(\sum_{\mathbf{k}'} g_{\mathbf{k}'} \right) \sum_{\mathbf{k}} \frac{1}{2E_0(\mathbf{k}) - E} \quad (2.27)$$

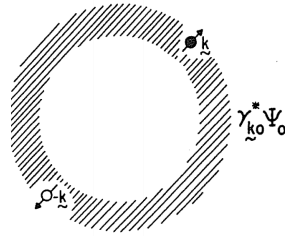
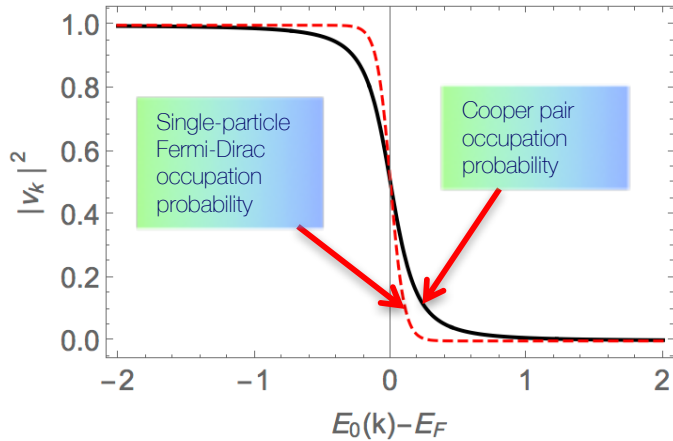
$$\frac{1}{V_0} = \sum_{\mathbf{k}} \frac{1}{2E_0(\mathbf{k}) - E} \Rightarrow \frac{1}{V_0} = \int_{E_F}^{E_F + \hbar\omega_D} \frac{N(\mathcal{E}) d\mathcal{E}}{2\mathcal{E} - E} \Rightarrow \frac{1}{N_0 V_0} \approx \int_{E_F}^{E_F + \hbar\omega_D} \frac{d\mathcal{E}}{2\mathcal{E} - E}$$

Pairing energy

$$\ln \left(\frac{2E_F + 2\hbar\omega_D - E}{2E_F - E} \right) \approx \frac{2}{N_0 V_0} \Rightarrow 2E_F - E \approx \frac{2\hbar\omega_D}{e^{\frac{2}{N_0 V_0}} - 1} \Rightarrow E \approx 2E_F - 2\hbar\omega_D e^{-\frac{2}{N_0 V_0}}$$

Total energy of two interacting electrons is *lower* than their single particle "Fermi" equilibrium value $2E_F \rightarrow$ Reason they pair.

Superconductivity: The BCS "condensate"



The BCS Hamiltonian

$$H_{BCS} = \sum_{\mathbf{k}, \sigma} E_0(\mathbf{k}) c_{\mathbf{k}\sigma}^\dagger c_{\mathbf{k}\sigma} - V_0 \sum_{\mathbf{k}, \mathbf{q}} c_{\mathbf{q}\uparrow}^\dagger c_{-\mathbf{q}\downarrow}^\dagger c_{-\mathbf{k}\downarrow} c_{\mathbf{k}\uparrow}$$

Fig. 6. A single particle excitation of the superconductor or in one-to-one correspondence with an excitation of the normal fermion system.

$$|\Psi_{\mathbf{k}}\rangle = u_{\mathbf{k}}|0\rangle + v_{\mathbf{k}}c_{\mathbf{k}\uparrow}^\dagger c_{-\mathbf{k}\downarrow}^\dagger|0\rangle = (u_{\mathbf{k}} + v_{\mathbf{k}}c_{\mathbf{k}\uparrow}^\dagger c_{-\mathbf{k}\downarrow}^\dagger)|0\rangle = e^{\alpha_{\mathbf{k}} b_{\mathbf{k}}^\dagger}|0\rangle$$

$$b_{\mathbf{k}}^\dagger = c_{\mathbf{k}\uparrow}^\dagger c_{-\mathbf{k}\downarrow}^\dagger \quad \text{Pair creation operator}$$

The BCS many-body wavefunction

$$|\Psi_{BCS}\rangle = \prod_{\mathbf{k}} (u_{\mathbf{k}} + v_{\mathbf{k}} b_{\mathbf{k}}^\dagger) |0\rangle = \prod_{\mathbf{k}} e^{\alpha_{\mathbf{k}} b_{\mathbf{k}}^\dagger} |0\rangle = e^{\sum_{\mathbf{k}} \alpha_{\mathbf{k}} b_{\mathbf{k}}^\dagger} |0\rangle$$

$$\langle \Psi_{BCS} | \Psi_{BCS} \rangle = \prod_{\mathbf{k}} \langle 0 | (u_{\mathbf{k}} + v_{\mathbf{k}} b_{\mathbf{k}}) (u_{\mathbf{k}} + v_{\mathbf{k}} b_{\mathbf{k}}^\dagger) |0\rangle = 1 \implies u_{\mathbf{k}}^2 + v_{\mathbf{k}}^2 = 1$$

Occupation probability of state \mathbf{k} $\langle \Psi_{BCS} | c_{\mathbf{k}\uparrow}^\dagger c_{\mathbf{k}\uparrow} | \Psi_{BCS} \rangle = v_{\mathbf{k}}^2$

$$H_{BCS} = \sum_{\mathbf{k}, \sigma} E_0(\mathbf{k}) c_{\mathbf{k}\sigma}^\dagger c_{\mathbf{k}\sigma} - V_0 \sum_{\mathbf{k}, \mathbf{q}} c_{\mathbf{q}\uparrow}^\dagger c_{-\mathbf{q}\downarrow}^\dagger c_{-\mathbf{k}\downarrow} c_{\mathbf{k}\uparrow}$$

Energy expectation value

$$\langle \Psi_{BCS} | H_{BCS} | \Psi_{BCS} \rangle = 2 \sum_{\mathbf{k}} E_0(\mathbf{k}) v_{\mathbf{k}}^2 - V_0 \sum_{\mathbf{k}, \mathbf{k}'} v_{\mathbf{k}} v_{\mathbf{k}'} u_{\mathbf{k}'} u_{\mathbf{k}}$$

minimize

$$\Delta = V_0 \sum_{\mathbf{k}} u_{\mathbf{k}} v_{\mathbf{k}}$$

$$v_{\mathbf{k}}^2 = \frac{1}{2} \left[1 - \frac{E_0(\mathbf{k}) - E_F}{\sqrt{(E_0(\mathbf{k}) - E_F)^2 + \Delta^2}} \right] \quad u_{\mathbf{k}}^2 = \frac{1}{2} \left[1 + \frac{E_0(\mathbf{k}) - E_F}{\sqrt{(E_0(\mathbf{k}) - E_F)^2 + \Delta^2}} \right]$$

$$\sum_{\mathbf{k}} u_{\mathbf{k}} v_{\mathbf{k}} = \frac{\Delta}{V_0} = \sum_{\mathbf{k}} \frac{\Delta}{2\sqrt{(E_0(\mathbf{k}) - E_F)^2 + \Delta^2}}$$

$$\Delta = \frac{\hbar\omega_D}{\sinh(\frac{1}{N_0 V_0})} \approx (2\hbar\omega_D) e^{-\frac{1}{N_0 V_0}}$$

Superconducting gap

1950: Landau Ginzburg Theory of Superconductivity

1951: Frohlich theory of electron-phonon interactions

1953: Isotope Effect in Superconductors

1956: BCS Microscopic Theory of Superconductivity

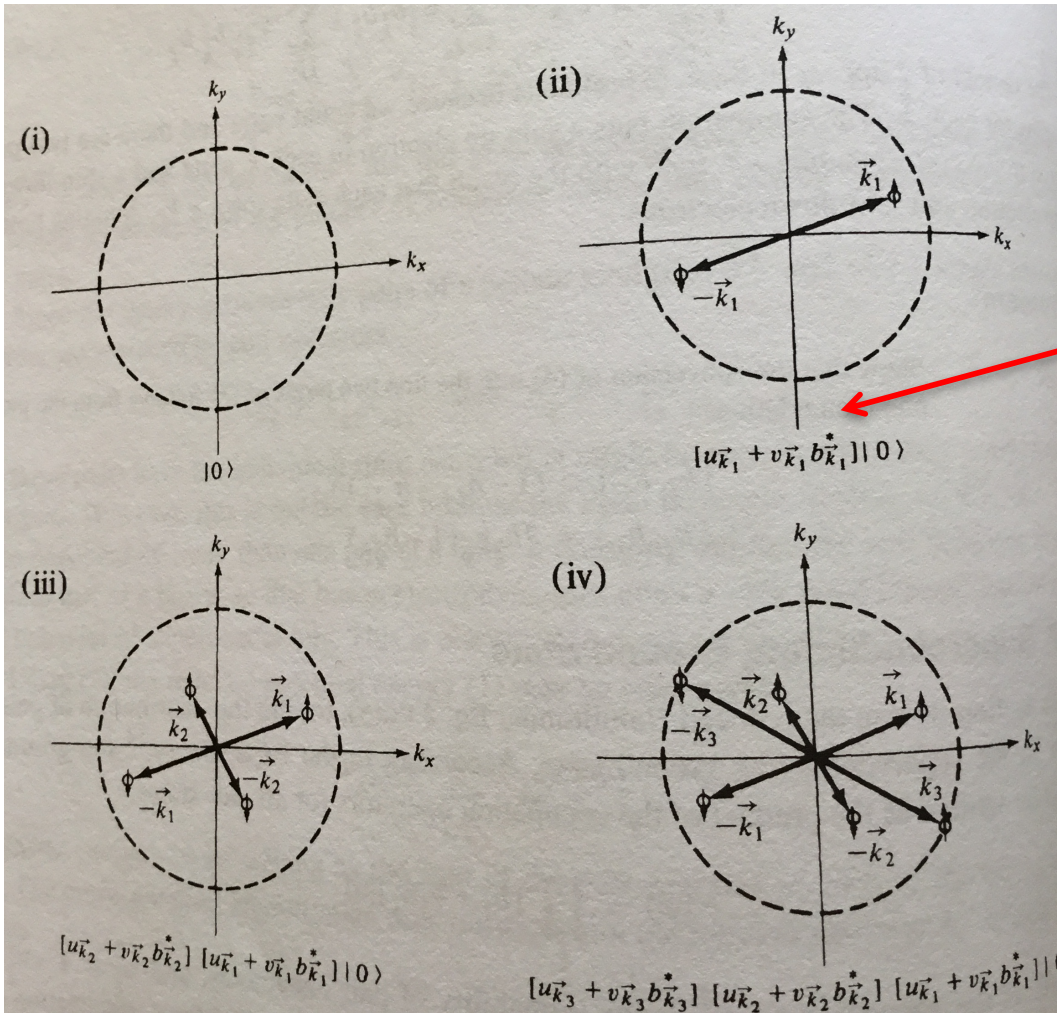
1960: Giaever Measurement of Superconductor gap

1962: Josephson Tunneling Effect

1987: High-temperature superconductivity in cuprates

200x: Topological superconductivity

Superconductivity: 2nd quantization in pictures



$$|\Psi_{\mathbf{k}}\rangle = u_{\mathbf{k}}|0\rangle + v_{\mathbf{k}}c_{\mathbf{k}\uparrow}^\dagger c_{-\mathbf{k}\downarrow}^\dagger|0\rangle = (u_{\mathbf{k}} + v_{\mathbf{k}}c_{\mathbf{k}\uparrow}^\dagger c_{-\mathbf{k}\downarrow}^\dagger)|0\rangle = e^{\alpha_{\mathbf{k}}b_{\mathbf{k}}^\dagger}|0\rangle$$

$$b_{\mathbf{k}}^\dagger = c_{\mathbf{k}\uparrow}^\dagger c_{-\mathbf{k}\downarrow}^\dagger$$

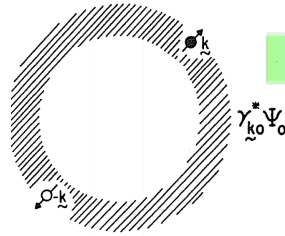
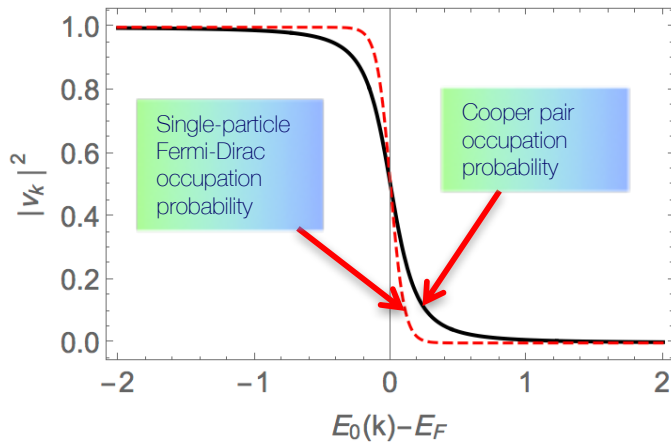
Pair creation operator

$$|\Psi_{BCS}\rangle = \prod_{\mathbf{k}}(u_{\mathbf{k}} + v_{\mathbf{k}}b_{\mathbf{k}}^\dagger)|0\rangle = \prod_{\mathbf{k}}e^{\alpha_{\mathbf{k}}b_{\mathbf{k}}^\dagger}|0\rangle = e^{\sum_{\mathbf{k}}\alpha_{\mathbf{k}}b_{\mathbf{k}}^\dagger}|0\rangle$$

The BCS many-body wavefunction

From: van Duzer and Turner

Superconductivity: The Bogoliubov approach



The BCS Hamiltonian

$$H_{BCS} = \sum_{\mathbf{k}, \sigma} E_0(\mathbf{k}) c_{\mathbf{k}\sigma}^\dagger c_{\mathbf{k}\sigma} - V_0 \sum_{\mathbf{k}, \mathbf{q}} c_{\mathbf{q}\uparrow}^\dagger c_{-\mathbf{q}\downarrow}^\dagger c_{-\mathbf{k}\downarrow} c_{\mathbf{k}, \uparrow}$$

Write energies with respect to the Fermi surface

$$H_{red} = \sum_{\mathbf{k}, \sigma} (E_0(\mathbf{k}) - E_F) c_{\mathbf{k}\sigma}^\dagger c_{\mathbf{k}\sigma} - V_0 \sum_{\mathbf{k}, \mathbf{q}} c_{\mathbf{q}\uparrow}^\dagger c_{-\mathbf{q}\downarrow}^\dagger c_{-\mathbf{k}\downarrow} c_{\mathbf{k}, \uparrow}$$

4th power in c's creation/annihilation operators

Convert to bilinear form, or 2nd power in c's

$$\sum_{\mathbf{k}, \mathbf{q}} c_{\mathbf{q}\uparrow}^\dagger c_{-\mathbf{q}\downarrow}^\dagger c_{-\mathbf{k}\downarrow} c_{\mathbf{k}, \uparrow} \approx \sum_{\mathbf{k}} \left(\underbrace{\langle c_{\mathbf{k}\uparrow}^\dagger c_{-\mathbf{k}\downarrow}^\dagger \rangle}_{b_{\mathbf{k}}^\dagger \approx \langle b_{\mathbf{k}}^\dagger \rangle} c_{-\mathbf{k}\downarrow} c_{\mathbf{k}, \uparrow} + \underbrace{\langle c_{-\mathbf{k}\downarrow} c_{\mathbf{k}, \uparrow} \rangle}_{b_{\mathbf{k}} \approx \langle b_{\mathbf{k}} \rangle} c_{\mathbf{k}\uparrow}^\dagger c_{-\mathbf{k}\downarrow}^\dagger \right)$$

"Expectation value" of pair occupation or un-occupation

$$H_{red} \approx \sum_{\mathbf{k}, \sigma} (E_0(\mathbf{k}) - E_F) c_{\mathbf{k}\sigma}^\dagger c_{\mathbf{k}\sigma} - \sum_{\mathbf{k}} (\Delta^* c_{-\mathbf{k}\downarrow} c_{\mathbf{k}\uparrow} + \Delta c_{\mathbf{k}\uparrow}^\dagger c_{-\mathbf{k}\downarrow}^\dagger)$$

$$c_{\mathbf{k}, \uparrow} = u_{\mathbf{k}}^* \gamma_{\mathbf{k}, \uparrow} + v_{\mathbf{k}} \gamma_{-\mathbf{k}, \downarrow}^\dagger$$

$$c_{-\mathbf{k}, \downarrow}^\dagger = -v_{\mathbf{k}}^* \gamma_{\mathbf{k}, \uparrow} + u_{\mathbf{k}} \gamma_{-\mathbf{k}, \downarrow}^\dagger$$

The bilinear form can now be diagonalized with linear transformation of c-operators using a general Bogoliubov-Valatin technique

$$H_{BdG} = \sum_{\mathbf{k}} E_{BdG}(\mathbf{k}) (\gamma_{\mathbf{k}\uparrow}^\dagger \gamma_{\mathbf{k}\uparrow} + \gamma_{-\mathbf{k}\downarrow}^\dagger \gamma_{-\mathbf{k}\downarrow}^\dagger)$$

$$E_{BdG}(\mathbf{k}) = \sqrt{(E_0(\mathbf{k}) - E_F)^2 + \Delta^2}$$

1950: Landau Ginzburg Theory of Superconductivity

1951: Frohlich theory of electron-phonon interactions

1953: Isotope Effect in Superconductors

1956: BCS Microscopic Theory of Superconductivity

1960: Giaever Measurement of Superconductor gap

1962: Josephson Tunneling Effect

1987: High-temperature superconductivity in cuprates

200x: Topological superconductivity

Superconductivity: Gap in excitation spectrum

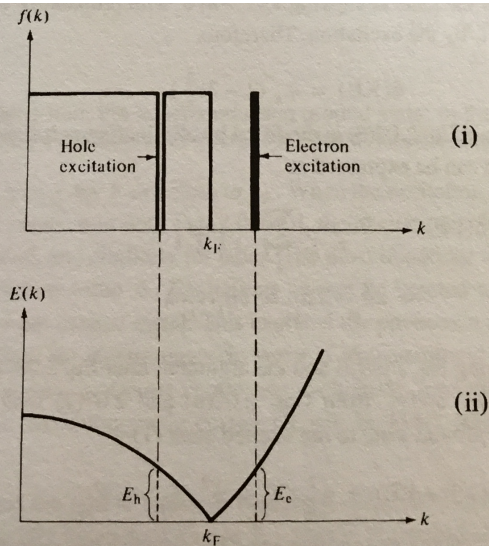


Figure 2.09a Hole and electron excitations in a normal metal: (i) Fermi function; (ii) excitation energies.

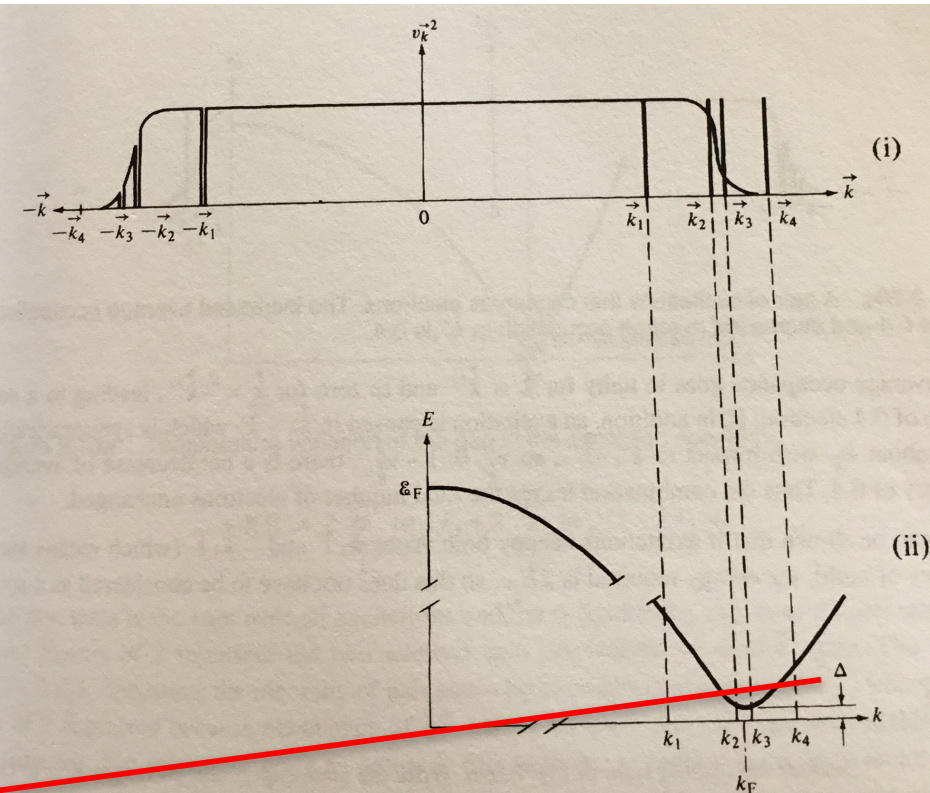


Figure 2.09b Excitations from the superconducting ground state: (i) the ground state with four quasiparticle excitations; (ii) the excitation energy for each of these excitations.

$$H_{BdG} = \sum_{\mathbf{k}} E_{BdG}(\mathbf{k}) (\gamma_{\mathbf{k}\uparrow}^\dagger \gamma_{\mathbf{k}\uparrow} + \gamma_{-\mathbf{k}\downarrow}^\dagger \gamma_{-\mathbf{k}\downarrow})$$

$$E_{BdG}(\mathbf{k}) = \sqrt{(E_0(\mathbf{k}) - E_F)^2 + \Delta^2}$$

From: van Duzer and Turner

Superconductivity

1911: Liquefaction of Helium

1912: Discovery of Superconductivity

1913: Discovery of Persistent Supercurrents

1920: Electronic Specific Heat of Superconductivity

1933: Discovery of Meissner Effect

1935: London theory of Meissner Effect

1950: Landau Ginzburg Theory of Superconductivity

1951: Frohlich theory of electron-phonon interactions

1953: Isotope Effect in Superconductors

1956: BCS Microscopic Theory of Superconductivity

1960: Giaever Measurement of Superconductor gap

1962: Josephson Tunneling Effect

1987: High-temperature superconductivity in cuprates

200x: Topological superconductivity

VOLUME 5, NUMBER 4

PHYSICAL REVIEW LETTERS

AUGUST 15, 1960

ENERGY GAP IN SUPERCONDUCTORS MEASURED BY ELECTRON TUNNELING

Ivar Giaever

General Electric Research Laboratory, Schenectady, New York

(Received July 5, 1960)

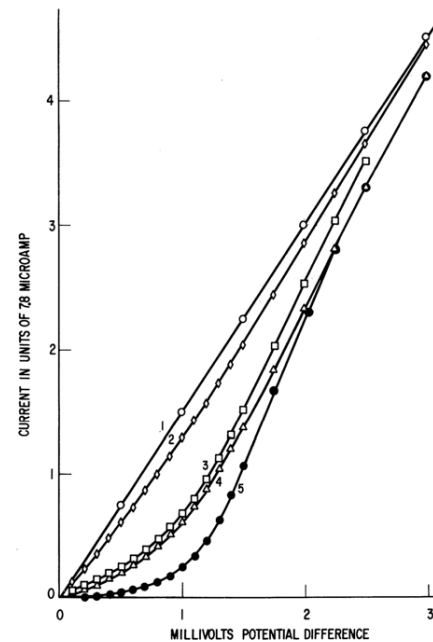


FIG. 1. Tunnel current between Al and Pb through Al_2O_3 film as a function of voltage. (1) $T=4.2^\circ\text{K}$ and 1.6°K , $H=2.7$ koe (Pb normal). (2) $T=4.2^\circ\text{K}$, $H=0.8$ koe. (3) $T=1.6^\circ\text{K}$, $H=0.8$ koe. (4) $T=4.2^\circ\text{K}$, $H=0$ (Pb superconducting). (5) $T=1.6^\circ\text{K}$, $H=0$ (Pb superconducting).

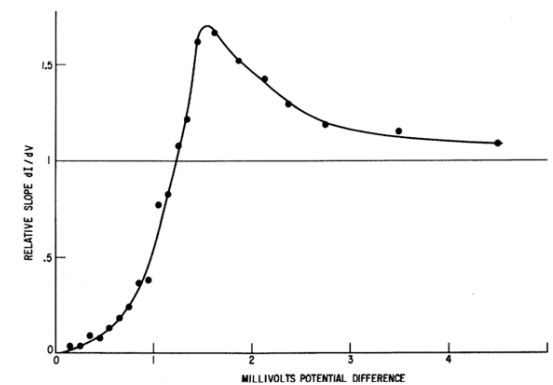
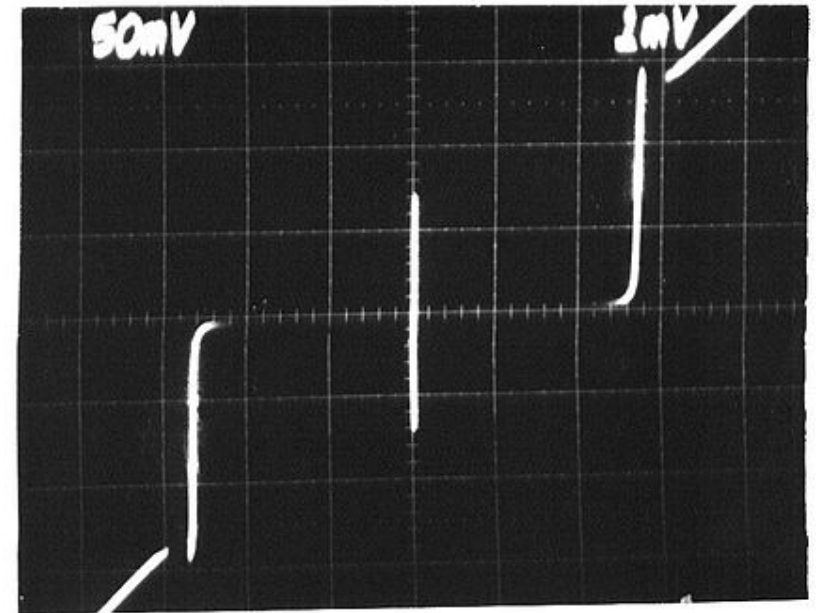


FIG. 2. From Fig. 1, slope dI/dV of curve 5 relative to slope of curve 1.

Superconductivity

- 1911: Liquefaction of Helium
- 1912: Discovery of Superconductivity
- 1913: Discovery of Persistent Supercurrents
- 1920: Electronic Specific Heat of Superconductivity
- 1933: Discovery of Meissner Effect
- 1935: London theory of Meissner Effect
- 1950: Landau Ginzburg Theory of Superconductivity
- 1951: Frohlich theory of electron-phonon interactions
- 1953: Isotope Effect in Superconductors
- 1956: BCS Microscopic Theory of Superconductivity
- 1960: Giaever Measurement of Superconductor gap
- 1962: Josephson Tunneling Effect**
- 1987: High-temperature superconductivity in cuprates
- 200x: Topological superconductivity

Current (I)



Voltage (V)

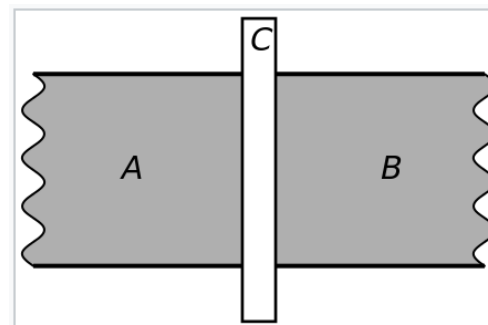


Diagram of a single Josephson junction. A and B represent superconductors, and C the weak link between them.

From Wikipedia

Superconductivity



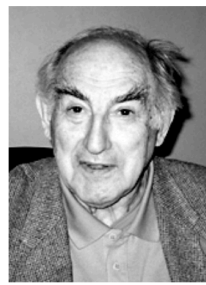
The Nobel Prize in Physics 2003
Alexei Abrikosov, Vitaly L. Ginzburg, Anthony J. Leggett

Share this: 20

The Nobel Prize in Physics 2003



Alexei A. Abrikosov
Prize share: 1/3



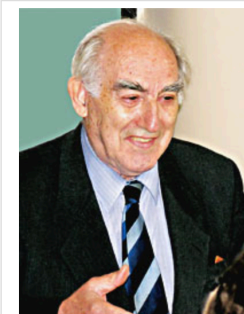
Vitaly L. Ginzburg
Prize share: 1/3



Anthony J. Leggett
Prize share: 1/3

The Nobel Prize in Physics 2003 was awarded jointly to Alexei A. Abrikosov, Vitaly L. Ginzburg and Anthony J. Leggett "for pioneering contributions to the theory of superconductors and superfluids".

Photos: Copyright © The Nobel Foundation



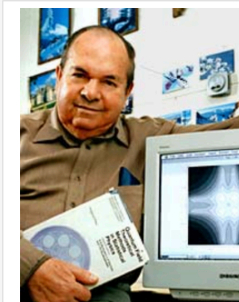
Vitaly L. Ginzburg
P.N. Lebedev Physical Institute, Moscow, Russia

The importance of order

Together with his colleague Lev Landau, **Vitaly Ginzburg** developed a phenomenological theory of superconductivity in the late 1940s. This theory proposes that those electrons that contribute to superconduction form a superfluid. The superconductor is described by a complex function Ψ called the order parameter, and $|\Psi|^2$ indicates the fraction of electrons that has condensed into a superfluid.

$$\frac{1}{2m^*} \left(-i\hbar\nabla - \frac{e}{c}A \right)^2 \Psi + \alpha\Psi + \beta|\Psi|^2\Psi = 0$$

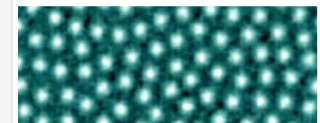
The Ginzburg-Landau order parameter Ψ is the solution of an equation similar to the quantum-mechanical wave equation.



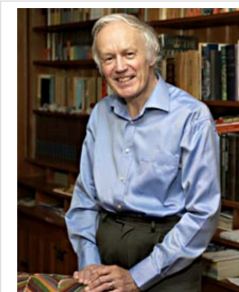
Alexei A. Abrikosov
Argonne National Laboratory, Argonne, Illinois, USA

Vortices give guidance

Landau's pupil, **Alexei Abrikosov**, realised almost immediately that Ginzburg and Landau's theory can also describe those superconductors (type II) that can coexist with strong magnetic fields. According to Abrikosov's theory this occurs because the superconductor allows the magnetic field to enter through vortices in the electron superfluid. These vortices can form regular structures, *Abrikosov lattices*, but disordered structures can also occur.



An Abrikosov lattice of vortices in a type-II superconductor. The magnetic field passes through the vortices.



Anthony J. Leggett
University of Illinois, Urbana, Illinois, USA

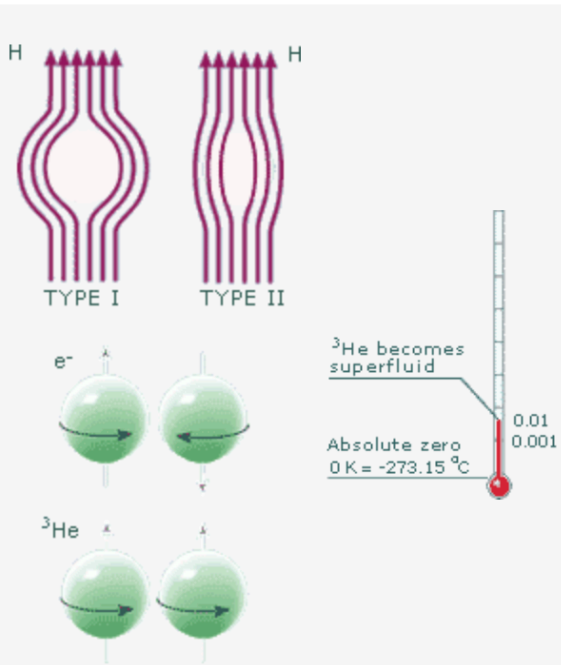
A fluid with directions

In the early 1970s **Anthony Leggett** developed a theory for the superfluid that is obtained when the rare gas isotope ^3He is cooled down to very low temperatures. This fluid has magnetic properties, which makes it anisotropic; it has different properties in different directions. In addition, the fluid has several states with different properties, called phases, in which several types of ordering phenomena occur. Here the magnetic properties are linked to the atoms' movements.



Every pair of ^3He atoms is described by its spin (fulldrawn green arrow) and its movement (broken red arrow). In Leggett's theory the phases A and B have different kinds of order. Which phase that appears depends on temperature, pressure and external magnetic field.

Superconductivity



Two types of superconductors

Type-I superconductors are characterised by a total so-called *Meissner effect*. This means that the superconductor completely expels a magnetic field. If the magnetic field becomes too strong, the superconductive property disappears abruptly. But there are other superconductors, often alloys, in which the Meissner effect is not total. Here a surrounding magnetic field can intrude partly and the materials can retain their superconductive property even in very strong magnetic fields.

It takes two

If electrons and ³He atoms are to condense into a superfluid liquid, they must first pair up. This can take place in two ways concerning the particles' magnetic properties, their so-called spin. This is described with an arrow – a compass needle. The spins are either opposite, in which case they counteract each other (electrons in a superconductor) or in the same direction so that they reinforce each other (³He atoms in a superfluid). In the latter case the superfluid can have magnetic properties.

Swirling superfluids

If a beaker containing a superfluid is rotated slowly, at first the fluid remains quite still. If the speed of rotation is increased, a vortex suddenly occurs, followed by more and more vortices. The rotation of the fluid is quantised and every vortex equals one quantum. Studies of the formation of vortices in superfluids can give us information about the way turbulence occurs. The electrons in a superconductor form a superfluid in which vortices also may occur if a magnetic field intrudes. The magnetic field is quantised and every vortex allows a quantum of magnetic flux to pass through. In a material where many vortices can occur, superconductivity can coexist with strong magnetic fields. Such materials can be used in the construction of strong magnets.

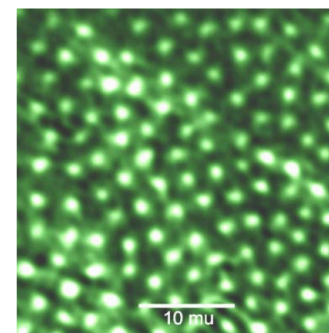
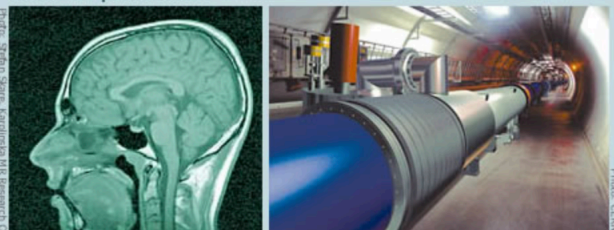


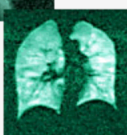
Figure 4. Abrikosov lattice of magnetic flux lines (vortices) in NbSe₂ – a type-II superconductor - visualised by magneto-optical imaging. The first pictures of such a vortex lattice were taken in 1967 by U. Essmann and H. Träuble, who sprinkled their sample surfaces with a ferromagnetic powder that arranges itself in a pattern reflecting the magnetic flux line structure.

Theories put to work



MRI image of a human brain

The resolution in magnetic resonance imaging (MRI) is partly dependent on the strength of the magnetic field. Nowadays strong superconducting magnets, all type II, are used.



The magnetism in ³He can be made uniform (hyperfolarisation). If this gas is inhaled, cavities such as the lungs can be imaged in a magnetic camera.

Particle accelerators

Powerful superconducting magnets are used in the LHC particle accelerator at CERN. They are cooled with superfluid helium (⁴He), which makes its way into all the cavities in the casing.

It all started in 1911!

1911 Heike Kammerlingh Onnes discovers superconductivity in mercury.
Nobel Prize in Physics 1913.

1938 Pyotr Kapitsa discovers superfluid ⁴He.
Nobel Prize in Physics 1978.

1947 Lev Landau proposes a theory for superfluid ⁴He.
Nobel Prize in Physics 1962.

1950 Vitaly Ginzburg and Lev Landau publish a phenomenological theory for superconductivity.
Nobel Prize in Physics 2003.

1957 Alexei Abrikosov builds on the work by Ginzburg and Landau and publishes a theory for superconductors of type II.
Nobel Prize in Physics 2003.

1957 John Bardeen, Leon Cooper and Robert Schrieffer publish a microscopic theory for superconductivity (type I).
Nobel Prize in Physics 1972.

1962 Brian Josephson predicts properties of supercurrents.
Nobel Prize in Physics 1973.

1972 David Lee, Douglas Osheroff and Robert Richardson discover superfluid ³He.
Nobel Prize in Physics 1996.

1972 Anthony Leggett proposes a theory for superfluid ³He.
Nobel Prize in Physics 2003.

1986 Georg Bednorz and Alex Müller discover high-temperature superconductors (type II).
Nobel Prize in Physics 1987.

Superconductivity

Pairing of electrons:

"di-electronic molecules" Cooper pairs

In simplest ("BCS") theory, Cooper pairs, once formed, must automatically **undergo Bose condensation!**

must all do **exactly the same thing at the same time** (also in nonequilibrium situation)

Single electrons in normal metal Cooper pairs in superconductor

What is superconductivity?

Kamerlingh Onnes discovered in 1911 superconductivity by measuring abrupt disappearance of electrical resistance of mercury.

Perfect diamagnetism (Meissner effect) equilibrium effect

Persistent currents, astronomically stable metastable effect

No a priori guarantee these two phenomena always go together! (but in fact seem to, in all (bulk 3D) "superconductors" known to date).

Physics of superconductivity

Spin of elementary particles: $\frac{n}{2}\hbar$

$\frac{n}{2} = 0, 1, 2, \dots$ bosons

$\frac{n}{2} = \frac{1}{2}, \frac{3}{2}, \frac{5}{2}, \dots$ fermions

At low temperatures:

Electrons in metals: spin 1/2 \Rightarrow fermions

But a compound object consisting of an even number of fermions has spin 0, 1, 2, ... \Rightarrow boson

Ex: $2p + 2n + 2e = {}^4\text{He atom} \Rightarrow$ can undergo Bose condensation

Qualitative explanation of the two major phenomena of superconductivity: London (1935), Ginzburg+Landau (1950)

Superconducting state is characterized by "macroscopic wave function" $\Psi(\mathbf{r})$ which behaves in (almost) all aspects like a single-particle Schrödinger wave function. Like that, it is a complex scalar quantity, so can write:

$$\Psi(\mathbf{r}) = |\Psi(\mathbf{r})|e^{i\varphi(\mathbf{r})} \quad \leftarrow \text{Phase, must be single-valued modulo } 2\pi$$

For a single particle in magnetic vector potential $\mathbf{A}(\mathbf{r})$

$$\hat{p} = -i\hbar\nabla \rightarrow \hat{p} - e\mathbf{A}(\mathbf{r})$$

$$\mathbf{j}(\mathbf{r}) = \frac{e}{2m}[\psi^*(\mathbf{r})(-i\hbar\nabla - e\mathbf{A}(\mathbf{r}))\psi(\mathbf{r}) - c.c.] = \frac{e}{m}|\psi(\mathbf{r})|^2[\nabla\varphi(\mathbf{r}) - e\mathbf{A}(\mathbf{r})]$$

Consequence 1: atomic diamagnetism

In absence of field, no current flows around nucleus $\Rightarrow \oint \nabla\varphi(\mathbf{r})d\mathbf{l} = 0 \Rightarrow \varphi = \text{const.}$

In presence of (weak) field, must still have $\oint \nabla\varphi(\mathbf{r})d\mathbf{l} = 0 \Rightarrow \varphi = \text{const.}$

But now

$$\mathbf{j}(\mathbf{r}) = \frac{e}{m}|\psi(\mathbf{r})|^2[\nabla\varphi(\mathbf{r}) - e\mathbf{A}(\mathbf{r})] = -\frac{|\psi(\mathbf{r})|^2}{m}e^2\mathbf{A}(\mathbf{r})$$

$$\mathbf{j}(\mathbf{r}) \propto -\mathbf{A}(\mathbf{r}) \quad (\text{diamagnetism})$$

By Ampere's law, this current generates magnetic field in a sense opposite to the original $\mathbf{B}(\mathbf{r})$, so tends to screen it out. But screening length is

$$\lambda_L = \sqrt{\frac{m}{\mu_0 e^2 n}} \gg \text{atomic size} \quad \leftarrow \text{So observable effect (e.g. in NMR) small}$$

Consequence 2: persistent currents

Imagine we have set up a current in ring in zero magnetic field (e.g. by starting with nonzero flux and turning it off)

Recall: $\mathbf{j}(\mathbf{r}) = \frac{e^*}{m}|\Psi(\mathbf{r})|^2[\nabla\varphi(\mathbf{r}) - e^*\mathbf{A}(\mathbf{r})]$

Since $\mathbf{A}(\mathbf{r}) = 0$ but $\mathbf{j}(\mathbf{r}) \neq 0$, must have $\nabla\varphi(\mathbf{r}) \neq 0$. However from single-valueness,

$$\oint \nabla\varphi(\mathbf{r})d\mathbf{l} = 2\pi n$$

$\mathbf{j} \propto n$ "winding number" = number of "turns" in Argand diagram

How to change n ? The only way is to depress $|\Psi(\mathbf{r})|$ to zero.

For an electron in an atom, nothing prevents this, e.g.

$$\psi_p(\mathbf{r}) \rightarrow a(t)\psi_p(\mathbf{r}) + b(t)\psi_S(\mathbf{r}) \rightarrow \psi_S(\mathbf{r})$$

$n=1$ orbitals $n=0$

$\psi_p(\mathbf{r}) \rightarrow 0$ at point $\theta = 0$ when $a(t) = b(t)$

Because TDSE (time-dependent Schrodinger equation) is linear ($E \propto |\Psi(\mathbf{r})|^2$), nothing prevents this!

$$E(t) = |a(t)|^2 E_p + |b(t)|^2 E_S = \text{monotonically decreasing}$$

However, in superconducting case

$$E \propto K|\Psi(\mathbf{r})|^2 + \mu|\Psi(\mathbf{r})|^4$$

\Rightarrow Free energy barrier

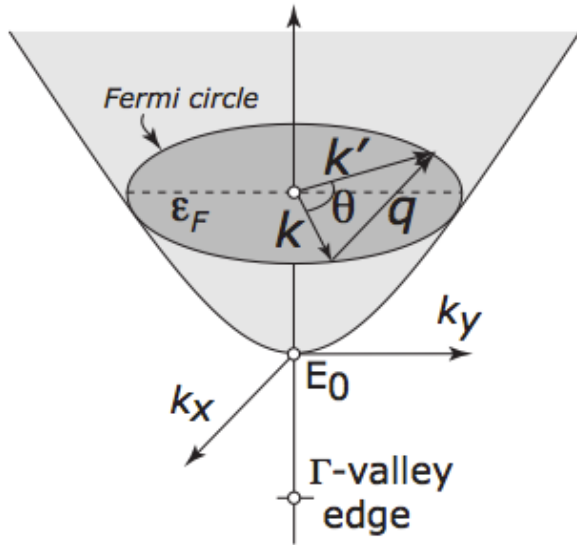
$\Rightarrow n$, and hence \mathbf{j} , topologically conserved.

Obvious question: where does $|\Psi(\mathbf{r})|^4$ term come from?

Handling Diffusive Transport in Low-Dimensions

Example: Transport in 2DEGs

2DEG electron wavefunction (note: \mathbf{k} , \mathbf{r} are in the 2D plane!)



$$\frac{1}{\sqrt{A}} e^{i\mathbf{k}\cdot\mathbf{r}} \chi(z) u_{n\mathbf{k}}(\mathbf{r}) \rightarrow S(\mathbf{k}, \mathbf{k}') = \frac{2\pi}{\hbar} |H_{\mathbf{k}, \mathbf{k}'}|^2 \delta(\epsilon_{\mathbf{k}} - \epsilon_{\mathbf{k}'})$$

envelope fn.

$$H_{\mathbf{k}, \mathbf{k}'} = \langle \mathbf{k}' | V(\mathbf{r}, z) | \mathbf{k} \rangle \cdot I_{\mathbf{k}, \mathbf{k}'}$$

$$I_{\mathbf{k}, \mathbf{k}'} \approx 1$$

$$\frac{1}{\tau_m(\mathbf{k})} = N_{2D} \sum_{k'} S(k', k) (1 - \cos \theta)$$

$$\frac{1}{\langle \tau_m \rangle} = n_{2D}^{imp} \frac{m^*}{2\pi \hbar^3 k_F^3} \int_0^{2k_F} |V(q)|^2 \frac{q^2}{\sqrt{1 - (q/2k_F)^2}} dq$$

$$1 - \cos \theta = q^2 / 2k_F^2$$

In general, scattering can lead to intersubband transitions...

$$V_{nm}(q) = \frac{1}{A} \int dz \left(\chi_n^*(z) \chi_m(z) \int d^2\mathbf{r} V(\mathbf{r}, z) e^{i\mathbf{q}\cdot\mathbf{r}} \right)$$

n, m are the subband indices.

Within the same subband: 'Electric quantum limit'

$$V(q) = V_{00}(q) = \frac{1}{A} F(q) V(q, z_0)$$

Screening in 2D

$$\epsilon_{2d}(q) = \epsilon(0) \left(1 + \frac{q_{TF}}{q} \right)$$

2D screening function

$$q_{TF} = \frac{m^* e^2}{2\pi \epsilon(0) \epsilon_0 \hbar^2} = \frac{2}{a_B^*}$$

Thomas-Fermi wavevector

$$V(q, z_0) = \frac{V_{uns}(q, z_0)}{\epsilon_{2d}(q)}$$

Screened 2D potential

Handling Diffusive Transport in Low-Dimensions

$$\rho(z) \rightarrow en_s \delta(z)$$

'perfect' 2D: Graphene, BN

$$\rho(r, z) = \rho(z) = en_s |\chi(z)|^2$$

Quasi-2D: MOSFETs/HEMTs

$$\chi_{n_z}(z) = \sqrt{\frac{2}{L_z}} \sin\left(\frac{n_z \pi}{L_z} z\right)$$

'Infinitely' deep square QW

$$\chi(z) = 0, z < 0$$

$$\chi(z) = \sqrt{\frac{b^3}{2}} z e^{-\frac{bz}{2}}, z \geq 0,$$

$$b = \left(33m^* e^2 n_s / 8\hbar^2 \epsilon_0 \epsilon_b\right)^{1/3}$$

Triangular QW:
Variational Wavefunction
(Fang-Howard)
Can handle multiple
subband occupation...

$$V(q) = \frac{1}{A} F(q) V(q, z_0)$$

$$F(q) = \eta^3 = \left(\frac{b}{b+q}\right)^3$$

Form factor

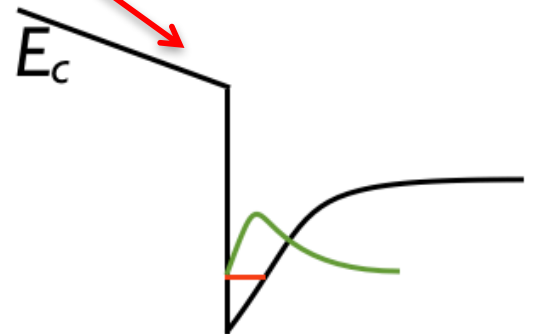
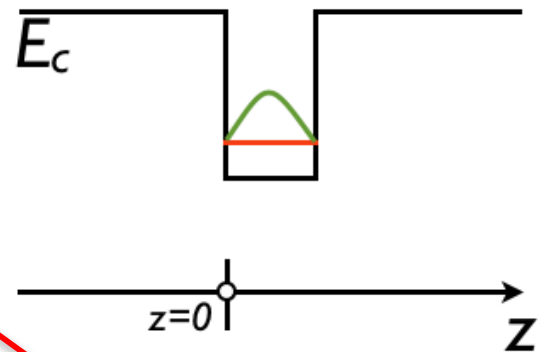
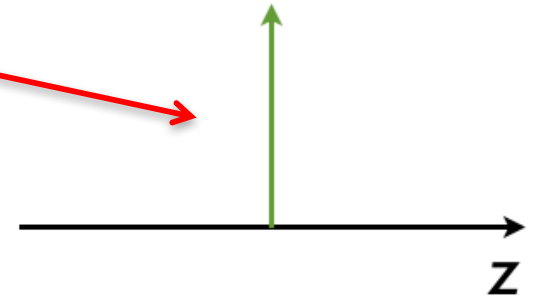
$$V(q, z_0) = \frac{V_{uns}(q, z_0)}{\epsilon_{2d}(q)}$$

Screened scattering potential

$$\epsilon_{2d}(q) = \epsilon(0) \left(1 + \frac{q_{TF}}{q} G(q)\right)$$

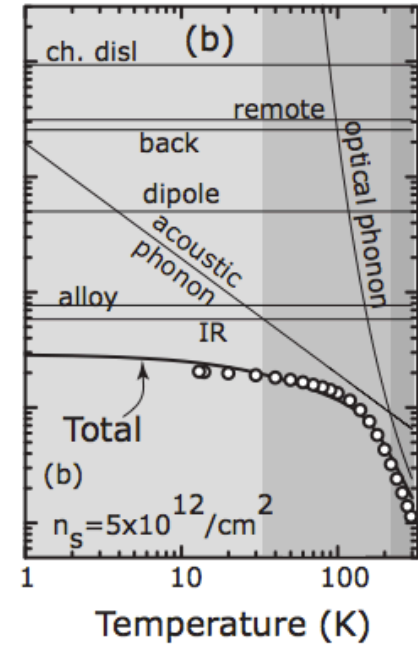
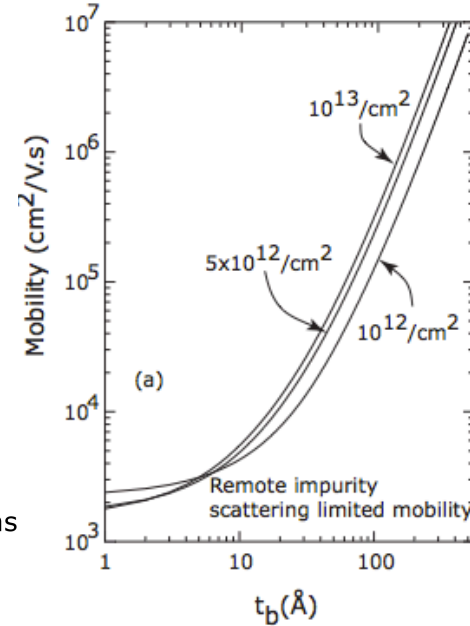
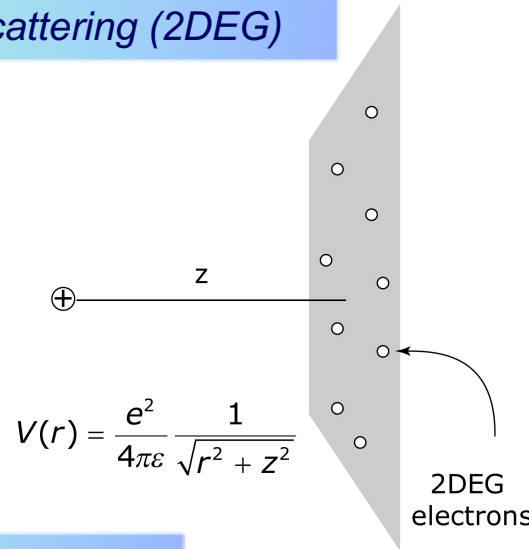
$$G(q) = \frac{1}{8} (2\eta^3 + 3\eta^2 + 3\eta)$$

Screening form factor



Handling Diffusive Transport in Low-Dimensions

Example: Remote Impurity Scattering (2DEG)



Screened remote Coulomb potential

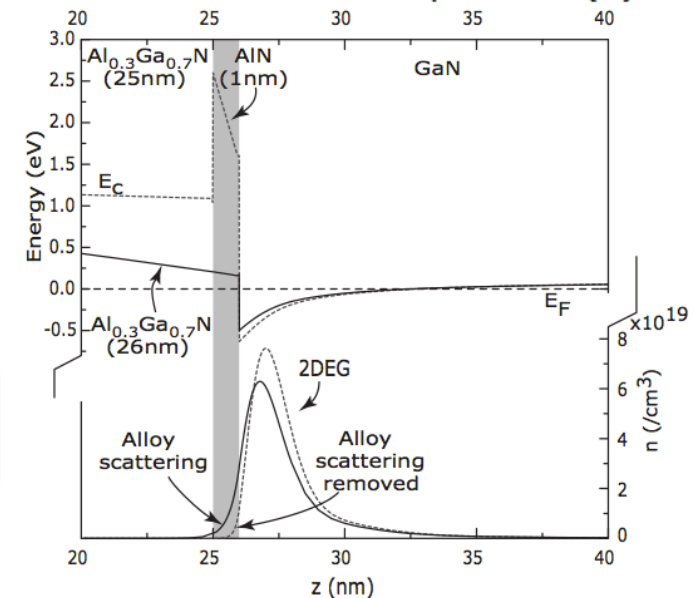
$$V(q) = \frac{V(q, z_0)}{\epsilon_{2d}(q)} = \int_0^\infty r dr \int_0^{2\pi} d\theta \frac{e^2}{4\pi\epsilon(q)\sqrt{r^2 + z_0^2}} e^{iqr \cos\theta} = \frac{e^2}{2\epsilon_0\epsilon(0)} \frac{e^{-qz_0}}{q + q_{TF}}$$

Scattering rate (note dependence on k_F)

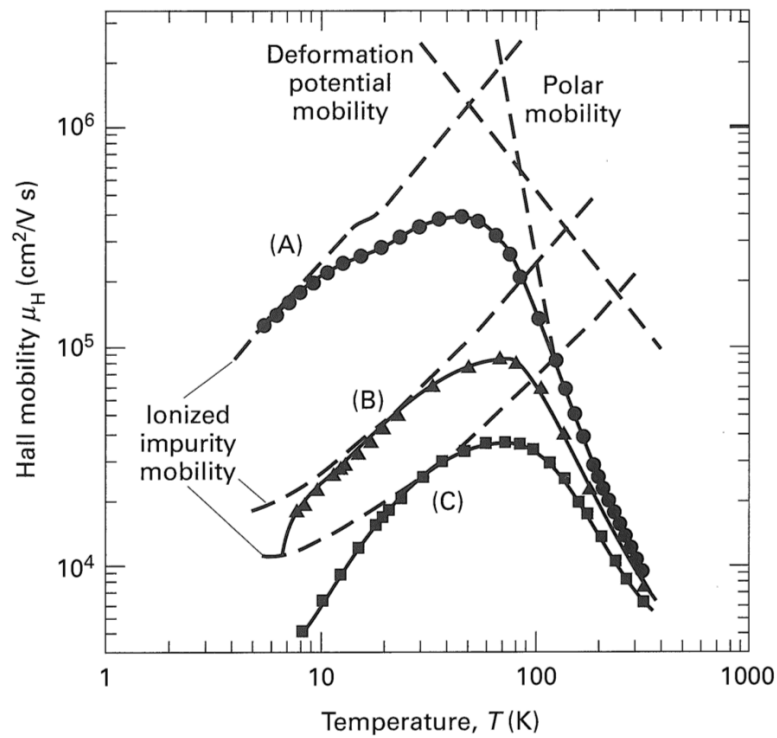
$$\frac{1}{\tau_{rem}(k_F)} = N_s \frac{m^*}{2\pi\hbar^3 k_F^3} \left(\frac{e^2}{2\epsilon_0\epsilon(0)} \right)^2 \int_0^{2k_F} dq \frac{F(q)e^{-2qt_b}}{(q + q_{TF}G(q))^2} \frac{q^2}{\sqrt{1 - \left(\frac{q}{2k_F}\right)^2}}$$

Averaging over distribution: No averaging necessary for degenerate 2DEGs because transport occurs by electrons at the Fermi energy!

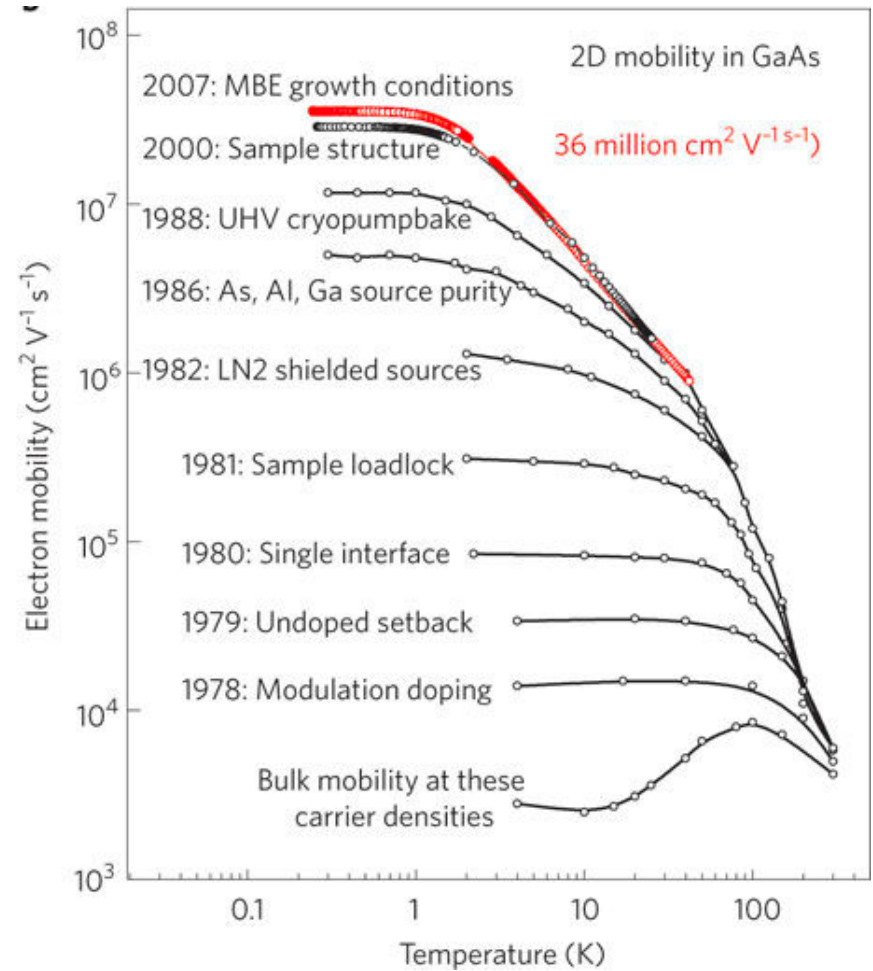
$$\frac{\partial f_0(E)}{\partial E} \approx \delta(E - E_F) \rightarrow \mu_{2DEG} \approx \frac{q\tau_m(k_F)}{m^*}$$



Transport in 3D vs 2D

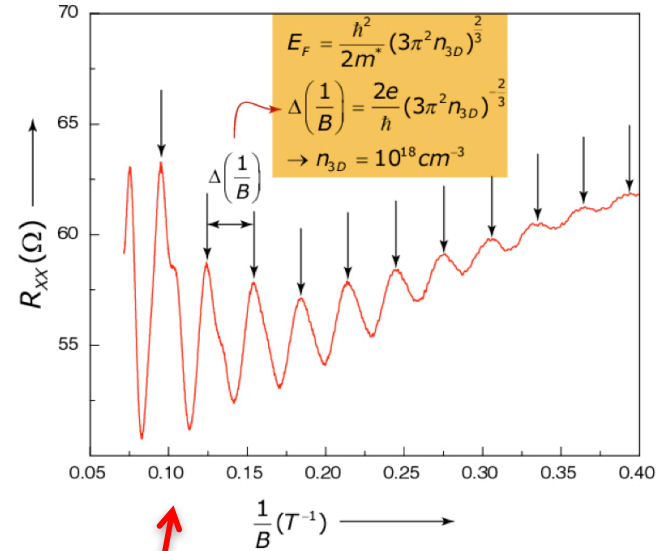
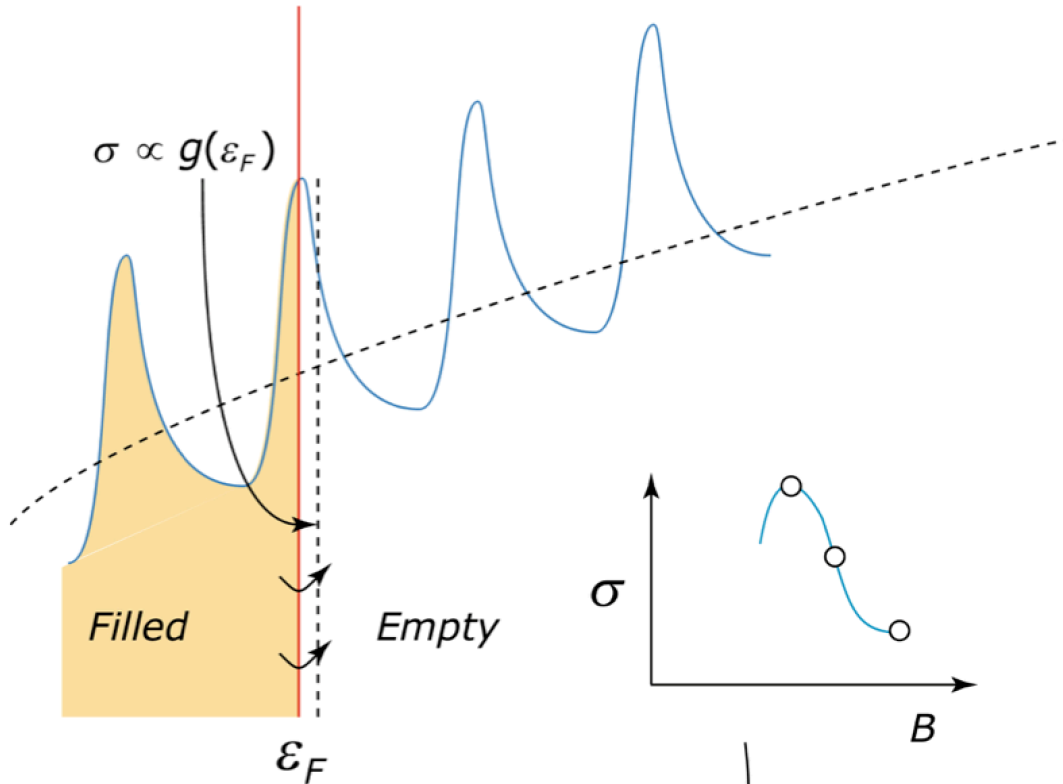


3D (Doped GaAs)



Modulation Doped GaAs

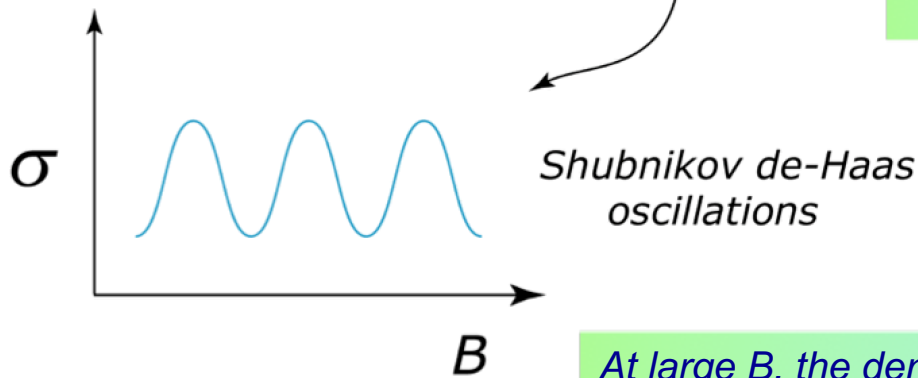
Shubnikov de Haas Oscillations



$$\Delta R_{xx} \propto f\left(\frac{m^* T}{B}\right) \cdot e^{-\omega_c \tau_q} \cdot \cos\left(\frac{2\pi \epsilon_F}{\hbar \omega_c}\right)$$

Dingle formula

Experimentally measured Shubnikov de-Haas oscillations



$$E = \frac{\hbar^2}{2m^*} (k_x^2 + k_y^2) \rightarrow E_n = \left(n + \frac{1}{2}\right) \hbar \omega_c$$

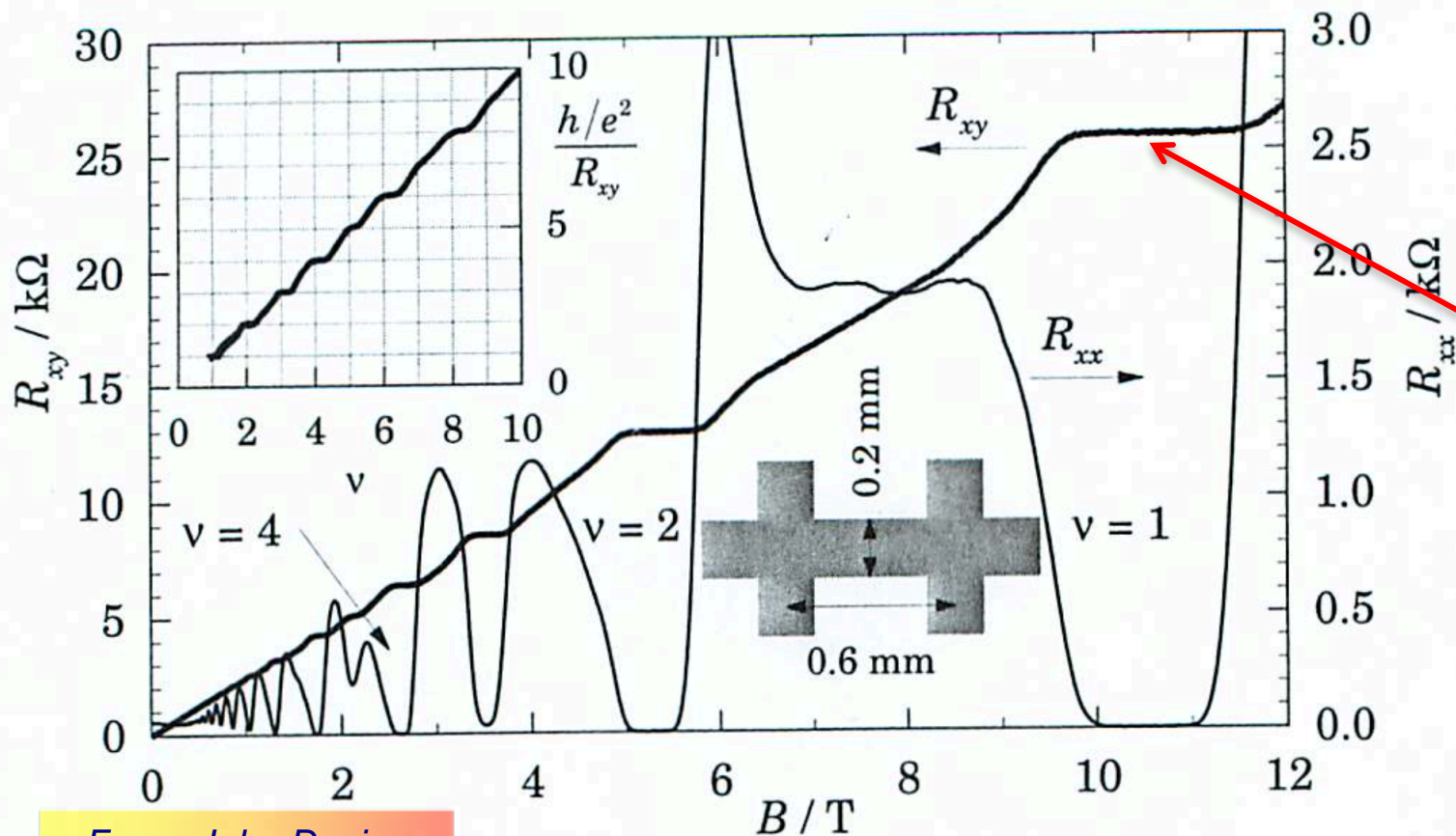
Landau levels

$\omega_c = \frac{eB}{m^*}$ cyclotron frequency

Energy eigenvalues with a B-field

At large B , the density of states collapses into bunches of energies called Landau levels. Conductivity is expected to oscillate \rightarrow SdH oscillations.

The Quantum Hall Effect



From: John Davies

Quantization of Hall conductance is precise to ~1 part in a billion!

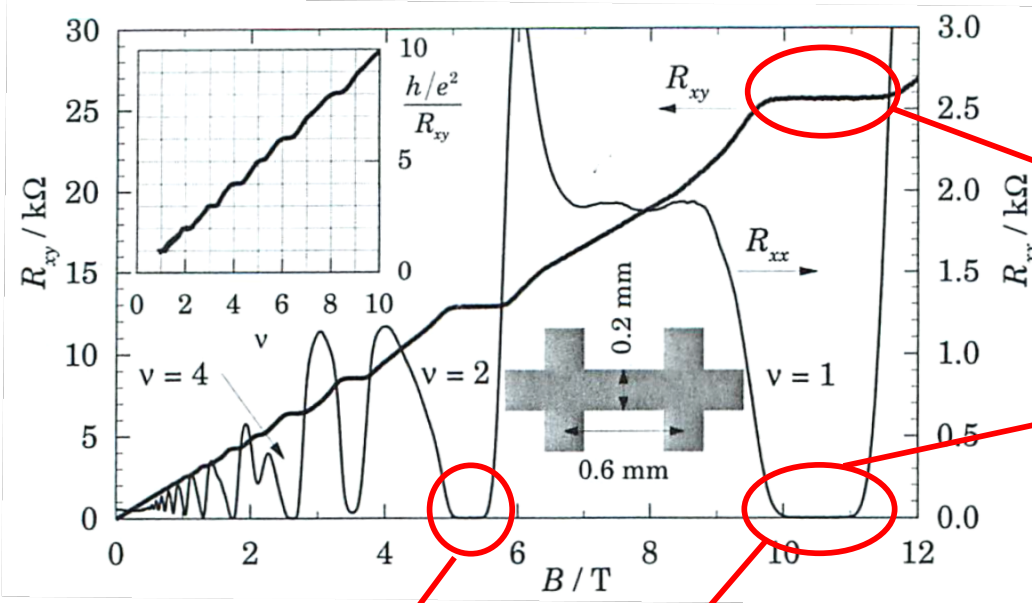
Why is it so precise?

$$\sigma_{xy} = \frac{e^2}{h} \times C$$

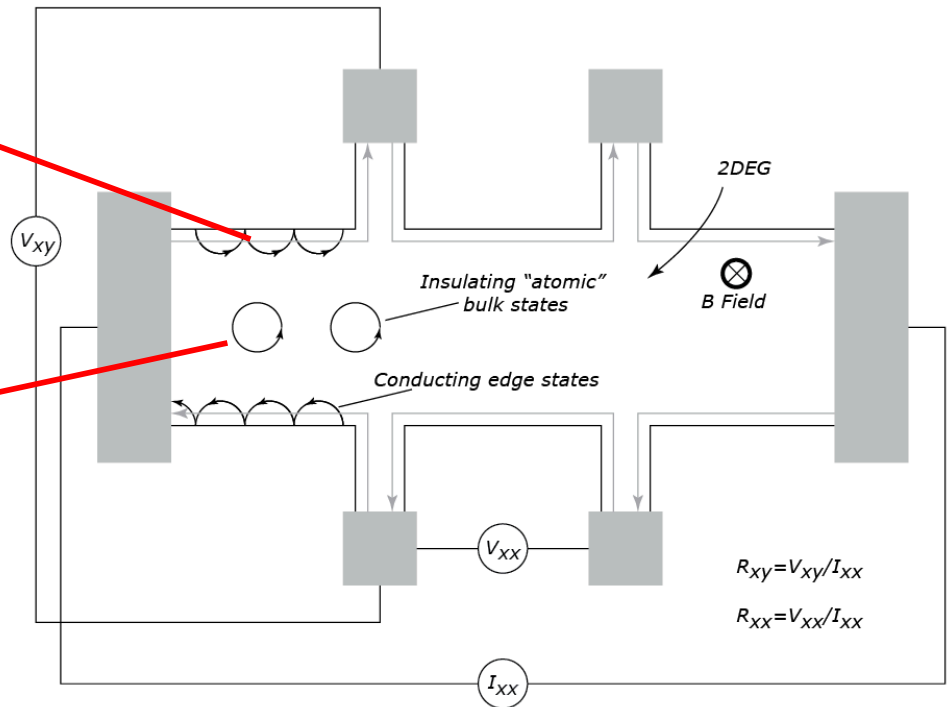
TKNN invariant:
Chern number, an integer!

The Quantum Hall Effect

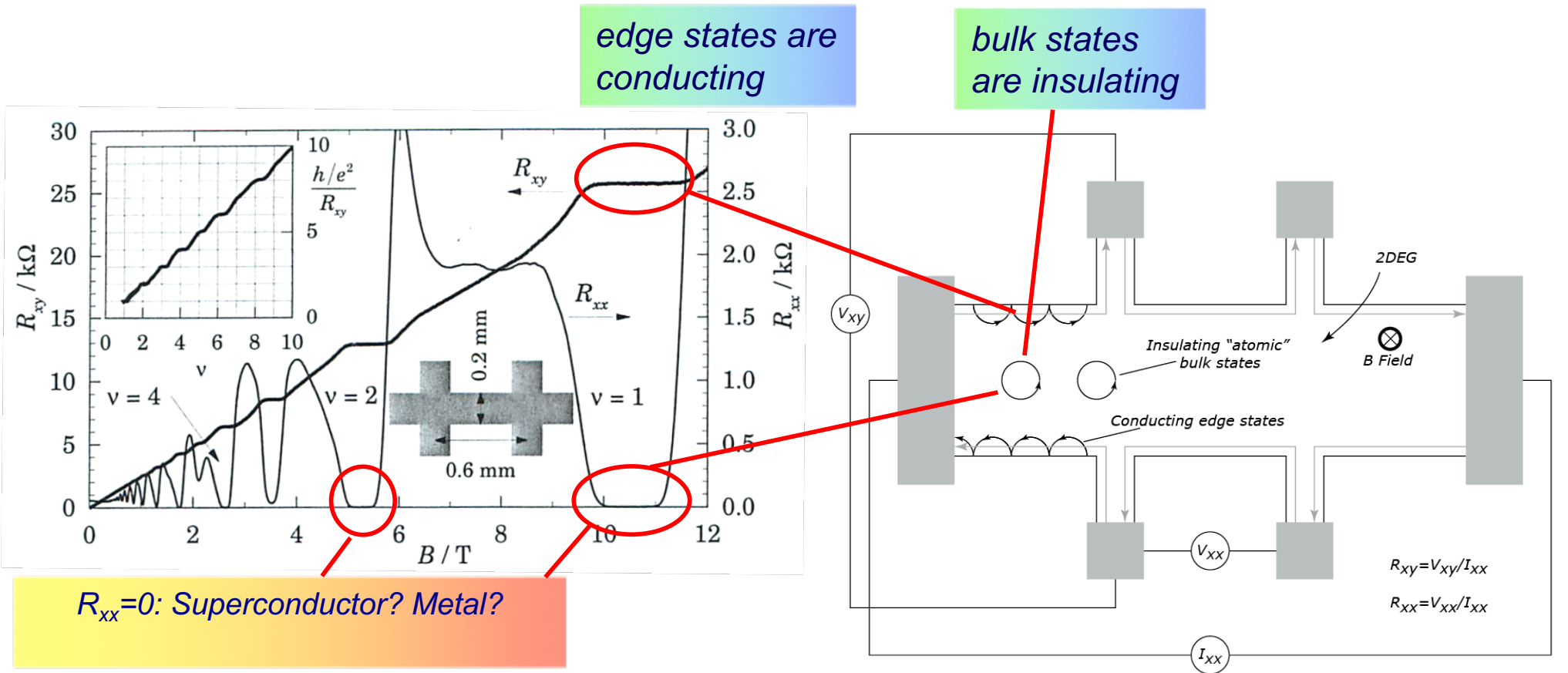
edge states are conducting



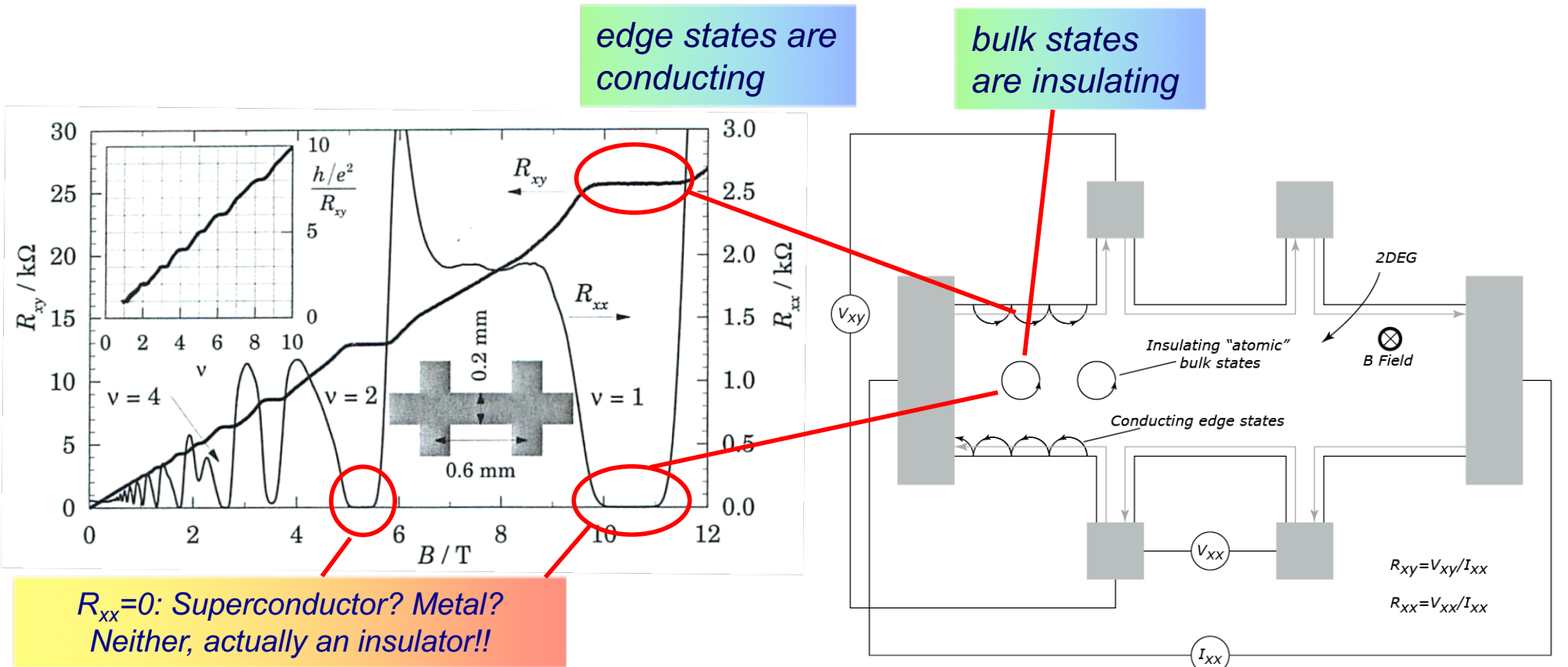
$R_{xx}=0$: Superconductor?



The Quantum Hall Effect



The Quantum Hall Effect



$$\begin{bmatrix} J_x \\ J_y \end{bmatrix} = \begin{bmatrix} \sigma_{xx} & \sigma_{xy} \\ \sigma_{yx} & \sigma_{yy} \end{bmatrix} \begin{bmatrix} E_x \\ E_y \end{bmatrix}$$

conductivity tensor

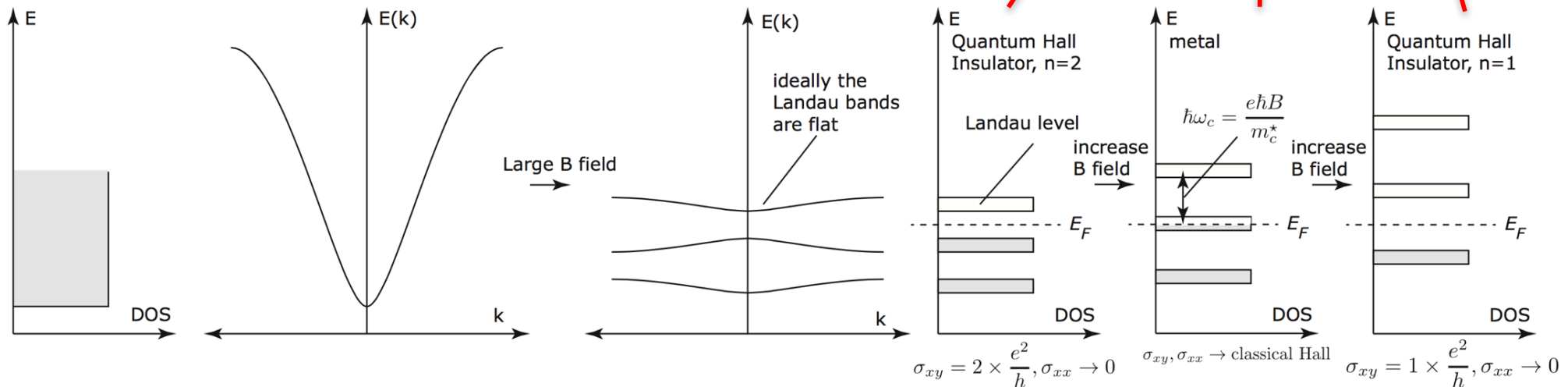
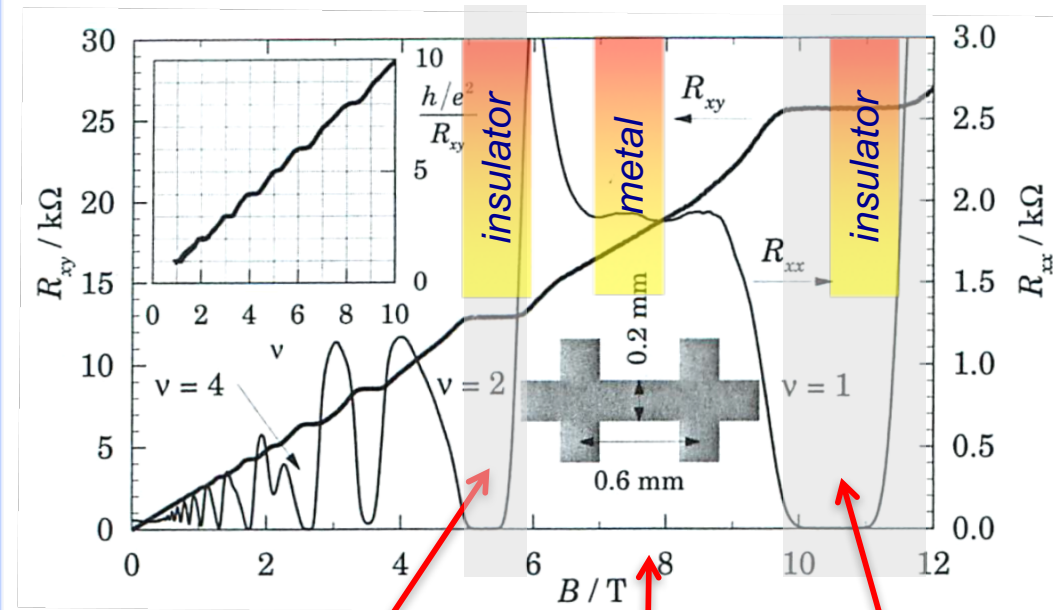
$$\begin{bmatrix} \sigma_{xx} & \sigma_{xy} \\ \sigma_{yx} & \sigma_{yy} \end{bmatrix} = \begin{bmatrix} \rho_{xx} & \rho_{xy} \\ \rho_{yx} & \rho_{yy} \end{bmatrix}^{-1} = \frac{1}{\rho_{xx}\rho_{yy} - \rho_{xy}\rho_{yx}} \begin{bmatrix} \rho_{yy} & -\rho_{xy} \\ -\rho_{yx} & \rho_{xx} \end{bmatrix}$$

For the QHE plateaus, $\rho_{xx} = \rho_{yy} = 0$, which implies that $\sigma_{xx} = 0$.

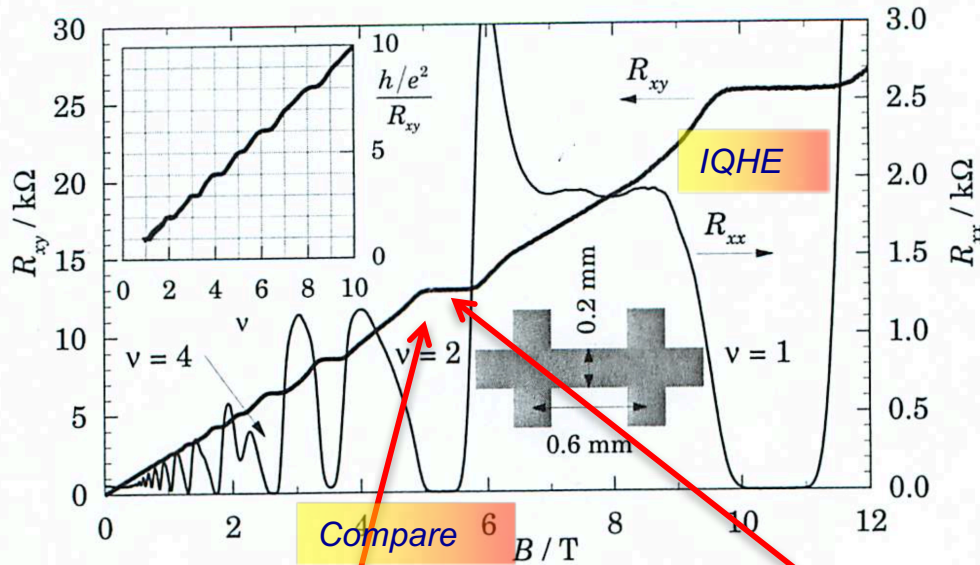
The Quantum Hall Effect

From a Landau-level picture, it is easy to see that:

- Landau level separation increases with B .
- If 2D electron gas density is constant, the DOS at the Fermi level E_F goes into gaps and inside Landau levels successively.
- When the E_F is inside a Landau level, the system behaves in the classical Hall effect, $R_{xy} = B/n_{2d}e$, and R_{xx} is a scattering-limited magnetoresistance.
- But when the E_F is in the gap of DOS between Landau levels, $R_{xx} \rightarrow 0$, and $R_{xy} = h/(e^2 \cdot \text{integer})$ to a very high degree of precision.
- $R_{xx} \rightarrow 0$ is justified because of low conductivity and insulating bulk states, but the very precise quantization of R_{xy} is a big surprise!



Quantum Hall Insulator & Topological Insulator



Parts per billion precision

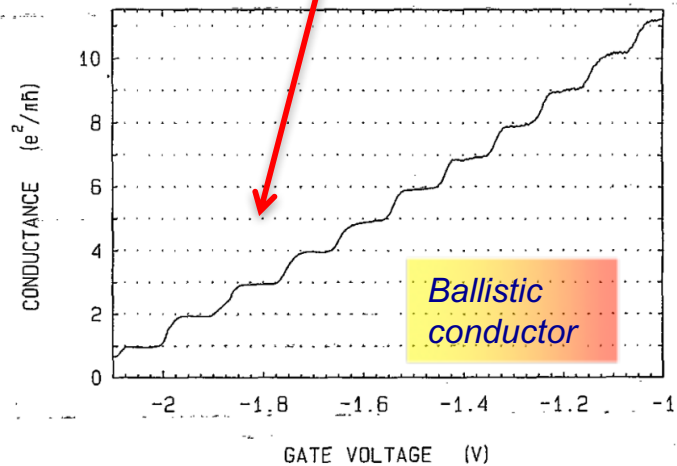
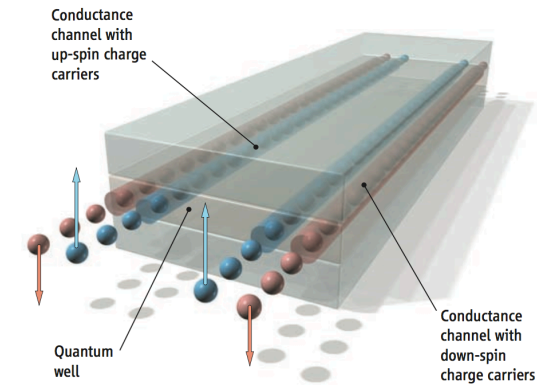


FIG. 2. Point-contact conductance as a function of gate voltage, obtained from the data of Fig. 1 after subtraction of the lead resistance. The conductance shows plateaus at multiples of $e^2/\pi h$.

Low precision

Quantum Spin Hall Insulator State in HgTe Quantum Wells

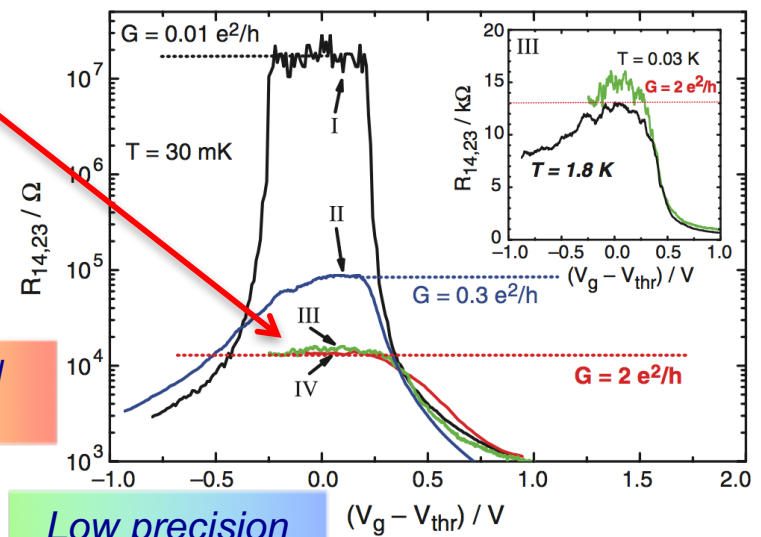
Markus König,¹ Steffen Wiedmann,¹ Christoph Brüne,¹ Andreas Roth,¹ Hartmut Buhmann,¹ Laurens W. Molenkamp,^{1*} Xiao-Liang Qi,² Shou-Cheng Zhang²



Schematic of the spin-polarized edge channels in a quantum spin Hall insulator.

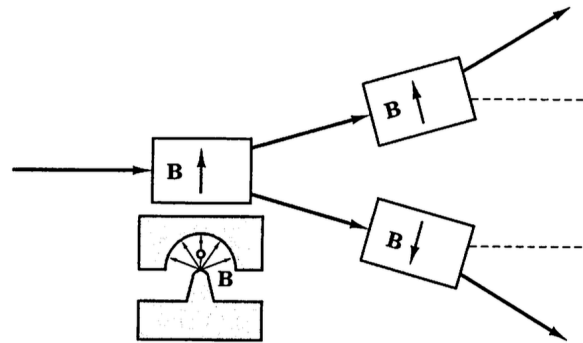
Compare

Topological insulator



Low precision

Electron spin is a consequence of relativity



1922 Stern-Gerlach experiment shows evidence of spin

1925 Uhlenbeck and Goudsmit propose spin as an intrinsic angular momentum of electrons

1927 Pauli introduces spin matrices and spin into the Schrodinger equation in an ad-hoc manner

1927 Dirac unifies special relativity and quantum mechanics and finds spin as a byproduct

$$\hat{H} = \hat{H}_0 + \mu_B \sigma \cdot \mathbf{B} + \mu_B \sigma \cdot \frac{\mathbf{E} \times \mathbf{v}}{2c^2} = \hat{H}_0 + \mu_B \sigma \cdot \mathbf{B} + \frac{\hbar}{4mc^2} \sigma \cdot [(\nabla V) \times \mathbf{v}]$$

Spin-less Energy

Extra terms because of spin

Extra terms because of spin

Crash course on special relativity

$$x' = x - vt, t' = t.$$

$$w' = \frac{dx'}{dt} = \frac{dx}{dt} - \frac{d(vt)}{dt} \implies w' = w - v.$$

$$a' = a \implies F' = ma' = F = ma$$

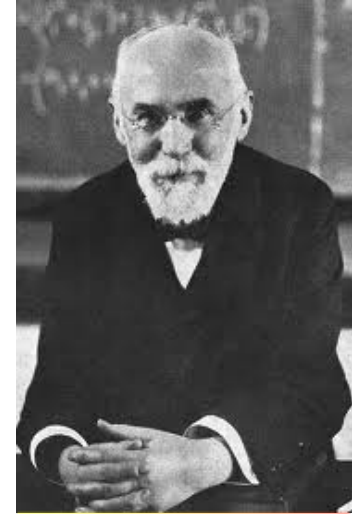
"Galilean" relativity theory of how coordinates transform from one reference frame to another.

Main idea: Constant velocity is NOT ABSOLUTE, but depends on the speed of the observer

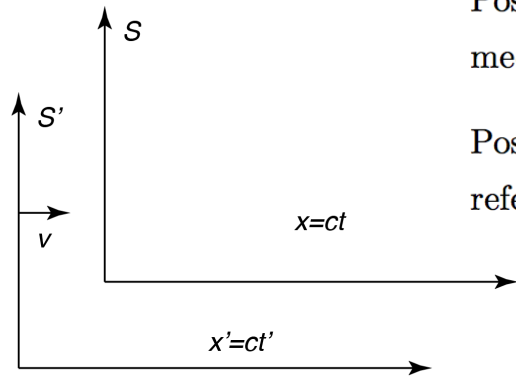
$$(\nabla^2 - \frac{1}{c^2} \frac{\partial^2}{\partial t^2}) \mathbf{E} = 0$$

$$c = \frac{1}{\sqrt{\epsilon_0 \mu_0}} = 3 \times 10^8 \text{ m/s.}$$

Maxwell's Equations: Speed of light emerges with no indication of observer. Experiments by Michelson/Morley show that the measured speed of light DOES NOT depend on the speed of the observer!



Lorentz



Postulate 1: All inertial observers are equally privileged wrt physical laws: laws of mechanics *and* laws of electromagnetism.

Einstein's two postulates to explain the strange behavior of light

Postulate 2: Velocity of light is a constant, independent of source, observer, or the reference frame!

$$\gamma = \frac{1}{\sqrt{1 - \frac{v^2}{c^2}}}$$

$$x' = \frac{x - vt}{\sqrt{1 - \frac{v^2}{c^2}}}, \text{ and}$$

$$t' = \frac{t - \frac{vx}{c^2}}{\sqrt{1 - \frac{v^2}{c^2}}}$$

Lorentz Transformation

$$x = ct \text{ and } x' = ct'$$

$$x' = \gamma(x - vt), \text{ and } x = \gamma(x' + vt')$$

$$w' = \frac{w - v}{1 - \frac{vw}{c^2}}, \text{ and } w = \frac{w' + v}{1 + \frac{vw'}{c^2}}$$

Crash course on special relativity

The views of space and time which I wish to lay before you have sprung from the soil of experimental physics, and therein lies their strength. Henceforth space by itself, and time by itself, are doomed to fade away into mere shadows, and only a kind of union of the two will preserve an independent reality.

— Hermann Minkowski, 1907^[4]

$$\Delta t' = \frac{\Delta t - \frac{v\Delta x}{c^2}}{\sqrt{1 - \left(\frac{v}{c}\right)^2}}$$

Space-time 4-vectors

$$X = (ct, x, y, z) = (x_0, x_1, x_2, x_3) = (x_0, \mathbf{r}) \quad X' = (ct', x', y', z')$$

$$x'_i = \frac{x_i - vt}{\sqrt{1 - \frac{v^2}{c^2}}} = \frac{x_i - \beta x_0}{\sqrt{1 - \beta^2}}$$

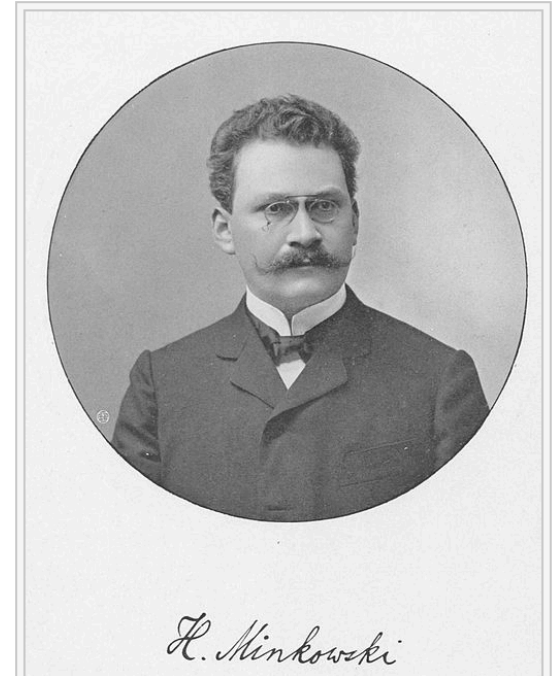
$$s^2 = X \cdot X = x_0^2 - x_1^2 - x_2^2 - x_3^2 = x_0^2 - |\mathbf{r}|^2$$

The Minkowski Norm is invariant for inertial observers!

$$X \cdot X' = X^T X' = X^T g X'$$

The Minkowski dot product for 4-vectors

$$g_{\mu\nu} = \begin{bmatrix} +1 & 0 & 0 & 0 \\ 0 & -1 & 0 & 0 \\ 0 & 0 & -1 & 0 \\ 0 & 0 & 0 & -1 \end{bmatrix}$$



H. Minkowski

Hermann Minkowski (1864 – 1909) was a German mathematician. He found that the theory of special relativity, introduced by his former student [Albert Einstein](#), could best be understood in a four-dimensional space, since known as the Minkowski spacetime.

wikipedia

Crash course on special relativity

$$t' = \frac{t - \frac{vx}{c^2}}{\sqrt{1 - \frac{v^2}{c^2}}}$$

Since time is relative, the only time all observers agree on is the “proper” time, or the time measured on the clock carried by the particle whose motion is being studied.



Einstein

$$\Delta t' = \frac{\Delta t - \frac{v\Delta x}{c^2}}{\sqrt{1 - (\frac{v}{c})^2}}$$



$$\Delta t = \frac{\Delta\tau}{\sqrt{1 - (\frac{v}{c})^2}} \implies \frac{dt}{d\tau} = \frac{1}{\sqrt{1 - (\frac{v}{c})^2}}$$

τ is the proper time

$$\frac{d(\dots)}{d\tau} = \frac{d(\dots)}{dt} \frac{dt}{d\tau}$$

$$V = \frac{dX}{d\tau} = \left(\frac{dx_0}{d\tau}, \frac{dx_1}{d\tau}, \frac{dx_2}{d\tau}, \frac{dx_3}{d\tau} \right) = \frac{1}{\sqrt{1 - \frac{v^2}{c^2}}} \left(\frac{dx_0}{dt}, \frac{dx_1}{dt}, \frac{dx_2}{dt}, \frac{dx_3}{dt} \right) = \frac{1}{\sqrt{1 - \frac{v^2}{c^2}}} \left(c, \frac{d\mathbf{r}}{dt} \right)$$

The 4-velocity. Note the time derivative is w.r.t. the proper time, not the time in the observer’s frame!

$$P = mV = (p_0, \mathbf{p}) = \left(\frac{mc}{\sqrt{1 - \frac{v^2}{c^2}}}, \frac{m\mathbf{v}}{\sqrt{1 - \frac{v^2}{c^2}}} \right)$$

The 4-momentum. Because space and time are tangled, the ‘momentum’ is strangely not a 3D vector, but a 4-D vector, with a strange connection between the mass of the particle and the speed of light!

Crash course on special relativity

$$P = mV = (p_0, \mathbf{p}) = \left(\frac{mc}{\sqrt{1 - \frac{v^2}{c^2}}}, \frac{m\mathbf{v}}{\sqrt{1 - \frac{v^2}{c^2}}} \right)$$

Einstein dissects the 4-momentum.

$$p = mv \left(1 - \frac{v^2}{c^2}\right)^{-\frac{1}{2}} \approx mv + \frac{1}{2}mv \left(\frac{v}{c}\right)^2 + \dots$$

Similar to classical momentum, but extra terms...

$$p_0 = mc \left(1 - \frac{v^2}{c^2}\right)^{-\frac{1}{2}} \approx mc + \frac{1}{2}m \frac{v^2}{c} + \dots \implies cp_0 = \boxed{mc^2} + \boxed{\frac{1}{2}mv^2} + \dots$$

Very different from classical momentum, but strangely connected to kinetic energy!

$$P = \left(\frac{E}{c}, \mathbf{p}\right) \quad E = cp_0 = \frac{mc^2}{\sqrt{1 - \frac{v^2}{c^2}}}$$

Rest energy

Kinetic energy

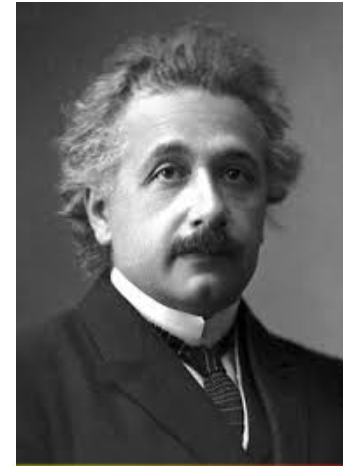
Minkowski Norm of 4-momentum is invariant for inertial observers!

Total energy of a particle

$$P \cdot P = (mc)^2 = p_0^2 - |\mathbf{p}|^2 = \frac{E^2}{c^2} - p^2 = (mc)^2 \implies E^2 = (mc^2)^2 + (cp)^2$$

$$K = \left(\frac{E}{c}, p\right) \text{ and } K \cdot K = (mc)^2 = 0 \implies \left(\frac{E}{c}\right)^2 - p^2 = 0 \implies E = cp$$

Total energy of a massless particle



Einstein

Making the Schrodinger equation relativistic

$$-\frac{\hbar^2}{2m}\nabla^2\psi = i\hbar\frac{\partial}{\partial t}\psi = E\psi$$

Schrodinger equation does not have the correct relativistic energy: there is no 'c'!

$$\hat{E} = i\hbar\frac{\partial}{\partial t}, \text{ and } p \rightarrow \hat{p} = -i\hbar\nabla:$$

Correct relativistic energy

$$\frac{E^2}{c^2} - p^2 = (mc)^2$$

$$\rightarrow \left[-\frac{1}{c^2}\frac{\partial^2}{\partial t^2} - (-i\hbar\nabla)^2\right]\psi = (mc)^2\psi$$

$$\left[\nabla^2 - \frac{1}{c^2}\frac{\partial^2}{\partial t^2}\right]\psi = \left(\frac{mc}{\hbar}\right)^2\psi = \left(\frac{2\pi}{\lambda}\right)^2\psi$$

The Klein-Gordon equation

Fails this requirement

$$\rho = \psi^*\psi \geq 0$$

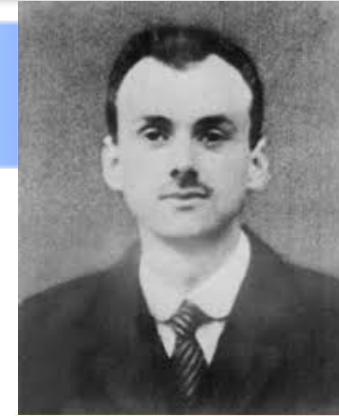
The Klein-Gordon equation appears a likely candidate for the relativistic quantum mechanics of electrons. However, the probability density of the particles it represents does not remain positive definite. It can represent spinless particles, but **NOT ELECTRONS!**

$\lambda = h/mc$ is a characteristic Compton wavelength

The Dirac Equation

$$\nabla^2 - \frac{1}{c^2} \frac{\partial^2}{\partial t^2} = \partial_x^2 + \partial_y^2 + \partial_z^2 - \frac{1}{c^2} \frac{\partial^2}{\partial t^2} = (A\partial_x + B\partial_y + C\partial_z + \frac{i}{c}D\partial_t)^2$$

Take the square root of the operator!



Dirac

$$A^2 = B^2 = C^2 = D^2 = 1, AB + BA = 0, \dots$$

A, B, C, D are not numbers, but **4x4!** matrices. Dirac's major realization, introduction of 4x4 matrices

$$(A\partial_x + B\partial_y + C\partial_z + \frac{i}{c}D\partial_t)\psi = (\frac{mc}{\hbar})\psi$$

$$\partial_0 = \frac{\partial}{c\partial t}, \partial_1 = \frac{\partial}{\partial x}, \partial_2 = \frac{\partial}{\partial y}, \partial_3 = \frac{\partial}{\partial z} \quad 4 \times 4 \text{ Dirac gamma matrices } \gamma^0, \gamma^1, \gamma^2, \gamma^3$$

$$(\gamma^0)^2 = +1 \text{ but } (\gamma^1)^2 = (\gamma^2)^2 = (\gamma^3)^2 = -1$$

rewrite

$$\text{Minkowski metric tensor } g \quad \{\gamma^\nu, \gamma^\mu\} = 2g^{\nu\mu}$$

Pauli spin matrices

$$\gamma^0 = \begin{bmatrix} +1 & 0 & 0 & 0 \\ 0 & +1 & 0 & 0 \\ 0 & 0 & -1 & 0 \\ 0 & 0 & 0 & -1 \end{bmatrix} = \begin{bmatrix} I_2 & 0 \\ 0 & -I_2 \end{bmatrix}$$

$$\gamma^1 = \begin{bmatrix} 0 & 0 & 0 & 1 \\ 0 & 0 & 1 & 0 \\ 0 & -1 & 0 & 0 \\ -1 & 0 & 0 & 0 \end{bmatrix} = \begin{bmatrix} 0 & \sigma_x \\ -\sigma_x & 0 \end{bmatrix}$$

$$\gamma^2 = \begin{bmatrix} 0 & 0 & 0 & -i \\ 0 & 0 & i & 0 \\ 0 & i & 0 & 0 \\ -i & 0 & 0 & 0 \end{bmatrix} = \begin{bmatrix} 0 & \sigma_y \\ -\sigma_y & 0 \end{bmatrix}$$

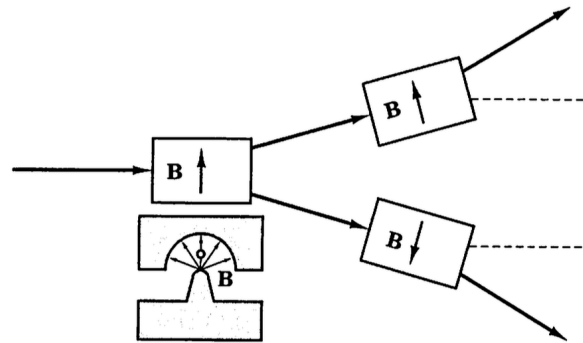
$$\gamma^3 = \begin{bmatrix} 0 & 0 & 1 & 0 \\ 0 & 0 & 0 & -1 \\ -1 & 0 & 0 & 0 \\ 0 & +1 & 0 & 0 \end{bmatrix} = \begin{bmatrix} 0 & \sigma_z \\ -\sigma_z & 0 \end{bmatrix}$$

The Dirac Equation for the electron

$$(i[\gamma^0\partial_0 + \gamma^1\partial_1 + \gamma^2\partial_2 + \gamma^3\partial_3] - \frac{mc}{\hbar})\psi = (i\gamma^\mu\partial_\mu - \frac{mc}{\hbar})\psi = 0$$

The Dirac equation predicts electron spin, and the existence of antimatter: positrons!

Electron spin is a consequence of relativity



1922 Stern-Gerlach experiment shows evidence of spin

1925 Uhlenbeck and Goudsmit propose spin as an intrinsic angular momentum of electrons

1927 Pauli introduces spin matrices and spin into the Schrodinger equation in an ad-hoc manner

1927 Dirac unifies special relativity and quantum mechanics and finds spin as a byproduct

$$\hat{H} = \hat{H}_0 + \mu_B \sigma \cdot \mathbf{B} + \mu_B \sigma \cdot \frac{\mathbf{E} \times \mathbf{v}}{2c^2} = \hat{H}_0 + \mu_B \sigma \cdot \mathbf{B} + \frac{\hbar}{4mc^2} \sigma \cdot [(\nabla V) \times \mathbf{v}]$$

Spin-less Energy

Extra terms because of spin

Extra terms because of spin

Asymmetry between x and p ...

$$\frac{d\mathbf{p}}{dt} = -e\nabla_r V + e\left(\frac{d\mathbf{x}}{dt} \times \mathbf{B}\right)$$

$$\frac{d\mathbf{x}}{dt} = \frac{1}{\hbar} \nabla_k E(k)$$

Asymmetry between x and p ...

$$\frac{d\mathbf{p}}{dt} = -e\nabla_r V + e\left(\frac{d\mathbf{x}}{dt} \times \mathbf{B}\right)$$

$$\frac{d\mathbf{x}}{dt} = \frac{1}{\hbar} \nabla_k E(k) \quad ??$$

Anomalous velocity terms in Bands

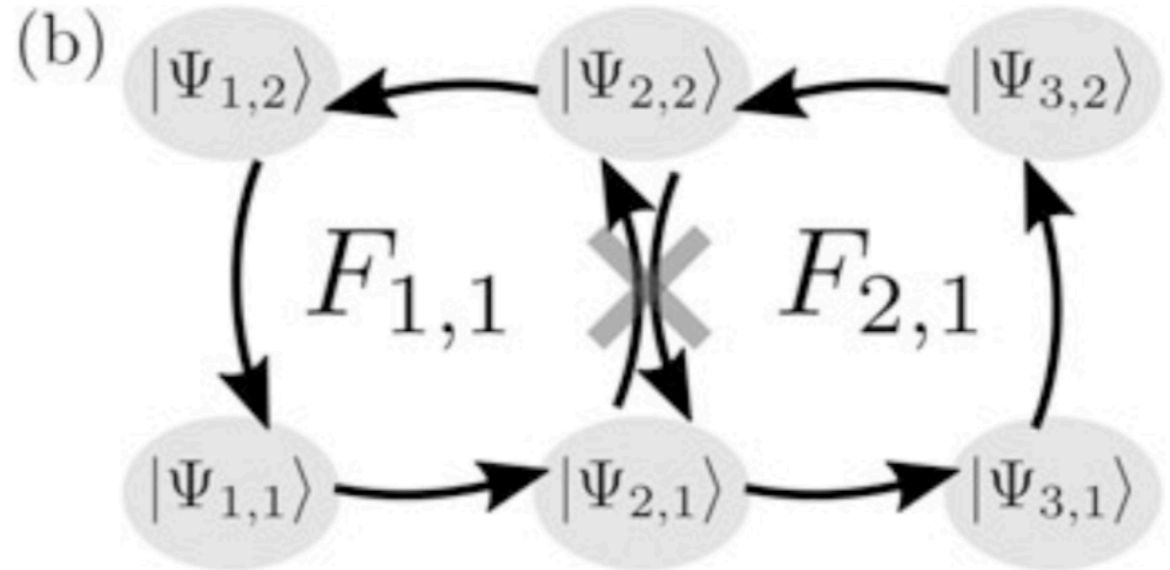
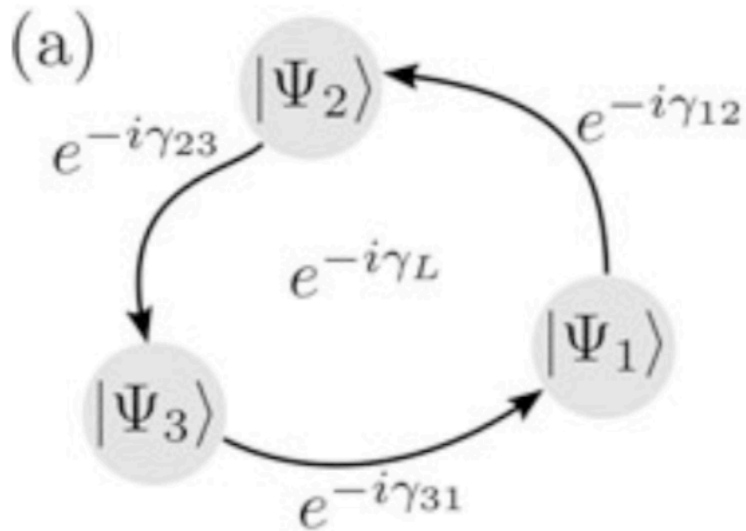
$$\frac{d\mathbf{p}}{dt} = -e\nabla_r V + e\left(\frac{d\mathbf{x}}{dt} \times \mathbf{B}\right)$$

$$\frac{d\mathbf{x}}{dt} = \frac{1}{\hbar}\nabla_k E(k) + \frac{d\mathbf{k}}{dt} \times \boldsymbol{\Omega} = \frac{1}{\hbar}\nabla_k E(k) + \frac{q}{\hbar}\mathbf{E} \times \boldsymbol{\Omega}$$

Note the dimensions here. Velocity is m/s, so the anomalous velocity term is also m/s. The units of $\boldsymbol{\Omega} = \nabla_k \times \mathcal{A} = \nabla_k \times i\langle n | \nabla_k | n \rangle = m^2$, and therefore the anomalous velocity unit is $\frac{1}{m \cdot s} \cdot m^2 = m/s$.

The discrete Berry Phase and Berry Flux

$$\gamma_L = -\arg e^{-i(\gamma_{12} + \gamma_{23} + \dots + \gamma_{N1})} = -\arg (\langle \Psi_1 | \Psi_2 \rangle \langle \Psi_2 | \Psi_3 \rangle \dots \langle \Psi_N | \Psi_1 \rangle)$$



$$\exp \left[-i \sum_{n=1}^{N-1} \sum_{m=1}^{M-1} F_{nm} \right] = e^{-i\gamma_L}$$

The Chern Number

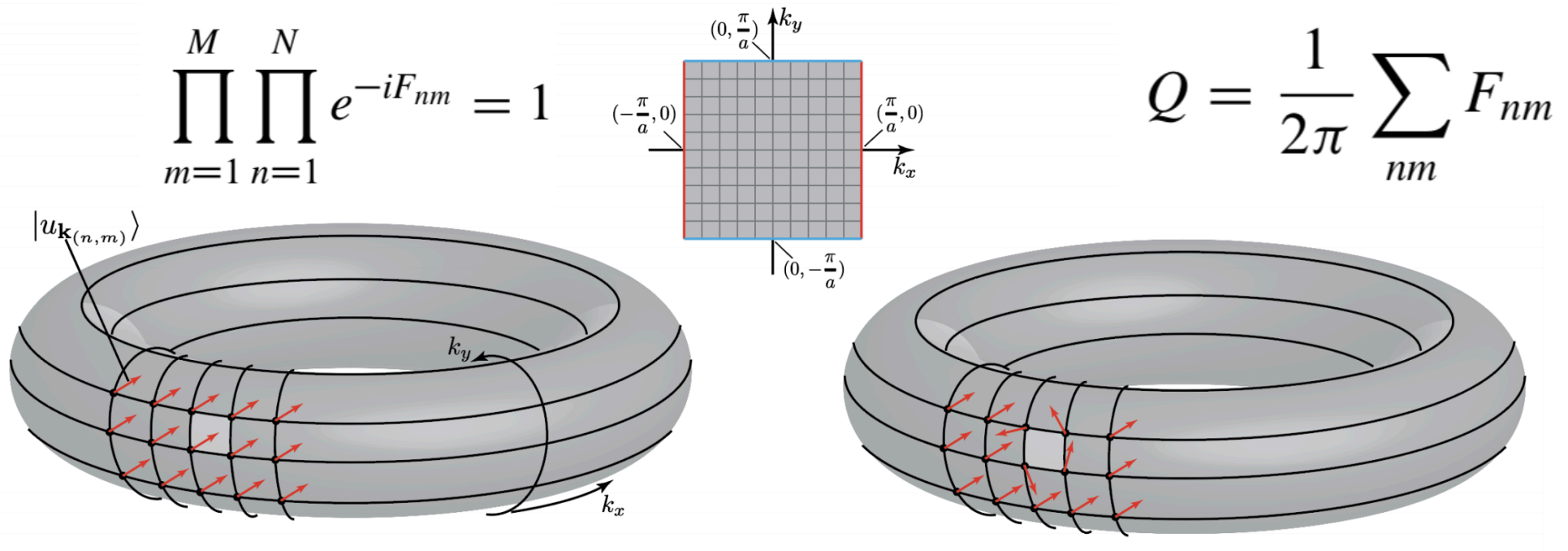


Figure 1: Berry phase and Chern Number.

We have found a simple picture for the Chern number: *The Chern number Q , that is, the sum of the Berry fluxes of all the plaquettes of a closed surface, is the number of vortices on the surface,*

$$Q = \frac{1}{2\pi} \sum_{nm} F_{nm} = \sum_{nm} Q_{nm} \in \mathbb{Z}. \quad (2.17)$$

Gauge Invariance \leftrightarrow Physical Observable

Classical Mechanics

$$[x, p_x] = 0$$

$$F = m \frac{d^2x}{dt^2}$$

$$-\nabla V$$

$$V + \lambda$$

"gauge"

Quantum Mechanics

$$[\hat{x}, \hat{p}_x] = i\hbar$$

$$\hat{H} = \frac{\hat{p}^2}{2m} + V \quad V + \lambda \Rightarrow E + \lambda$$

$$|\psi\rangle = \sum_n a_n |n\rangle$$

$$\hat{H} |n\rangle = E_n |n\rangle$$

$$i\hbar \frac{\partial}{\partial t} |\psi\rangle = \hat{H} |\psi\rangle$$

$$\langle m | n \rangle = \delta_{mn}$$

$$\langle x | p \rangle = \frac{e^{i p x / \hbar}}{\sqrt{2\pi\hbar}}$$

$$|\psi|^2 = \text{Prob}$$

Electromagnetism

$$\vec{E} = -\nabla V$$

$$V + \lambda$$

scalar 'gauge'

$$\vec{B} = \nabla \times \vec{A}$$

$$\vec{A} + \vec{C}$$

"Vector gauge"

To get physics right,

$$\nabla \times \vec{A} = \nabla \times (\vec{A} + \vec{C})$$

$$\nabla \times \vec{C} = 0 \text{ 'curl-free'}$$

$$\nabla^2$$

$$\nabla \times \nabla^2 = 0 \text{ (} d^2=0 \text{)}$$

Physical Qty \rightarrow Gauge Invariant

[But: is the reverse true?]

Berry phase: YES!

\rightarrow Polarization
 \rightarrow Magnetization

Quantum Berry Phase

FOR A CLOSED PATH,

γ_n IS GAUGE INVARIANT !!

$$\gamma_n = \oint_C d\vec{R} \cdot i \langle n(\vec{R}) | \frac{\partial}{\partial \vec{R}} | n(\vec{R}) \rangle = \oint_C d\vec{R} \cdot \vec{A}_n(\vec{R})$$

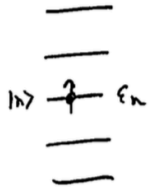
is the Berry Phase!

γ_n depends only on the GEOMETRIC aspect of the closed path & NOT on 't' \Rightarrow GEOMETRICAL PHASE!!

Q.M.

'Stationary' States

Say e'vals are: E_n + $|\psi\rangle = |n\rangle$



$$i\hbar \frac{\partial}{\partial t} |n\rangle = E_n |n\rangle$$

$$|n(t)\rangle = |n(0)\rangle e^{-\frac{i}{\hbar} \int_0^t E_n dt'}$$

'Dynamical' phase!

Precision $\langle\langle - \rangle\rangle$ Topology

Let us consider the Hamiltonian $H|\Psi\rangle = E\Psi$.

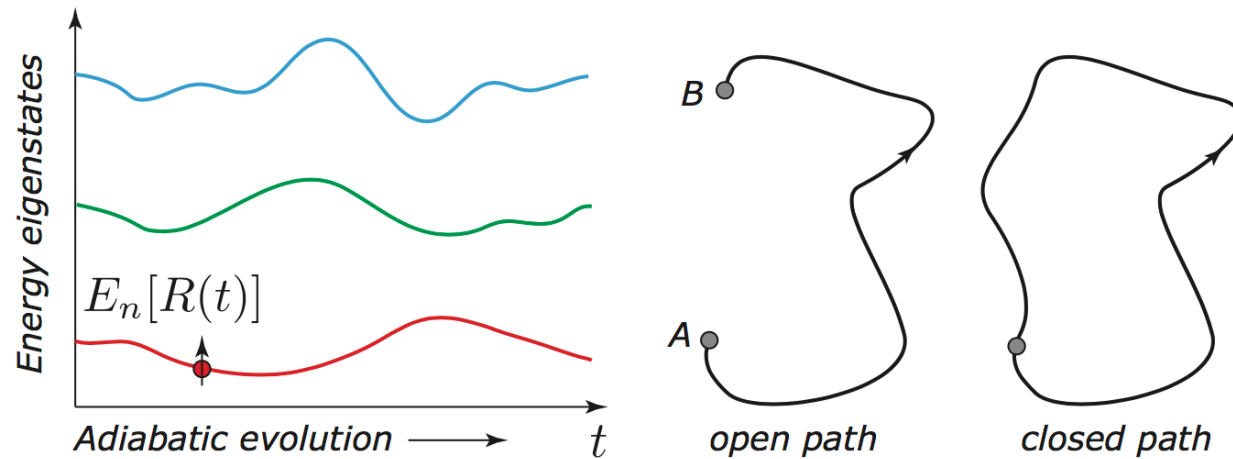
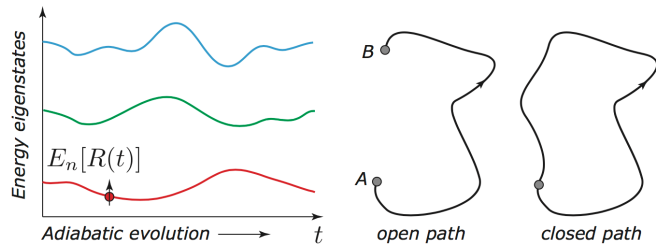


FIGURE 53.2: Berry phase derivation in quantum mechanics.

Berry Phase in Electron Bands



Every band will have its own Berry phase. Let each band be labeled $E_n(\mathbf{k})$, where \mathbf{k} is the wavevector, $|n(\mathbf{k})\rangle$ the eigenvector and $E_n(\mathbf{k})$ the corresponding eigenvalue.

Then the Berry phase of the band is given by

$$\gamma_n = i \oint d\mathbf{k} \cdot \underbrace{\langle n(\mathbf{k}) | \nabla_{\mathbf{k}} | n(\mathbf{k}) \rangle}_{\mathcal{A}_n(\mathbf{k})} \quad (53.3)$$

which is a line integral of a quantity $\mathcal{A}_n(\mathbf{k})$ over a closed loop. This quantity is called the Berry connection, and is analogous to the magnetic vector potential \mathbf{A} , whose curl is the magnetic field $\mathbf{B} = \nabla \times \mathbf{A}$. In analogy to the magnetic field \mathbf{B} , the Berry curvature is defined as $\mathbf{\Omega}_n(\mathbf{k}) = \nabla \times \mathcal{A}_n(\mathbf{k})$. Thus, we have the analogies $\mathcal{A}_n(\mathbf{k}) \leftrightarrow \mathbf{A}$ and $\mathbf{\Omega}_n(\mathbf{k}) \leftrightarrow \mathbf{B}$. For example, the line integral of the magnetic vector potential gives us the electromagnetic phase $e^{i\phi} = e^{i\frac{q}{\hbar} \int d\mathbf{l} \cdot \mathbf{A}}$. Drawing analogy with Stoke's theorem $\oint d\mathbf{l} \cdot \mathbf{A} = \int_S d\mathbf{S} \cdot \nabla \times \mathbf{A} = \int_S d\mathbf{S} \cdot \mathbf{B}$ for the magnetic flux, we realize that the Berry phase is an analogous flux

Berry curvature

$$\gamma_n = i \oint d\mathbf{k} \cdot \mathcal{A}_n(\mathbf{k}) = i \int_S d\mathbf{S} \cdot \mathbf{\Omega}_n(\mathbf{k}). \quad (53.4)$$

$$\Omega_{\nu\mu}^n = i \sum_{n \neq n'} \frac{\langle n | \partial_{R^\mu} H | n' \rangle \langle n' | \partial_{R^\nu} H | n \rangle - \langle n | \partial_{R^\nu} H | n' \rangle \langle n' | \partial_{R^\mu} H | n \rangle}{(E_n - E_{n'})^2}$$

Give me the bandstructure and eigenstates, and I can calculate the Berry Curvature

Electron Transport in 3D vs 2D

$$\mathbf{v}_n(\mathbf{k}) = \frac{1}{\hbar} \frac{\partial E_n}{\partial \mathbf{k}} - i \left(\left\langle \frac{\partial}{\partial \mathbf{k}} \left| \frac{\partial}{\partial t} \right\rangle - \left\langle \frac{\partial}{\partial t} \left| \frac{\partial}{\partial \mathbf{k}} \right\rangle \right)$$

Berry curvature

$$\mathbf{j} = \frac{1}{V} \sum_{n\mathbf{k}} -e\mathbf{v}_n(\mathbf{k}) = \frac{e^2}{\hbar} \sum_n \int \frac{d^2\mathbf{k}}{(2\pi)^2} \boldsymbol{\Omega}_n(\mathbf{k}) \times \mathbf{E}$$

$$\sigma_{xy} = \frac{e^2}{h} \sum_n \frac{1}{2\pi} \int d^2\mathbf{k} \Omega_n(\mathbf{k})$$

$$\sigma_{xy} = \frac{e^2}{h} \times C$$

Chern Number

Reason for the fantastic precision of IQHE



The Nobel Prize in Physics 2016
David J. Thouless, F. Duncan M. Haldane, J. Michael Kosterlitz

Share this: 1.9K

The Nobel Prize in Physics 2016



Photo: A. Mahmoud
David J. Thouless
Prize share: 1/2



Photo: A. Mahmoud
F. Duncan M. Haldane
Prize share: 1/4



Photo: A. Mahmoud
J. Michael Kosterlitz
Prize share: 1/4

The Nobel Prize in Physics 2016 was awarded with one half to David J. Thouless, and the other half to F. Duncan M. Haldane and J. Michael Kosterlitz "for theoretical discoveries of topological phase transitions and topological phases of matter".

VOLUME 49, NUMBER 6

PHYSICAL REVIEW LETTERS

9 AUGUST 1982

Quantized Hall Conductance in a Two-Dimensional Periodic Potential

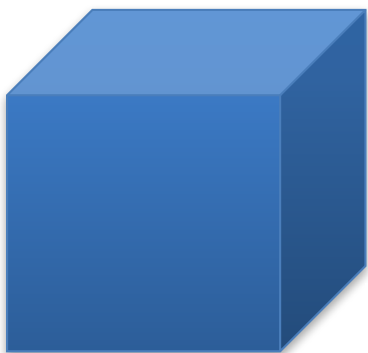
D. J. Thouless, M. Kohmoto,^(a) M. P. Nightingale, and M. den Nijs
Department of Physics, University of Washington, Seattle, Washington 98195
(Received 30 April 1982)

The Hall conductance of a two-dimensional electron gas has been studied in a uniform magnetic field and a periodic substrate potential U . The Kubo formula is written in a form that makes apparent the quantization when the Fermi energy lies in a gap. Explicit expressions have been obtained for the Hall conductance for both large and small $U/\hbar\omega_c$.

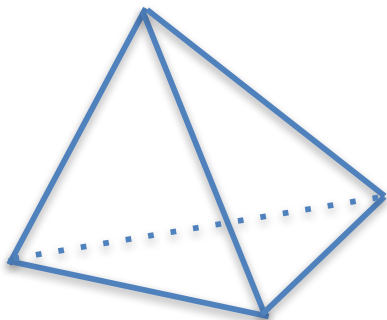
PACS numbers: 72.15.Gd, 72.20. Mg, 73.90.+b

The Euler Characteristic of Polyhedra

V is the number of vertices, E the number of edges, and F the number of faces



$$\chi = 2$$



$$\chi = 2$$

$$V - E + F = \chi$$

The Euler Characteristic

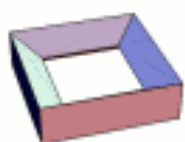
Convex Polygons (Cube, Tetrahedron, ...)

Images from Fukimoto Lab



$$\chi = 2$$

sphere



$$\chi = 0$$

donut



$$\chi = -2$$

double donut

$$\chi = 2 - 2g$$

g =number of holes, or 'handles'

Topologically equivalent to



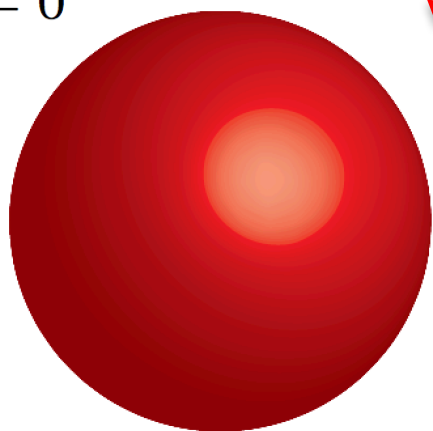
Euler

The Gauss-Bonnet Theorem

$$\int_{\theta=0}^{\pi} \int_{\phi=0}^{2\pi} \frac{1}{R^2} R^2 \sin \theta d\theta d\phi = 4\pi$$

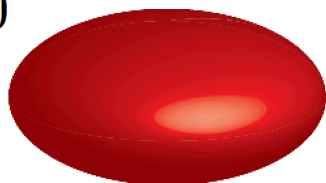
$$\kappa_1 = \kappa_2 = 1/R$$

$g = 0$



sphere

$g = 0$



football

$g = 1$



donut

$$z = z(x, y)$$

Equation of the surface

$$z(x, y) \approx a_0 + a_1 x^2 + a_2 y^2 + a_3 xy$$

Taylor expansion

$$z(x, y) \approx \frac{1}{2} \begin{bmatrix} x & y \end{bmatrix} \begin{bmatrix} \frac{\partial^2 z}{\partial x^2} & \frac{\partial^2 z}{\partial x \partial y} \\ \frac{\partial^2 z}{\partial y \partial x} & \frac{\partial^2 z}{\partial y^2} \end{bmatrix} \begin{bmatrix} x \\ y \end{bmatrix}$$

Hessian Matrix

eigenvalues κ_1, κ_2

Local curvatures

$$\int_S \kappa_1 \kappa_2 dA = 2\pi \chi = 2\pi(2 - 2g).$$

The Gauss-Bonnet Theorem

g =number of holes, or 'handles'

$$\Omega = \kappa_1 \kappa_2$$

total curvature

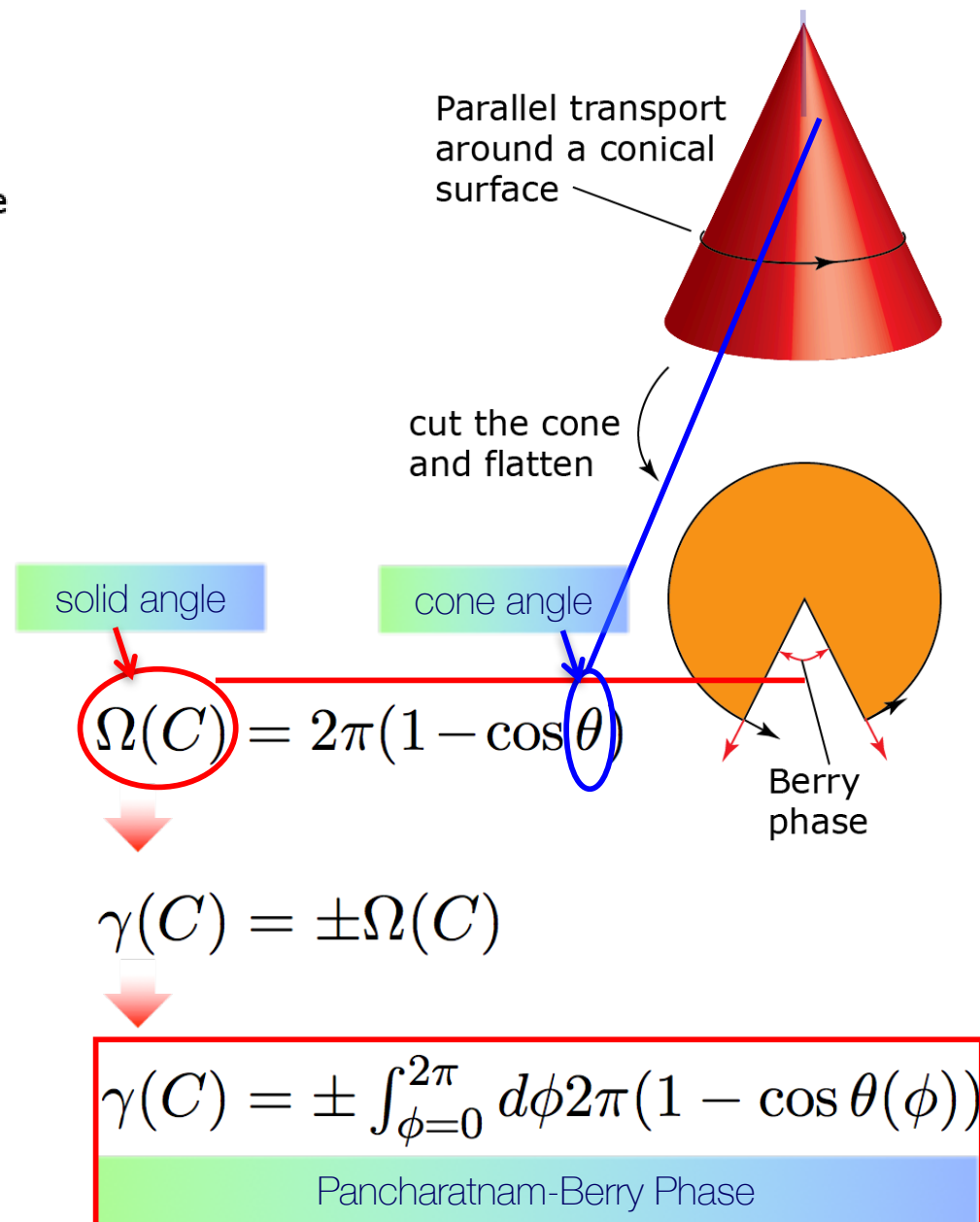
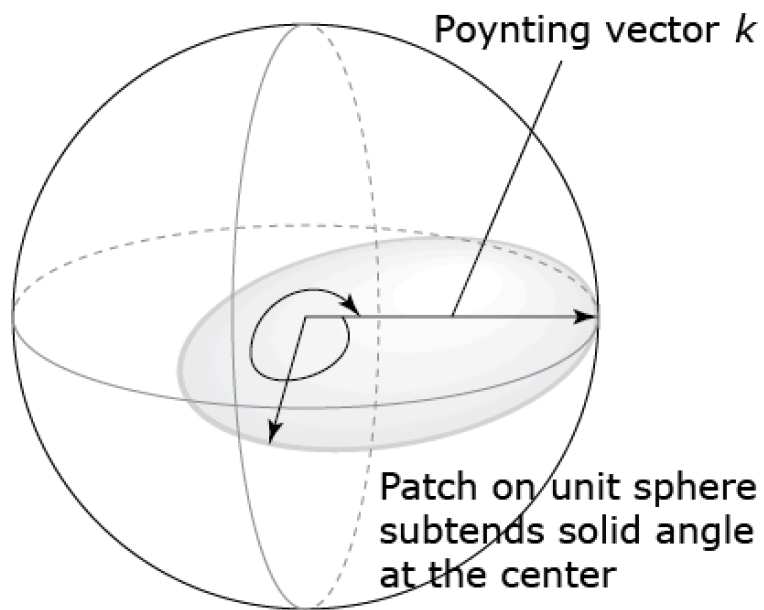
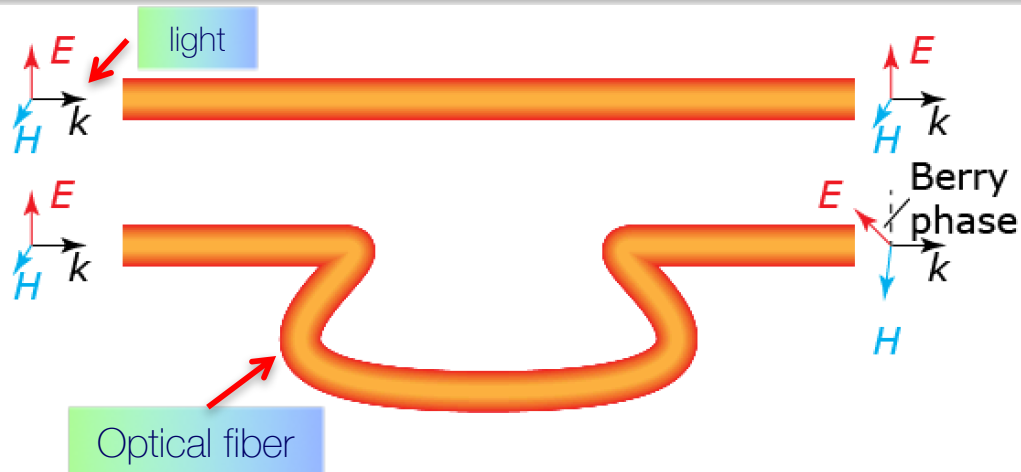
$$\frac{1}{2\pi} \int_S \Omega dA = C$$

Chern number, an integer!

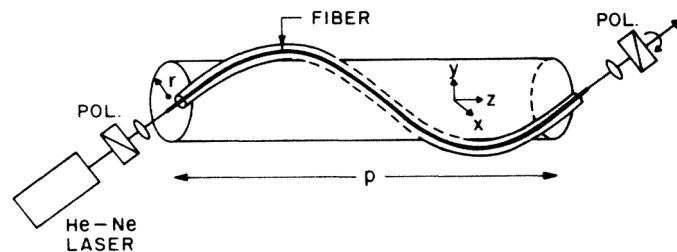


Gauss

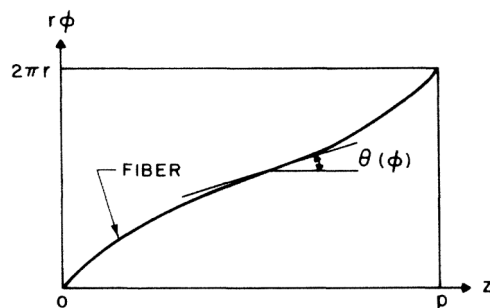
The Pancharatnam-Berry Phase



The Pancharatnam-Berry Phase: Experiment



(a)



(b)

FIG. 1. (a) Experimental setup; (b) geometry used to calculate the solid angle in momentum space of a nonuniformly wound fiber on a cylinder.

Observation of Berry's Topological Phase by Use of an Optical Fiber

Akira Tomita^(a)

AT&T Bell Laboratories, Murray Hill, New Jersey 07974

and

Raymond Y. Chiao

Department of Physics, University of California, Berkeley, California 94720

(Received 28 February 1986)

We report the first experimental verification of Berry's topological phase. The key element in the experiment was a single-mode, helically wound optical fiber, inside which a photon of a given helicity could be adiabatically transported around a closed path in momentum space. The experiment confirmed at the classical level that the angle of rotation of linearly polarized light in this fiber gives a direct measure of Berry's phase. The topological nature of this effect was also verified, i.e., the rotation was found to be independent of deformations of fiber path if the solid angle of the path in momentum space stayed constant.

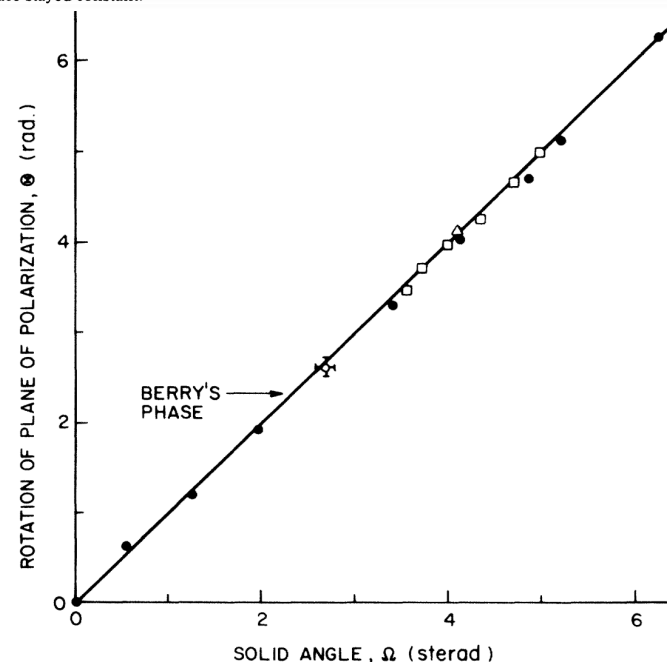
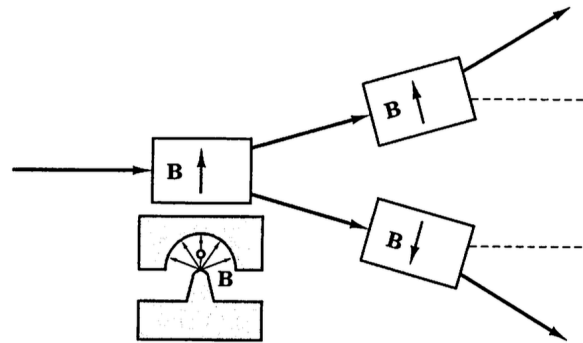


FIG. 3. Measured angle of rotation of linearly polarized light vs calculated solid angle in momentum space, Eq. (3). Open circles represent the data for uniform helices; squares and triangle represent nonuniform helices (see Fig. 2); solid circles represent arbitrary planar paths. The solid line is the theoretical prediction based on Berry's phase, Eq. (4).

Electron spin is a consequence of relativity



1922 Stern-Gerlach experiment shows evidence of spin

1925 Uhlenbeck and Goudsmit propose spin as an intrinsic angular momentum of electrons

1927 Pauli introduces spin matrices and spin into the Schrodinger equation in an ad-hoc manner

1927 Dirac unifies special relativity and quantum mechanics and finds spin as a byproduct

$$\hat{H} = \hat{H}_0 + \mu_B \sigma \cdot \mathbf{B} + \mu_B \sigma \cdot \frac{\mathbf{E} \times \mathbf{v}}{2c^2} = \hat{H}_0 + \mu_B \sigma \cdot \mathbf{B} + \frac{\hbar}{4mc^2} \sigma \cdot [(\nabla V) \times \mathbf{v}]$$

Spin-less Energy

Extra terms because of spin

Extra terms because of spin

Berry Phase of ANY 2-Band System

Problem 4.5) Topological Insulators and Berry Phases

In class, we discussed that every 2×2 Hermitian Hamiltonian matrix can be written as $H_2 = \begin{pmatrix} h_0(k)+h_z(k) & h_x(k)-ih_y(k) \\ h_x(k)+ih_y(k) & h_0(k)-h_z(k) \end{pmatrix}$, and can be decomposed into the form $H_2 = h_0(k)I + h_x(k)\sigma_x + h_y(k)\sigma_y + h_z(k)\sigma_z = h_0(k)I + \vec{h} \cdot \vec{\sigma}$, where $\vec{h} = [h_x(k), h_y(k), h_z(k)]$, σ 's are the Pauli spin matrices, and I is the identity matrix.

(a) By drawing analogy to the Hamiltonian of an electron in a magnetic field and Zeeman splitting, show that the eigenvalues form two bands $E_{\pm}(k) = h_0(k) \pm |\vec{h}(k)|$, and the gap at k is $E_g(k) = E_+(k) - E_-(k) = 2|\vec{h}(k)|$. Show that the eigenfunctions are not well behaved near points in k -space where the gap closes. Recall from our discussion of the Dirac monopole that this is a signature of non-trivial Chern-numbers.

Berry Phase of ANY 2-Band System

$$\hat{H}(\mathbf{d}) = d_x \hat{\sigma}_x + d_y \hat{\sigma}_y + d_z \hat{\sigma}_z = \mathbf{d} \cdot \hat{\sigma}$$

$$\mathbf{d} = (d_x, d_y, d_z)$$

$$\cos \theta = \frac{d_z}{|\mathbf{d}|}, \quad e^{i\varphi} = \frac{d_x + id_y}{\sqrt{d_x^2 + d_y^2}}$$

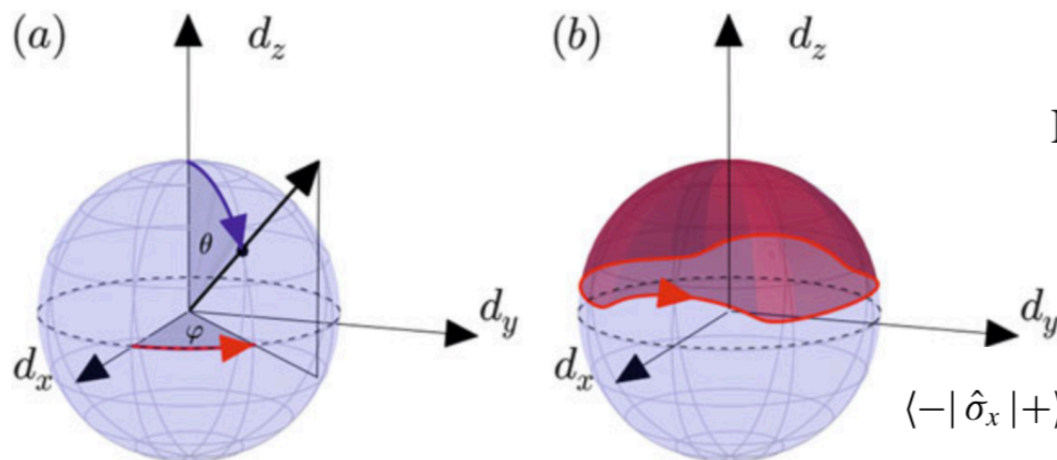


Fig. 2.2 The Bloch sphere. A generic traceless gapped two-level Hamiltonian is a linear combination of Pauli matrices, $\hat{H}(\mathbf{d}) = \mathbf{d} \cdot \hat{\sigma}$. This can be identified with a point in $\mathbb{R}^3 \setminus \{0\}$. The eigenenergies are given by the distance of the point from the origin, the eigenstates depend only on the direction of the vector \mathbf{d} , i.e., on the angles θ and φ , as defined in subfigure (a) and in Eq. (2.62). The Berry phase of a closed curve \mathcal{C} is half the area enclosed by the curve when it is projected onto the surface of the Bloch sphere

$$\hat{H}(\mathbf{d}) |\pm_{\mathbf{d}}\rangle = \pm |\mathbf{d}| |\pm_{\mathbf{d}}\rangle$$

$$|+_{\mathbf{d}}\rangle = e^{i\alpha(\theta, \varphi)} \begin{pmatrix} e^{-i\varphi/2} \cos \theta/2 \\ e^{i\varphi/2} \sin \theta/2 \end{pmatrix}$$

$$\gamma_-(\mathcal{C}) = \oint_{\mathcal{C}} \mathbf{A}(\mathbf{d}) d\mathbf{d}$$

$$\mathbf{A}(\mathbf{d}) = i \langle -_{\mathbf{d}} | \nabla_{\mathbf{d}} | -_{\mathbf{d}} \rangle$$

$$\mathbf{B}^{\pm}(\mathbf{d}) = -\text{Im} \frac{\langle \pm | \nabla_{\mathbf{d}} \hat{H} | \mp \rangle \times \langle \mp | \nabla_{\mathbf{d}} \hat{H} | \pm \rangle}{4\mathbf{d}^2}$$

$$\nabla_{\mathbf{d}} \hat{H} = \hat{\sigma} \quad | +_{\mathbf{d}} \rangle = \begin{pmatrix} 1 \\ 0 \end{pmatrix} \quad | -_{\mathbf{d}} \rangle = \begin{pmatrix} 0 \\ 1 \end{pmatrix}$$

$$\langle - | \hat{\sigma}_x | + \rangle = (0 \ 1) \begin{pmatrix} 0 & 1 \\ 1 & 0 \end{pmatrix} \begin{pmatrix} 1 \\ 0 \end{pmatrix} = 1 \quad \langle - | \sigma_y | + \rangle = i; \\ \langle - | \sigma_z | + \rangle = 0.$$

$$\mathbf{B}^{\pm}(\mathbf{d}) = \pm \frac{\mathbf{d}}{|\mathbf{d}|} \frac{1}{2d^2} \quad \gamma_-(\mathcal{C}) = \frac{1}{2} \Omega_{\mathcal{C}}$$

Anomalous velocity term due to Berry Phase

$$|u_n\rangle - i\hbar \sum_{n' \neq n} \frac{|u_{n'}\rangle \langle u_{n'} | \partial u_n / \partial t \rangle}{\epsilon_n - \epsilon_{n'}}$$

Perturbation in eigenfunction

$$v_n(q) = \frac{\partial \epsilon_n(q)}{\hbar \partial q}$$

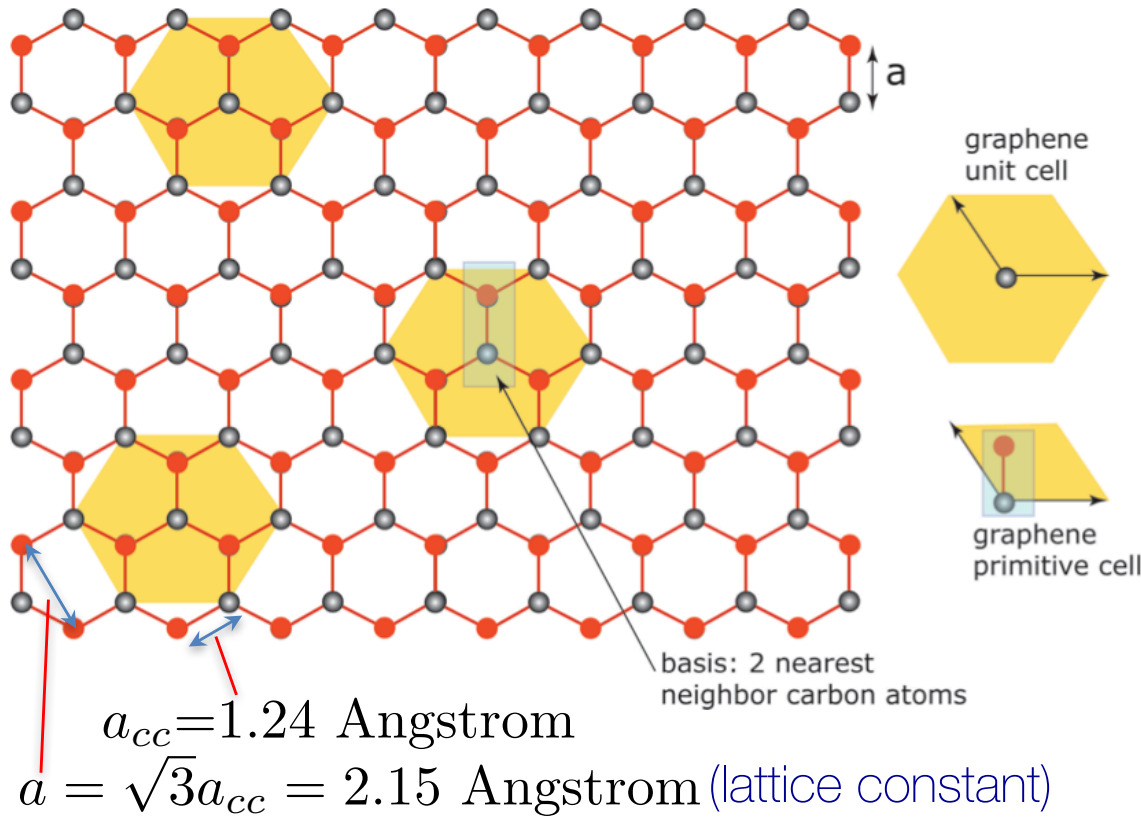
$$-i \sum_{n' \neq n} \left\{ \frac{\langle u_n | \partial H / \partial q | u_{n'} \rangle \langle u_{n'} | \partial u_n / \partial t \rangle}{\epsilon_n - \epsilon_{n'}} - \text{c.c.} \right\}$$

$$\frac{d\mathbf{x}}{dt} = \frac{1}{\hbar} \nabla_k E(k) + \frac{d\mathbf{k}}{dt} \times \boldsymbol{\Omega} = \frac{1}{\hbar} \nabla_k E(k) + \frac{q}{\hbar} \mathbf{E} \times \boldsymbol{\Omega}$$

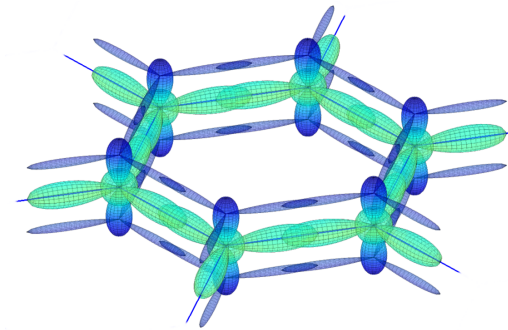
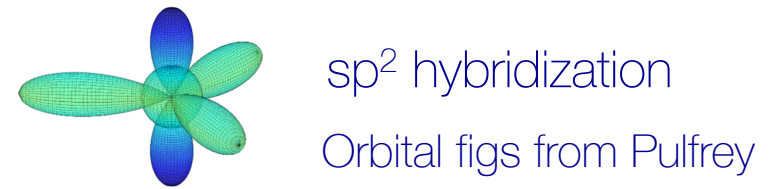
Berry curvature velocity term

$$\frac{d\mathbf{p}}{dt} = -e \nabla_r V + e \left(\frac{d\mathbf{x}}{dt} \times \mathbf{B} \right)$$

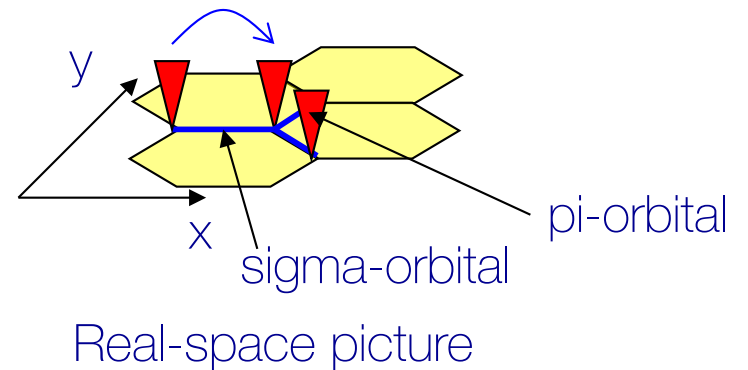
Example: Graphene



- Sigma-orbitals hold the atoms together. (3 electrons/carbon atom, one left over)
- Pi-orbitals are responsible for conduction. (1 electron/carbon atom)



Hopping energy: $\gamma_0 \approx 3$ eV



Graphene Bandstructure

$$v_F = \frac{3}{2} a_{cc} \frac{\gamma_0}{\hbar} \sim 10^8 \frac{cm}{s}$$



Hamiltonian of pi-electrons with 1st nearest neighbor interaction

$$\hbar v_F \begin{bmatrix} 0 & k_x - ik_y \\ k_x + ik_y & 0 \end{bmatrix} \begin{bmatrix} F_A(r) \\ F_B(r) \end{bmatrix} = \mathcal{E}(k_x, k_y) \begin{bmatrix} F_A(r) \\ F_B(r) \end{bmatrix}$$

pseudo-spin

$$\hbar v_F (\boldsymbol{\sigma} \cdot \mathbf{k}) \mathbf{F}(\mathbf{r}) = \mathcal{E}(k_x, k_y) \mathbf{F}(\mathbf{r})$$

solve!

Eigenvectors:

$$\langle \mathbf{r} | k \rangle = \frac{1}{\sqrt{2}} e^{i\mathbf{k} \cdot \mathbf{r}} \begin{pmatrix} 1 \\ \pm e^{-i\theta_k} \end{pmatrix}$$

$$\theta_k = \tan^{-1} \left(\frac{k_y}{k_x} \right)$$

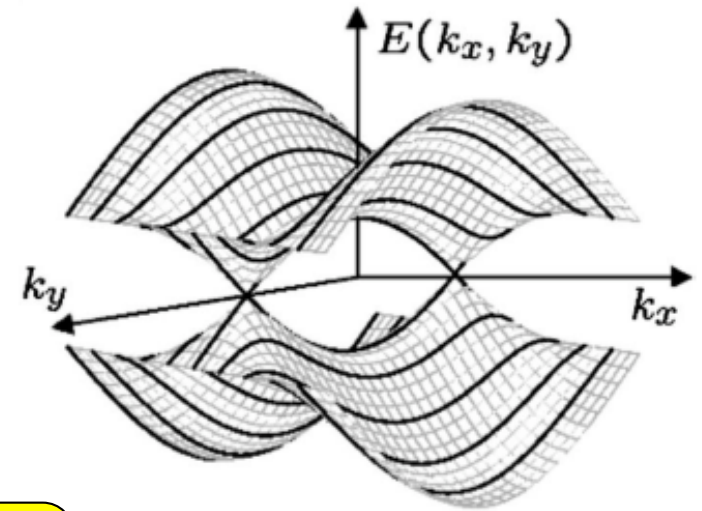
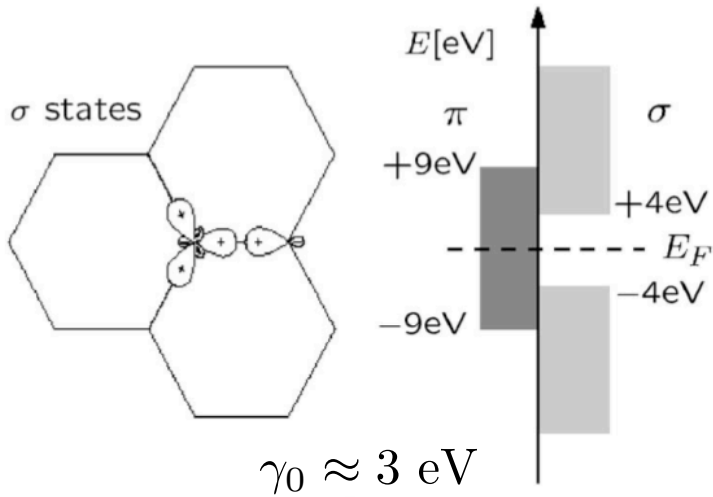
Bandstructure

$$\mathcal{E}(k_x, k_y) = \mathcal{E}_F \pm \gamma_0 \sqrt{1 + 4 \cos\left(\frac{\sqrt{3}k_x a}{2}\right) \cos\left(\frac{k_y a}{2}\right) + 4 \cos^2\left(\frac{k_y a}{2}\right)}$$

Some features: $\mathcal{E}(0, 0) = \mathcal{E}_F \pm 3\gamma_0 \rightarrow \begin{pmatrix} 3\gamma_0 \sim +9eV: \text{antibonding} \\ -3\gamma_0 \sim -9eV: \text{bonding} \end{pmatrix} \rightarrow \Gamma\text{-point}$

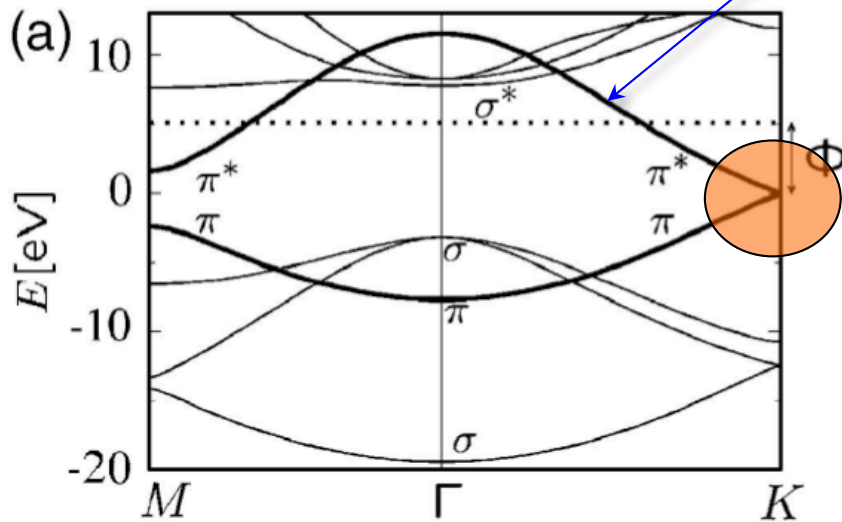
$\mathcal{E}(0, \frac{4\pi}{3a}) = \mathcal{E}_F \pm 0 \rightarrow$ No gap (Dirac point), wavelength: $\lambda = \frac{3a}{2} \rightarrow \mathcal{K}\text{-point}$

Graphene Bandstructure



$$\mathcal{E}(k_x, k_y) = \mathcal{E}_F \pm \gamma_0 \sqrt{1 + 4 \cos\left(\frac{\sqrt{3}k_x a}{2}\right) \cos\left(\frac{k_y a}{2}\right) + 4 \cos^2\left(\frac{k_y a}{2}\right)}$$

- Expand around the Dirac point



$$\mathcal{E}(k_x, k_y) \approx \hbar v_F \sqrt{k_x^2 + k_y^2}$$

$v_F \sim 10^8 \text{ cm/s}$

Conical!
Linear dispersion

$g_{spin} = 2$
 $g_{valley} = 2$

- Reviews of Modern Physics, 79 677 (2007).

Graphene with a gap: the Valley Hall Effect

$$\frac{d\mathbf{x}}{dt} = \frac{1}{\hbar} \nabla_{\mathbf{k}} E(\mathbf{k}) + \frac{d\mathbf{k}}{dt} \times \boldsymbol{\Omega} = \frac{1}{\hbar} \nabla_{\mathbf{k}} E(\mathbf{k}) + \frac{q}{\hbar} \mathbf{E} \times \boldsymbol{\Omega}$$

$$H = \frac{\sqrt{3}}{2} at(q_x \tau_z \sigma_x + q_y \sigma_y) + \frac{\Delta}{2} \sigma_z$$

Gapped graphene Hamiltonian

$$\boldsymbol{\Omega}(\mathbf{q}) = \tau_z \frac{3a^2 \Delta t^2}{2(\Delta^2 + 3q^2 a^2 t^2)^{3/2}}$$

Berry curvature in "Gapped" Graphene

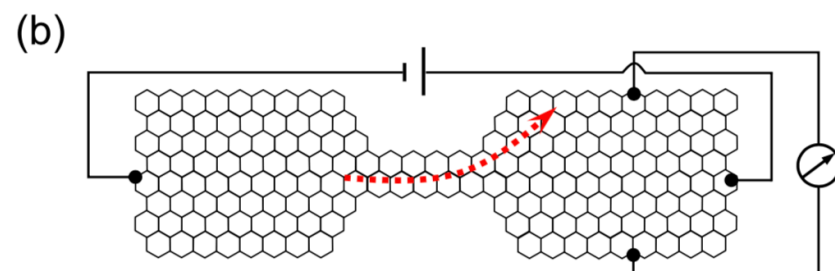
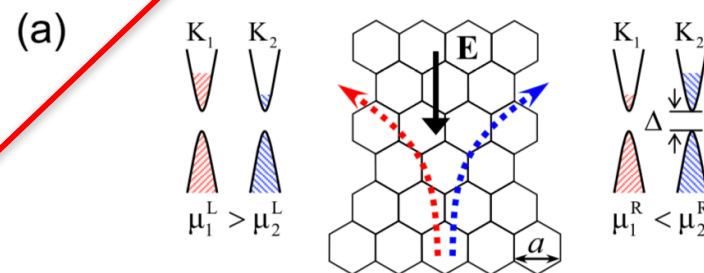
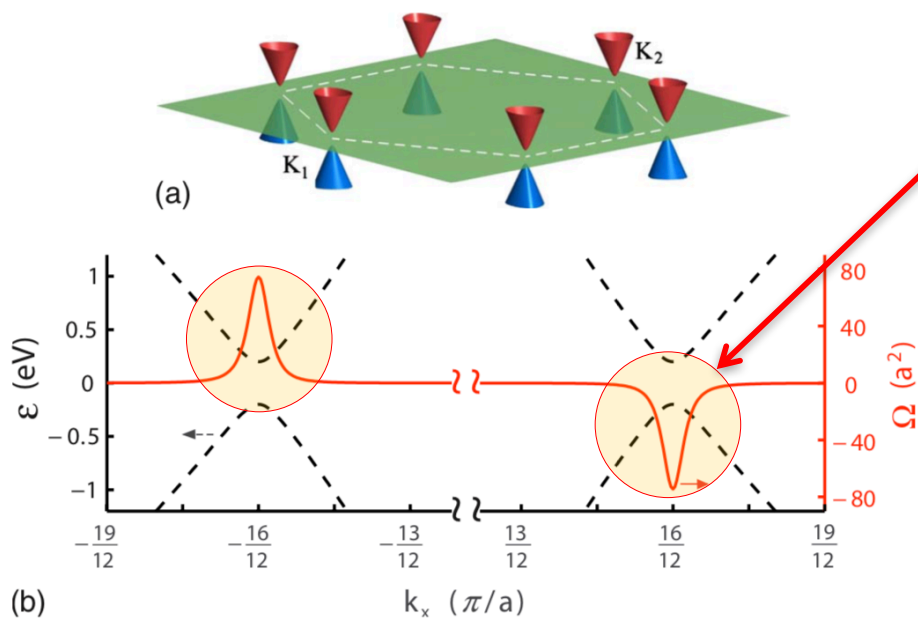


FIG. 2 (color online). Electric generation (a) and detection (b) of the valley polarization. (a) An in-plane electric field will generate a transverse valley current, which leads to a net valley polarization on the sample edges. (b) A valley polarization created by the valley filter [6] results in a transverse voltage across the sample.

The SSH Model of a Topological Insulator



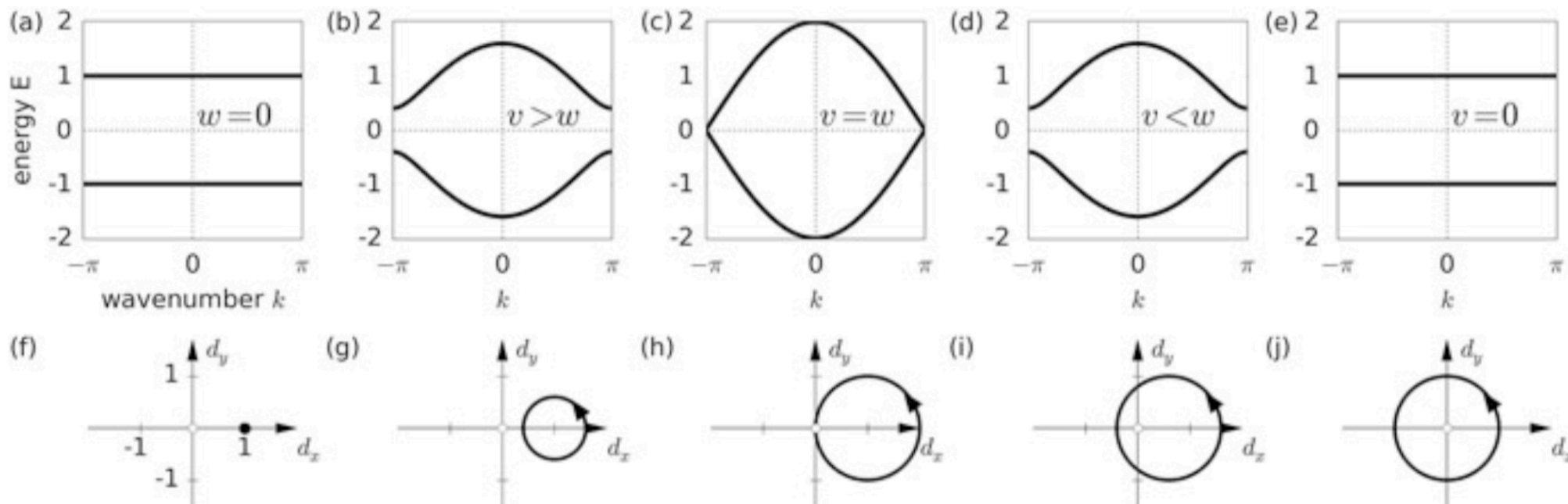
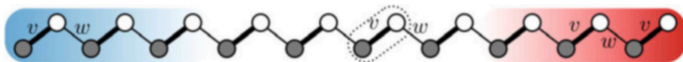
$$\begin{pmatrix} 0 & v & 0 & 0 & 0 & 0 & 0 & w \\ v & 0 & w & 0 & 0 & 0 & 0 & 0 \\ 0 & w & 0 & v & 0 & 0 & 0 & 0 \\ 0 & 0 & v & 0 & w & 0 & 0 & 0 \\ 0 & 0 & 0 & w & 0 & v & 0 & 0 \\ 0 & 0 & 0 & 0 & v & 0 & w & 0 \\ 0 & 0 & 0 & 0 & 0 & w & 0 & v \\ w & 0 & 0 & 0 & 0 & 0 & v & 0 \end{pmatrix} \begin{pmatrix} a(k)e^{ik} \\ b(k)e^{ik} \\ a(k)e^{2ik} \\ b(k)e^{2ik} \\ a(k)e^{3ik} \\ b(k)e^{3ik} \\ a(k)e^{Nik} \\ b(k)e^{Nik} \end{pmatrix} = E(k) \begin{pmatrix} a(k)e^{ik} \\ b(k)e^{ik} \\ a(k)e^{2ik} \\ b(k)e^{2ik} \\ a(k)e^{3ik} \\ b(k)e^{3ik} \\ a(k)e^{Nik} \\ b(k)e^{Nik} \end{pmatrix}$$

A representative Hamiltonian of finite 4 unit cell SSH chain

$$H(k) = \begin{pmatrix} 0 & v + we^{-ik} \\ v + we^{ik} & 0 \end{pmatrix}; \quad H(k) \begin{pmatrix} a(k) \\ b(k) \end{pmatrix} = E(k) \begin{pmatrix} a(k) \\ b(k) \end{pmatrix}$$

The SSH "bulk" Hamiltonian for a long (or periodic) 1D chain

The SSH Model of a Topological Insulator



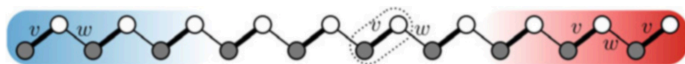
$$H(k) = \begin{pmatrix} 0 & v + we^{-ik} \\ v + we^{ik} & 0 \end{pmatrix}; \quad H(k) \begin{pmatrix} a(k) \\ b(k) \end{pmatrix} = E(k) \begin{pmatrix} a(k) \\ b(k) \end{pmatrix}$$

The SSH "bulk" Hamiltonian for a long (or periodic) 1D chain

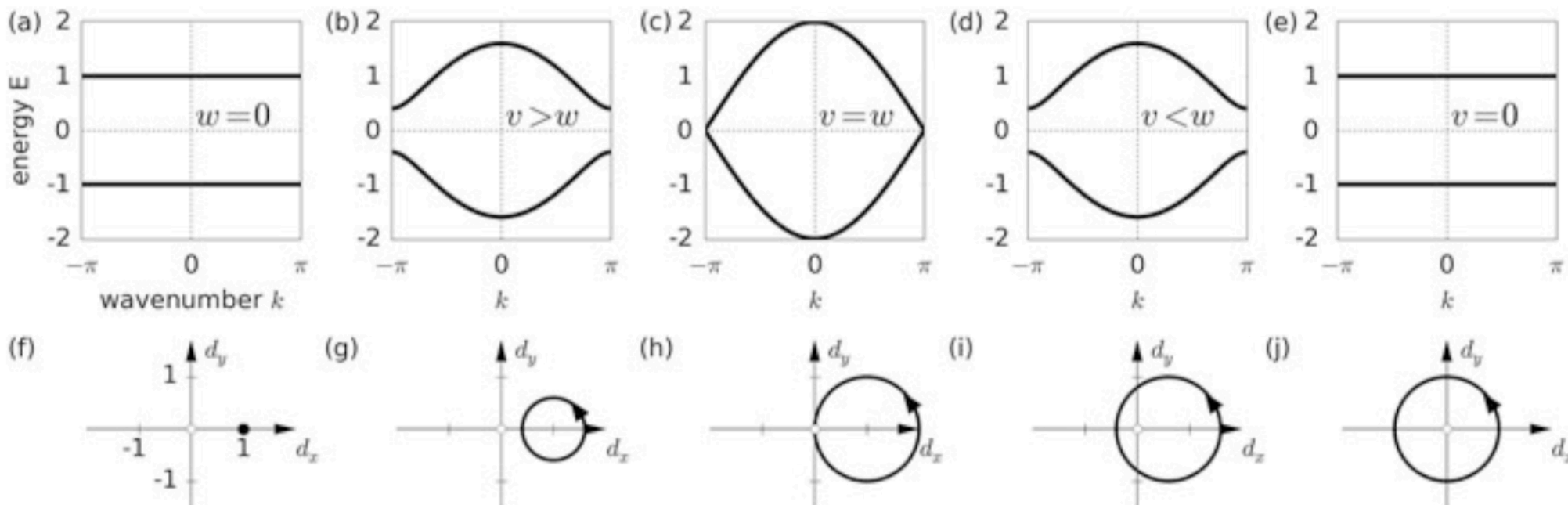
$$H(k) = d_0(k)\hat{\sigma}_0 + d_x(k)\hat{\sigma}_x + d_y(k)\hat{\sigma}_y + d_z(k)\hat{\sigma}_z = d_0(k)\hat{\sigma}_0 + \mathbf{d}(k)\hat{\boldsymbol{\sigma}}$$

$$d_x(k) = v + w \cos k; \quad d_y(k) = w \sin k; \quad d_z(k) = 0.$$

The SSH Model of a Topological Insulator



What's different?



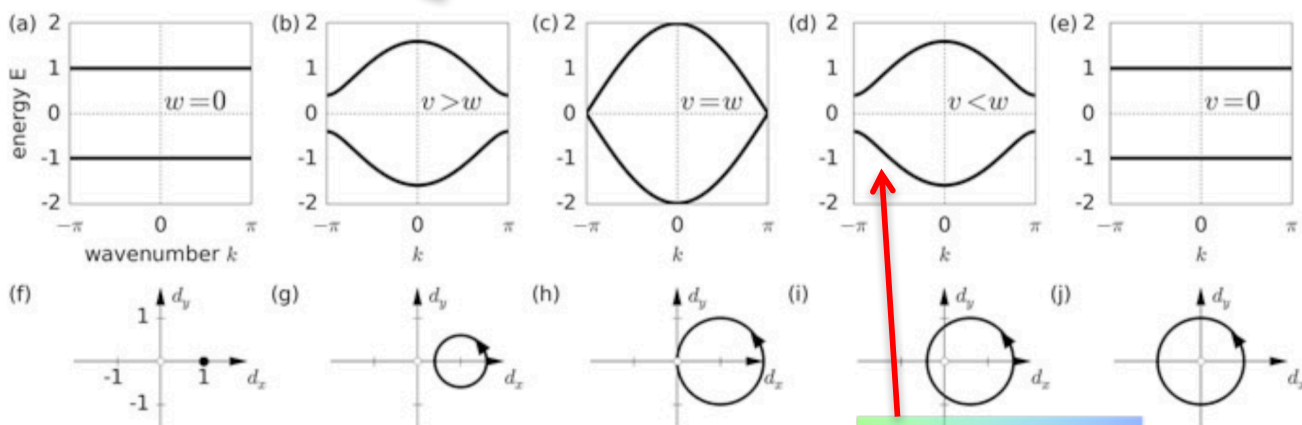
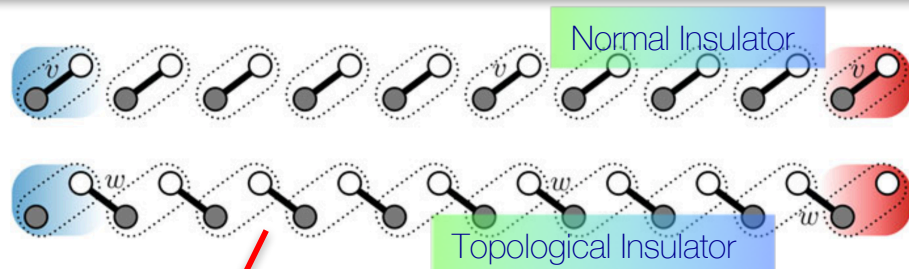
$$H(k) = \begin{pmatrix} 0 & v + we^{-ik} \\ v + we^{ik} & 0 \end{pmatrix}; \quad H(k) \begin{pmatrix} a(k) \\ b(k) \end{pmatrix} = E(k) \begin{pmatrix} a(k) \\ b(k) \end{pmatrix}$$

The SSH "bulk" Hamiltonian for a long (or periodic) 1D chain

$$H(k) = d_0(k)\hat{\sigma}_0 + d_x(k)\hat{\sigma}_x + d_y(k)\hat{\sigma}_y + d_z(k)\hat{\sigma}_z = d_0(k)\hat{\sigma}_0 + \mathbf{d}(k)\hat{\boldsymbol{\sigma}}$$

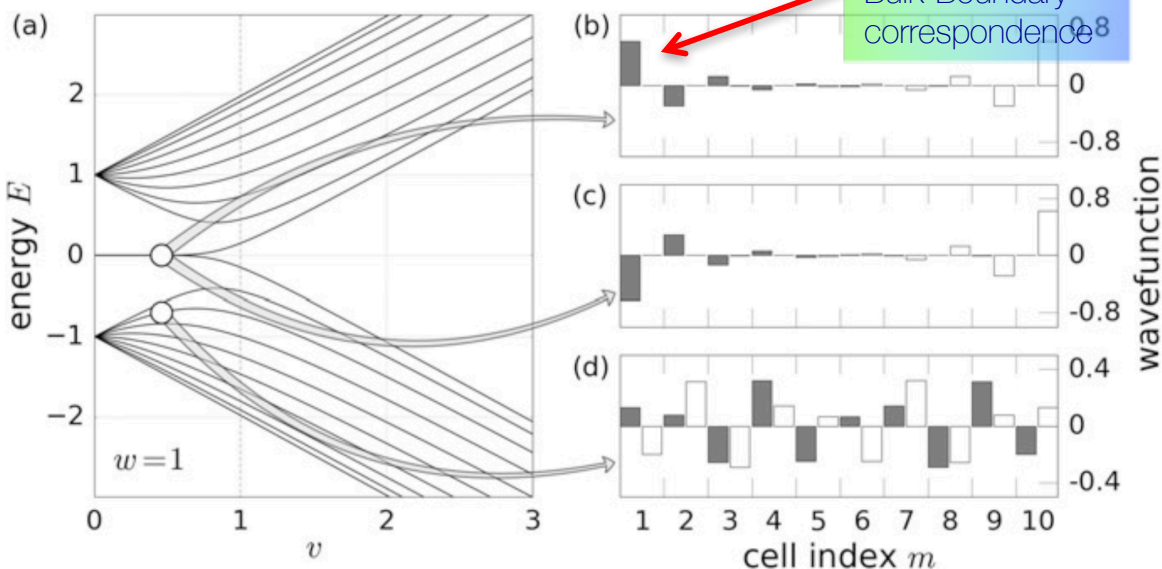
$$d_x(k) = v + w \cos k; \quad d_y(k) = w \sin k; \quad d_z(k) = 0.$$

The SSH Model of a Topological Insulator



$$H(k) = \begin{pmatrix} 0 & h(k) \\ h^*(k) & 0 \end{pmatrix}$$

$$h(k) = d_x(k) - id_y(k).$$

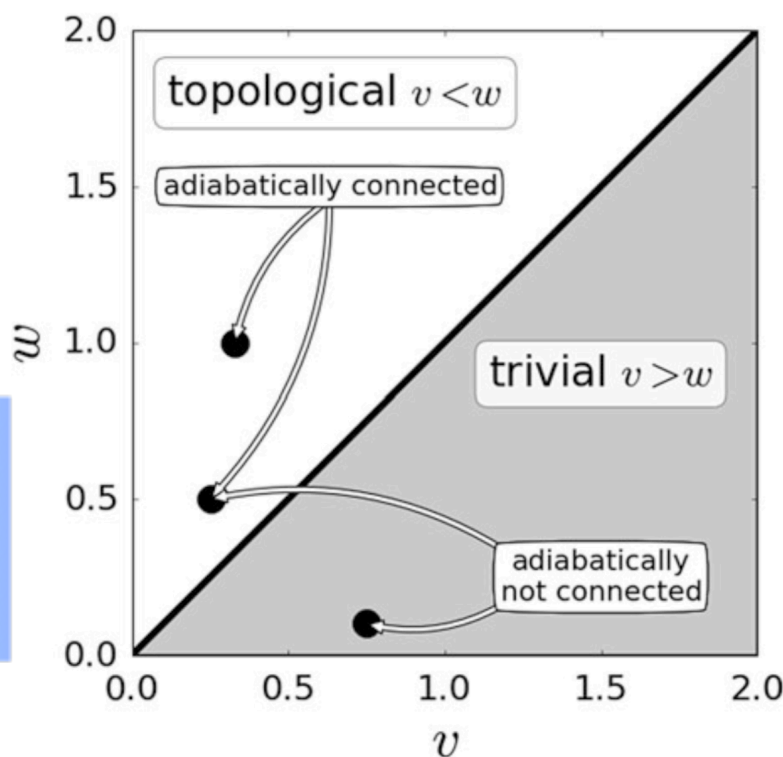
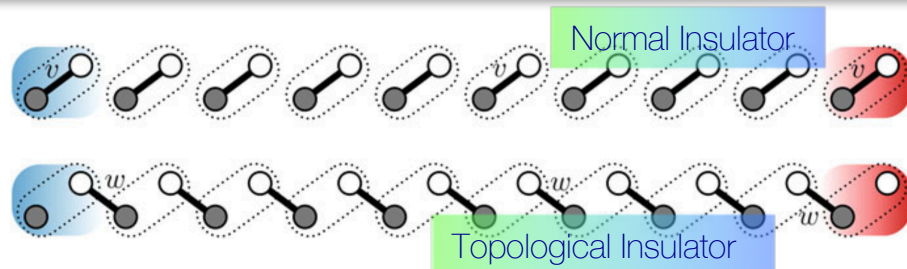
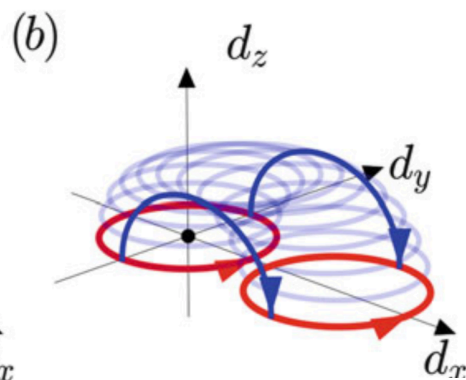
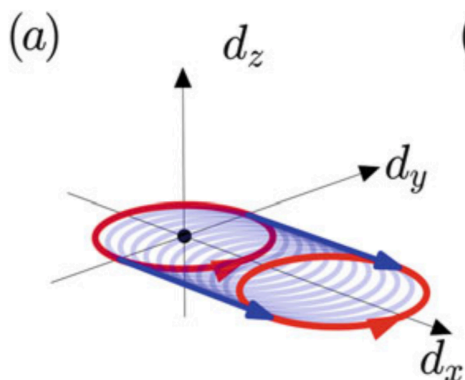
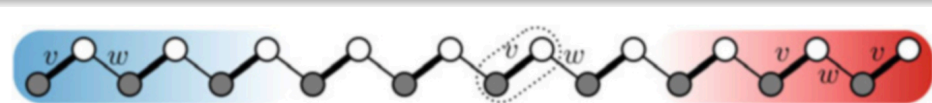


Bulk-Boundary correspondence

$$\nu = \frac{1}{2\pi i} \int_{-\pi}^{\pi} dk \frac{d}{dk} \log h(k)$$

Winding number

The SSH Model of a 1D Topological Insulator



Topological phases of the SSH chain, and of any crystal can be classified in this manner

$$H(k) = \begin{pmatrix} 0 & h(k) \\ h^*(k) & 0 \end{pmatrix}$$

$$h(k) = d_x(k) - id_y(k).$$

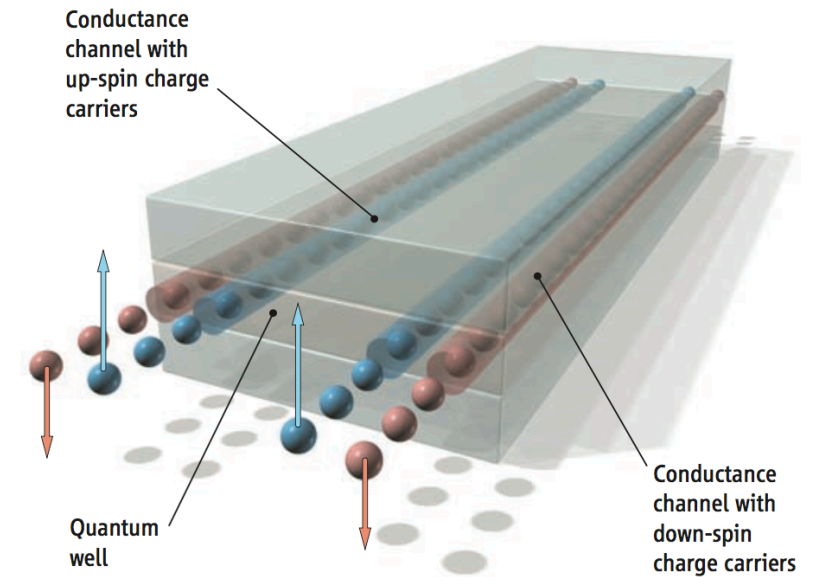
$$\nu = \frac{1}{2\pi i} \int_{-\pi}^{\pi} dk \frac{d}{dk} \log h(k)$$

Winding number

2D Topological Insulators: 1D Edge States

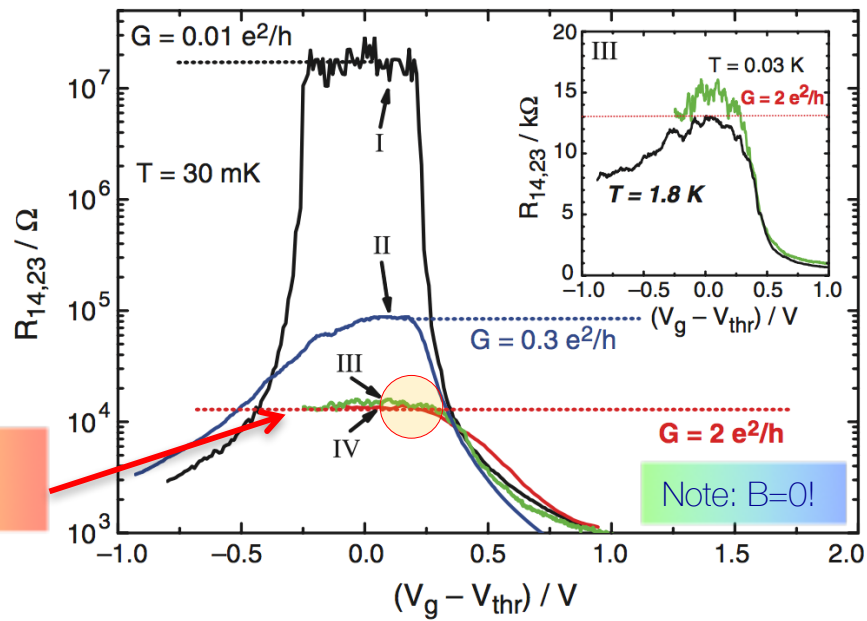
Quantum Spin Hall Insulator State in HgTe Quantum Wells

Markus König,¹ Steffen Wiedmann,¹ Christoph Brüne,¹ Andreas Roth,¹ Hartmut Buhmann,¹ Laurens W. Molenkamp,^{1*} Xiao-Liang Qi,² Shou-Cheng Zhang²

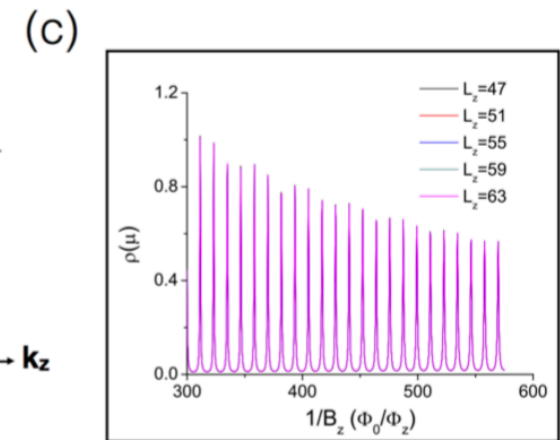
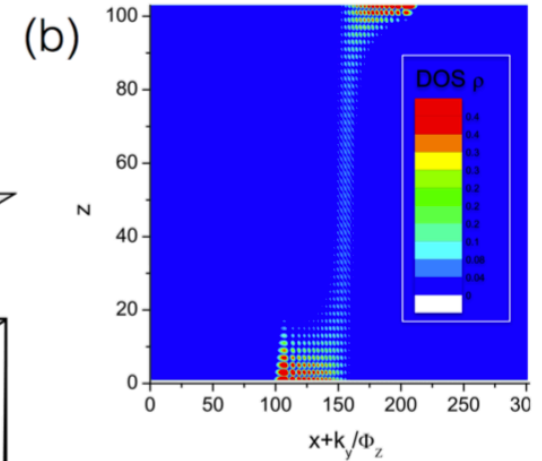
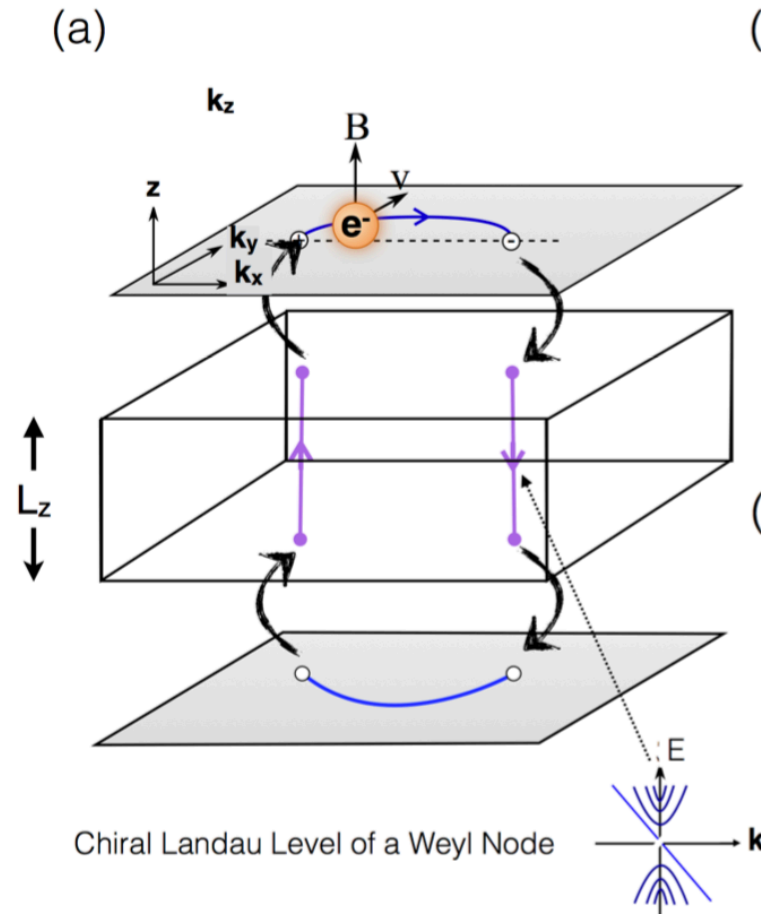
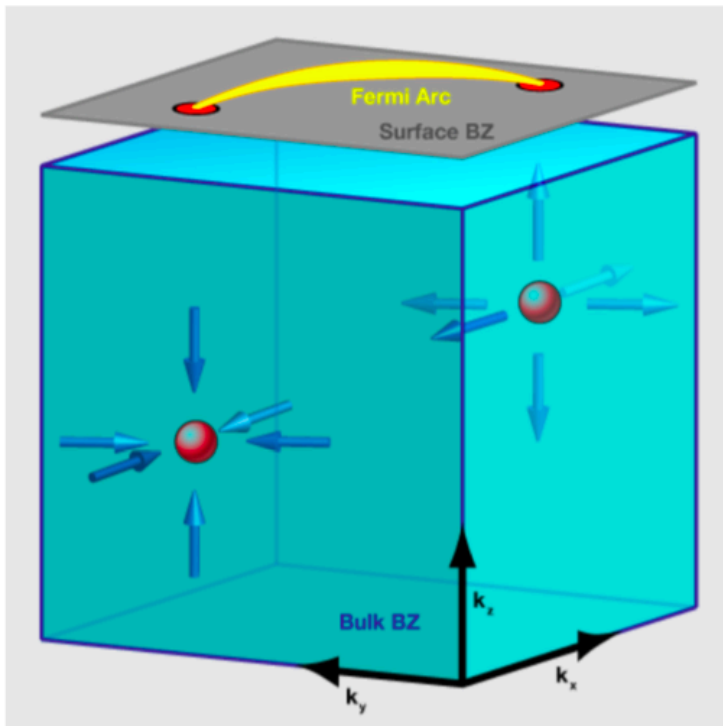


Schematic of the spin-polarized edge channels in a quantum spin Hall insulator.

Living on the edge!



Weyl Semimetals: Dirac cone bulk + Fermi Arc Surface





End